Vertical Distribution Of Selected Trace Elements

Within the Fruitland Number Eight Coal Seam

Near Farmington, New Mexico

By

D. T. Kendrick

Submitted in Partial Fufillment

of the Requirements for the Degree of

Master of Science in Geology

New Mexico Institute of Mining and Technology

Socorro, New Mexico

December 1985

## ACKNOWLEDGMENTS

## ABSTRACT

Two drill cores penetrating the 14 ft. thick Fruitland No. 8 coal seam were sampled at 30 and 33 points each. These samples represent 0.2 to 0.4 vertical feet of drill core each. Sampling recovered approximately 41 % of the coal thickness in both drill cores.

Abundances were determined for 33 trace and minor elements utilizing AA, ISE, INAA, and a potentiometric titration technique. Proximate analyses were also made.

The rare earth elements (REE) show an unexpected fractionation within the coal seam. The light rare earth elements (LREE) show strong correlations with the determined ash content. But the heavy rare earth elements (HREE) show very low correlations with ash. Chondrite normalized REE plots reveal a HREE enrichment in coal samples adjacent to partings. This indicates a preferential mobilization of the HREE from the source materials within the partings into the surrounding coal. This mobilization was the result of intense chemical weathering of the parting constituents in the highly acidic peat environment.

Most of the elements analyzed for can be distributed into one of four groups based on their vertical distribution profiles.

Group I (Ce, Cs, Eu, F, Hf, La, Li, Lu, Na, Nd, Rb, Sc, Sm, Ta, Tb, Th, U, and Yb) show a strong association with the occurrence of partings (tonsteins). The source of these elements is considered to be allogenic mineral matter, which constitutes the majority of the ash forming constituents.

Elements in this group are subdivided into two sub-groups, Ia and Ib, depending upon whether or not the element shows redistribution from the parting into the surrounding coal. Group Ia elements show no redistribution, while those in Ib show varying degrees of redistribution.

Group II (Ni, and Sb) shows distribution profiles where abundances increase sharply at one or both seam boundaries. This type of distribution is interpreted as secondary enrichment during a post depositional stage.

Group III (Ca and Mn) elements show markedly increased abundances just above partings, where cleat development and filling by authigenic minerals is most prominent. The build-up of these elements above the partings is thought to be related to the partings impermeability.

Group IV (As, Cr, Cu, Pb, Se, and Zn) elements show distribution profiles in which zones of increased abundance occur in stratigraphically similar positions in both drill cores. These zones are unrelated to the occurrence of partings or to the seam boundaries. Further the zones of increased abundance for one element are not coincident in location with those for other elements in this group.

# TABLE OF CONTENTS

TABLE OF CONTENTS (cont.)

TABLE OF CONTENTS (cont.)

# LIST OF TABLES

## TABLES IN APPENDICIES

LIST OF FIGURES

LIST OF FIGURES IN APPENDICIES

LIST OF FIGURES IN APPENDICIES (cont.)

LIST OF FIGURES IN APPENDICIES (cont.)

LIST OF FIGURES IN APPENDICIES (cont.)

LIST OF FIGURES IN APPENDICIES (cont.)

LIST OF FIGURES IN APPENDICIES (cont.)

INTRODUCTION

The study of trace elements in coal has received considerable attention in recent years, coincident with increasing coal consumption. Much of the work has been in the form of washability studies designed to determine the organic versus inorganic affinity of various trace and minor elements. But Balkassoon and Kuellmer (1982) suggest that most trace element abundance in coal is dominated by depositional factors, and only under special circumstances of low ash coal do contributions by plants become significant.

As Finkelman et al. (1979) point out, the results of float-sink separations can be misleading. This primarily results from rafting of minute mineral grains by intimately associated organic material, shifting the mineral grain into a lighter specific gravity fraction than it would occupy if complete separation were achieved. The very small mineral grains once thought insignificant in terms of trace element contribution have been shown to account for nearly all of an element's abundance in a given sample (Finkelman and Stanton, 1978).

The majority of work done on trace elements in coal has dealt with coal from the midwest and eastern U.S. In studies of coal from the western U.S., very few have considered coal

from New Mexico, even though New Mexico is a significant producer in the region.

Studies which have examined lateral variations in trace element abundance within a coal seam, include Zubovic (1966b), and Kaplan, Carr, and Kelter (1983). But very few workers have attempted a detailed study of the vertical distribution of trace elements within a coal seam.

The purpose of this study was to determine the vertical distribution of selected trace elements within a relatively thick Upper Cretaceous coal bed from the San Juan Basin. The sampling scheme was designed so as to produce detailed and accurate vertical profiles of trace element abundances within the coal bed. The profiles were examined to determine what factors might affect the element distribution. A correlation analysis was performed on the analytical data to aid in grouping those elements behaving in a similar manner.


GEOLOGIC SETTING


The Fruitland Formation crops out and is actively mined for coal along the northwestern margin of the San Juan Basin. The San Juan Basin is a late Cretaceous to early Tertiary structural depression located at the eastern margin of the Colorado Plateau (figure 1). The basin is strongly

SAN JUAN
MINE

COLORADO

NEW MEXICO

FARMINGTON

SAN   JUAN

BASIN

20 MILES

ALBUQUERQUE

OUTCROP OF FRUITLAND
FORMATION – KIRTLAND SHALE

NEW MEXICO
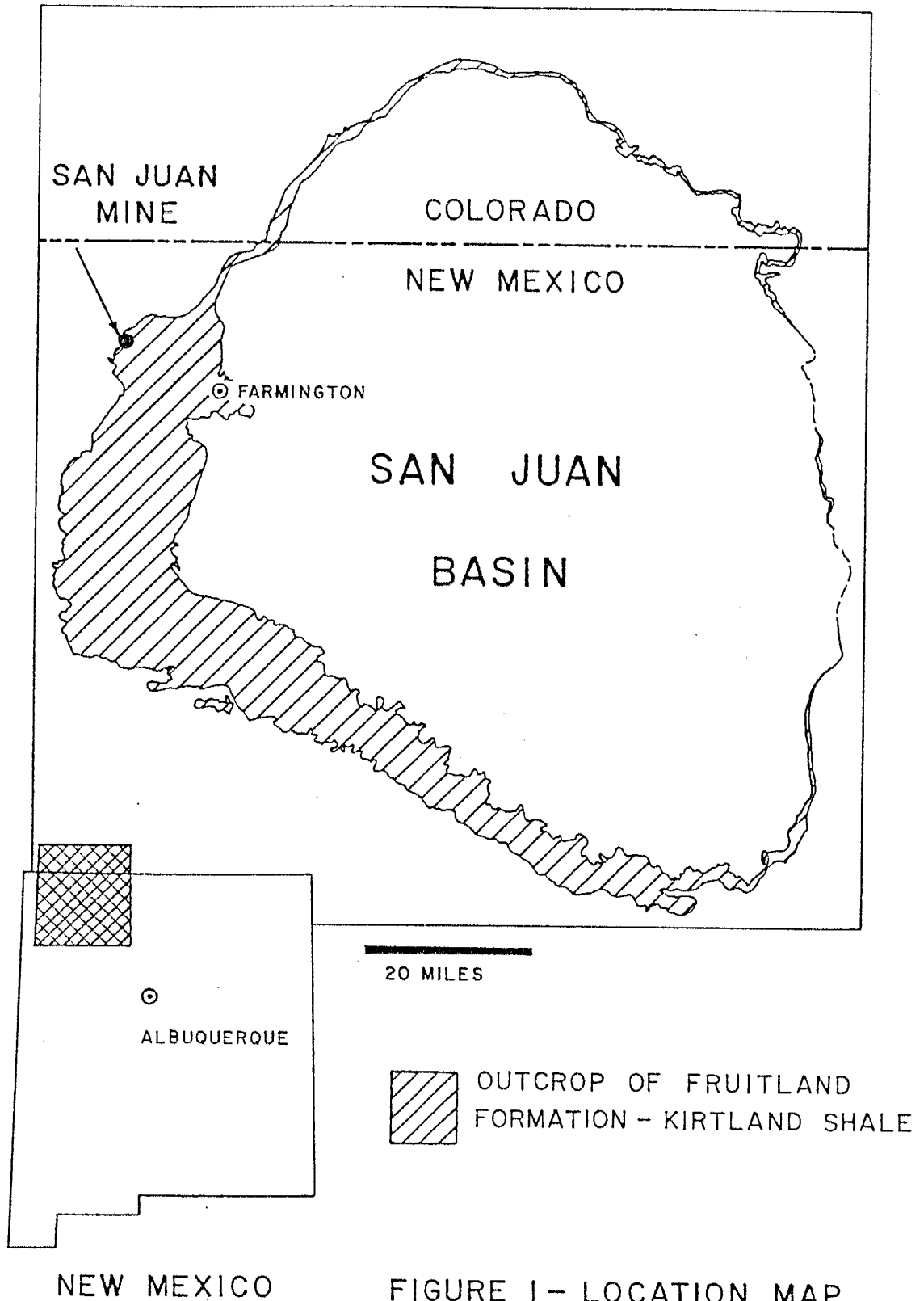
FIGURE I – LOCATION MAP

Shows the location of the San
Juan Mine within the San Juan
Basin (after Fassett & Hinds
1971)

asymetrical, with its axis trending northwest-southeast. The central portion of the basin is separated from the adjacent highlands by a number of monoclines.

The basin contains sedimentary rocks ranging in age from Cambrian to Quaternary, with a maximum known thickness in excess of 14,000 feet (Fassett and Hinds, 1971). Upper Cretaceous rocks are 6,000 feet or more in thickness, and were deposited in environments ranging from fluvial to shallow marine (Fassett and Hinds, 1971). Several major transgressive-regressive episodes are recorded in the intertonguing of marine shales with littoral sandstones and associated fluvial sequences. The youngest transgressive phase, which is of interest in this study, is represented by the Lewis Shale, a light gray to black marine shale. The Pictured Cliffs Sandstone overlying the Lewis Shale represents the transition from open marine sedimentation, to littoral sedimentation dominated by long shore currents (Fassett and Hinds, 1971).

Pictured Cliffs progradation proceeded at different rates over different portions of the basin resulting in stillstands, where relatively great thicknesses of Pictured Cliffs Sandstone were built up. The major thicknesses of Fruitland coal occur shoreward of these stratigraphic rises in the Pictured Cliffs Sandstone (Fassett and Hinds, 1971), see figure 2 for a diagrammatic cross section of this.

SOUTHWEST

Swamp

Sea level          NORTHEAST

(A) SHORELINE REGRESSION

SOUTHWEST

Swamp

Sea level          NORTHEAST

(B) SHORELINE STABILITY

SOUTHWEST

Sea level          NORTHEAST

(C) SHORELINE TRANSGRESSION

SOUTHWEST

Swamp

Sea level          NORTHEAST

(D) SHORELINE REGRESSION

| Marine shale | Marine sandstone | Continental deposits | Coal | Fluvial sandstone |
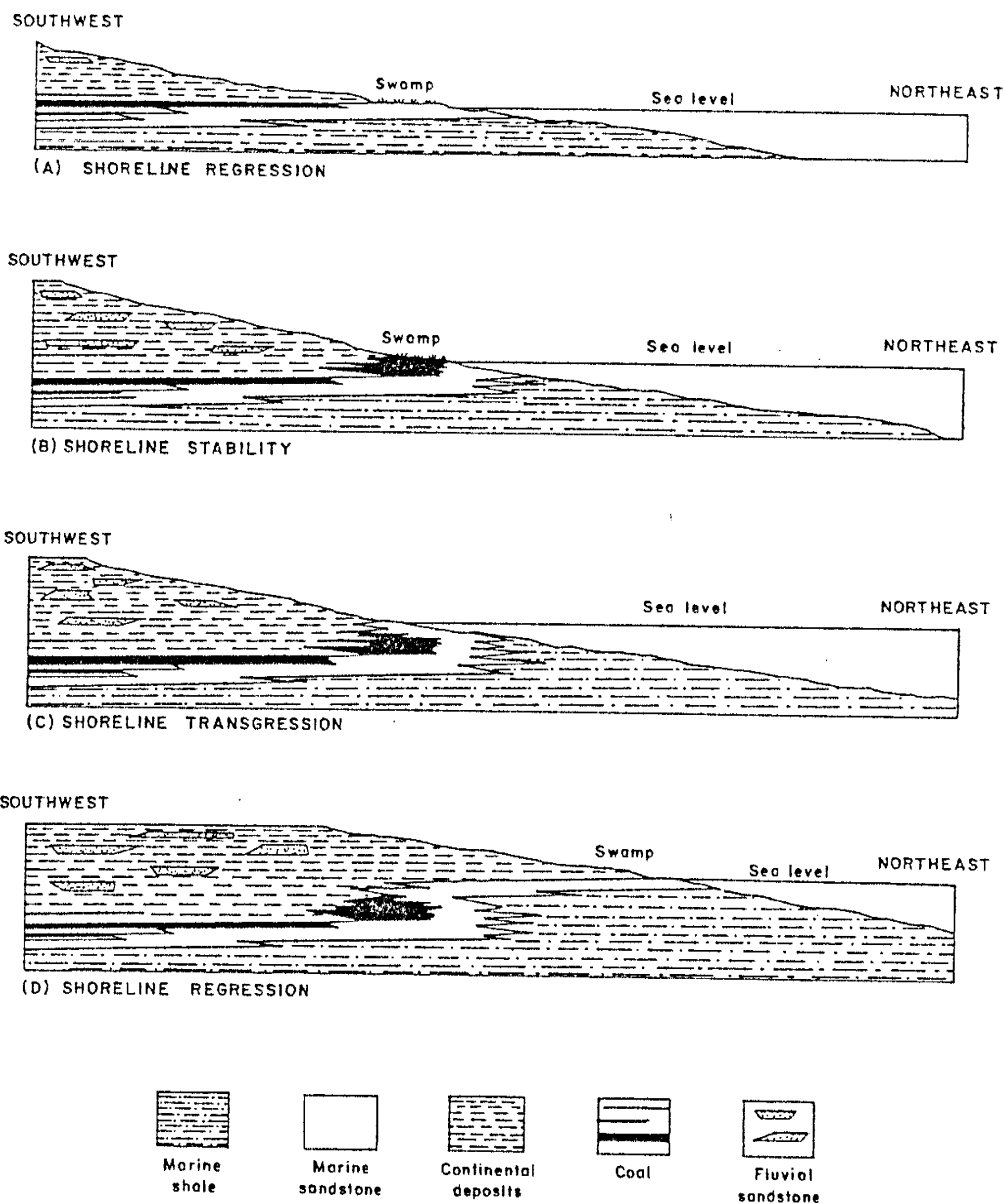
Figure 2                              (AFTER FASSETT & HINDS, 1971)
Diagramatic cross section illustrating the depositional
relationships between the Lewis Shale (Marine shale),
Pictured Cliffs Sandstone (Marine sandstone), and the
Fruitland Formation (Continental deposits, Coal, and
Fluvial sandstone). The stillstands occur during B
Shoreline stability, which gives rise to relatively
great thicknesses of coal shoreward of the beach facies.

The Fruitland Formation conformably overlies the Pictured Cliffs Sandstone. The Fruitland Formation represents a spectrum of environments from upper delta plain silts and shales to lower delta plain sands, silts, shales, coals, and even brackish water limestones. The major minable coal beds occur within the lower fifth of the Fruitland Formation (Fassett and Hinds, 1971). These are generally orientated parallel to the northwest-southeast paleo-strandline in their long dimension. They wedge out abruptly against the Pictured Cliffs sandstone bodies to the northeast, while to the southwest they grade gradually into floodplane deposits (Fassett and Hinds, 1971).

The contact between the Fruitland Formation and the overlying Kirtland Shale is arbitrarily drawn at the top of the upper most coal or carbonaceous shale bed (Fassett and Hinds, 1971). The Lower Shale Member of the Kirtland is dominantly a gray shale containing sparse interbeds of siltstone and sandstone. The Upper Member of the Kirtland Shale is dominated by sandstones interbedded with lesser amounts of silts and shales.

## LOCATION AND SAMPLING

### Location and Description of the San Juan Mine Area

The San Juan Mine, (figure 1), is an open pit strip mine operated by Utah International. The Mine is currently recovering coal from two seams within the lower Fruitland Formation. The upper, or number nine seam averages 4.5 feet thick and is separated from the lower, or number eight seam by 110 feet of sandstones, siltstones and shales. The number eight seam, which is of interest in this study, averages 13.8 feet in thickness over the lease area, and lies within ten to twenty feet of the top of the Pictured Cliffs Sandstone. The number eight seam dips approximately two degrees to the southeast.

Two drill cores penetrating the number eight seam were obtained for this study, and are designated Pinon Test No. 1, and Pinon Test No. 2. Figure 3 shows the location of these drill holes within the Fruitland Coal Field. The Drill holes are approximately 1500 feet apart. Pinon Test No. 2 is situated up dip from Pinon Test No. 1.

In general the core quality and recovery was good. But because the entire seam thickness could not be contained within the core tube used, two runs were required. Consequently a small amount of core was lost. The actual

R 15 W     R 14 W     R 13 W     R 12 W

T 32 N

T 31 N

T 30 N

T 29 N

PINON TEST No. 2

PINON TEST No. 1

SECTION 9

0     1000     2000

SCALE IN FEET

FRUITLAND COAL FIELD
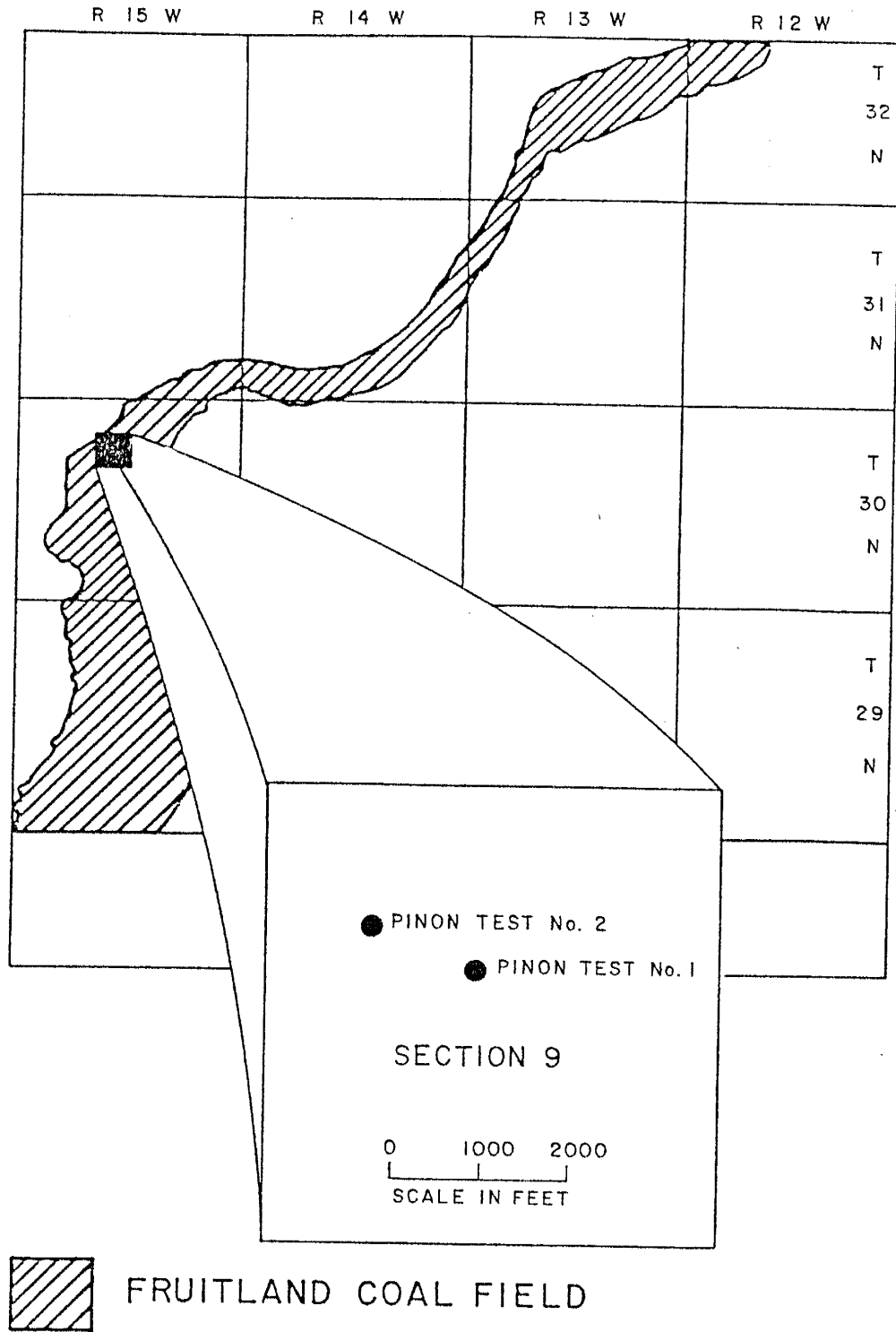
FIGURE 3 — LOCATION OF DRILL CORES WITHIN THE FRUITLAND COAL FIELD

amount of core lost could not be determined precisely, which may account for the disparity in seam thickness between the two holes. This difference could, however, easily represent a real variation in seam thickness.

## Description of the Number Eight Seam

Figure 4 is a correlation diagram for the two drill holes. This also gives the location of the observed partings, the bounding sediment lithologies, and coal lithotypes.

The lower boundary of the seam shows a sharp contact with the underlying carbonaceous claystone. Although a well developed root horizon was not observed, the coal is apparently autochthonous due to the lack of clastic characteristics.

As coring of Pinon Test No.1 started in the claystone overlying the coal seam, the total thickness of the overlying claystone at this location could not be determined. But more importantly for the interpretations of this study, it is not known if the sandstone observed in Pinon Test No. 2 lies directly on top of the cored interval or if some unknown thickness of claystone is present.

LITHOTYPE
AND
LITHOLOGY

CLARAIN

DURAIN

FUSAIN

PARTING

SANDSTONE

CLAYSTONE

CARBONACEOUS
CLAYSTONE

PINON TEST No. 2

PINON TEST No. 1

INTERVAL
NOT
RECOVERED

INTERVAL
NOT
RECOVERED

No. 8 COAL SEAM

No. 8 COAL SEAM
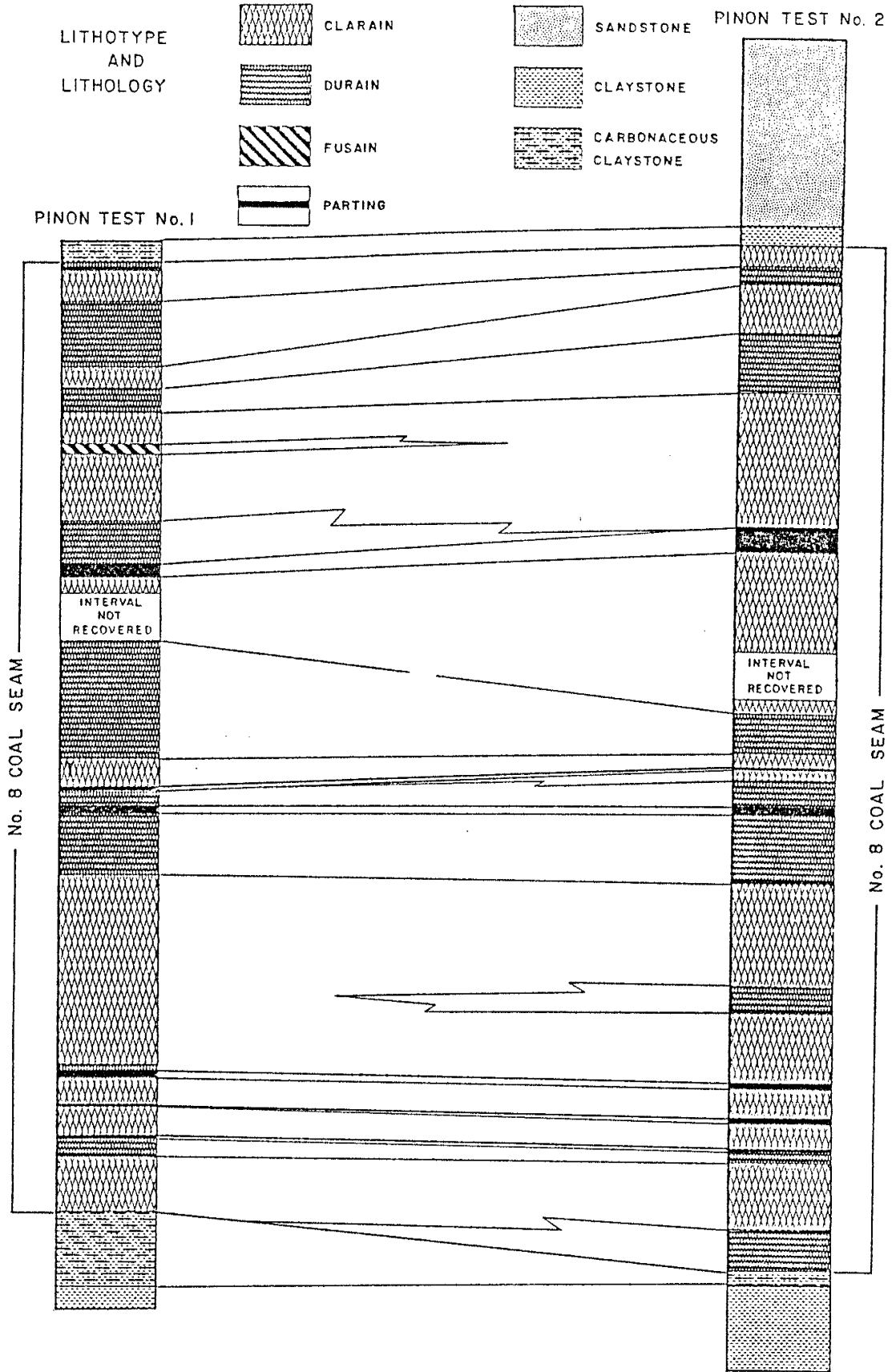
FIGURE 4    CORRELATION OF DRILL CORES

The dominant lithotypes alternate between clarain and durain. The coal is evenly banded, with band thickness varying from thin (0.5 - 2.0 mm) to medium (2.0 - 5.0 mm). Sparce thin bands of vitrain are common, though volumetrically unimportant. Sparce amounts of megascopically visible resinite occur throughout the coal thickness. These generally occur as irregularly shaped bodies extruded into cleat fractures, although ellipsoid shaped bodies were also observed.

A fusain zone occurs approximately three feet from the top of the seam in Pinon Test No. 1. As seen in figure 4 this zone is not continuous between the two drill holes. A cursory examination of several polished sections of this zone revealed the dominant maceral to be fusinite, with minor amounts of semifusinite, vitrinite, and resinite. The increased porosity, due to the abundance of fusinite, favored deposition of significant amounts of pyrite. This pyrite occurs both as cell lumen and microcleat fillings, indicating a secondary origin.

Six partings ranging in thickness from 0.4 ft. to less than 0.02 ft. split the seam. X-Ray diffraction (XRD) analysis of these partings showed kaolinite to be the dominant mineral, with other clays accounting for less than one part per ten of the total clay fraction. Other minerals identified were quartz, calcite, and pyrite. Examination of

the hand specimens indicates that the bulk of the calcite
and pyrite occur as authigenic phases. The dominance of
kaolinite (Raymond et al., 1985), the uniform thickness and
spatial distribution over the mine area, along with the
identification of remnant glass shards, identifies these
partings, or tonsteins, as volcanic ash falls (Mackowsky,
1982).

The similarity in major mineralogy, and the remarkable
similarity of the rare earth element (REE) distributions
between the partings and the claystone overlying the seam
indicate that the claystone is similar in origin. Further
this claystone shows a moderate abundance of mixed layer
clays and the presence of calcic feldspars (labradorite, or
anorthite, tentatively identified by XRD).

Cleat fractures are well developed, and range in
thickness from hairline fractures to separations as great as
0.1 inch, which occurs adjacent to parting No. 6, see
figures 5 and 6. These are commonly filled with calcite and
sparse amounts of pyrite, although some sulfate minerals,
(gypsum and jarosite) were noted in the upper portions of
both holes.

## Sampling Scheme

The sampling scheme was designed with the assumption that many of the elements would show maximum variations at seam boundaries or partings. Thus the sampling density is greatest at these features. A minimum sample size of 0.2 vertical feet of core (approximately 350 g.) was necessary to provide enough sample to run all the planned analyses.

The sample locations, shown in figures 5 and 6, were determined in the following manner. Samples were first located at the partings. Because some of the partings were less than the 0.2 foot minimum sample size, these samples also contain coal adjacent to the parting. If a parting was greater than 0.2 foot in thickness, such as parting No. 6, the entire parting was taken as one sample.

Samples were located immediately above and below each parting sample. Where the partings were closely spaced one intermediate sample served as the adjacent sample for two partings.

To sample the seam boundaries two samples were located in the coal and one in the bounding lithology. An additional sample was taken in the overlying sandstone which was recovered in Pinon Test No. 2.
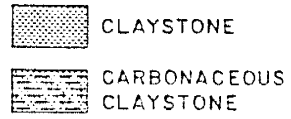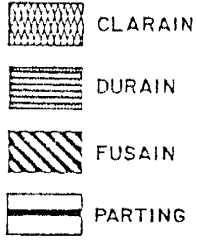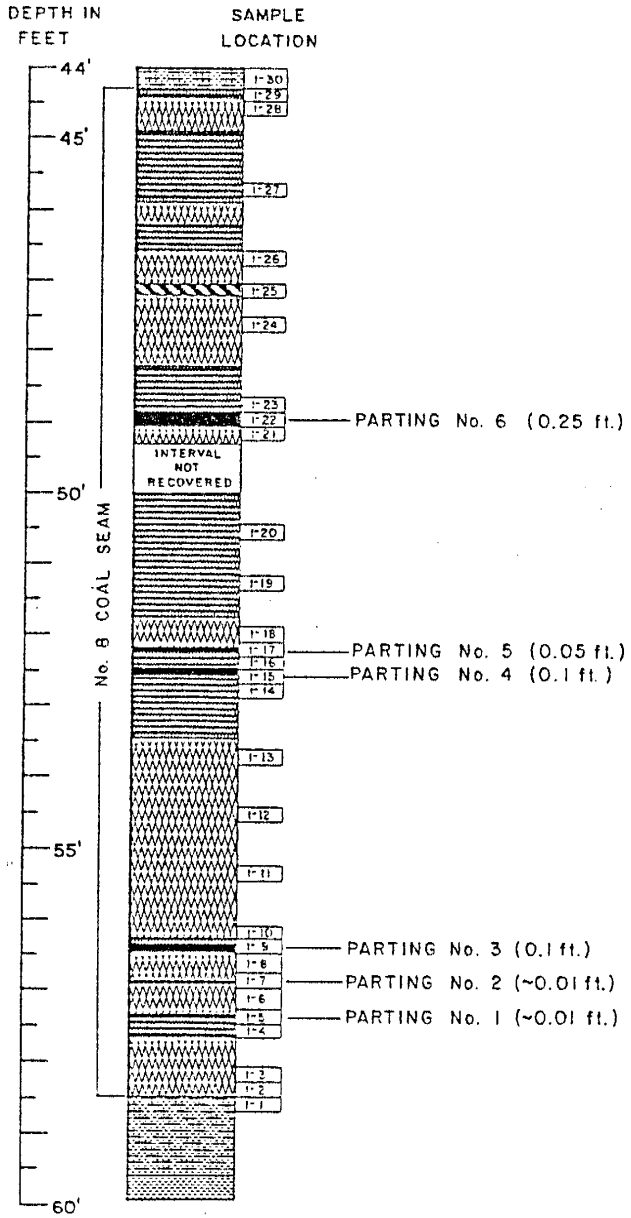
Figure 5 - Stratigraphic column of
Pinon Test No. 1.
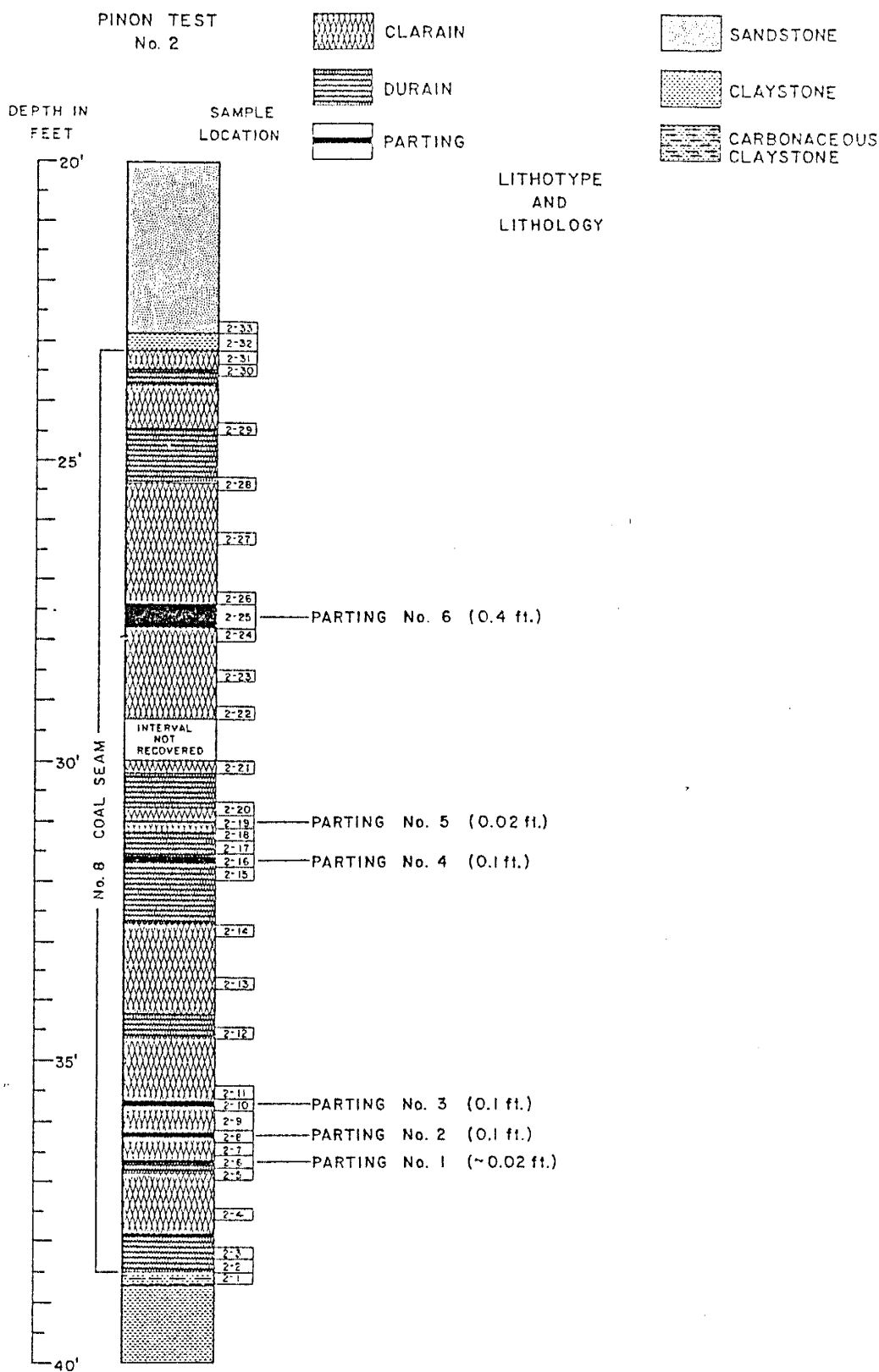
Figure 6 - Stratigraphic column of
Pinon Test No. 2.

The other sample points, representing coal distal to the partings, were located at points 1/4, 1/2, and 3/4 of the distance between the parting sample clusters. An additional sample was located in the fusinite zone of Pinon Test No. 1, because of its anomalous lithotype. This scheme samples about 41 % of the seam thickness in both holes.

## Sample Preparation

Figure 7 is a flow chart illustrating the processing necessary to produce the analysis sample stock. Throughout sample processing and analysis, contamination was a major concern. To minimize intersample contamination a ceramic mortar and pestle, which could be easily cleaned between each sample, was used for the initial crushing. A tungsten carbide rotary mill was used to pulverize the samples, thus limiting trace metal contamination to tungsten, and cobalt. This was cleaned between each sample with compressed air, and by wiping down the interior surfaces with acetone. Glass jars were used to store the analysis sample stock. These were washed, rinsed with dilute hydrochloric acid, followed by a final rinse with deionized water. Further details on sample preparation specific to a given analytical technique are discussed in Appendix IV.

# FIGURE 7—SAMPLE PROCESSING FLOW CHART

CORE WAS SAMPLED BY REMOVING 0.2 TO 0.4 FEET PER SAMPLE, APPROXIMATELY 320 TO 640 g.

INDIVIDUAL SAMPLES WERE REDUCED TO 1/2" x 1/4" IN A CERAMIC MORTAR AND PESTLE.

SAMPLES WERE SPLIT IN A RIFFLE SAMPLE SPLITTER.

1/2 OF EACH SAMPLE WAS SEALED IN A PLASTIC BAG, AND RESERVED AS A BACK-UP SAMPLE.

THE SECOND HALF WAS REDUCED TO APPROXIMATELY 60 MESH, IN A TUNGSTEN-CARBIDE ROTARY MILL.

THE 60 MESH SAMPLE WAS BLENDED, AND ABOUT 20g SPLIT OFF.

THE REMAINDER OF THE 60 MESH SAMPLE WAS STORED FOR PROXIMATE, A.A., AND S.I.E. ANALYSES.

THE 20g. SPLIT WAS REDUCED TO APPROXIMATELY 200 MESH WITH A MULLITE MORTAR AND PESTLE.

THE 200 MESH SAMPLE WAS OVEN DRIED AT 105°C AND STORED IN A DESICCATOR.

THE DRIED 200 MESH SAMPLE STOCK WAS USED FOR THE I.N.A.A. AND TOTAL SULFUR ANALYSIS.

ANALYTICAL METHODS

Table 1 lists the elements for which abundances were determined, by the analytical technique used.

TABLE 1

TRACE AND MINOR ELEMENTS BY ANALYTICAL TECHNIQUE

| | |
|---|---|
| Instrumental Neutron Activation Analysis | As, Ba, Br, Ca, Ce, Cr, Cs<br>Eu, Fe, Hf, La, Lu, Na, Nd<br>Rb, Sb, Sc, Se, Sm, Sr, Ta<br>Tb, Th, U, Yb |
| Atomic Absorption Spectrophotometry | Cu, Li, Mn, Ni, Pb, Zn |
| Specific Ion Electrode | F |
| Potentiometric Titration | S |

In addition to the elemental analyses, proximate analyses were performed for each sample yielding values for moisture, ash, volatile matter, fixed carbon, and heating value (BTU). Each of the analytical methods is discussed briefly in Appendix IV.

DATA REDUCTION


Ash Normalizing The Data


Many of the elements studied show strong relationships
with the partings and claystones, which are dominantly
allogenic mineral matter. The abundance of allogenic mineral
matter therefore influences the abundance of these elements.
To see if other factors, such as position within the seam,
are influencing the distribution of these elements we need
to look at the abundance expressed as a concentration per
unit allogenic mineral matter. For most of the samples in
this study the abundance of allogenic mineral matter is
approximated by the determined ash content. Therefore the
data were divided by (or normalized to) the determined ash
content, which gives a concentration per unit ash.


Correlation Analysis


Any analysis of a large amount of numerical data
generally requires some kind of statistical treatment. In
this study the information sought was a measure of the
concomitant variation between paired variables, or how the
variation in one variable is linked to the variation in the
second.

To accomplish this a Pearson Product-Moment Correlation Analysis was performed on the data set. The data set includes all values listed in Tables A and B in Appendix I. For those values listed as, upper limits only, in Tables A and B, that value was used in the computation of the correlation coefficient. Missing values were excluded from the calculations which determined the correlation coefficients.

Pearson correlation coefficients were calculated using a group of computer programs collectively known as the Statistical Package for the Social Sciences, (SPSS), (Nie et al., 1975).

The subroutine for Pearson Correlation Coefficients produces as output, the correlation coefficient r, the number of cases used to compute the r value, and a value P, which is the result of a two tailed significance test for each correlation coefficient, r.

The r, which is a measure of the association indicating the strength of the linear relationship between the two variables, can range from -1 to +1. A negative value for r indicates an inverse relationship between the two variables, while a positive r indicates a normal, or positive relationship. An r value of 0 indicates that no linear relationship exists between the variables, while an r of either +1 or -1 indicates a perfect linear correlation.

The tests of significance of the correlation
coefficient determine the probability that the observed
relationship exists from random variation. Thus a P value of
0 indicates a high level of confidence in the observed
relationship.


RESULTS


Data Presentation


Elemental abundances and the proximate results, are
located in Appendix I, in tables A, and B, for Pinon Test
No. 1 and Pinon Test No. 2 respectively. All values, except
moisture, are presented on a moisture free basis. The
moisture values are presented on an as received basis.
Determinations of the precision and accuracy for each
element are given in Appendix IV under the appropriate
analytical technique.


Summary of the Correlation Analysis


The proximate analysis parameters, moisture, ash,
volatile matter, fixed carbon, and heating value (BTU) were
included in the correlation analysis. In general those
parameters measuring the organic constituents (volatile

matter, fixed carbon, and BTU) correlate with each other to a very high degree, and show strong negative correlations with the ash content. Moisture shows no significant correlation with any of the other proximate parameters.

Only ash shows significant positive correlations with any of the analyzed elements. The correlation coefficients for the various elements on ash range from -0.31 for Br to 0.91 for Ce. An r of 0.65 was arbitrarily chosen as being a significant correlation. Eleven of the 33 elements determined were correlative with ash at this limit. This is nearly one third of the analyzed elements. Table 2 lists these elements and their associated correlation coefficients.

TABLE 2

Elements Showing A Significant Correlation With Ash

| ELEMENT | r value | ELEMENT | r value |
|---------|---------|---------|---------|
| Ce | 0.91 | Th | 0.80 |
| Nd | 0.89 | Rb | 0.79 |
| La | 0.89 | F | 0.79 |
| Sm | 0.86 | Hf | 0.73 |
| Eu | 0.83 | Na | 0.67 |
| Ta | 0.81 | | |

It should be noted that the list contains some, but not all of the rare earth elements (REE) determined. The significance of this will be discussed in a later section dealing specifically with the REE.

While a relatively large number of elements show significant positive correlations with ash, none of the elements show a significant positive correlation with volatile matter, fixed carbon, or heating value. Further those elements showing a significant negative correlation with these 'organic' parameters are the same elements showing a positive correlation with ash. Thus based only on the correlation analysis there appears to be no positive relationship between any of the analyzed elements and the organic parameters measured.

While the greatest number of elements showing significant correlation coefficients among themselves also correlate with ash, there are other groups of correlative elements which do not correlate with ash, or ash correlative elements at significant levels. These are: Fe, S, and As, with a mutual correlation of 0.78 or greater; Ca and Mn with a correlation of 0.68; and Cr and Cs with a correlation of 0.69.

The Rare Earth Elements


Because of their unique geochemical properties the rare earth elements (REE) will be treated as a group. The REE, also referred to as the lanthanide series, includes lanthanum (atomic number 57) to lutetium (atomic number 71). Abundances for eight of the REE, (La, Ce, Nd, Sm, Eu, Tb, Yb, and Lu) were determined in this study.

Figures A-1 through A-16 (in appendix II) show the distribution profiles for the REE in the two drill cores. The profiles show a strong association between tonstein occurrences and greater REE abundances. A secondary trend was observed in which samples situated adjacent to partings showed an increase in the concentration of the heavier REE (Tb, Yb, and Lu). Visually this results in a broadening of the abundance peak associated with the parting. For example, compare the shape of the La profiles (figures A-1 and A-2) with that of the Lu profiles (figures A-15 and A-16).

Another method of examining REE data is to construct chondrite normalized rare earth plots. These plots are generated by plotting the chondrite normalized sample abundance on the ordinate versus the atomic number on the abscissa. The resulting diagram shows variations in the REE abundances relative to an accepted standard, namely chondritic meteorites.

Figure 8 A-V) shows chondrite normalized plots for the data from both drill cores. Each pair of diagrams (A and B for example) show samples from similar stratigraphic positions in the two drill cores. The value in parentheses is the determined ash content rounded to the nearest whole percent.

As Fleet (1984) states the bulk of the REE transported in fluvial systems is contained in the detrital or allogenic fraction, with the dissolved fraction accounting for only a few percent of the total REE abundance. Therefore we can assume that the bulk of the REE entering the coal swamp were incorporated within allogenic mineral matter. If the REE remain in association with allogenic mineral matter during the diagenetic history of the coal bed, then the REE should show a high degree of correlation with the ash content.

In looking at figure 8 we see that over all this is true. Samples such as 2-29 (figure 8-H) which have a low ash content plot lower on the vertical axis than samples with a high ash content, such as 2-25 (figure 8-F).

Figure 8-F illustrates the relationship between samples in which a fractionation of the REE is apparent. This diagram shows the patterns for a parting and the two adjacent coal samples. The abundances of the HREE are very similar in both the parting and the adjacent coal. But the abundances of the LREE are much lower in the coal than the

parting. Visually this results in a flatter slope for the patterns of coal samples which are located adjacent to partings, when compared to the patterns for both partings, and coal samples distal to partings.

Where the partings are very thin compared to the sample thickness, a mixing of the parting and adjacent coal occurs. Figure 8, plots I and J, and S and T exhibit this mixing. The slopes of these parting sample patterns are intermediate between those which are strictly parting material and those which are strictly coal.

As stated earlier the REE should show a strong association with the ash content since this approximates the abundance of allogenic mineral matter in these samples. In this line of reasoning the abundance of organic matter can be thought of as a diluting factor. This can be compensated for by normalizing the data to the determined ash content prior to constructing the chondrite normalized REE plot. The effect of this on the plots in figure 8 would be to move the patterns up the ordinate a distance inversely proportional to the ash content.

Figures 9 and 10 show field diagrams plotted on an ash normalized basis for the samples from both drill cores. In each figure two fields are plotted. The stippled pattern shows the field enclosing the REE patterns for all of the coal samples situated adjacent to partings or claystones.

The cross-hatched pattern shows the field enclosing the remaining REE patterns. We can see from these diagrams that the coal samples situated adjacent to partings or claystones are significantly enriched in the HREE compared to the remaining samples, when expressed on a ash normalized basis.

In figure 9, sample 1-25 is plotted as a separate line because it lies a considerable distance from the cluster of data forming the field. This is a result of the large abundance of authigenic mineral matter (pyrite) contributing to the determined ash content of this sample. As can be seen by comparing the two figures, the variability of REE concentrations is greater in Pinon Test No. 1 than in Pinon Test No. 2.
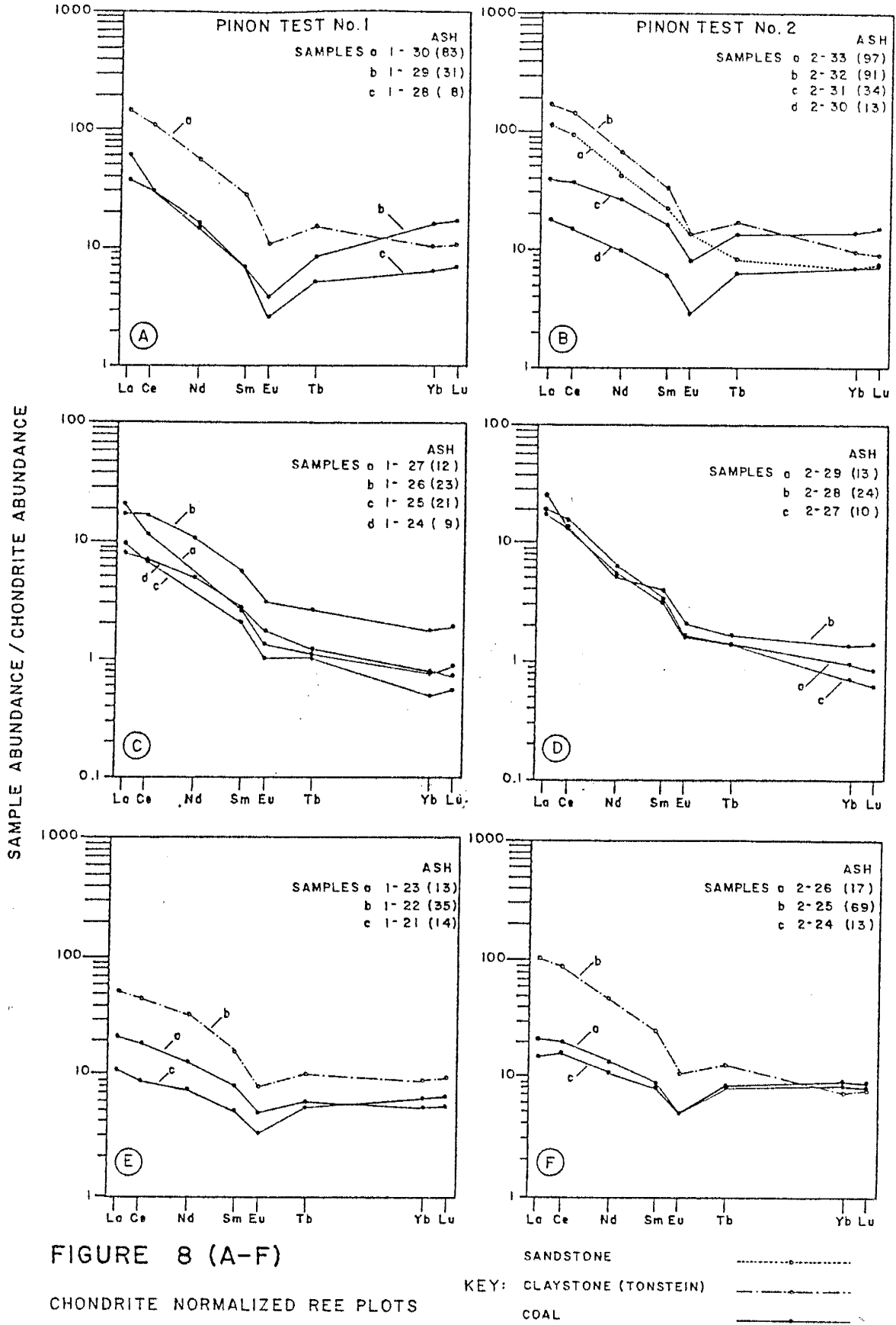
FIGURE 8 (A-F)

CHONDRITE NORMALIZED REE PLOTS
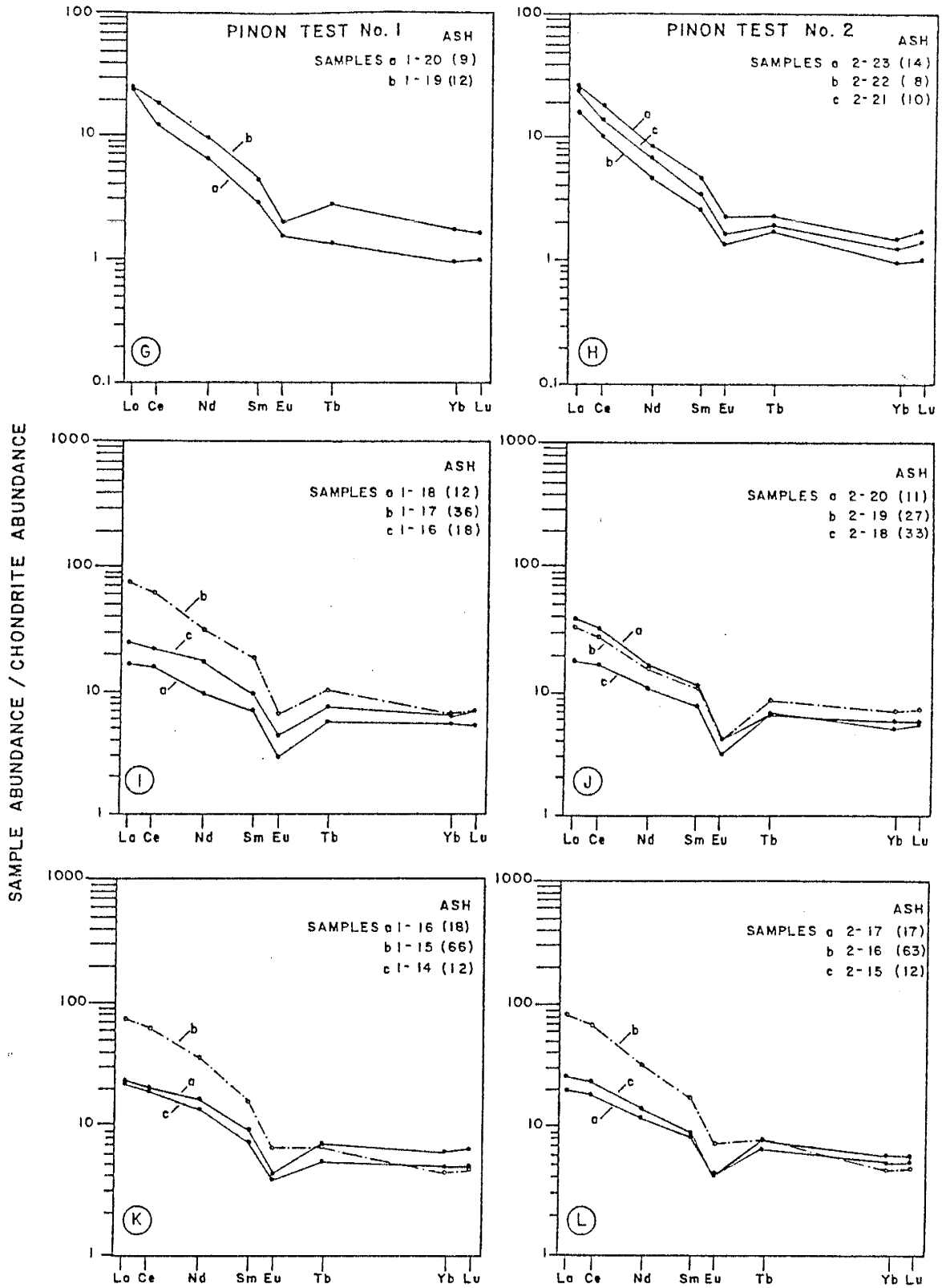
FIGURE 8 (G–L)

CHONDRITE NORMALIZED REE PLOTS

KEY:

CLAYSTONE (TONSTEIN) ————————
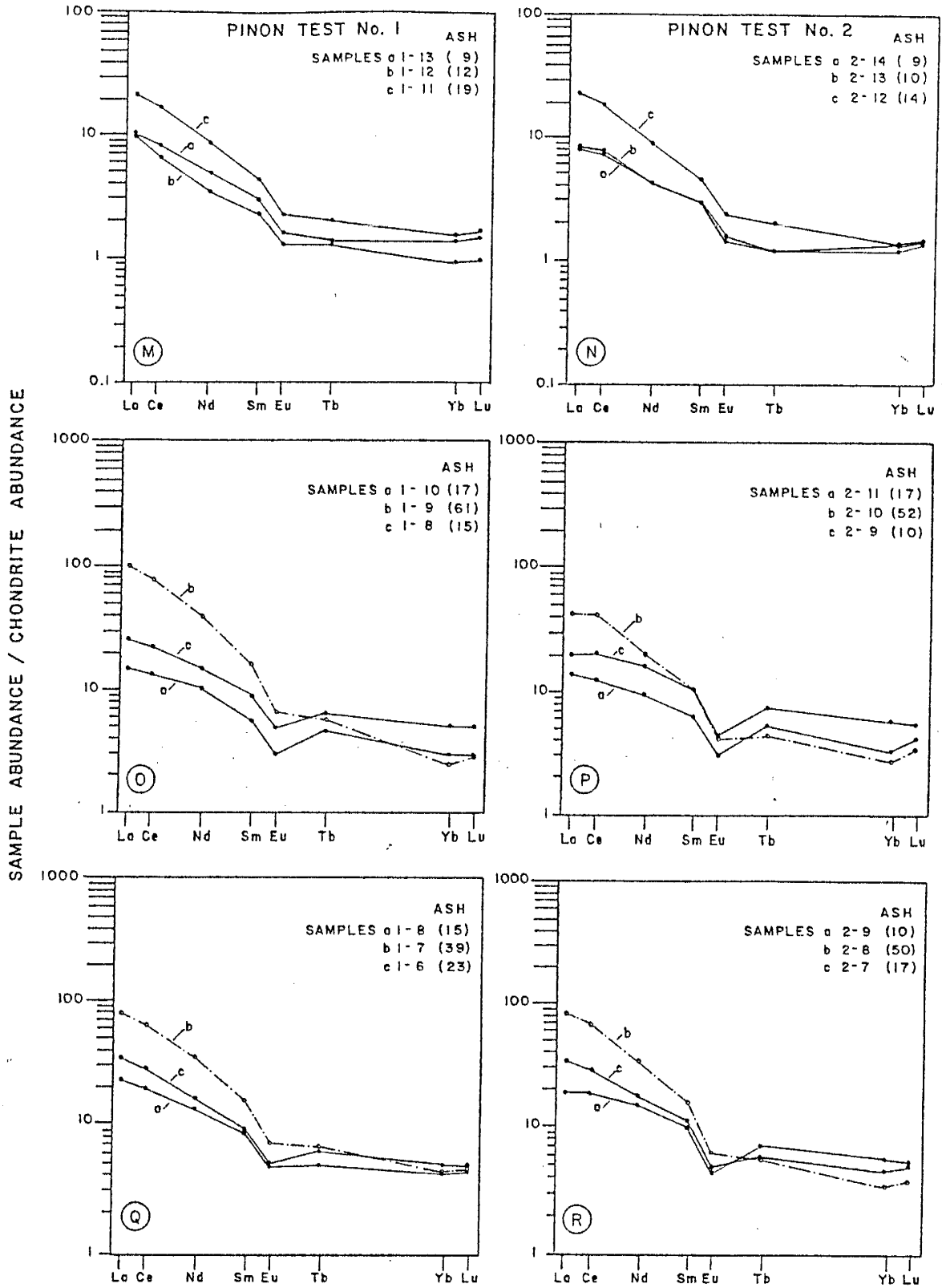
COAL ————————

FIGURE 8 (M-R)

CHONDRITE NORMALIZED REE PLOTS

KEY:

CLAYSTONE (TONSTEIN) —·—·—

COAL ———

PINON TEST No. 1

ASH

SAMPLES a 1-6 (23)
b 1-5 (42)
c 1-4 (18)

La Ce   Nd   Sm Eu   Tb   Yb Lu

Ⓢ

PINON TEST No. 2

ASH

SAMPLES a 2-7 (17)
b 2-6 (19)
c 2-5 (10)

La Ce   Nd   Sm Eu   Tb   Yb Lu

Ⓣ

ASH

SAMPLES a 1-3 (19)
b 1-2 (15)
c 1-1 (47)

La Ce   Nd   Sm Eu   Tb   Yb Lu

Ⓤ

ASH

SAMPLES a 2-4 (10)
b 2-3 (24)
c 2-2 (30)
d 2-1 (65)

La Ce   Nd   Sm Eu   Tb   Yb Lu

Ⓥ

SAMPLE ABUNDANCE / CHONDRITE ABUNDANCE
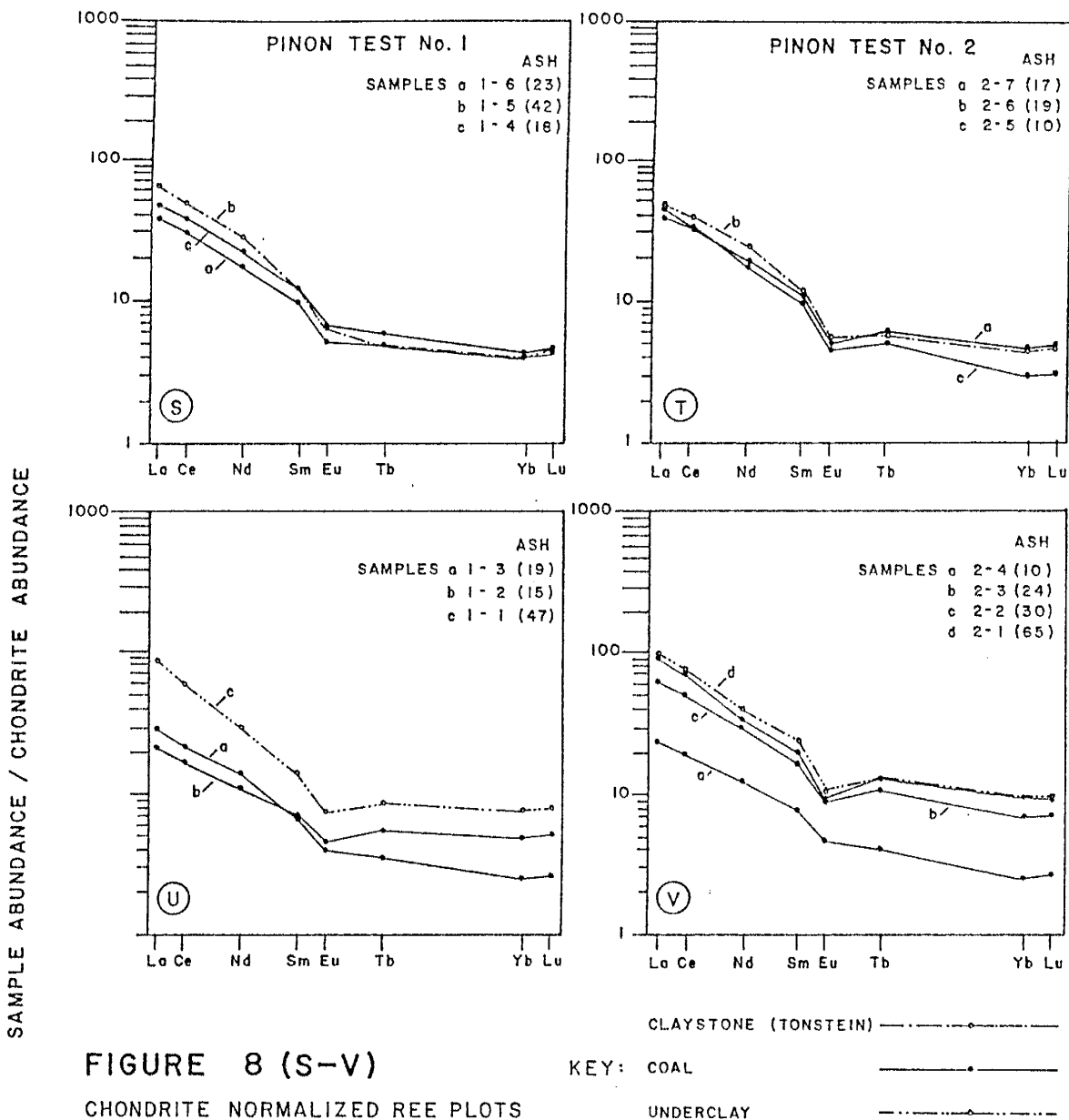
# FIGURE 8 (S-V)

CHONDRITE NORMALIZED REE PLOTS

KEY:

CLAYSTONE (TONSTEIN) —·——·—·——·—

COAL       ———·———·——

UNDERCLAY —··——··—o—·——··—

Chondrite normalized rare earth element plots for all of
the samples in this study. Each pair of diagrams (A & B
for example) show samples from similar stratigraphic
positions in the two drill cores. The value in parenth-
eses is the ash content rounded to the nearest whole
percent.
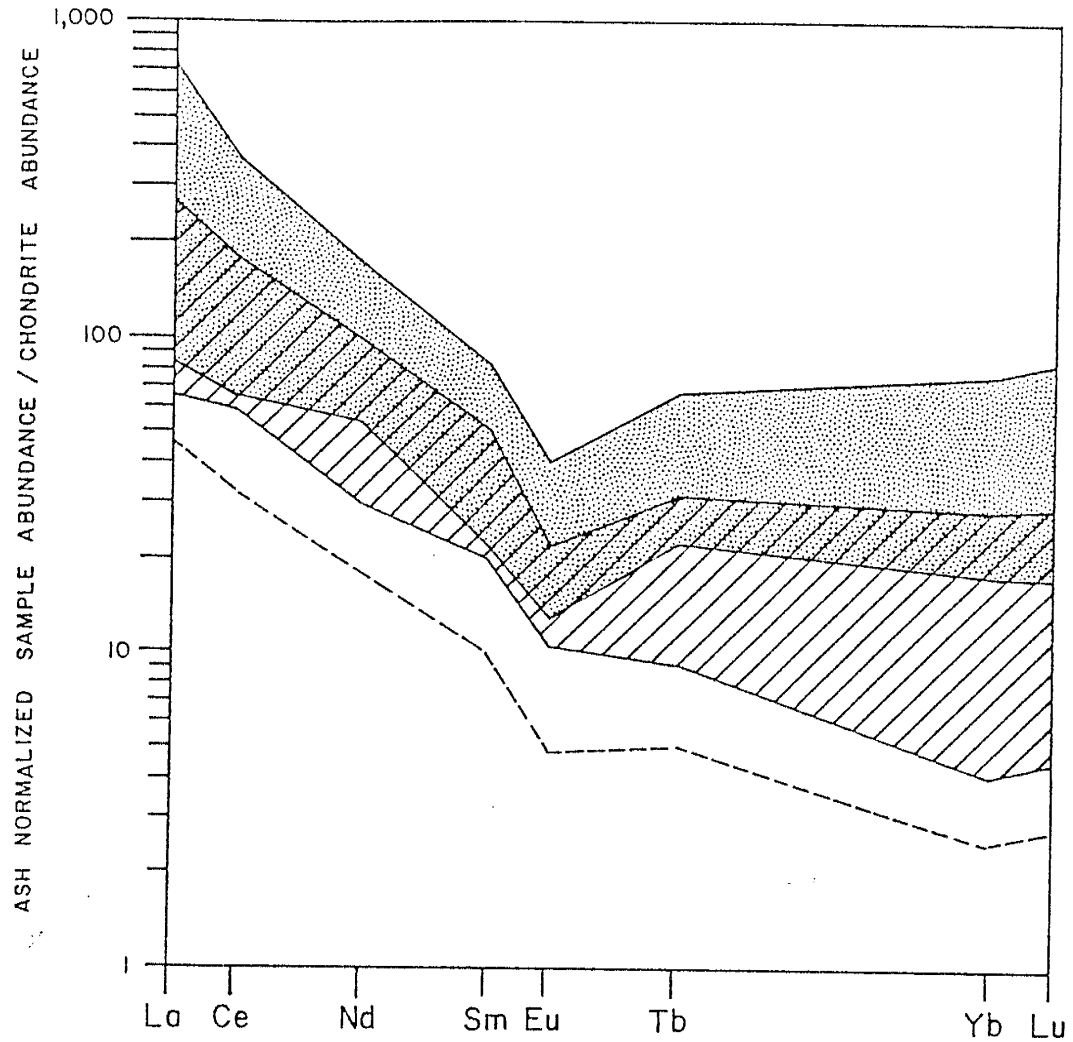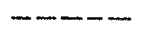
Figure 9 - Chondrite normalized rare earth element field diagram for ash normalized data, Pinon Test No. 1.

PINON TEST No. 2
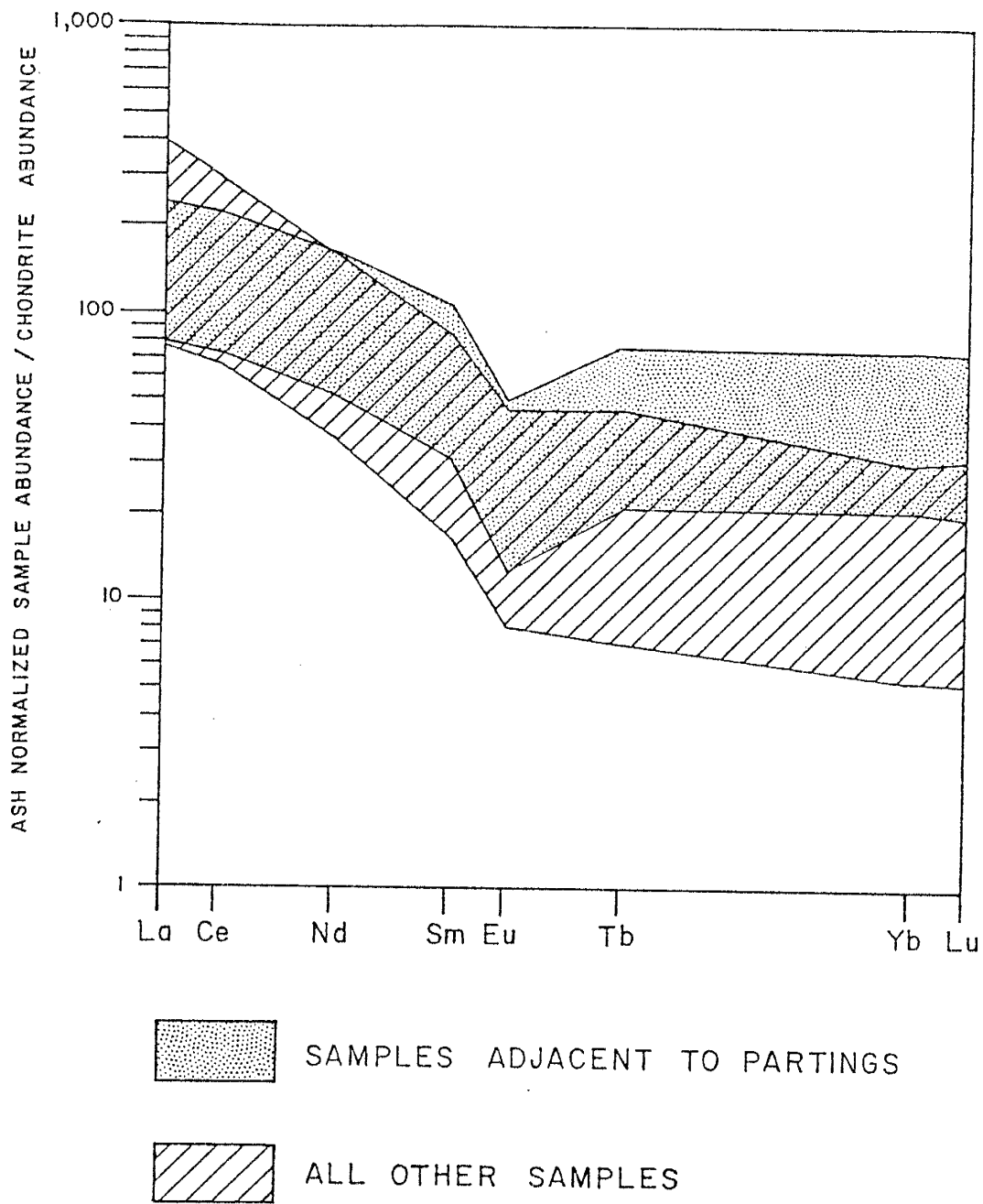


Figure 10 - Chondrite normalized rare earth element field diagram for ash normalized data, Pinon Test No. 2.

Other Trace and Minor Elements

The distribution profiles for the remainder of the
trace and minor elements are shown in figures A-17 through
A-70 in appendix III.

DISCUSSION

Distribution of the Rare Earth Elements

Previous studies of the rare earth elements (REE) show
conflicting results as to their organic versus inorganic
affinity. In the study by Gluskoter et al. (1977) the light
rare earth elements (LREE) generally showed inorganic
affinities, while the heavy rare earth elements (HREE)
showed both organic and inorganic affinities. In the data of
Kuhn et al. (1978), the REE showed clear organic affinities.
In a study of 13 coals from Bulgaria, Eskenazy (1978) found
a relative increase of the HREE in low-ash coals, an
increase in the absolute REE concentration with increasing
ash content, and a REE pattern that approached that for
shales in high-ash coals. This is very similar to what was
observed in this study.

Finkelman (1980), found the REE patterns of ashed coal
samples from the Appalachian Basin to be nearly identical to
a composite of 40 North American shales (NASC), as given by

Haskin and Paster (1979). Tsui et al. (1979) found that the REE patterns for coal ash from the Illinois Basin are nearly identical to the NASC.

Fleet (1984) has suggested that the bulk of rare earth elements in most sedimentary environments are held within the clay fraction and/or accessory minerals such as zircon and apatite. But Finkelman (1980) describes the bulk of the REE in the Waynesburg samples, as occurring in phosphate minerals, principally monazite and xenotime, which he interpretates as authigenic. The presence of authigenic REE minerals requires either a sufficient supply of dissolved REE entering the peat swamp, which seems unlikely, or mobilization of REE from existing allogenic minerals. Finkelman (1980) indicates that the latter might have been accomplished by organic complexes.

Many authors feel that the REE can be fractionated during chemical weathering of rock materials, but that no further fractionation takes place during the transport of these weathering products in fluvial systems (Fleet, 1984; Balashov, 1967; and others). Nesbitt (1979) showed how a REE pattern very similar to the NASC could be produced by weathering a granodiorite in a humid climate in the presence of organic matter.

Balashov (1964) stated that the stability of rare earth organic complexes increases with increasing atomic number. Whereas Nesbitt (1979) stated that the clay minerals kaolinite and illite accomodate the LREE better than the HREE. Another way of looking at this relationship between the LREE and the HREE in this study is to plot the REE by atomic number on the abscissa versus their correlation coefficient with the determed ash content on the ordinate. Figure 11 is such a plot. In this figure we see that the LREE all show about the same degree of correlation with the ash content, which follows the predicted behavior of the REE in general. The HREE, on the other hand, show much lower correlations with the ash content.

In searching for an explanation for the observed behavior of the REE in this study we note that the ionic potential (charge/ionic radius) of the REE increases with increasing atomic number. And further that this series of elements crosses the boundary (at $Z/r = 3$) between the soluble cation field and the hydrolysate element field (Siegel, 1974). When this boundary is plotted on figure 11 we see that it coincides with the observed change in behavior of the REE.
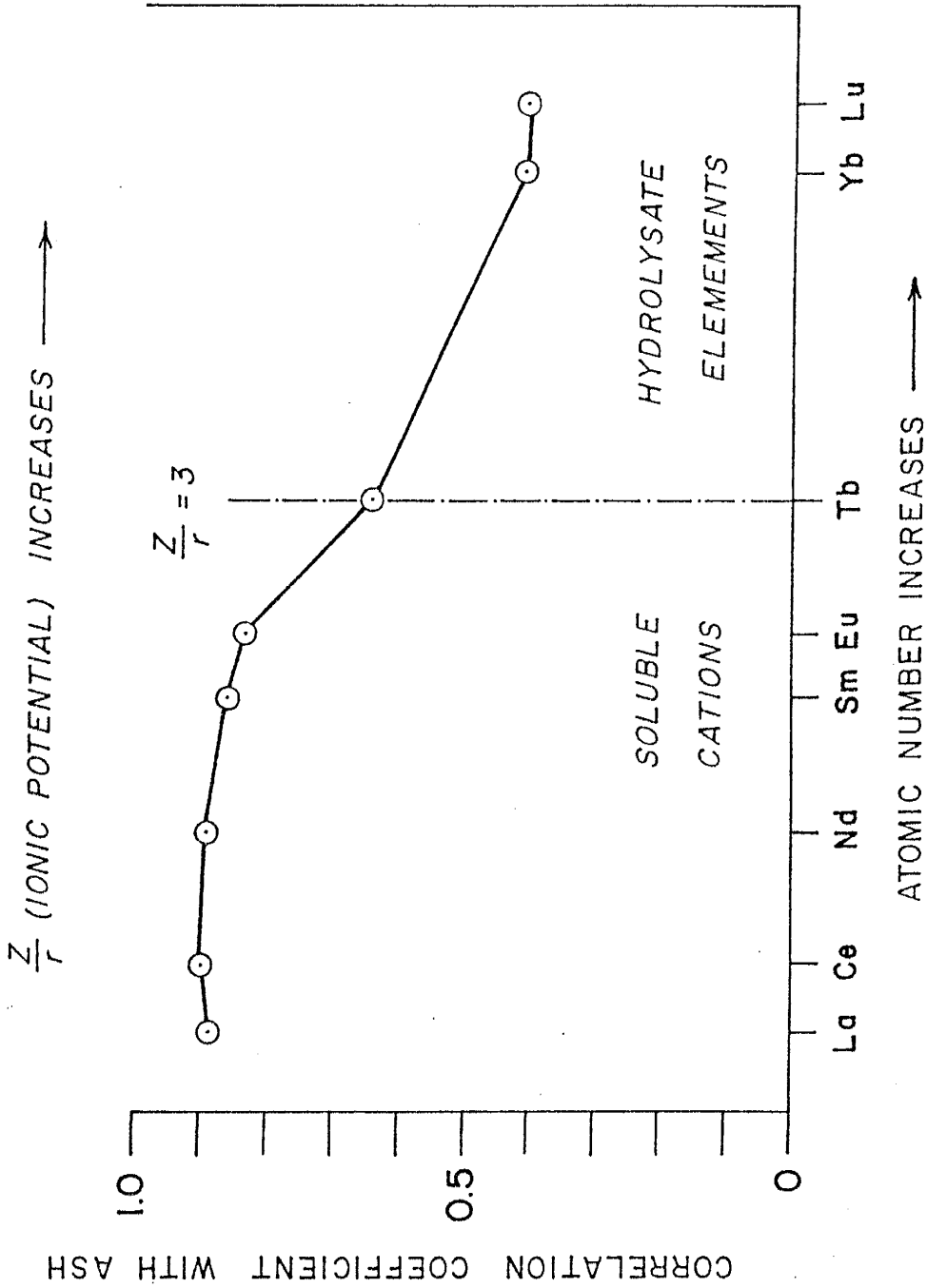
Figure 11 – Correlation of the rare earth elements with the determined ash content. Ionic radii from Siegel, 1974 (table 3-9), field boundaries from Siegel, 1974 (figure 4-9).

Model Explaining the Distribution of the REE

With all of this information in hand we can now propose a model to explain the distribution of the REE in this study. The partings, which represent volcanic ash falls, were extensively weathered in the highly acidic peat environment. The REE were liberated during the breakdown of their parent minerals. The LREE were preferentially accomodated in the clay minerals, which were forming as weathering products. The HREE were preferentially hydrolyzed or bound within organic complexes and allowed to migrate away from the parting. These mobilized REE could subsequently form authigenic REE phosphates (monazite and xenotime), such as observed by Finkelman (1980).

Distribution of the Other Trace and Minor Elements

Antimony: (refer to figures A-17 and A-18)

In various float-sink studies antimony has displayed both inorganic and organic affinities, Gluskoter et al. (1977), but as Finkelman (1980) points out this may be due to the rafting effect of minute stibnite grains dispersed in an organic matrix.

The distribution patterns for this study show a consistent, significant increase in the antimony concentration within the upper one half foot of the seam. This type of pattern, similar to nickel, indicates secondary enrichment. A careful examination of the profiles shows small increases of antimony content adjacent to some partings. For example see figure A-17, sample 1-21 and the region containing samples 1-4 through 1-10. A similar trend is observed in Pinon Test No. 2, although in this core there appears to be a preferential enrichment above partings, see figure A-18 samples 2-20 and 2-11.

Arsenic: (refer to figures A-19 and A-20)

Because of the relatively high correlation coefficient between arsenic, iron, and sulfur, an association of arsenic with the mineral pyrite seems likely, as this is a common mode of occurrence. During a detailed study of the mode of occurrence of pyrite in the Upper Freeport coal, (Appalachian Region), Minkin et al. (1980) found the arsenic to be totaly associated with pyrite. Most of the arsenic was in solid solution with pyrite, and apparently of epigenetic origin. Their evidence for this was location of the arsenic in distinct rims around the outside of the pyrite grains, and by its occurrence in limited stratigraphic intervals.

The distribution of arsenic in the samples of this study shows a pattern similar to that described by Minkin et al. (1980) in that the major occurrences of arsenic are limited to a discreet stratigraphic interval, which also shows an above average abundance of pyrite.

This zone of increased pyrite abundance coincides with the location of a fusinite zone in Pinon Test No. 1, see figure 29, sample 1-25. Because of the predominance of fusinite, the zone shows a marked increase in porosity, which has only partially been filled by secondary minerals. Although this fusinite zone could not be found in the core from Pinon Test No. 2, the arsenic anomaly is located in a similar stratigraphic horizon. Therefore it appears that the major abundances of arsenic present in these samples occur in association with pyrite, but their stratigraphic location is controlled by relative permeability.

Barium: (refer to figures A-21 and A-22)

The distribution profiles of barium show a general increase in both the average concentration and variability towards the top of the seam. Both holes show a significant increase in Ba concentration at approximately the same stratigraphic position, which corresponds to an increase in the occurrence of sulfate in the megascopic description of the cores.

The anomalous concentration of 31,600 ppm for sample number 1-29, figure A-21, is almost certainly in error. It probably resulted from a combination of incomplete sample blending and a non-representative sample aliquot.

The distribution pattern exhibited by barium conforms to the general trend for the occurrence of sulfate minerals in San Juan Basin coals. Sulfate minerals commonly occur in the upper portions of coal seams as oxidation products of sulfide minerals, principally pyrite, with contributions by sulfate rich ground waters. This strongly indicates the occurrence of barium as the sulfate, barite.

Bromine: (refer to figures A-23 and A-24)

The distribution profiles for bromine differ dramatically between the two drill holes. One feature common to both is a relative depletion at partings and seam boundaries. Finkelman (1980), Gluskoter et al. (1977) and Kuhn et al. (1980) all list bromine as strongly organic in its aff nities. While the depletion at partings tends to concur with this mode of occurrence, the large disparity in average bromine concentration for two sample sets spaced so closely invalidates most conclusions which could be drawn from the vertical profiles.

Calcium: (refer to figures A-25 and A-26)

The most characteristic feature of the distribution profiles for calcium is a significant increase in the abundance immediately above major partings. Other concentration maxima occur spaced in between partings. The locations of these features agree with the maximum abundances of calcite occurring as cleat filling material, which were observed in the megascopic description of the drill cores.

In light of the fact that there were no other major contributors of calcium identified in the hand specimen it can be concluded that the distribution of calcium, in general, represents the distribution of calcite. This does not infer that all of the calcium is present as calcite, but rather the major features of the calcium distribution are attributable to the distribution of calcite.

Cesium: (refer to figures A-27 and A-28)

The profiles for cesium clearly show a strong association with clay rich zones. The mean value for all samples is 0.67 ppm, while the mean for the data excluding the partings and bounding claystones is 0.28 ppm. This shows an enrichment in the clay rich samples. This is in general agreement with the data of Gluskoter et al. (1977), Finkelman (1980), and others.

Chromium: (refer to figures A-29 and A-30)

The chromium profiles generated for this study show generally elevated concentrations in the bounding claystones and sandstone, and in the coal sections in between partings. These zones of elevated concentration are located in stratigraphically similar horizons in both drill holes. Further there is no apparent relationship between the chromium content and ash content. Evidence of this is the low correlation coefficient (0.34) between chromium and ash. Both holes show a relative increase in chromium content at the No. 6 parting, samples 1-22 in figure A-29 and sample 2-25 in figure A-30, but partings lower in the seam show inconsistent trends between the two holes.

This type of distribution pattern is consistent with Szilagyi's (1971) suggestion of an epigenetic origin for the chromium in Hungarian coals. Other authors, such as Finkelman (1980) and Nichols (1968) demonstrate an association between chromium and clay minerals in their float-sink data.

The distribution of chromium within the No. 8 seam is interpreted as epigenetic in origin due to its apparent stratigraphically controled occurrence. The chromium could be associated with clay minerals rather than the organic matter, with its location controled by differences in relative porosity. This would explain the low correlation

coefficient between chromium and ash. To confirm this a detailed study analyzing the mode of occurrence of chromium and the textural relationships involved would be necessary, which is clearly beyond the scope of this study.

Copper: (refer to figures A-31 and A-32)

The copper profiles generated from the data of this study are similar in nature to the profiles generated for chromium, but there is no significant correlation between Cu and Cr. The major peaks in copper concentration are consistent in their stratigraphic location between holes, however, these peaks do not coincide with chromium peaks. The nature of the distribution patterns would favor an epigenetic origin, but there is no decisive evidence for this.

Fluorine: (refer to figures A-33 and A-34)

Except for the anomalously high concentration peak at sample number 1-24, figure A-33, the fluorine concentration closely follows the occurrences of partings and claystones. This pattern would suggest an association of fluorine with clay minerals or a fluorine bearing mineral which was either a component of the volcanic ash, or a weathering product of it. In either case the present occurrence appears to have remained stable within the partings, as no evidence of

redistribution is seen in the profiles. No explanation can be offered for the anomalous concentration in sample 1-24.

Hafnium: (refer to figures A-35 and A-36)

The patterns for hafnium show a strong association with both the partings and bounding claystones. This association is corroborated by the relatively high correlation coefficient (r = 0.73) between Hf and ash.

Hafnium shows a very strong geochemical association with zirconium in most continential rocks, showing average Zr/Hf ratios of about 40 (Erlank et al., 1978). It therefore seems likely that the bulk of the hafnium observed in these samples originates from allogenic zircon, with minor contributions from other zirconium-hafnium bearing minerals.

The data of this study show an apparent mobilization of hafnium from the source material (the parting constituents) to the surrounding organic rich phase. The evidence for this is the broadening of the hafnium abundance peaks associated with the partings (figures A-35 and A-36). Another method of examining this relationship is to plot the hafnium profiles on an ash normalized basis (figures A-37 and A-38). It is clear from these figures that the abundance of Hf, per unit ash, is greater both above and below the partings than within them. This type of distribution profile strongly indicates mobilization.

The idea of zircon being susceptible to chemical weathering is not new. In a discussion of the merits of using Zr/Hf ratios of sediments as indicators of the ratio in parent rocks Erlank et al. (1978) caution that hafnium rich zircon seem to be more rapidly broken down as a result of either lattice defects due to the presence of hafnium, or metamic alteration due to the radioactive decay of uranium accompanying the hafnium. And Ronov et al. (1961) calls upon the hydrolysis of zirconium and hafnium (in zircon) to help explain a systematic change in the Zr/Hf ratio from oxidizing acidic environments to reducing acidic environments. Thus it seems that zircon may be subjected to hydrolysis in highly acidic and very reducing environments, such as peat swamps.

Iron: (refer to figures A-39 and A-40)

The most common association of iron in coal is with the mineral pyrite. The samples from this study appear to follow this trend. This is evident by the relatively high correlation coefficient of iron and sulfur. This certainly does not mean that all of the iron is tied up in the mineral pyrite. For example the distribution profiles show an abundance of iron in the claystones bounding the seam. This is due to jarosite, an iron sulfate, which was observed in the upper portions of Pinon Test No. 2. What the correlation coefficient does indicate is a reasonably consistent ratio

between the total iron in the sample with the pyritic iron, and similarly for the total sulfur with the pyritic sulfur.

Lead: (refer to figures A-41 and A-42)

The very large value of 232 ppm for sample 1-30 is probably the result of contamination, although the source of this contamination is unknown. Excluding this feature the patterns are very similar for both holes. The major features are two maxima, one occurring in samples 1-16 and 2-17 and another in samples 1-19 and 2-21. This type of stratigraphically dependent profile is also exhibited by other chalcophile elements such as copper, chromium, and arsenic. No clear relationship can be established between any of these elements based either on correlation coefficients or location of their relative maxima. It does seem likely that similar mechanisms are operating on these elements to produce distribution patterns similar in type.

Several authors have described the occurrence of lead as a sulfide, or associated with sulfide minerals (Brown and Swain, 1964), and (Finkelman, 1980). Finkelman also describes the occurrence of clausthalite (PbSe), and the substitution of lead for barium in barite, especially in sulfide poor coals. Although the mode of occurrence of lead in samples from this study can not be interpreted from the data collected, the major features of the profiles do not

suggest an association of lead with sulfate minerals or sulfides such as pyrite.

Lithium: (refer to figures A-43 and A-44)

The profiles for lithium show a relatively high degree of association with the partings, but the correlation coefficient between lithium and ash is only (0.33). This probably results from the anomalous concentration just above parting number three in both holes, samples 1-10 and 2-12. The occurrence of this anomalous lithium concentration in a low ash coal sample contradicts the general trend in which lithium is associated with allogenic mineral matter. Further it contradicts the association of lithium with clay minerals in coals as observed by Finkelman (1980) and Gluskoter et al. (1977).

Manganese: (refer to figures A-45 and A-46)

The distribution patterns for manganese are very similar to those for calcium. For example both elements show relative maxima immediately above parting No. 6 in both drill cores. As stated earlier the manganese is probably occurring as a manganese carbonate in association with the calcite, or it is substituting into the calcite lattice.

Nickel: (refer to figures A-47 and A-48)

Several authors have shown nickel to have strong organic affinities, Zubovic (1966A), Gluskoter et al. (1977), and Kuhn et al. (1978). Zubovic (1966A) proposed nickel to be bounded as chelated complexes when it shows organic affinities, while Filby et al. (1977) proposes a porphyrin association. Other authors have shown an inorganic association for nickel, such as Finkelman (1980), who describes an association of nickel with the sulfides galena, sphalerite, pyrite, and clausthalite.

The distribution patterns exhibited by nickel in this study clearly show progressive enrichment towards the seam boundaries. In addition the patterns show a relative depletion at the partings and claystones. These features indicate both a secondary origin, and an organic association for the nickel.

Rubidium: (refer to figures A-49 and A-50)

The profiles for rubidium show a strong association with the partings and bounding claystones, especially in Pinon Test No. 2. Rubidium also exhibits a strong correlation coefficient with ash, (r = 0.79).

Geochemically rubidium follows potassium in its distribution, and therefore should occur in kaolinite, K-feldspars and micas. This would explain its abundance in the feldspatholithic sandstone, and its association with the clay-rich samples.

Scandium: (refer to figures A-51 and A-52)

The profiles for scandium show a strong association for the partings and bounding claystones. But the correlation coefficient between scandium and ash is only 0.49. In looking at figures A-51 and A-52 we see that the scandium profiles exhibit mobilization of scandium from the partings into the adjacent coal.

This would concur with Finkelman's (1980) observation that the organic association of scandium increases with increasing rank. It seems likely, therefore that the process responsible for the mobilization of scandium is occurring throughout the history of the seam. And given more time and/or temperature, a greater redistribution will result.

Selenium: (refer to figures A-53 and A-54)

The profiles for selenium are very similar in nature to those for chromium and copper, in that the patterns for both holes show relative maxima at similar stratigraphic positions. Thus the distribution of selenium appears to be

related to that of several other chalcophile elements. But again no significant correlation exists between selenium and any of the other chalcophile elements.

Sodium: (refer to figures A-55 and A-56)

The distribution patterns for sodium show elevated abundances at partings, and significantly elevated abundances in the claystones and sandstones overlying the seam. The relatively high sodium content of the overlying claystone is attributed to sodium bearing clays, tentatively identified by (XRD). The marked sodium increase observed in the sandstone is explained by the presence sodium bearing feldspars, and lithic fragments. The apparent lack of sodium in the partings can be accounted for by the effects of severe leaching in the peat environment.

Strontium: (refer to figures A-57 and A-58)

In both drill cores the strontium values show relative maxima at some, but not all partings. Relative maxima or peaks also occur at positions unrelated to parting location, most notably just below parting number four in Pinon Test No. 1, sample 1-13 in figure A-57.

Both holes show a slight but noticeable increase in the average background values towards the top of the seam. In addition to this both holes show a very large increase in

the strontium concentration near the top of the sampled interval. This maximum concentration does not occur in similar stratigraphic positions in both holes though. In Pinon Test No. 1 it occurs in the uppermost coal sample, (1-29), whereas in Pinon Test No. 2 it occurs in the claystone and sandstone samples (2-32 and 2-33), overlying the coal seam.

It seems plausible that the mode of occurrence of strontium in these dissimilar lithologies is also different. The strontium values for the claystones overlying the seam are nearly identical for both holes, as are the values for the underclay samples.

The profiles suggest multiple modes of occurrence for strontium within the sampled interval. The strontium in the claystones probably occurs as species adsorbed on clays, with minor contributions from the carbonate minerals present. The strontium abundances within the seam not accountable for by clays or carbonates are probably due to an organic association such as described by Finkelman (1980).

Sulfur: (refer to figures A-59 and A-60)

The most readily observed occurrence of sulfur is in the mineral pyrite, which accounts for most of the sulfur in sample number 1-25. Pyrite is not the only major occurrence

of sulfur in the seam. Both gypsum and jarosite were present in sufficient quantities to be observed in the megascopic description of the core. Although gypsum is probably present throughout the seam, it was only observed megascopicaly in the upper portions of the seam. And jarosite was only observed in the upper foot of Pinon Test No. 2. This indicates a difference in the late stage diagenetic environments between the two drill holes. This is probably related to the proximity of the overlying sandstone, which would be a conduit for oxidizing fluids. Because of the consistency in the total sulfur abundance throughout the seam profile, it is assumed that the sulfates are forming at the expense of sulfides and possibly organically bound sulfur.

Tantalum: (refer to figures A-61 and A-62)

The profiles for both holes show a strong relationship between the tantalum concentrations and both the partings and claystones. This relationship is corroborated by a correlation coefficient of (0.81) for tantalum with ash. The profiles show little evidence for mobilization of tantalum.

Thorium: (refer to figures A-63 and A-64)

The thorium profiles are strikingly similar to the tantalum profiles, showing a strong association with the partings and bounding claystones. This observation is confirmed by the high correlation coefficient (r = 0.92) of thorium with tantalum. This indicates a similar source, although not necessarily similar mineralogy for these two elements. Further these elements appear to be in very stable mineral phases.

Uranium: (refer to figures A-65 and A-66)

The profiles for uranium show an association with the partings and the overlying claystone. But the correlation coefficient for uranium with ash is only (0.57). When these profiles are replotted on an ash normalized basis, (see figures A-67 and A-68), the concentration of uranium in the coal samples adjacent to the partings and claystones becomes significantly elevated. This indicates mobilization of the uranium from the partings into the coal samples.

It is not known whether the resulting uranium phase is a mineral or an organic compound. Of note is the greater abundance of uranium below the major partings than above them, indicating a preferential downward movement of the mobilized uranium.

Zinc: (refer to figures A-69 and A-70)

Although the data for zinc are significantly lower in their precision and accuracy than the rest of the data, some interpretations can be made if caution is used. Both holes show an increase in the zinc concentration within several tenths of a foot from the top of the seam. This would indicate a secondary origin for at least some of the zinc.

A significant point is the low concentration of sample 1-25, which represents a zone of significant pyrite crystallization. Sample 2-27, from Pinon Test No. 2, which is from a similar stratigraphic location shows an extremely elevated zinc concentration. This indicates that the zinc maxima are probably due to secondary enrichment associated with sulfide mineralization, but independent of pyrite. The overall greater variability of the concentration in Pinon Test No. 2 probably represents some unidentified lateral variation between the two holes.

Summary of the Distribution Profile Types

In general there are four types of distribution profiles recognized in this study. These profiles are characterized, in figure 12, as Type Ia, Type Ib, Type II, Type III, and Type IV. Elements showing these types of distribution profiles are accordingly grouped, (Group Ia,

Group Ib, and so forth). Table 3 shows this grouping. Some elements can not be clearly categorized on this criteria. These elements are barium, bromine, iron, strontium, and sulfur.

TABLE 3

GROUPING OF ELEMENTS

BASED ON THEIR VERTICAL DISTRIBUTION PROFILES

| Group Ia | Group Ib | Group II | Group III | Group IV |
|----------|----------|----------|-----------|----------|
| Ce | Hf | Ni | Ca | As |
| Cs | Lu | Sb | Mn | Cr |
| Eu | Na | | | Cu |
| F | Sc | | | Pb |
| La | Tb | | | Se |
| Li | U | | | Zn |
| Nd | Yb | | | |
| Rb | | | | |
| Sm | | | | |
| Ta | | | | |
| Th | | | | |
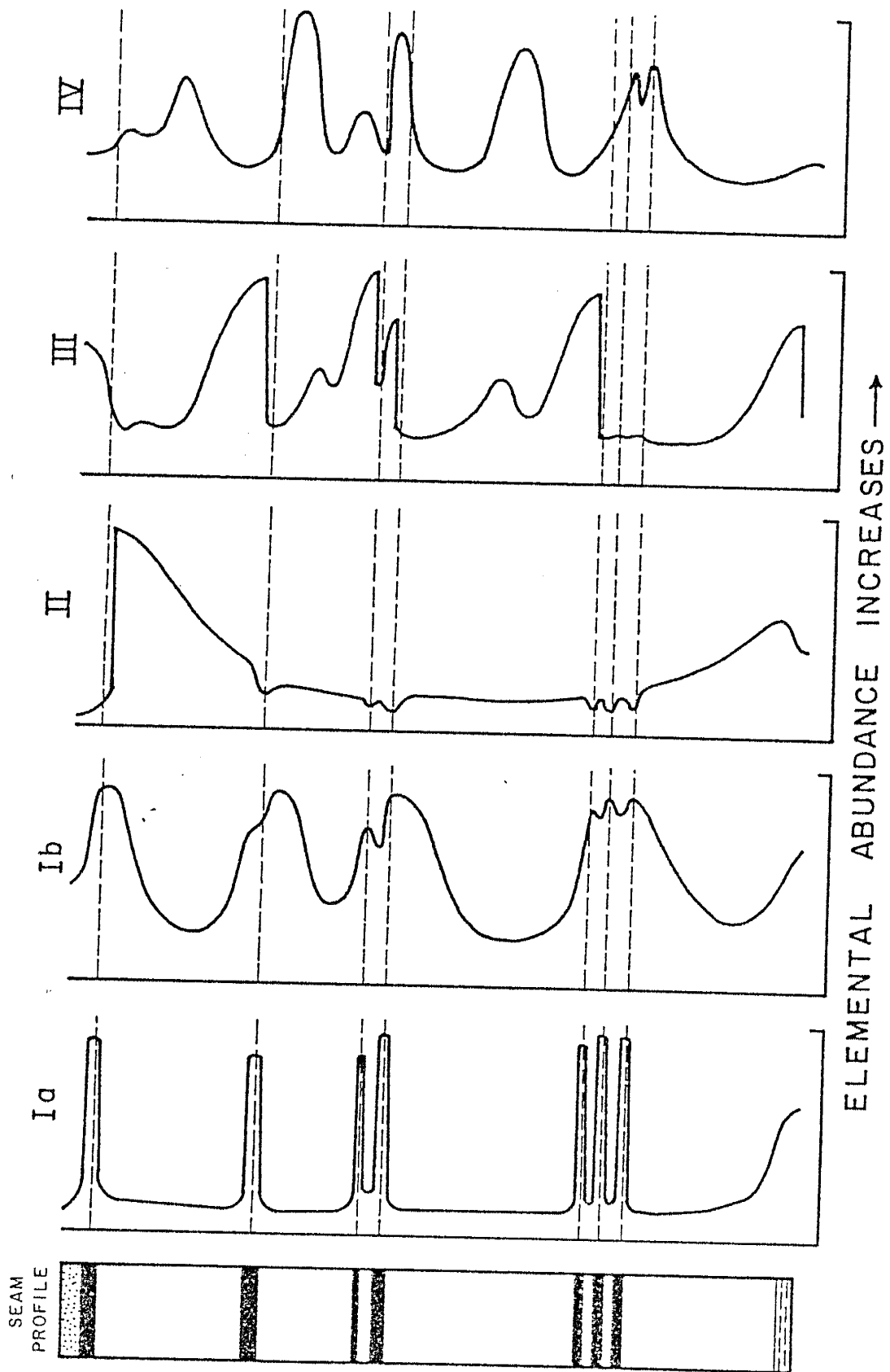
FIGURE 12 — SUMMARY OF DISTRIBUTION PROFILE TYPES

Group I elements show a strong association with partings and the bounding claystones. Group I can be subdivided into two subgroups depending upon whether the element shows elevated abundances strictly within the parting (Ia), or shows elevated abundances in the coal adjacent to the parting (Ib). Group Ia elements show a high degree of correlation with the determined ash content. Group Ib elements show varying degrees of enrichment within the coal fraction, and consequently lower correlation coefficients with the determined ash content.

Group II elements are characterized as showing significant increases in abundance at one or both seam boundaries.

Group III elements produce patterns which show significant concentration increases just above, but not within major partings. Other areas of increased concentration lie in between major partings. Both of these areas coincide with zones of significant cleat development, and filling by secondary minerals.

The most common cleat filling mineral is calcite, followed by pyrite, and then gypsum in the upper portions of the seam. The textural relationships indicate that the pyrite was present before precipitation of the calcite occurred.

Group IV elements produce patterns which show significant increases in abundance at different stratigraphic positions, which are apparently independent of parameters such as ash content, and location relative to partings. Moreover the stratigraphic location of these maxima is consistent in both drill cores. Since all of the elements showing this type of distribution are considered to be chalcophile elements, it is not unexpected that they should show similar behavior. It should be stressed, however, that the stratigraphic locations of the maxima are not the same for the different elements.

CONCLUSIONS

1. The rare earth elements exhibit a significant fractionation within the coal bed studied. Heavy rare earth element enrichment of coal adjacent to partings is the result of selective mobilization of the heavy rare earth elements during intense chemical weathering of the parting constituents in the highly acidic peat environment.

2. For a large number of the elements studied, the vertical distribution is controlled by the location and thickness of partings. These elements are: Ce, Cs, Eu, F, Hf, La, Li, Lu, Na, Nd, Rb, Sc, Sm, Ta, Tb, Th, U, and Yb.

The elements Ce, Cs, Eu, F, La, Li, Nd, Rb, Sm, Ta, and Th show elevated abundances strictly within the partings. This indicates little redistribution of these elements into the surrounding coal.

The elements Hf, Lu, Na, Sc, Tb, U, and Yb show elevated abundances both within the partings and within the coal immediately adjacent to the partings. This suggests a remobilization of the elements during a post depositional stage of the peat, probably occurring mostly before compaction and dewatering had rendered the partings impermeable.

3. The clay rich partings act as impermeable barriers, and as such control the deposition of late stage cleat filling minerals, principally carbonates and sulfates.

4. Two elements (Ni, and Sb) show significantly elevated abundances at one or both seam boundaries. This profile shape is interpreted as secondary enrichment, with the source fluids being derived from adjacent rocks. Thus the permeability of these surrounding rocks will affect the magnitude of this type of enrichment.

5. The presence of Fusinite in sufficient abundances to form fusain bands greatly enhances pyrite occurrences, by providing zones of increased porosity.

6. Arsenic shows a strong association with the occurrence of pyrite, and is believed to be substituting into the pyrite lattice.

7. The chalcophile elements (Cr, Cu, Pb, Se, and Zn) show elevated abundances in their distribution profiles which are stratigraphically dependent. The mechanisms controlling their distributions are not clearly understood, but probably involve either differential input of these elements into the swamp at different times, or differences in permeability at various stratigraphic locations allowing contact with epigenetic fluids bearing these elements.

SUGGESTIONS FOR FURTHER WORK

To better understand the effects of chemical weathering on trace element distribution in tonsteins and the accompanying coal we must know something about the starting composition and mineralogy, and the resulting abundances and mineralogy. A good way to study this would be to sample a tonstein and its bounding lithologies within a coal bed, and the adjacent facies. By analyzing these samples with an SEM and XRD the mineralogies in these two different geochemical environments could be studied. By examining textural relationships of the accessory mineral phases in both environments one could, hopefully, determine authigenic versus allogenic origins.

Elemental abundances, determined by INAA, for both bulk samples and mineral separates would allow the determination of distribution coefficients for the various mineral phases in both types of environments. Analyses such as this might shed some light on the mobility of elements such as hafnium.

REFERENCES

American Society for Testing and Materials, 1980, Annual book of ASTM standards, part 26, gaseous fuels; coal and coke; atmospheric analysis: American Society for Testing and Materials, Philadelphia PA, 934 p.

Balashov, Yu. A., and Khitrov, V. I., 1967, Composition of the Rare Earths in the Clastic Material Carried by the Volga River: Geochemistry Internat. (USSR) English Translation. v. 4, p. 404-407.

Balashov, Yu. A., Ronov, A. A., and Turanskaya, N. V., 1964, The Effect of Climate and Facies Environment on the Fractionation of the Rare Earths During Sedimentation: Geochemistry (USSR) English Translation. p. 951-969

Balkissoon, I. L., and Kuellmer, F. J., 1982, Statistical Analysis of Litrature Data on the Organic/Inorganic Association of Elements in Coal: GSA Abstracts with Programs. v. 14, no. 7, p. 438.

Beaty, R. D., 1978, Concepts, Instrumentation, and Techniques in Atomic Absorption Spectrophotometry: Perkin-Elmer Corp., 49 p.

Brown, H. R., and Swain, D. J., 1964, Inorganic Constituents of Australian Coals. Part I, Nature and Mode of Occurrence: Journal of the Institute of Fuel, v. 37, p. 422-440.

Erlank, A. J., Smith, H. S., Merchant, J. W., Cardoso, M. P., and Ahrenus, L. H., 1978, Behavior [of Hafnium] During Weathering and Alteration of Rocks. in Wedepohl,K. H., Correns, C. W., Shaw, P. M., Turekian, K. K., and Zemann, J., eds., Handbook of Geochemistry: Springer-Verlag. Ch. 72, p. 72-G-1.

Eskenazy, G., 1978, Rare-Earth Elements in Some Coal Basins of Bulgaria: Geological Balcanica, v. 8, no. 2, p. 81-88. in Finkelman, R. B., 1980, Modes of Occurrence of Trace Elements in Coal [Ph.D. Dissertation]: University of Maryland, 1980, 301 p.

Fassett, J. E., and Hinds, J. S., 1971, Geology and Fuel Resources of the Fruitland Formation and Kirtland Shale of the San Juan Basin, New Mexico and Colorado: U.S. Geol. Surv. Prof. Paper 676, 76 p.

Filby, R. H., Shah, K. R., and Sautter, C. A., 1977, A Study of Trace Element Distribution in the Solvent Refined Coal (SRC) Process Using Neutron Activation Analysis: J. Radioanal. Chem., v. 37, p. 693-704.

Finkelman, R. B., 1980, Modes of Occurrence of Trace Elements in Coal [Ph.D. Dissertation]: University of Maryland, 1980, 301 p.

Finkelman, R. B., and Stanton, R. W., 1978, Identification and Significance of Accessory Minerals from a Bituminous Coal: Fuel v. 57, p. 763-768.

Finkelman, R. B., Stanton, R. W., Cecil, C. B., and Minkin, J. A., 1979, Modes of occurrence of Selected Trace Elements in Several Appalachian Coals: American Chemical Society Preprints, Fuel Chemistry Division, v. 24, no. 1, p. 236-241.

Fleet, A. J., 1984, Aqueous and Sedimentary Geochemistry of the Rare Earth Elements. in Henderson, P., ed., Rare Earth Element Geochemistry: Elsevier, Amsterdam, Ch. 10, p. 343-369.

Gluskoter, H. J., Ruch, R. R., Miller, W. G., Cahill, R. A., Dreher, G. B., and Kuhn, J. K., 1977, Trace Elements in Coal: Occurrence and Distribution: Ill. St. Geol. Surv. Circular 499, 154 p.

Gladney, E. S., Burns, C. E., Perrin, D. R., Roelandts, I., and Gills, T. E., 1982, 1982 Compilation of Elemental Concentration Data for NBS Biological, Geological, and Environmental Standard Reference Materials: NBS Special Publication 260-88, 200 p.

Haskin, L. A., and Paster, T. P., 1979, Geochemistry and Mineralogy of the Rare Earths. in Gschneidner, K. A. Jr., and Eyring, L., ed's., Handbook on the Physics and Chemistry of the Rare Earths: North-Holland Publishing Co. Ch. 21, p. 1-80.

Jacobs, J. W., Korotev, R. L., Blanchard, D. P., and Haskin, L. A., 1977, A Well Tested Procedure for Instrumental Neutron Activation Analysis of Silicate Rocks and Minerals: J. Radioanal. Chem. v. 40, p. 98-114.

Kaplan, S. S., Carr, J. D., and Kelter, P. B., 1983, Analysis of the Trace Element Content of Coals from the Wabaunsee Group, Southeastern Nebraska: The Mountain Geologist, v. 20, no. 1, p. 1-4

Kuhn, J. K., Fiene, F., and Harvey, R., 1978, Geochemical
    Evaluation and Characterization of a Pittsburgh No. 8
    and a Rosebud Seam Coal: Deptartment of Energy,
    Morgantown Energy Technology Center, Document METC/
    CR-78/8, 40+Xiii p. in Finkelman, R. B., 1980,
    Modes of Occurrence of Trace Elements in Coal [Ph.D.
    Dissertation]: University of Maryland, 1980, 301 p.

Lundstrom, D. J., and Korotev, R. L., 1982, Teabags:
    Computer Program for Instrumental Neutron Activation
    Analysis: J. Radioanal. Chem. v. 70, p. 439-458.

Mackowsky, M.-Th., 1982, Minerals and Trace Elements
    Occurring in Coal. in Stach, E., Mackowsky, M-Th.,
    Techmuller, M., Taylor, G. H., Chandra, D., and
    Techmuller, R., 1982, Stach's Textbook of Coal
    Petrology: Gebruder Borntraeger, Berlin-Stuttgart,
    p. 153-170.

Minkin, J. A., Finkelman, R. B., Thompson, C. L.,
    Cecil, C. B., Stanton, R. W., and Chao, E. C. T., 1980
    Arsenic- and Selenium-Bearing Pyrite in Upper Freeport
    Coal, Indiana County, Pennsylvania. Submitted to IX
    International Carboniferous Congress. in Finkelman,
    R. B., 1980, Modes of Occurrence of Trace Elements in
    Coal [Ph.D. Dissertation]: University of Maryland,
    1980, 301 p.

Nesbitt, W. A., 1979, Mobility and Fractionation of Rare
    Earth Elements During Weathering of a Granodiorite:
    Nature, v. 279, p. 206-210.

Nichols, G. D., 1968, The Geochemistry of Coal-Bearing
    Strata. in Coal and Coal-Bearing Strata. D.
    Murchison and T. S. Westoll, ed. American Edition:
    American Elsevier, N.Y., p. 269-307.

Nie, N. H., Hull, C. H., Jenkins, J. G., Steinbrenner, K.,
    and Bent, D. H., 1975, Statistical Package for the
    Social Sciencies (SPSS): McGraw-Hill, 675 p.

Raymond, R. Jr., Bisch, D. L., Archuleta, L. M., and Cohen,
    A. D., 1985, Volcanic and Sedimentary Origins Remain
    Distinctive in Clay-Rich Horizions of Costa Rican
    Lignites and Peats: GSA Abstracts with Programs, v. 17,
    no. 7, p. 695.

Ronov, A. B., Vainshtein, E. E., and Tuzova, A. M., 1961,
    Geochemistry of Hafnium, Zirconium, and Some Other
    Hydrolysate Elements in Clays: Geochemistry (USSR)
    English Translation. v. 4,
    p. 343-355.

Siegel, F. R., 1974, Applied Geochemistry: John Wiley and
    Sons Inc. 353 p.

Swanson, V. E., Medlin, J. H., Hatch, J. R., Coleman, S. L.,
    Wood, G. H. Jr., Woodruff, S. D., and Hildebrand, R. T.,
    1976, Collection, Chemical Analysis, and Evaluation of
    Coal Samples in 1975: U.S. Geol. Surv. Open-file
    Report 76-468, 503 p.

Szilagyi, M., 1971, The Role of Organic Material in the
    Distribution of Mo, V, and Cr in Coal Fields: Economic
    Geology, v. 66, p. 1075-1078.

Taylor, S. R., and Gorton, M. P, 1977, Geochemical
    Application of Spark Source Mass Spectrography-III.
    Element Sinsitivity, percision and Accuracy: Geochimica
    et Cosmochimica Acta, v. 41, p. 1375-1380.

Thomas, J. Jr., Gluskoter, H. J., 1974, Determination of
    Fluoride in Coal with the Fluoride Ion-Selective
    Electrode: Anal. Chem. v. 46, no. 9, p. 1321-1323.

Tsui, F. F., Cahill, R. A., and Frost, J. K., 1979,
    Concentrations of Rare Earth Elements of Coals in the
    Illinois Basin: Ninth International Congress of
    Carboniferous Stratigraphy and Geology. Urbana,
    Illinois, May 1979, p. 218. in Finkelman, R. B.,
    1980, Modes of Occurrence of Trace Elements in Coal
    [Ph.D. Dissertation]: University of Maryland, 1980,
    301 p.

Zubovic, P., 1966a, Physiochemical Properties of Certain
    Minor Elements as Controlling Factors in Their
    Distribution in Coal. in Gould, R. F., ed., Coal
    Science: American Chemical Society Publications,
    Advances in Chemistry, no. 55, Washington D. C.,
    p. 221-246.

Zubovic, P., 1966b, Minor Element Distribution in Coal
    Samples of the Interior Province. in Gould, R. F.,
    ed., Coal Science: American Chemical Society
    Publications, Advances in Chemistry, no. 55, Washington
    D. C., p. 232-274

APPENDIX I

TABLE A

ANALYTICAL DATA FOR PINON TEST No. 1

| SAMPLE | As | Ba | Br | Ca | Ce | Co |
|---|---|---|---|---|---|---|
| | (ppm) | (ppm) | (ppm) | (%) | (ppm) | (ppm) |
| 1-01 | 0.88 | 94. | 1.05 | 0.22 | 49.1 | 8.12 |
| 1-02 | 0.78 | * 20. | 2.57 | 0.30 | 14.4 | 11.5 |
| 1-03 | 3.06 | 67. | 1.53 | 1.00 | 18.2 | 6.86 |
| 1-04 | 1.40 | 55. | 1.61 | 0.42 | 31.5 | 4.16 |
| 1-05 | 0.32 | 128. | 0.54 | 0.34 | 40.3 | 4.09 |
| 1-06 | 2.35 | 482. | 5.2 | 0.69 | 24.7 | 4.10 |
| 1-07 | 2.71 | 303. | 0.46 | 0.26 | 55.6 | 4.19 |
| 1-08 | 1.60 | 208. | 1.99 | 0.09 | 17.2 | 4.20 |
| 1-09 | 0.33 | 111. | 0.26 | 0.36 | 61.1 | 2.00 |
| 1-10 | 0.67 | 215. | 4.5 | 0.38 | 10.4 | 2.99 |
| 1-11 | 0.61 | 33. | 4.8 | 0.24 | 13.9 | 2.11 |
| 1-12 | 3.00 | 226. | 1.76 | 2.92 | 5.7 | 4.05 |
| 1-13 | 0.81 | 917. | 7.0 | 0.19 | 6.9 | 3.30 |
| 1-14 | 0.22 | 1008. | 2.43 | 1.04 | 17.0 | 4.80 |
| 1-15 | 0.17 | 305. | * 0.16 | 0.36 | 52.7 | 3.24 |
| 1-16 | 0.20 | 247. | 0.83 | 0.29 | 17.7 | 5.51 |
| 1-17 | 0.33 | 420. | 0.58 | 0.74 | 50.3 | 3.49 |
| 1-18 | 1.78 | 947. | 0.78 | 0.81 | 12.7 | 5.55 |
| 1-19 | 0.50 | 32. | 0.77 | 1.02 | 15.1 | 5.47 |
| 1-20 | 0.53 | 26. | 0.87 | 1.19 | 10.3 | 4.41 |
| 1-21 | 0.34 | 707. | 0.86 | 0.63 | 7.3 | 5.65 |
| 1-22 | 0.45 | 757. | 0.43 | 0.42 | 37.8 | 5.35 |
| 1-23 | 1.37 | 619. | 0.61 | 2.10 | 15.7 | 6.42 |
| 1-24 | 2.98 | 2370. | 0.69 | 0.90 | 9.5 | 5.89 |
| 1-25 | 53.8 | 99. | 4.2 | 1.77 | 5.3 | 6.08 |
| 1-26 | 1.08 | 566. | 0.54 | 0.38 | 13.6 | 5.12 |
| 1-27 | 0.76 | 4720. | 0.55 | 0.49 | 5.8 | 2.90 |
| 1-28 | 3.45 | 898. | 0.45 | 0.11 | 24.1 | 5.14 |
| 1-29 | 4.42 | 31600. | * 0.29 | * 0.03 | 24.1 | 5.69 |
| 1-30 | 1.54 | 627. | * 0.04 | 0.51 | 89.1 | 3.87 |

*    value is reported as an upper limit only

Note: The cobalt values are given for informational
purposes only. Contamination of the samples by
cobalt is likely to have occurred during grinding.

TABLE A (cont.)

| SAMPLE | Cr | Cs | Cu | Eu | F | Fe |
|--------|------|-------|------|-------|------|------|
|        | (ppm) | (ppm) | (ppm) | (ppm) | (ppm) | (%) |
| 1-01 | 11.1 | 3.38 | 27.0 | 0.568 | 134. | 1.370 |
| 1-02 | 5.27 | 0.267 | 22.3 | 0.339 | 33. | 0.415 |
| 1-03 | 5.60 | 0.320 | 18.2 | 0.302 | 33. | 0.243 |
| 1-04 | 8.41 | 0.401 | 21.2 | 0.503 | 30. | 0.243 |
| 1-05 | 7.59 | 1.98 | 17.1 | 0.476 | 109. | 0.345 |
| 1-06 | 6.68 | 1.03 | 12.9 | 0.384 | 50. | 0.310 |
| 1-07 | 5.00 | 0.590 | 17.5 | 0.557 | 93. | 0.452 |
| 1-08 | 3.29 | 0.234 | 23.6 | 0.359 | 30. | 0.232 |
| 1-09 | 3.20 | 1.07 | 12.6 | 0.470 | 149. | 0.550 |
| 1-10 | 4.44 | 0.356 | 14.8 | 0.216 | 37. | 0.265 |
| 1-11 | 9.09 | 0.235 | 34.8 | 0.173 | 26. | 0.238 |
| 1-12 | 3.73 | 0.145 | 12.6 | 0.096 | 50. | 0.592 |
| 1-13 | 2.67 | 0.111 | 12.5 | 0.121 | 20. | 0.302 |
| 1-14 | 4.03 | 0.130 | 10.8 | 0.286 | 20. | 0.285 |
| 1-15 | 4.66 | 0.669 | 7.6 | 0.523 | 102. | 0.327 |
| 1-16 | 5.13 | 0.238 | 22.0 | 0.317 | 28. | 0.236 |
| 1-17 | 5.5 | 4.31 | 7.2 | 0.486 | 88. | 0.274 |
| 1-18 | 1.86 | 0.141 | 6.3 | 0.214 | 22. | 0.268 |
| 1-19 | 3.67 | 0.076 | 11.4 | 0.148 | 20. | 0.212 |
| 1-20 | 4.55 | 0.043 | 6.7 | 0.112 | 18. | 0.208 |
| 1-21 | 1.12 | 0.118 | 5.5 | 0.240 | 27. | 0.323 |
| 1-22 | 6.53 | 0.482 | 16.2 | 0.605 | 136. | 0.551 |
| 1-23 | 2.04 | 0.068 | 7.4 | 0.358 | 25. | 0.470 |
| 1-24 | 1.85 | 0.099 | 18.0 | 0.099 | 216. | 0.627 |
| 1-25 | 1.63 | 0.021 | 6.0 | 0.073 | 23. | 4.89 |
| 1-26 | 9.52 | 0.298 | 20.7 | 0.225 | 65. | 0.221 |
| 1-27 | 2.24 | 0.065 | 5.1 | 0.128 | 45. | 0.235 |
| 1-28 | 0.81 | 0.083 | 7.2 | 0.185 | 94. | 0.955 |
| 1-29 | 1.9 | 0.205 | 11.3 | 0.272 | 109. | 1.04 |
| 1-30 | 5.8 | 1.439 | 49.4 | 0.757 | 353. | 1.88 |

TABLE A (cont.)

| SAMPLE | Hf | La | Li | Lu | Mn | Na |
|--------|------|-------|------|-------|------|--------|
| | (ppm) | (ppm) | (ppm) | (ppm) | (ppm) | (%) |
| 1-01 | 2.53 | 27.55 | 19.9 | 0.272 | 21.4 | 0.1275 |
| 1-02 | 1.49 | 7.00 | 18.3 | 0.176 | 10.3 | 0.0824 |
| 1-03 | 1.84 | 9.31 | 21.6 | 0.090 | 11.9 | 0.0930 |
| 1-04 | 2.40 | 15.01 | 42.3 | 0.155 | 5.9 | 0.1144 |
| 1-05 | 3.10 | 19.87 | 22.1 | 0.149 | 10.9 | 0.1925 |
| 1-06 | 2.74 | 11.73 | 21.5 | 0.145 | 6.7 | 0.1359 |
| 1-07 | 4.26 | 26.55 | 41.5 | 0.151 | 4.8 | 0.1342 |
| 1-08 | 3.89 | 7.56 | 33.2 | 0.163 | 5.7 | 0.0823 |
| 1-09 | 5.17 | 30.07 | 54.6 | 0.093 | 7.9 | 0.1855 |
| 1-10 | 3.73 | 4.40 | 69.4 | 0.097 | 9.6 | 0.0814 |
| 1-11 | 2.35 | 6.99 | 45.8 | 0.056 | 8.2 | 0.0783 |
| 1-12 | 1.04 | 3.24 | 18.5 | 0.035 | 62.9 | 0.0887 |
| 1-13 | 0.79 | 3.28 | 14.5 | 0.050 | 12.2 | 0.0735 |
| 1-14 | 2.53 | 7.36 | 25.1 | 0.168 | 22.9 | 0.0855 |
| 1-15 | 2.82 | 23.82 | 47.4 | 0.151 | 14.4 | 0.332 |
| 1-16 | 3.28 | 7.75 | 30.4 | 0.227 | 19.3 | 0.1019 |
| 1-17 | 5.92 | 23.53 | 23.1 | 0.230 | 19.0 | 0.1838 |
| 1-18 | 2.01 | 5.33 | 10.2 | 0.179 | 15.5 | 0.1104 |
| 1-19 | 0.66 | 8.06 | 8.6 | 0.053 | 8.5 | 0.0966 |
| 1-20 | 0.45 | 7.50 | 4.6 | 0.032 | 13.4 | 0.0943 |
| 1-21 | 2.52 | 3.60 | 13.6 | 0.227 | 12.4 | 0.1185 |
| 1-22 | 7.06 | 16.43 | 26.8 | 0.325 | 8.8 | 0.280 |
| 1-23 | 2.34 | 6.99 | 5.5 | 0.188 | 43.6 | 0.1201 |
| 1-24 | 0.43 | 6.60 | 7.2 | 0.030 | 6.0 | 0.1437 |
| 1-25 | 0.32 | 3.05 | 10.6 | 0.019 | 8.7 | 0.0950 |
| 1-26 | 2.27 | 5.37 | 20.7 | 0.064 | 8.2 | 0.1366 |
| 1-27 | 0.86 | 2.48 | 13.5 | 0.025 | 21.5 | 0.1351 |
| 1-28 | 0.51 | 18.96 | 4.9 | 0.222 | 11.0 | 0.2063 |
| 1-29 | 5.28 | 11.5 | 18.2 | 0.545 | 12.7 | 0.510 |
| 1-30 | 5.78 | 45.7 | 14.9 | 0.341 | 11.9 | 1.677 |

TABLE A (cont.)

| SAMPLE | Nd | Ni | Pb | Rb | S | Sb |
|--------|------|------|-------|---------|--------|--------|
|        | (ppm)| (ppm)| (ppm) | (ppm)   | (%)    | (ppm)  |
| 1-01 | 18.0 | 7.7 | 15.0 | 21.2 | 1.394 | 2.16 |
| 1-02 | 6.6 | 8.3 | 10.3 | 1.3 | 0.911 | 1.06 |
| 1-03 | 8.6 | 6.6 | 11.7 | 1.7 | 0.705 | 0.232 |
| 1-04 | 13.4 | 3.7 | 9.4 | 2.4 | 0.627 | 0.358 |
| 1-05 | 17.0 | 2.0 | 9.4 | 23.9 | 0.518 | 0.347 |
| 1-06 | 10.3 | 2.7 | 8.1 | 8.0 | 0.689 | 0.807 |
| 1-07 | 21.9 | 1.6 | 14.2 | 11.3 | 0.793 | 0.360 |
| 1-08 | 8.5 | 4.5 | 14.0 | 1.6 | 0.677 | 0.824 |
| 1-09 | 22.4 | 1.0 | 10.2 | 13.2 | 0.613 | 0.526 |
| 1-10 | 6.0 | 3.4 | 13.7 | 2.1 | 0.762 | 0.874 |
| 1-11 | 5.4 | 2.3 | 20.0 | 0.9 | 0.620 | 0.160 |
| 1-12 | 2.1 | 2.1 | 1.7 | * 0.5 | 0.971 | 0.207 |
| 1-13 | 3.0 | 2.7 | 1.9 | * 0.4 | 0.702 | 0.179 |
| 1-14 | 8.8 | 2.1 | 2.8 | 0.6 | 0.677 | 0.401 |
| 1-15 | 22.4 | 0.6 | 30.6 | 17.2 | 0.311 | 0.206 |
| 1-16 | 10.4 | 2.4 | 37.4 | 2.0 | 0.559 | 0.469 |
| 1-17 | 18.8 | 1.2 | 17.1 | 4.5 | 0.490 | 0.506 |
| 1-18 | 5.9 | 2.1 | 8.0 | * 0.6 | 0.633 | 0.736 |
| 1-19 | 5.9 | 1.9 | 50.9 | * 0.5 | 0.486 | 0.143 |
| 1-20 | 4.0 | 2.6 | 18.5 | * 0.4 | 0.596 | 0.098 |
| 1-21 | 4.6 | 0.6 | 2.5 | * 0.6 | 1.057 | 1.066 |
| 1-22 | 20.5 | 1.4 | 14.0 | 3.7 | 0.801 | 0.573 |
| 1-23 | 8.1 | 2.3 | 2.5 | * 0.8 | 0.992 | 0.634 |
| 1-24 | ND | 3.0 | 0.3 | * 0.8 | 1.139 | 0.125 |
| 1-25 | ND | 2.4 | 11.6 | * 1.5 | 6.131 | 0.191 |
| 1-26 | 6.4 | 2.5 | 5.5 | 1.8 | 0.818 | 0.291 |
| 1-27 | 2.9 | 3.3 | 0.2 | 0.7 | 0.908 | 0.152 |
| 1-28 | 8.4 | 4.9 | 4.4 | * 0.5 | 1.854 | 8.44 |
| 1-29 | 9.3 | 2.9 | 7.6 | 5.5 | 2.748 | 8.07 |
| 1-30 | 34.6 | 1.6 | 242. | 12.8 | 0.702 | 0.81 |

\*  value is reported as an upper limit only

ND  value is reported as not detectable

TABLE A (cont.)

| SAMPLE | Sc | Se | Sm | Sr | Ta | Tb |
|--------|------|------|------|------|-------|-------|
| | (ppm) | (ppm) | (ppm) | (ppm) | (ppm) | (ppm) |
| 1-01 | 4.55 | 2.48 | 2.77 | 85. | 0.466 | 0.445 |
| 1-02 | 2.97 | 2.11 | 1.39 | 43. | 0.195 | 0.278 |
| 1-03 | 2.14 | 2.25 | 1.34 | 57. | 0.315 | 0.181 |
| 1-04 | 3.93 | 3.49 | 2.38 | 51. | 0.484 | 0.305 |
| 1-05 | 3.16 | 2.71 | 2.39 | 53. | 0.937 | 0.249 |
| 1-06 | 3.09 | 2.68 | 1.89 | 135. | 0.488 | 0.248 |
| 1-07 | 2.99 | 2.37 | 3.24 | 207. | 0.602 | 0.355 |
| 1-08 | 4.37 | 1.86 | 1.74 | 116. | 0.248 | 0.320 |
| 1-09 | 2.45 | 1.88 | 2.97 | 98. | 0.944 | 0.280 |
| 1-10 | 3.67 | 1.96 | 1.06 | 73. | 0.493 | 0.231 |
| 1-11 | 2.83 | 4.35 | 0.89 | 39. | 0.445 | 0.107 |
| 1-12 | 1.41 | 1.78 | 0.46 | 159. | 0.142 | 0.068 |
| 1-13 | 1.04 | 1.76 | 0.59 | 299. | 0.132 | 0.071 |
| 1-14 | 2.76 | 1.95 | 1.52 | 159. | 0.315 | 0.267 |
| 1-15 | 2.92 | 2.37 | 3.23 | 78. | 2.35 | 0.354 |
| 1-16 | 4.78 | 1.68 | 1.90 | 125. | 0.554 | 0.377 |
| 1-17 | 5.73 | 1.86 | 3.52 | 87. | 1.32 | 0.508 |
| 1-18 | 3.80 | 1.60 | 1.36 | 119. | 0.119 | 0.289 |
| 1-19 | 1.05 | 1.76 | 0.86 | 64. | 0.110 | 0.139 |
| 1-20 | 0.74 | 0.66 | 0.55 | 71. | 0.061 | 0.067 |
| 1-21 | 3.24 | 1.12 | 0.98 | 122. | 0.109 | 0.277 |
| 1-22 | 6.79 | 4.30 | 3.18 | 235. | 0.972 | 0.531 |
| 1-23 | 2.27 | 1.43 | 1.64 | 66. | 0.110 | 0.311 |
| 1-24 | 0.71 | 1.40 | 0.50 | 117. | 0.073 | 0.056 |
| 1-25 | 0.72 | 2.94 | 0.40 | 81. | 0.060 | 0.052 |
| 1-26 | 2.84 | 3.68 | 1.06 | 76. | 0.478 | 0.130 |
| 1-27 | 0.87 | 1.00 | 0.53 | 160. | 0.119 | 0.062 |
| 1-28 | 1.46 | 0.90 | 1.31 | 92. | 0.058 | 0.249 |
| 1-29 | 4.31 | 1.12 | 1.31 | 459. | 1.107 | 0.407 |
| 1-30 | 4.32 | 1.75 | 5.34 | 178. | 1.990 | 0.730 |

TABLE A (cont.)

| SAMPLE | Th | U | Yb | Zn | MOIST | ASH |
|--------|------|------|------|------|-------|------|
| | (ppm) | (ppm) | (ppm) | (ppm) | (%) | (%) |
| 1-01 | 5.56 | 1.62 | 1.667 | 11.2 | 7.90 | 47.25 |
| 1-02 | 2.96 | 1.36 | 1.077 | 3.5 | 7.48 | 14.89 |
| 1-03 | 2.97 | 1.11 | 0.551 | 4.3 | 7.24 | 18.98 |
| 1-04 | 4.33 | 2.11 | 0.959 | 3.3 | 6.66 | 17.51 |
| 1-05 | 4.74 | 2.29 | 0.885 | 4.1 | 5.75 | 41.99 |
| 1-06 | 4.13 | 2.15 | 0.906 | 2.3 | 7.19 | 22.58 |
| 1-07 | 7.57 | 2.83 | 0.950 | 3.4 | 6.94 | 38.66 |
| 1-08 | 5.59 | 3.76 | 1.065 | 3.9 | 7.67 | 14.94 |
| 1-09 | 18.86 | 4.72 | 0.524 | 7.0 | 7.63 | 61.29 |
| 1-10 | 7.58 | 2.92 | 0.643 | 2.3 | 8.18 | 17.37 |
| 1-11 | 4.31 | 1.32 | 0.337 | 6.0 | 6.00 | 19.40 |
| 1-12 | 1.68 | 0.58 | 0.206 | 5.0 | 8.36 | 11.83 |
| 1-13 | 1.66 | 0.48 | 0.297 | 3.6 | 8.52 | 8.79 |
| 1-14 | 3.93 | 4.39 | 1.081 | 3.0 | 8.15 | 12.04 |
| 1-15 | 16.63 | 4.07 | 0.948 | 9.3 | 5.65 | 65.58 |
| 1-16 | 9.14 | 4.97 | 1.410 | 10.9 | 7.24 | 18.00 |
| 1-17 | 21.94 | 5.03 | 1.45 | 11.7 | 7.30 | 36.28 |
| 1-18 | 1.88 | 2.11 | 1.169 | 4.4 | 8.55 | 11.76 |
| 1-19 | 1.37 | 0.47 | 0.376 | 10.2 | 7.88 | 11.92 |
| 1-20 | 0.70 | 0.29 | 0.202 | 4.7 | 9.13 | 9.01 |
| 1-21 | 1.89 | 3.74 | 1.423 | 0.8 | 11.03 | 14.09 |
| 1-22 | 12.52 | 5.85 | 2.018 | 4.6 | 9.53 | 34.56 |
| 1-23 | 2.32 | 2.94 | 1.190 | 2.7 | 10.25 | 13.32 |
| 1-24 | 0.75 | 0.15 | 0.165 | 4.1 | 9.72 | 9.23 |
| 1-25 | 0.69 | 0.23 | 0.108 | 2.0 | 5.95 | 20.55 |
| 1-26 | 5.63 | 1.96 | 0.378 | 10.5 | 6.58 | 23.03 |
| 1-27 | 0.97 | 0.50 | 0.175 | 11.2 | 7.92 | 12.03 |
| 1-28 | 0.80 | 1.41 | 1.30 | 33.6 | 10.25 | 8.38 |
| 1-29 | 9.01 | 11.30 | 3.30 | 18.70 | 9.44 | 30.80 |
| 1-30 | 32.70 | 11.70 | 2.11 | 193. | 11.42 | 82.65 |

TABLE A (cont.)

| SAMPLE | V.M. | F.C. | BTU |
|--------|------|------|-----|
| | (%) | (%) | BTU |
| 1-01 | 26.09 | 26.66 | 6955. |
| 1-02 | 40.96 | 44.15 | 12032. |
| 1-03 | 38.92 | 42.10 | 11437. |
| 1-04 | 39.21 | 43.28 | 11701. |
| 1-05 | 29.05 | 28.96 | 7525. |
| 1-06 | 36.58 | 40.84 | 10716. |
| 1-07 | 29.75 | 31.59 | 8020. |
| 1-08 | 39.05 | 46.01 | 12005. |
| 1-09 | 21.20 | 17.51 | 4653. |
| 1-10 | 36.56 | 46.07 | 11295. |
| 1-11 | 36.02 | 44.58 | 11523. |
| 1-12 | 39.12 | 49.05 | 12252. |
| 1-13 | 35.65 | 55.56 | 12745. |
| 1-14 | 35.41 | 52.55 | 12261. |
| 1-15 | 21.15 | 13.28 | 4667. |
| 1-16 | 36.37 | 45.64 | 11585. |
| 1-17 | 31.71 | 32.01 | 8540. |
| 1-18 | 40.49 | 47.75 | 12286. |
| 1-19 | 39.08 | 49.00 | 12302. |
| 1-20 | 40.47 | 50.52 | 12652. |
| 1-21 | 37.20 | 48.71 | 11857. |
| 1-22 | 29.56 | 35.88 | 8641. |
| 1-23 | 38.53 | 48.15 | 11806. |
| 1-24 | 41.44 | 49.33 | 12733. |
| 1-25 | 33.08 | 46.37 | 11323. |
| 1-26 | 36.59 | 40.38 | 10849. |
| 1-27 | 41.20 | 46.77 | 12265. |
| 1-28 | 40.71 | 50.91 | 12640. |
| 1-29 | 33.35 | 35.85 | 9492. |
| 1-30 | 11.73 | 5.62 | 1632. |

V.M. = Volatile Matter
F.C. = Fixed Carbon

TABLE B

ANALYTICAL DATA FOR PINON TEST No. 2

| SAMPLE | As | Ba | Br | Ca | Ce | Co |
|--------|------|------|------|------|------|------|
|        | (ppm) | (ppm) | (ppm) | (%) | (ppm) | (ppm) |
| 2-01 | 1.03 | 165. | 0.49 | 0.32 | 62.0 | 6.98 |
| 2-02 | 2.70 | 54. | 0.38 | 2.07 | 40.4 | 5.66 |
| 2-03 | 1.82 | 106. | 0.92 | 0.21 | 55.8 | 6.35 |
| 2-04 | 0.57 | 9. | 0.86 | 0.19 | 15.3 | 3.56 |
| 2-05 | 3.53 | 561. | 0.75 | 0.29 | 25.3 | 3.82 |
| 2-06 | 0.67 | 110. | 0.64 | 0.16 | 30.1 | 3.36 |
| 2-07 | 0.51 | 125. | 0.65 | 0.12 | 24.7 | 4.27 |
| 2-08 | 0.31 | 149. | 0.38 | 0.19 | 58.2 | 1.99 |
| 2-09 | 0.41 | 20. | 0.90 | 0.29 | 15.9 | 2.99 |
| 2-10 | 2.83 | 131. | 0.20 | 1.67 | 32.7 | 1.37 |
| 2-11 | 0.58 | 109. | 0.84 | 3.12 | 9.8 | 2.20 |
| 2-12 | 1.60 | 30. | 0.78 | 0.29 | 15.2 | 1.47 |
| 2-13 | 0.60 | 67. | 0.88 | 0.72 | 6.6 | 1.82 |
| 2-14 | 0.25 | 183. | 0.65 | 1.64 | 6.0 | 2.40 |
| 2-15 | 0.32 | 397. | 1.14 | 0.65 | 20.5 | 3.30 |
| 2-16 | 0.20 | 257. | 0.18 | 0.09 | 56.6 | 2.51 |
| 2-17 | 0.26 | 147. | 0.95 | 2.20 | 16.0 | 4.35 |
| 2-18 | 0.60 | 1526. | 0.52 | 1.88 | 25.4 | 3.06 |
| 2-19 | 1.23 | 724. | 0.44 | 2.94 | 22.0 | 2.90 |
| 2-20 | 1.48 | 683. | 0.97 | 2.00 | 13.2 | 2.83 |
| 2-21 | 0.50 | 117. | 1.04 | 0.79 | 11.8 | 3.25 |
| 2-22 | 0.23 | 159. | 1.27 | 0.63 | 8.6 | 3.65 |
| 2-23 | 2.39 | 136. | 1.23 | 2.25 | 15.0 | 6.50 |
| 2-24 | 1.65 | 1933. | 1.18 | 0.08 | 12.7 | 6.41 |
| 2-25 | 0.68 | 349. | 0.22 | 1.24 | 70.0 | 2.36 |
| 2-26 | 0.54 | 340. | 0.87 | 3.90 | 16.1 | 5.40 |
| 2-27 | 0.98 | 1124. | 1.09 | 0.33 | 11.5 | 4.42 |
| 2-28 | 17.6 | 6507. | 1.11 | 0.74 | 13.0 | 11.2 |
| 2-29 | 3.26 | 2404. | 1.22 | 0.49 | 11.2 | 18.4 |
| 2-30 | 2.69 | 30. | 1.26 | 0.13 | 11.4 | 43.6 |
| 2-31 | 4.15 | 747. | 2.63 | 0.06 | 28.9 | 33.8 |
| 2-32 | 0.91 | 358. | 0.85 | 0.39 | 116.6 | 105.7 |
| 2-33 | 2.70 | 751. | 0.10 | 1.20 | 67.1 | 13.5 |

Note: The cobalt values are given for informational
purposes only. Contamination of the samples by
cobalt is likely to have occurred during grinding.

TABLE B (cont.)

| SAMPLE | Cr | Cs | Cu | Eu | F | Fe |
|--------|------|-------|------|-------|------|-------|
| | (ppm) | (ppm) | (ppm) | (ppm) | (ppm) | (%) |
| 2-01 | 18.4 | 7.27 | 17.3 | 0.742 | 259. | 2.007 |
| 2-02 | 10.2 | 1.77 | 18.5 | 0.629 | 121. | 0.539 |
| 2-03 | 8.80 | 2.22 | 18.9 | 0.643 | 116. | 0.439 |
| 2-04 | 4.00 | 0.228 | 19.1 | 0.335 | 32. | 0.120 |
| 2-05 | 4.70 | 0.145 | 9.2 | 0.314 | 22. | 0.482 |
| 2-06 | 6.10 | 0.347 | 33.1 | 0.410 | 50. | 0.181 |
| 2-07 | 5.90 | 0.306 | 23.5 | 0.368 | 43. | 0.227 |
| 2-08 | 2.60 | 0.582 | 35.3 | 0.477 | 130. | 0.357 |
| 2-09 | 3.00 | 0.160 | 30.7 | 0.344 | 20. | 0.202 |
| 2-10 | 2.50 | 0.638 | 14.7 | 0.298 | 109. | 0.787 |
| 2-11 | 4.30 | 0.306 | 11.1 | 0.222 | 73. | 0.246 |
| 2-12 | 7.50 | 0.133 | 59.6 | 0.172 | 21. | 0.274 |
| 2-13 | 4.90 | 0.091 | 48.7 | 0.104 | 26. | 0.267 |
| 2-14 | 2.35 | 0.084 | 13.2 | 0.115 | 25. | 0.252 |
| 2-15 | 4.30 | 0.133 | 8.7 | 0.322 | 25. | 0.334 |
| 2-16 | 4.70 | 0.731 | 4.2 | 0.563 | 113. | 0.402 |
| 2-17 | 3.90 | 0.217 | 12.5 | 0.305 | 26. | 0.347 |
| 2-18 | 3.50 | 0.450 | 36.5 | 0.297 | 68. | 0.578 |
| 2-19 | 2.40 | 0.255 | 16.9 | 0.295 | 67. | 0.502 |
| 2-20 | 1.60 | 0.192 | 4.3 | 0.215 | 28. | 0.296 |
| 2-21 | 7.69 | 0.111 | 13.2 | 0.120 | 29. | 0.255 |
| 2-22 | 5.20 | 0.092 | 8.1 | 0.099 | 26. | 0.195 |
| 2-23 | 2.90 | 0.200 | 13.0 | 0.165 | 27. | 0.611 |
| 2-24 | 4.10 | 0.346 | 51.4 | 0.352 | 39. | 0.442 |
| 2-25 | 4.70 | 1.28 | 12.1 | 0.776 | 209. | 1.187 |
| 2-26 | 2.29 | 0.305 | 9.5 | 0.345 | 106. | 0.391 |
| 2-27 | 3.01 | 0.050 | 12.4 | 0.118 | 45. | 0.284 |
| 2-28 | 9.80 | 0.263 | 29.1 | 0.155 | 74. | 0.524 |
| 2-29 | 2.24 | 0.082 | 9.7 | 0.122 | 59. | 0.265 |
| 2-30 | 1.66 | 0.080 | 8.7 | 0.203 | 70. | 0.484 |
| 2-31 | 6.20 | 0.207 | 22.7 | 0.556 | 108. | 1.303 |
| 2-32 | 3.30 | 1.69 | 7.7 | 0.986 | MV | 1.780 |
| 2-33 | 10.7 | 2.86 | 4.9 | 0.942 | MV | 0.705 |

Mv    (missing value) value could not be determined

TABLE B (cont.)

| SAMPLE | Hf | La | Li | Lu | Mn | Na |
|---|---|---|---|---|---|---|
| | (ppm) | (ppm) | (ppm) | (ppm) | (ppm) | (%) |
| 2-01 | 4.41 | 31.16 | 18.2 | 0.309 | 16.2 | 0.1391 |
| 2-02 | 2.20 | 19.19 | 14.5 | 0.301 | 43.7 | 0.0472 |
| 2-03 | 1.75 | 28.50 | 9.5 | 0.230 | 14.4 | 0.0461 |
| 2-04 | 1.40 | 7.31 | 19.4 | 0.087 | 15.9 | 0.0646 |
| 2-05 | 1.03 | 13.23 | 25.1 | 0.099 | 9.5 | 0.0406 |
| 2-06 | 2.55 | 14.36 | 34.2 | 0.149 | 10.6 | 0.0514 |
| 2-07 | 2.28 | 11.52 | 24.6 | 0.161 | 15.0 | 0.0570 |
| 2-08 | 4.46 | 26.99 | 42.7 | 0.128 | 12.6 | 0.0839 |
| 2-09 | 2.72 | 6.06 | 32.5 | 0.178 | 14.8 | 0.0303 |
| 2-10 | 5.19 | 13.10 | 38.2 | 0.097 | 21.1 | 0.0741 |
| 2-11 | 3.96 | 4.12 | 27.4 | 0.108 | 46.7 | 0.0523 |
| 2-12 | 1.77 | 7.28 | 39.9 | 0.047 | 10.8 | 0.0411 |
| 2-13 | 1.88 | 2.74 | 30.1 | 0.044 | 11.7 | 0.0336 |
| 2-14 | 0.67 | 2.59 | 12.5 | 0.047 | 10.6 | 0.0379 |
| 2-15 | 2.10 | 8.71 | 23.4 | 0.187 | 24.1 | 0.4010 |
| 2-16 | 3.15 | 26.60 | 50.7 | 0.166 | 11.7 | 0.2436 |
| 2-17 | 2.69 | 6.65 | 18.0 | 0.207 | 70.6 | 0.0796 |
| 2-18 | 2.63 | 11.82 | 24.3 | 0.174 | 45.5 | 0.1124 |
| 2-19 | 5.69 | 10.27 | 22.8 | 0.232 | 48.7 | 0.0760 |
| 2-20 | 1.99 | 5.59 | 9.1 | 0.186 | 32.5 | 0.0816 |
| 2-21 | 0.59 | 7.36 | 8.7 | 0.045 | 12.9 | 0.0485 |
| 2-22 | 0.44 | 5.18 | 6.8 | 0.033 | 10.4 | 0.0469 |
| 2-23 | 0.81 | 8.34 | 11.7 | 0.056 | 21.4 | 0.0631 |
| 2-24 | 4.19 | 4.69 | 13.5 | 0.290 | 15.1 | 0.1590 |
| 2-25 | 6.81 | 31.37 | 33.7 | 0.247 | 18.1 | 0.2790 |
| 2-26 | 4.14 | 6.46 | 5.7 | 0.268 | 43.2 | 0.0794 |
| 2-27 | 0.53 | 8.25 | 15.6 | 0.029 | 10.8 | 0.0404 |
| 2-28 | 2.01 | 5.73 | 20.4 | 0.048 | 17.0 | 0.1270 |
| 2-29 | 0.47 | 6.03 | 10.9 | 0.021 | 23.7 | 0.1252 |
| 2-30 | 0.62 | 5.34 | 8.0 | 0.236 | 50.8 | 0.2850 |
| 2-31 | 2.74 | 11.85 | 13.6 | 0.483 | 29.3 | 0.2890 |
| 2-32 | 7.90 | 53.50 | 31.6 | 0.284 | 34.2 | 0.8120 |
| 2-33 | 5.77 | 35.27 | 12.2 | 0.245 | 32.4 | 2.440 |

TABLE B (cont.)

| SAMPLE | Nd | Ni | Pb | Rb | S | Sb |
|--------|------|------|------|------|-------|-------|
| | (ppm) | (ppm) | (ppm) | (ppm) | (%) | (ppm) |
| 2-01 | 24.5 | 3.5 | 12.1 | 50.0 | 0.772 | 0.858 |
| 2-02 | 17.7 | 2.4 | 11.4 | 11.1 | 0.675 | 1.001 |
| 2-03 | 21.5 | 3.6 | 8.8 | 11.5 | 0.805 | 0.612 |
| 2-04 | 7.2 | 4.8 | 7.5 | 0.6 | 0.712 | 0.158 |
| 2-05 | 10.1 | 2.8 | 2.6 | 1.0 | 0.846 | 0.211 |
| 2-06 | 14.1 | 2.3 | 14.3 | 3.0 | 0.582 | 0.206 |
| 2-07 | 11.2 | 2.6 | 11.4 | 3.4 | 0.726 | 0.524 |
| 2-08 | 21.2 | 0.6 | 8.2 | 13.4 | 0.575 | 0.247 |
| 2-09 | 9.3 | 2.2 | 14.6 | 1.1 | 0.722 | 0.876 |
| 2-10 | 11.4 | 0.6 | 7.5 | 8.8 | 1.048 | 0.479 |
| 2-11 | 5.6 | 1.9 | 8.1 | 2.8 | 0.709 | 1.35 |
| 2-12 | 5.5 | 1.5 | 9.7 | 1.1 | 0.714 | 0.178 |
| 2-13 | 2.6 | 1.4 | 7.5 | 0.5 | 0.673 | 0.173 |
| 2-14 | 2.6 | 1.6 | 2.9 | 0.2 | 0.624 | 0.231 |
| 2-15 | 8.9 | 1.4 | 8.3 | 0.3 | 0.643 | 0.302 |
| 2-16 | 20.4 | 0.4 | 16.8 | 16.0 | 0.335 | 0.221 |
| 2-17 | 7.7 | 2.0 | 34.7 | 0.4 | 0.624 | 0.566 |
| 2-18 | 10.1 | 1.0 | 8.2 | 7.1 | 0.746 | 0.678 |
| 2-19 | 9.3 | 1.8 | 9.7 | 3.0 | 0.670 | 0.923 |
| 2-20 | 6.4 | 2.6 | 3.0 | 1.0 | 0.734 | 1.144 |
| 2-21 | 4.2 | 2.5 | 50.4 | 0.5 | 0.567 | 0.149 |
| 2-22 | 2.9 | 3.2 | 3.8 | 0.1 | 0.527 | 0.107 |
| 2-23 | 5.3 | 2.0 | 5.0 | 1.2 | 0.831 | 0.187 |
| 2-24 | 6.2 | 2.4 | 7.9 | 0.3 | 1.051 | 0.843 |
| 2-25 | 28.0 | 0.2 | 15.3 | 12.6 | 0.590 | 0.693 |
| 2-26 | 7.9 | 2.6 | 6.1 | 1.1 | 0.883 | 0.912 |
| 2-27 | 3.8 | 2.4 | 2.3 | ND | 0.670 | 0.147 |
| 2-28 | 3.0 | 1.4 | 2.4 | 2.5 | 1.268 | 0.495 |
| 2-29 | 3.3 | 3.3 | 0.6 | 0.2 | 0.832 | 0.125 |
| 2-30 | 5.6 | 9.4 | 7.4 | 2.8 | 1.139 | 8.63 |
| 2-31 | 15.1 | 12.3 | 11.0 | 2.8 | 1.022 | 5.45 |
| 2-32 | 40.2 | 1.2 | 29.1 | 15.6 | 0.418 | 0.903 |
| 2-33 | 26.2 | 1.2 | 8.2 | 56.9 | 0.063 | 0.670 |

TABLE B (cont.)

| SAMPLE | Sc | Se | Sm | Sr | Ta | Tb |
|--------|------|------|------|------|-------|-------|
| | (ppm) | (ppm) | (ppm) | (ppm) | (ppm) | (ppm) |
| 2-01 | 7.59 | 1.67 | 4.46 | 82. | 1.083 | 0.630 |
| 2-02 | 5.51 | 2.12 | 3.09 | 32. | 0.380 | 0.630 |
| 2-03 | 4.60 | 2.41 | 3.74 | 32. | 0.304 | 0.520 |
| 2-04 | 2.22 | 1.65 | 1.47 | 21. | 0.205 | 0.199 |
| 2-05 | 2.24 | 1.79 | 1.74 | 53. | 0.115 | 0.247 |
| 2-06 | 2.98 | 3.21 | 2.24 | 32. | 0.511 | 0.276 |
| 2-07 | 3.05 | 2.01 | 2.09 | 20. | 0.409 | 0.297 |
| 2-08 | 2.17 | 1.36 | 3.15 | 23. | 0.612 | 0.280 |
| 2-09 | 4.14 | 1.38 | 1.97 | 14. | 0.165 | 0.361 |
| 2-10 | 2.79 | 2.04 | 1.93 | 41. | 0.874 | 0.220 |
| 2-11 | 3.55 | 1.96 | 1.20 | 37. | 0.674 | 0.262 |
| 2-12 | 2.46 | 5.20 | 0.91 | 18. | 0.385 | 0.098 |
| 2-13 | 1.84 | 1.73 | 0.59 | 35. | 0.453 | 0.059 |
| 2-14 | 1.00 | 1.21 | 0.58 | 39. | 0.108 | 0.059 |
| 2-15 | 3.12 | 1.42 | 1.87 | 38. | 0.368 | 0.349 |
| 2-16 | 3.21 | 1.84 | 3.62 | 55. | 2.51 | 0.410 |
| 2-17 | 3.81 | 1.10 | 1.77 | 32. | 0.393 | 0.410 |
| 2-18 | 3.70 | 1.15 | 2.12 | 108. | 0.604 | 0.327 |
| 2-19 | 5.40 | 1.71 | 2.01 | 103. | 0.996 | 0.420 |
| 2-20 | 2.96 | 1.31 | 1.44 | 57. | 0.098 | 0.317 |
| 2-21 | 0.87 | 1.15 | 0.69 | 24. | 0.096 | 0.096 |
| 2-22 | 0.67 | 1.29 | 0.50 | 34. | 0.079 | 0.085 |
| 2-23 | 1.34 | 1.55 | 0.93 | 37. | 0.249 | 0.114 |
| 2-24 | 3.94 | 2.34 | 1.50 | 83. | 0.192 | 0.390 |
| 2-25 | 6.37 | 3.40 | 4.73 | 104. | 1.63 | 0.610 |
| 2-26 | 3.61 | 1.02 | 1.69 | 83. | 0.247 | 0.409 |
| 2-27 | 1.14 | 1.16 | 0.66 | 62. | 0.091 | 0.073 |
| 2-28 | 1.71 | 3.05 | 0.78 | 116. | 0.555 | 0.084 |
| 2-29 | 0.91 | 0.93 | 0.63 | 79. | 0.085 | 0.070 |
| 2-30 | 1.64 | 1.22 | 1.11 | 75. | 0.185 | 0.298 |
| 2-31 | 7.31 | 1.48 | 3.01 | 48. | 0.676 | 0.640 |
| 2-32 | 5.17 | 0.50 | 6.58 | 182. | 2.88 | 0.800 |
| 2-33 | 4.02 | 0.17 | 4.16 | 423. | 0.613 | 0.394 |

TABLE B (cont.)

| SAMPLE | Th | U | Yb | Zn | MOIST | ASH |
|--------|------|------|------|------|-------|------|
| | (ppm) | (ppm) | (ppm) | (ppm) | (%) | (%) |
| 2-01 | 13.29 | 3.02 | 1.980 | 9.7 | 9.35 | 64.93 |
| 2-02 | 5.98 | 4.41 | 1.976 | 13.6 | 7.99 | 29.73 |
| 2-03 | 4.49 | 3.36 | 1.440 | 4.8 | 9.73 | 23.55 |
| 2-04 | 2.64 | 1.17 | 0.531 | 6.8 | 8.28 | 10.31 |
| 2-05 | 2.03 | 0.94 | 0.602 | 4.6 | 7.43 | 9.90 |
| 2-06 | 3.84 | 1.73 | 0.883 | 3.2 | 5.66 | 18.80 |
| 2-07 | 4.50 | 2.18 | 0.986 | 5.4 | 8.29 | 17.42 |
| 2-08 | 6.39 | 2.27 | 0.736 | 4.3 | 6.29 | 50.33 |
| 2-09 | 5.19 | 3.62 | 1.21 | 1.4 | 8.15 | 9.70 |
| 2-10 | 14.80 | 4.06 | 0.576 | 4.0 | 6.66 | 52.19 |
| 2-11 | 9.16 | 4.32 | 0.766 | 2.5 | 9.34 | 16.80 |
| 2-12 | 3.72 | 1.29 | 0.291 | 2.0 | 6.45 | 14.36 |
| 2-13 | 6.61 | 1.16 | 0.250 | 5.6 | 7.17 | 10.22 |
| 2-14 | 1.44 | 0.50 | 0.257 | 3.6 | 8.34 | 9.12 |
| 2-15 | 4.88 | 4.94 | 1.156 | 18.7 | 7.62 | 11.88 |
| 2-16 | 21.64 | 5.08 | 1.030 | 5.4 | 5.39 | 63.38 |
| 2-17 | 5.82 | 6.58 | 1.363 | 15.6 | 7.66 | 17.30 |
| 2-18 | 8.55 | 3.15 | 1.045 | 9.1 | 8.11 | 33.29 |
| 2-19 | 13.28 | 5.14 | 1.467 | 16.3 | 7.69 | 26.75 |
| 2-20 | 1.33 | 3.43 | 1.202 | 7.3 | 9.46 | 10.95 |
| 2-21 | 1.10 | 0.38 | 0.260 | 30.9 | 8.61 | 9.81 |
| 2-22 | 0.74 | 0.27 | 0.197 | 3.9 | 10.05 | 8.04 |
| 2-23 | 2.06 | 1.03 | 0.313 | 3.3 | 10.46 | 14.13 |
| 2-24 | 4.81 | 6.37 | 1.925 | 6.7 | 9.83 | 12.81 |
| 2-25 | 20.09 | 4.84 | 1.500 | 12.1 | 8.91 | 68.73 |
| 2-26 | 3.97 | 4.00 | 1.708 | 9.7 | 9.45 | 16.76 |
| 2-27 | 1.08 | 0.31 | 0.208 | 290. | 9.33 | 9.56 |
| 2-28 | 7.56 | 1.46 | 0.296 | 6.2 | 15.38 | 24.24 |
| 2-29 | 0.84 | 0.48 | 0.154 | 7.5 | 15.06 | 12.53 |
| 2-30 | 1.61 | 2.39 | 1.442 | 79.4 | 21.59 | 13.40 |
| 2-31 | 8.86 | 10.38 | 2.84 | 32.5 | 16.40 | 33.94 |
| 2-32 | 43.20 | 12.08 | 1.93 | 25.7 | 15.03 | 90.96 |
| 2-33 | 7.47 | 4.83 | 1.45 | 22.4 | 5.35 | 97.06 |

TABLE B (cont.)

| SAMPLE | V.M. | F.C. | BTU |
|--------|------|------|-----|
| | (%) | (%) | BTU |
| 2-01 | 19.80 | 15.28 | 4160. |
| 2-02 | 35.16 | 35.12 | 9454. |
| 2-03 | 34.70 | 41.76 | 10496. |
| 2-04 | 43.33 | 46.36 | 12645. |
| 2-05 | 44.93 | 45.17 | 12745. |
| 2-06 | 44.43 | 36.77 | 11624. |
| 2-07 | 39.80 | 42.79 | 11411. |
| 2-08 | 27.24 | 22.43 | 6521. |
| 2-09 | 43.48 | 46.82 | 12644. |
| 2-10 | 27.47 | 20.35 | 5658. |
| 2-11 | 39.45 | 43.75 | 11191. |
| 2-12 | 41.96 | 43.68 | 12142. |
| 2-13 | 43.19 | 46.59 | 12639. |
| 2-14 | 40.68 | 50.21 | 12496. |
| 2-15 | 37.78 | 50.35 | 12289. |
| 2-16 | 21.43 | 15.20 | 4091. |
| 2-17 | 37.40 | 45.31 | 11344. |
| 2-18 | 32.72 | 33.99 | 8801. |
| 2-19 | 40.68 | 32.58 | 9747. |
| 2-20 | 40.70 | 48.35 | 12191. |
| 2-21 | 39.48 | 50.72 | 12645. |
| 2-22 | 40.76 | 51.20 | 12852. |
| 2-23 | 35.37 | 50.51 | 11715. |
| 2-24 | 36.91 | 50.28 | 12040. |
| 2-25 | 18.26 | 13.01 | 3162. |
| 2-26 | 39.46 | 43.78 | 11128. |
| 2-27 | 41.86 | 48.59 | 12271. |
| 2-28 | 36.59 | 39.18 | 8850. |
| 2-29 | 41.65 | 45.83 | 10401. |
| 2-30 | 43.32 | 43.28 | 8935. |
| 2-31 | 33.77 | 32.29 | 7028. |
| 2-32 | MV | MV | MV |
| 2-33 | MV | MV | MV |

V.M. = Volatile Matter
F.C. = Fixed Carbon
Mv   = (missing value) value could
       not be determined.

APPENDIX II

DISTRIBUTION PROFILES

FOR THE RARE EARTH ELEMENTS
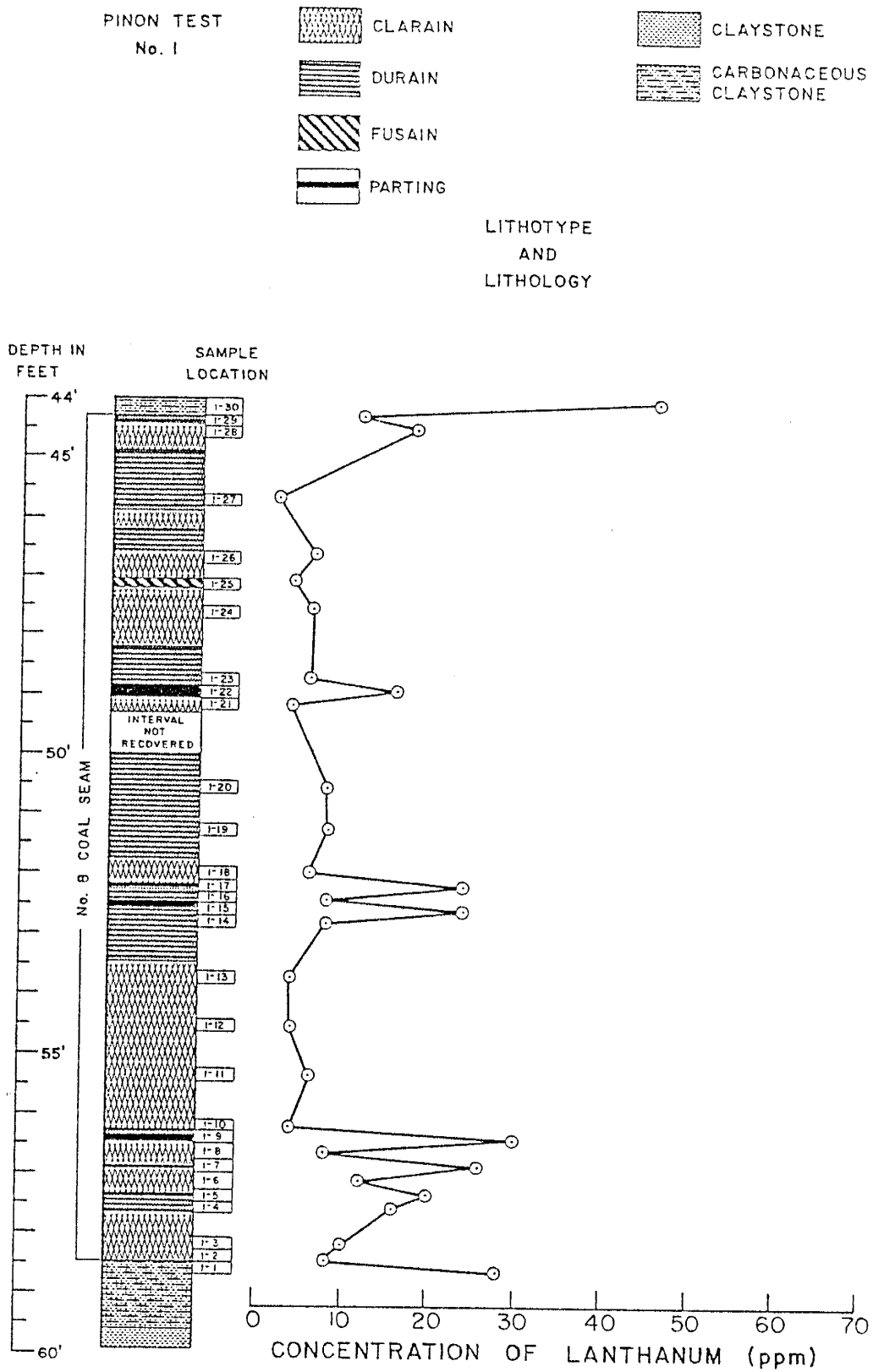
Figure A-1 - Distribution of Lanthanum
in Pinon Test No. 1.
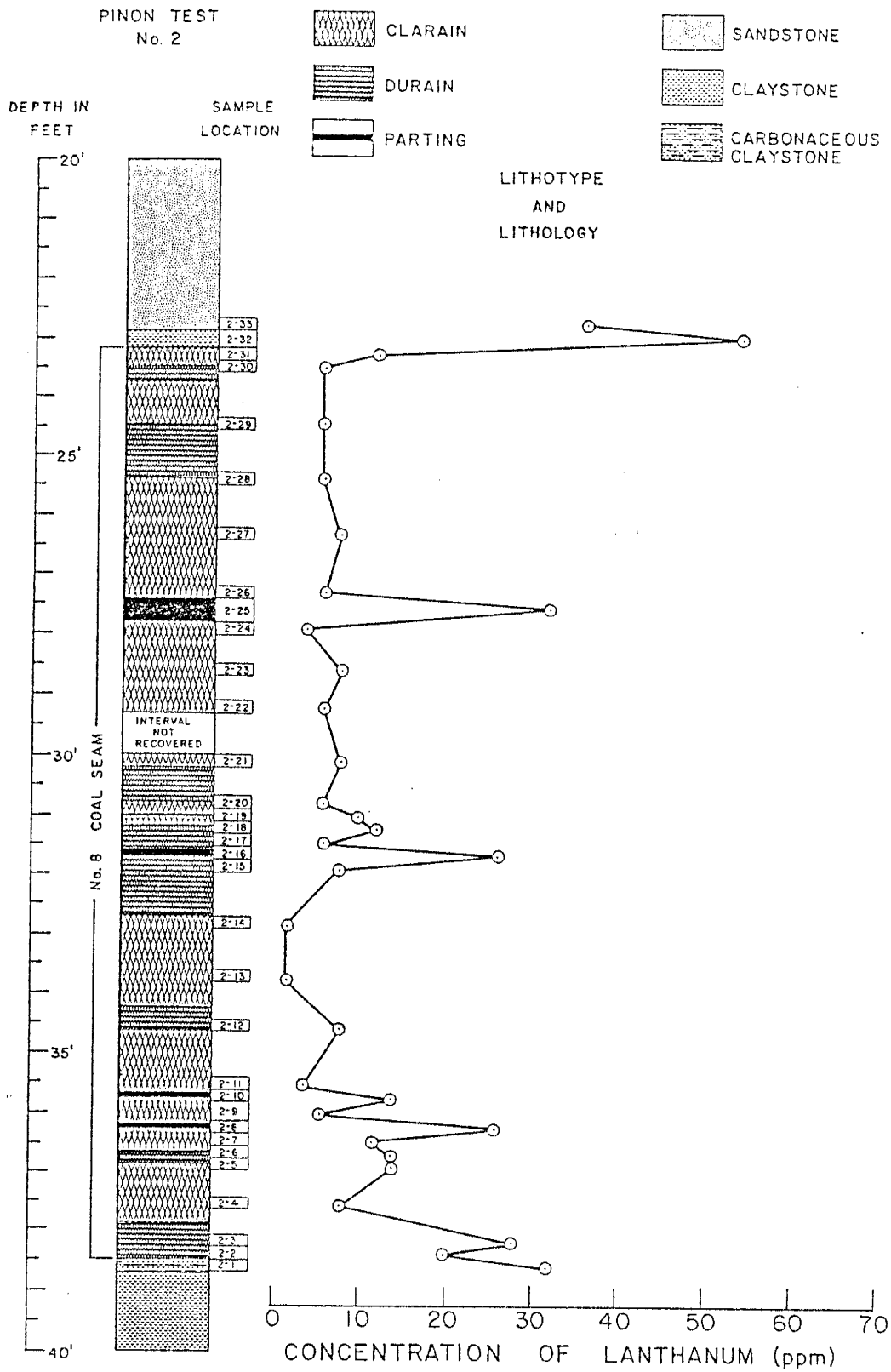
Figure A-2 — Distribution of Lanthanum
in Pinon Test No. 2.
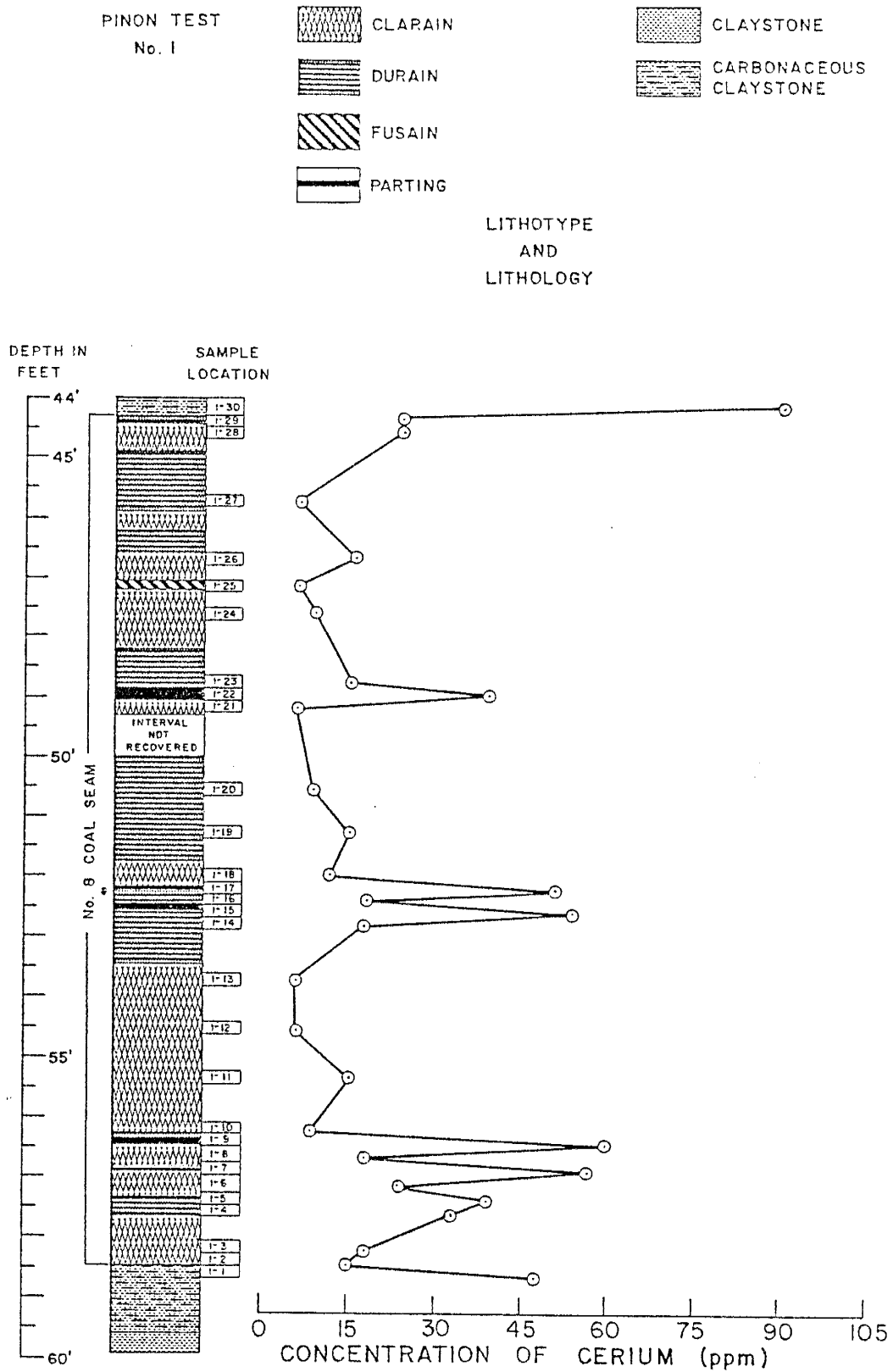
Figure A-3 – Distribution of Cerium
in Pinon Test No. 1.
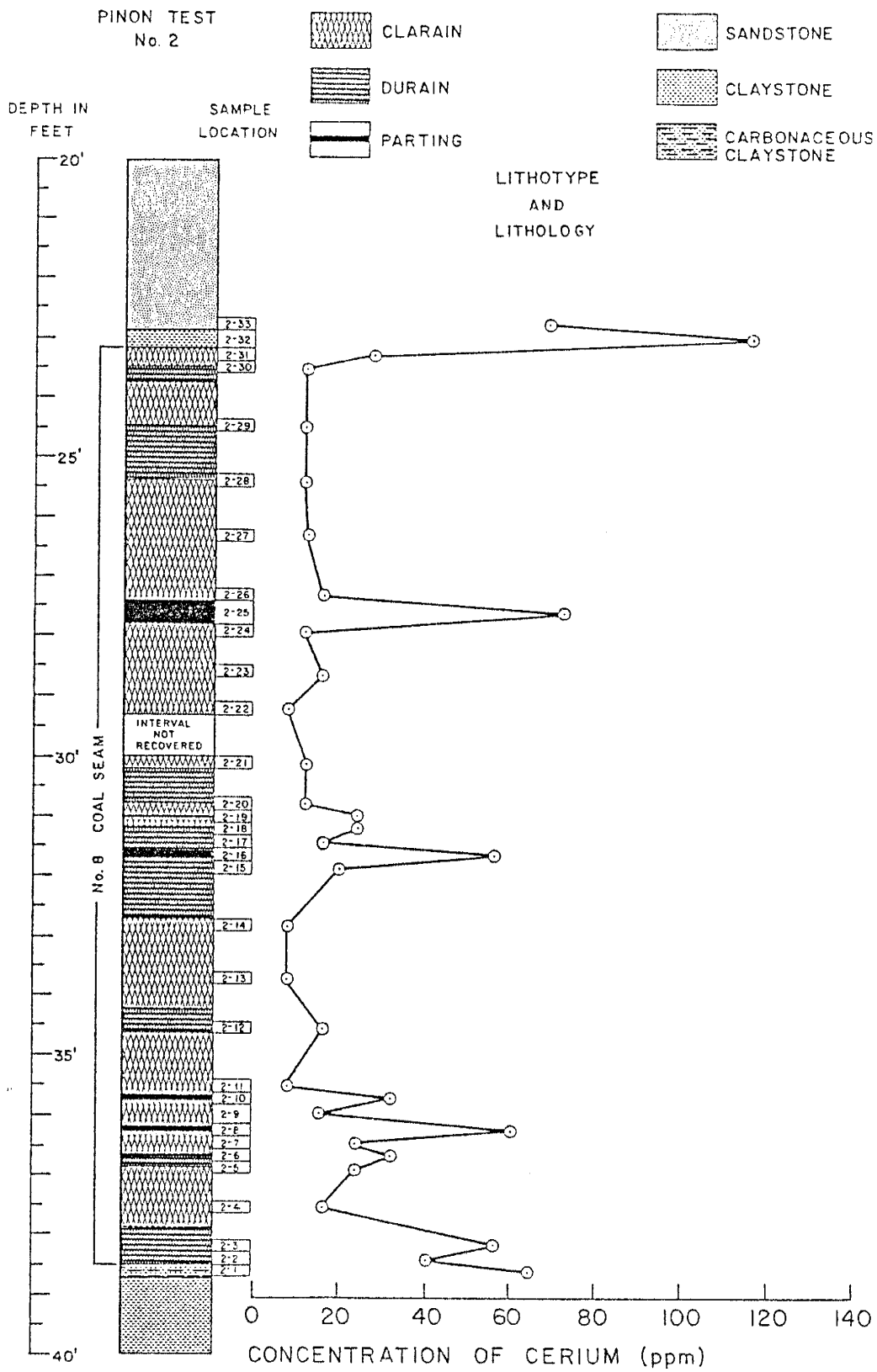
Figure A-4 – Distribution of Cerium
in Pinon Test No. 2.
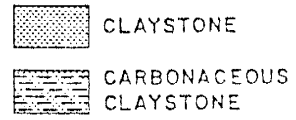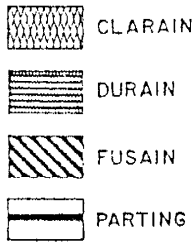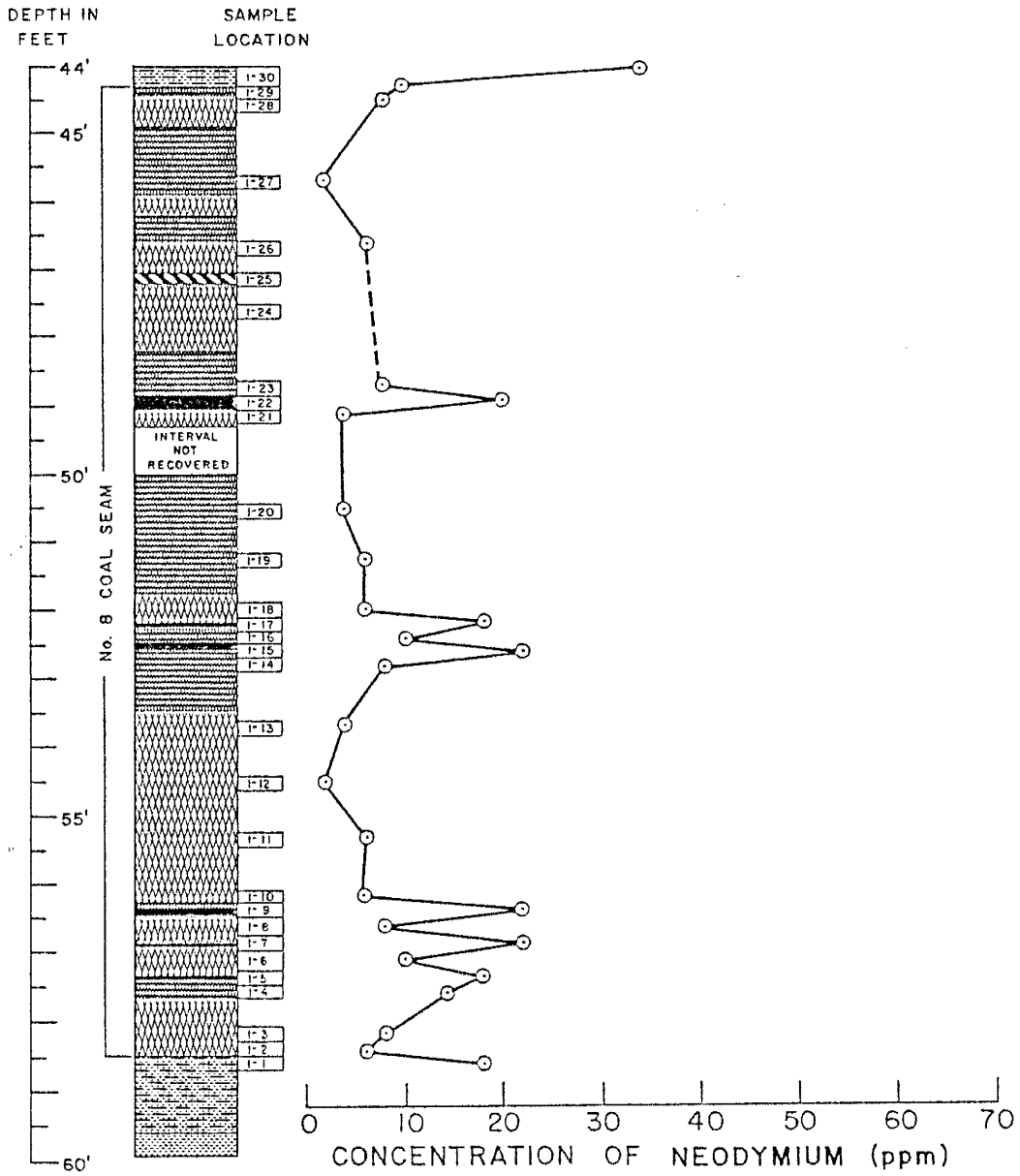
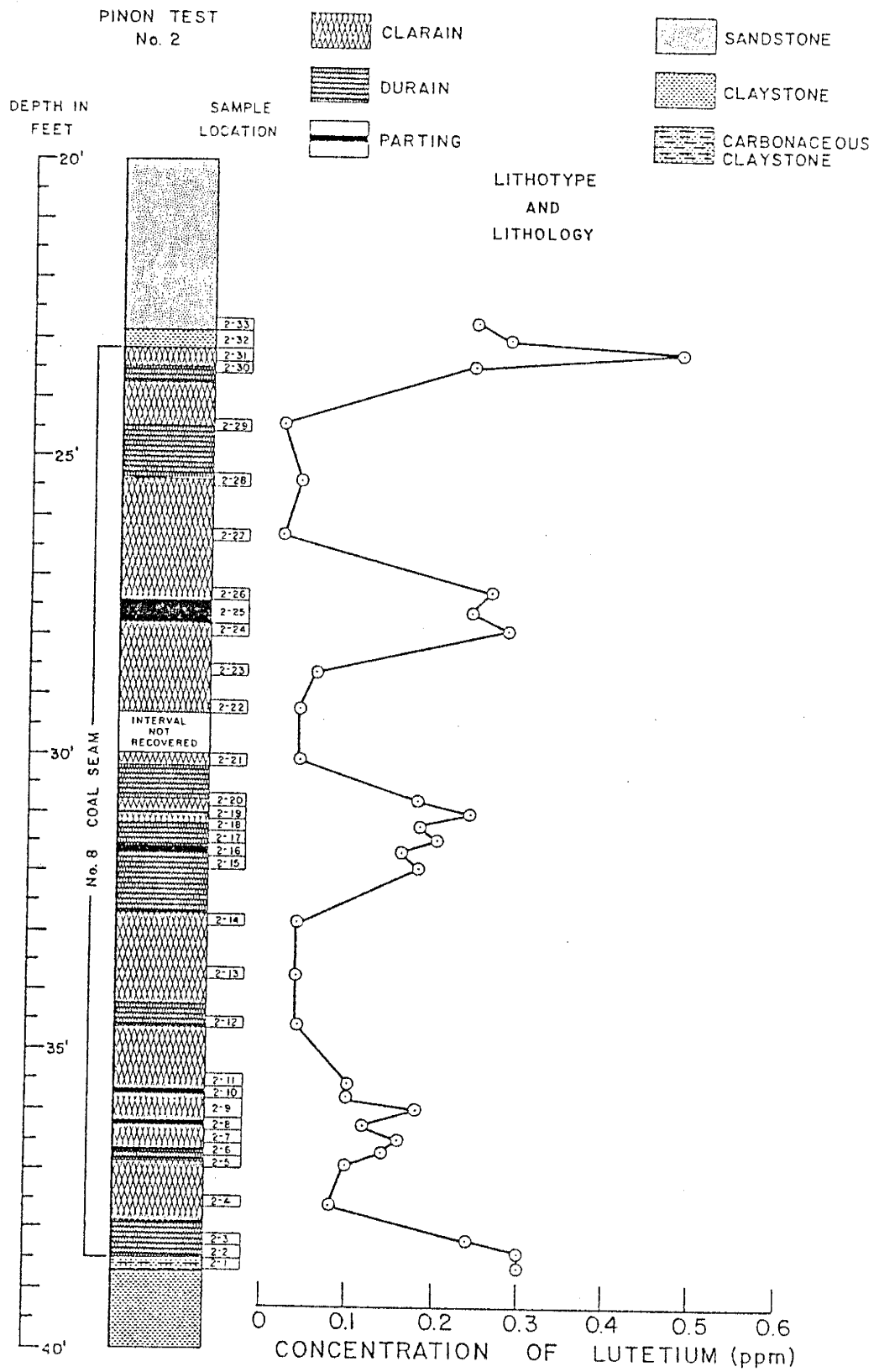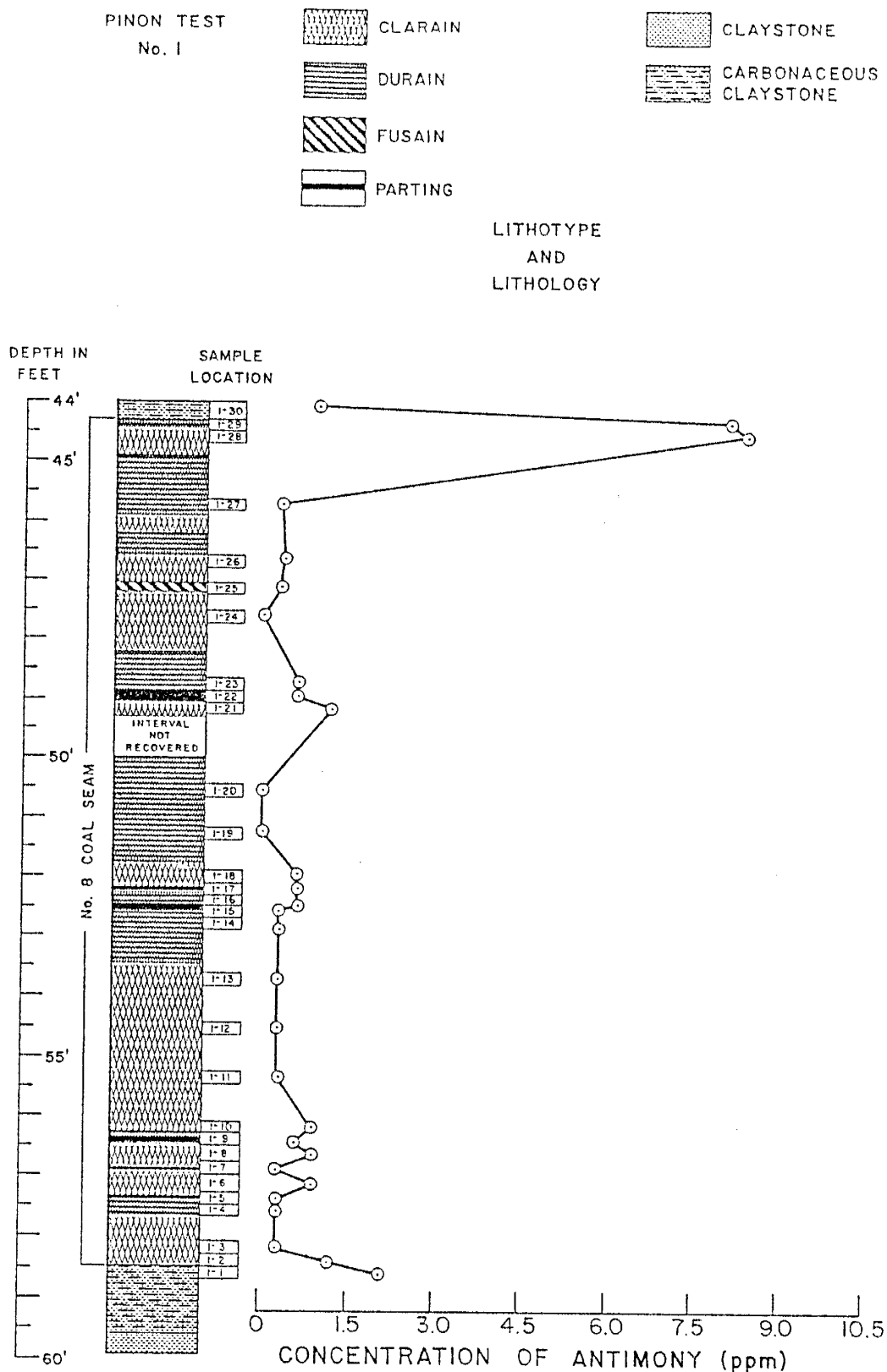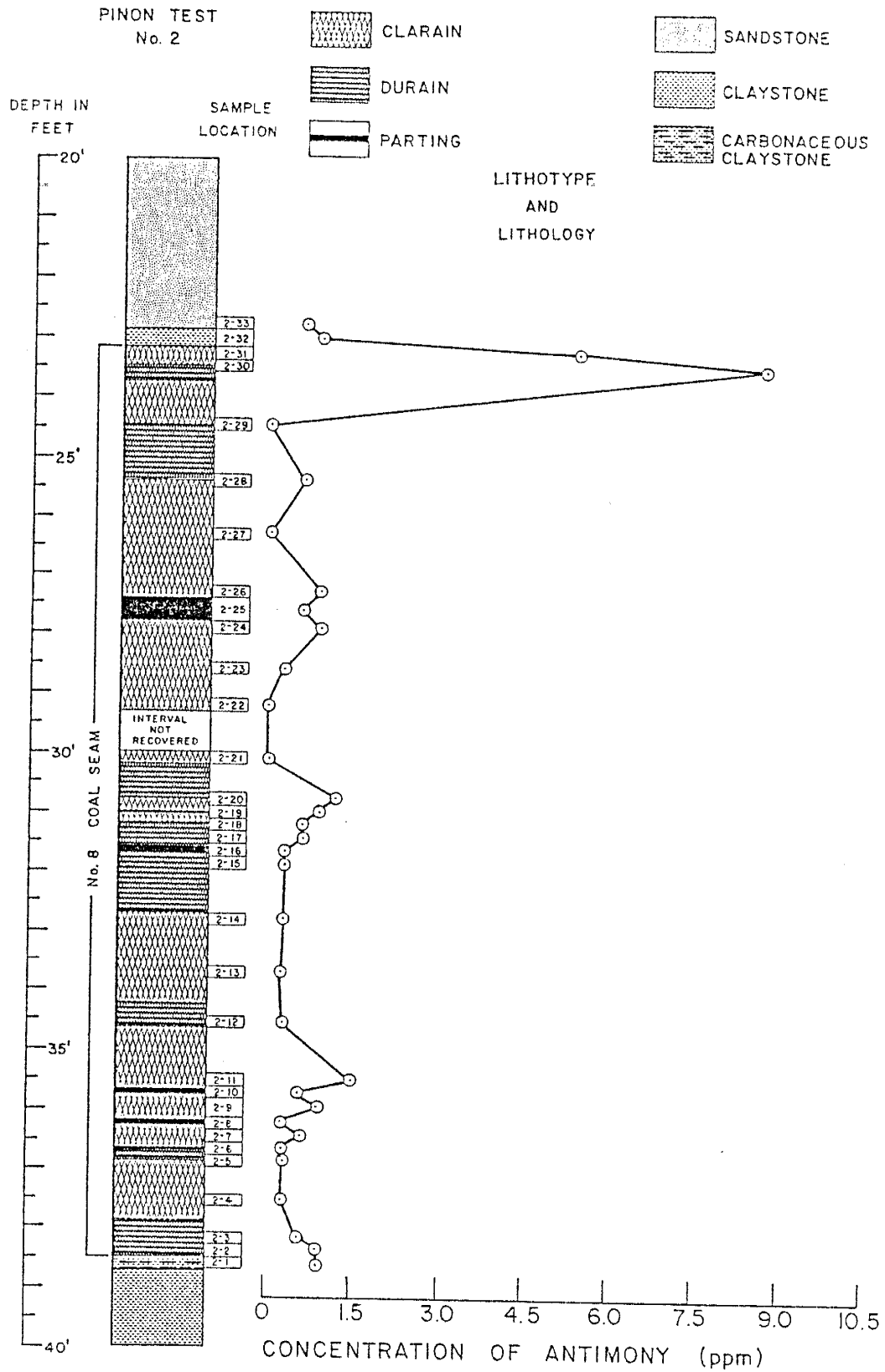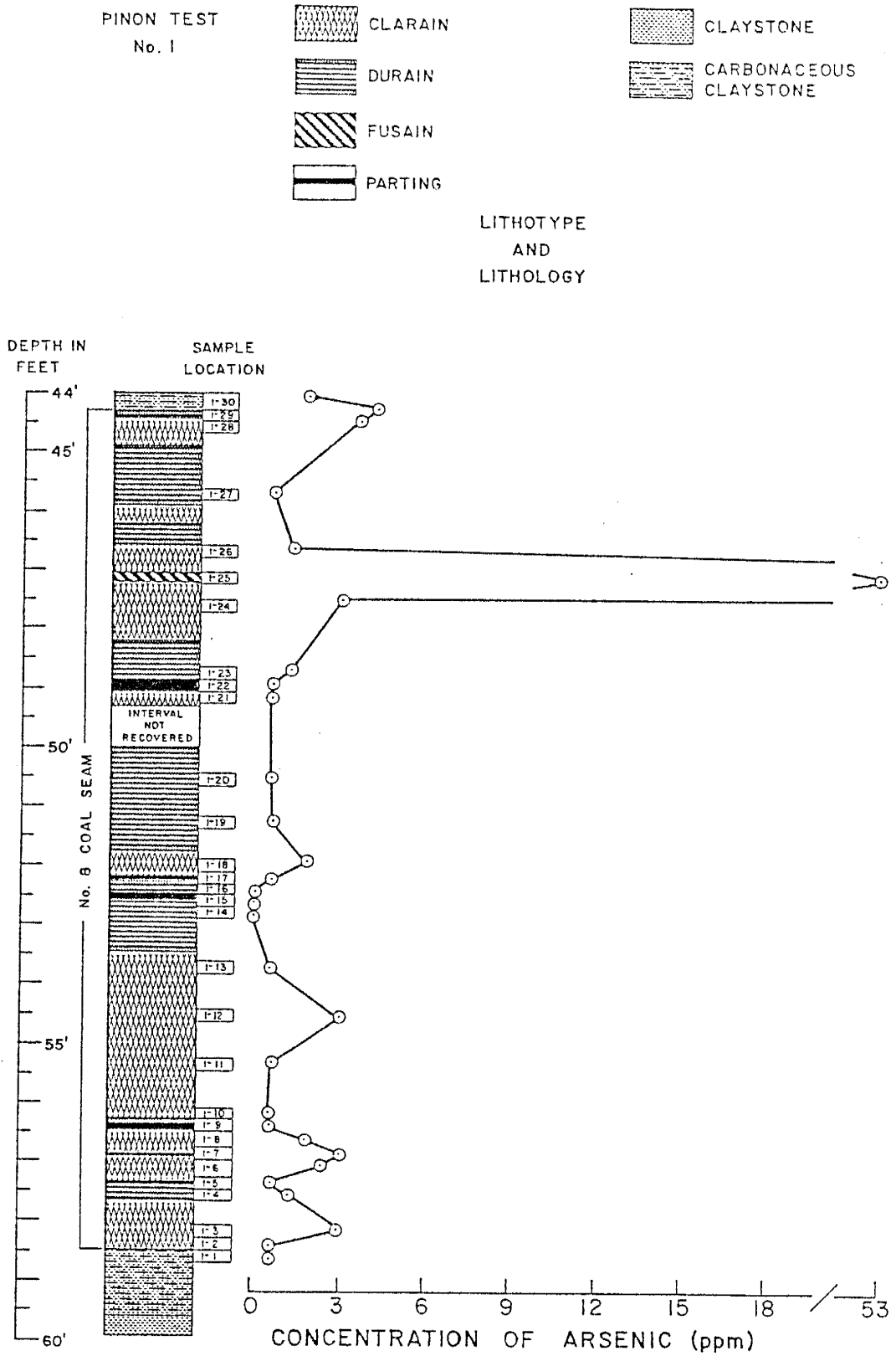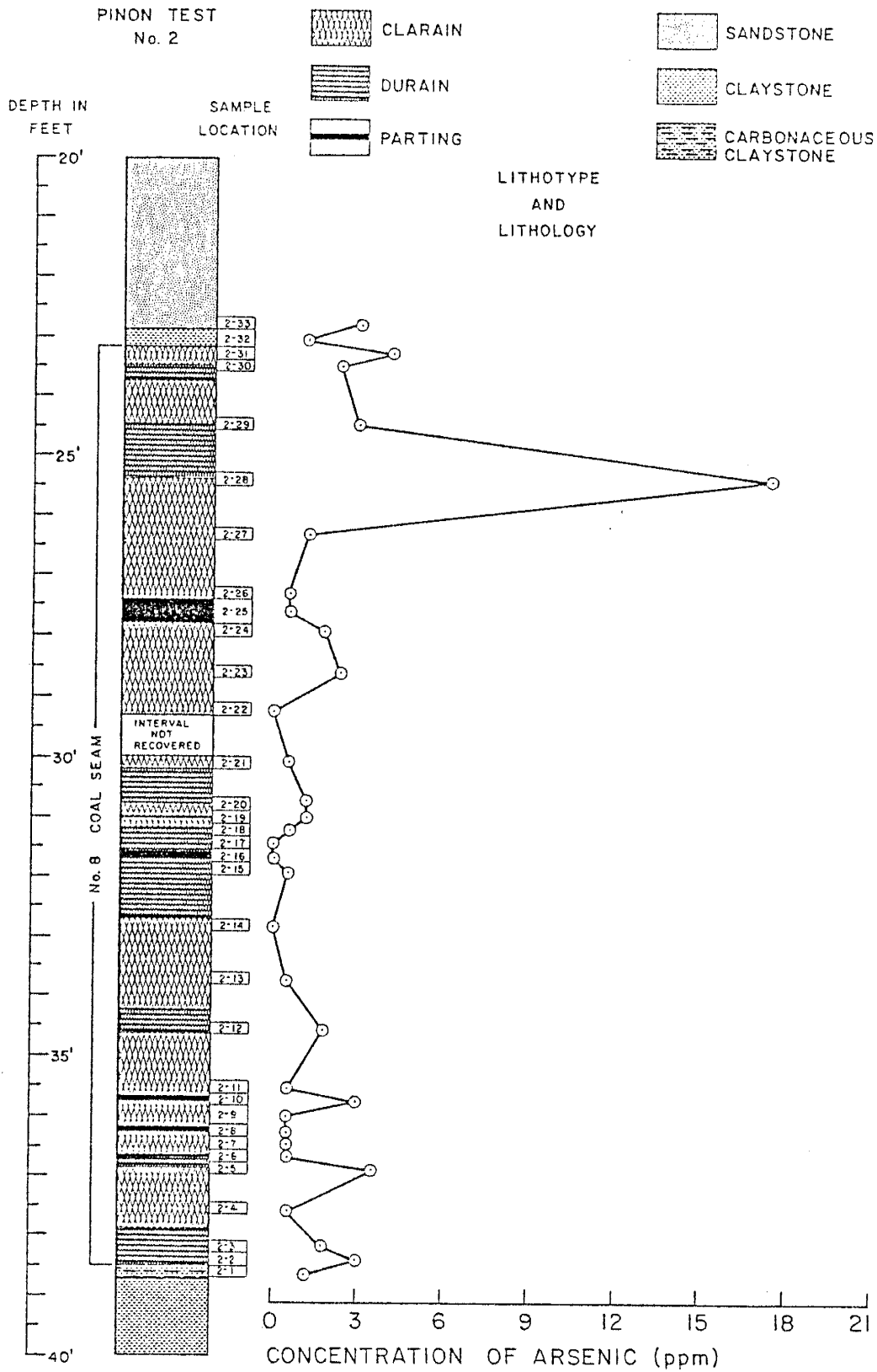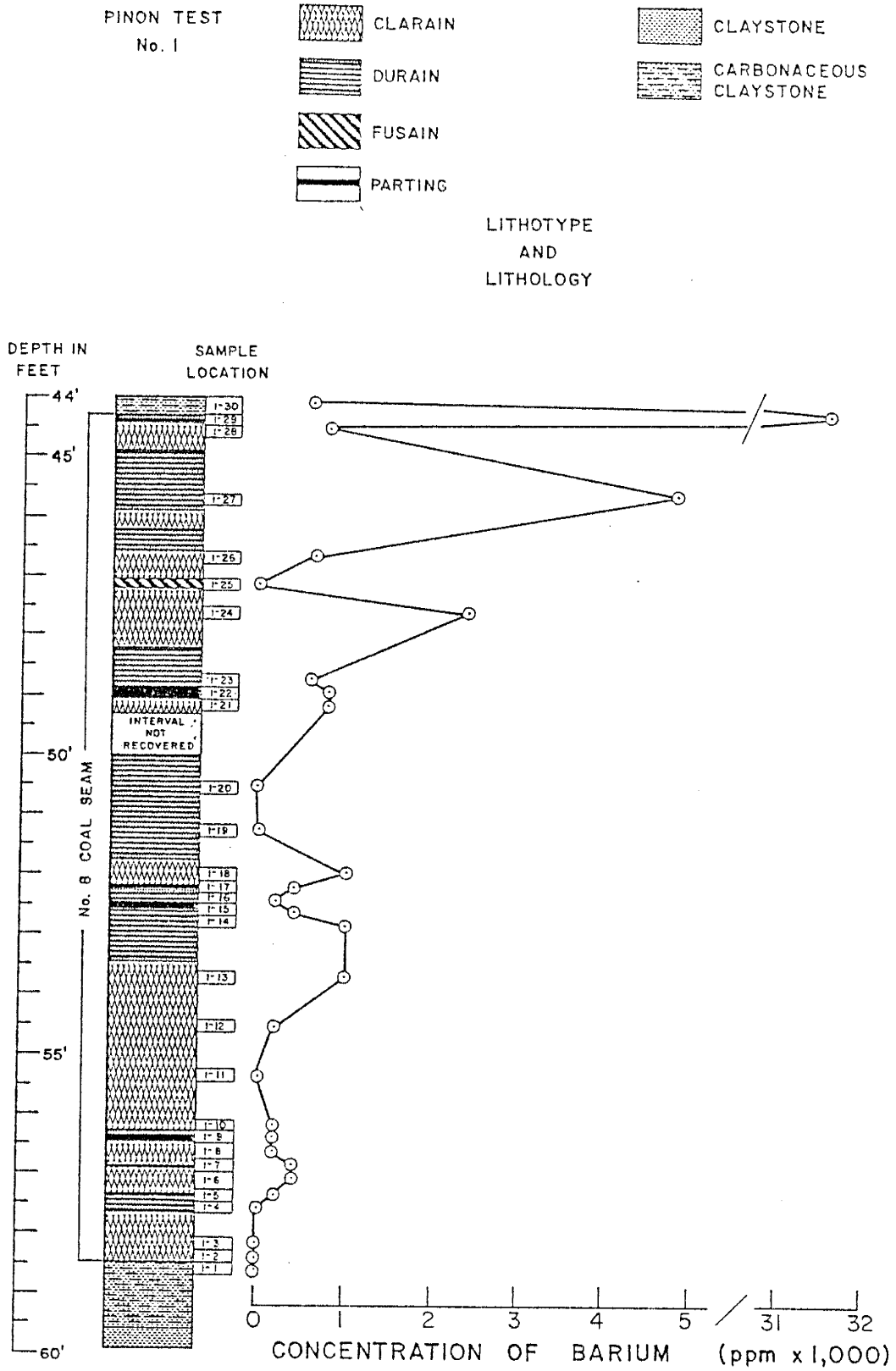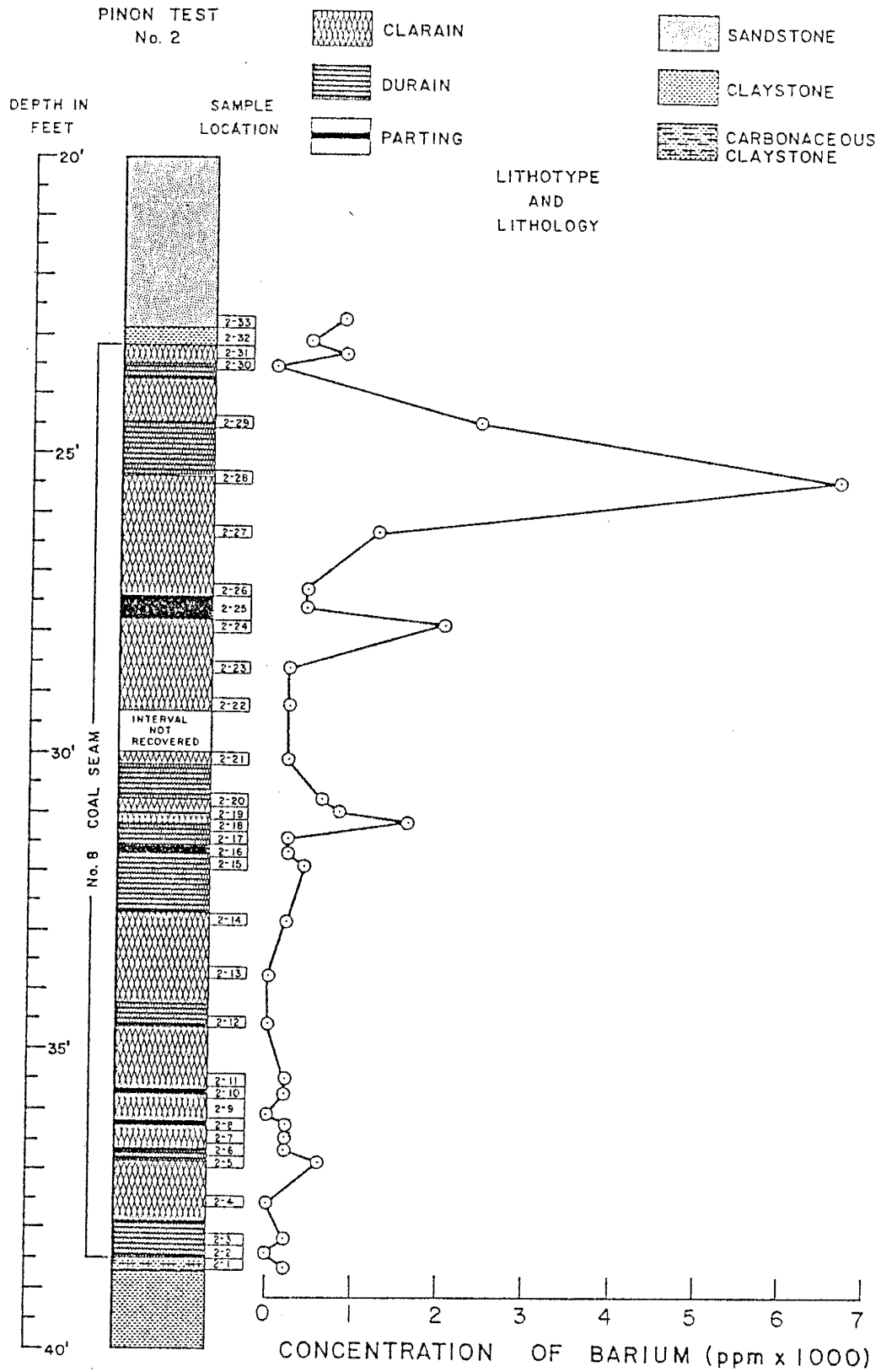Figure A-5 - Distribution of Neodymium
in Pinon Test No. 1.
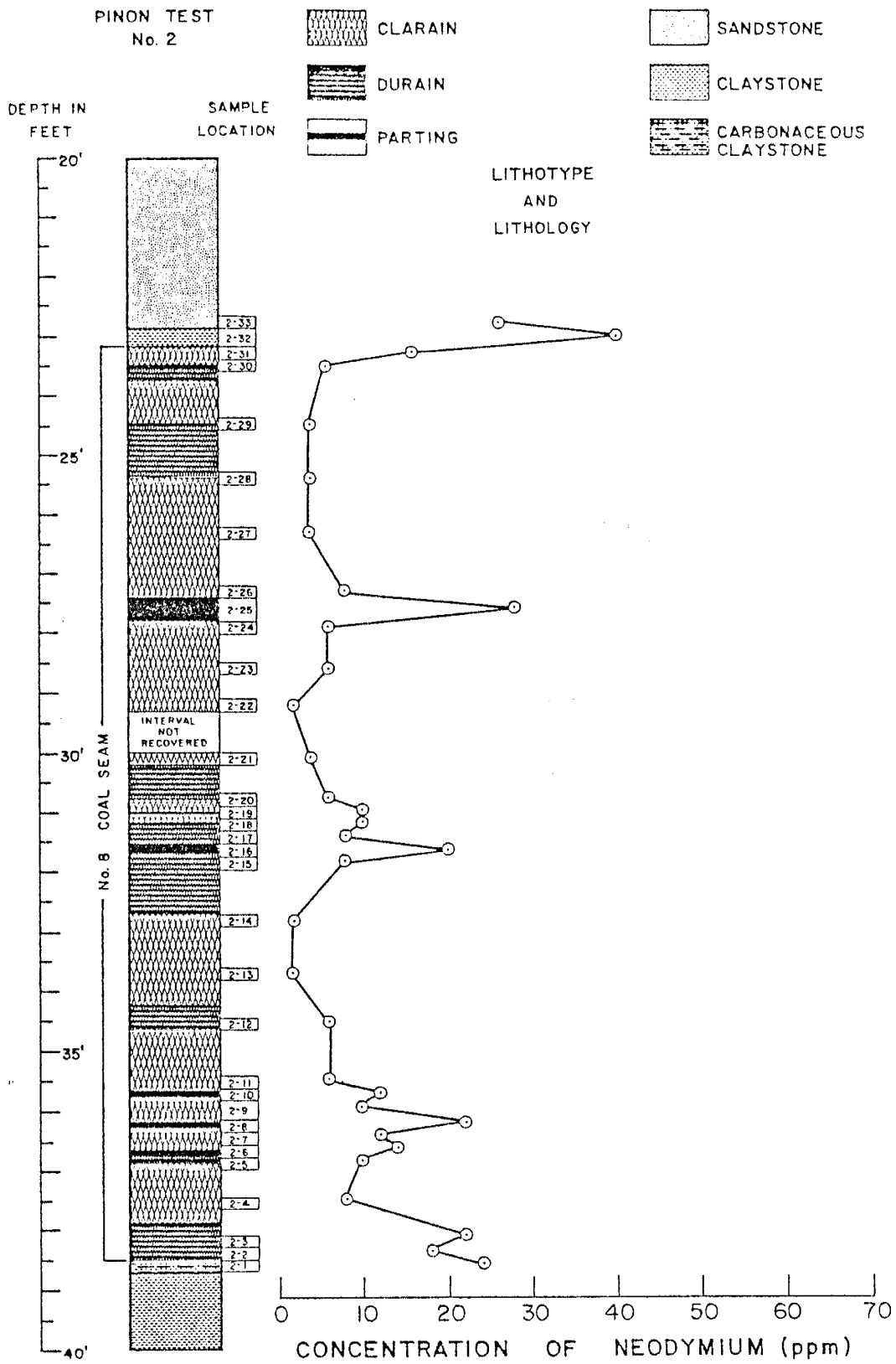
Figure A-6 - Distribution of Neodymium
in Pinon Test No. 2.
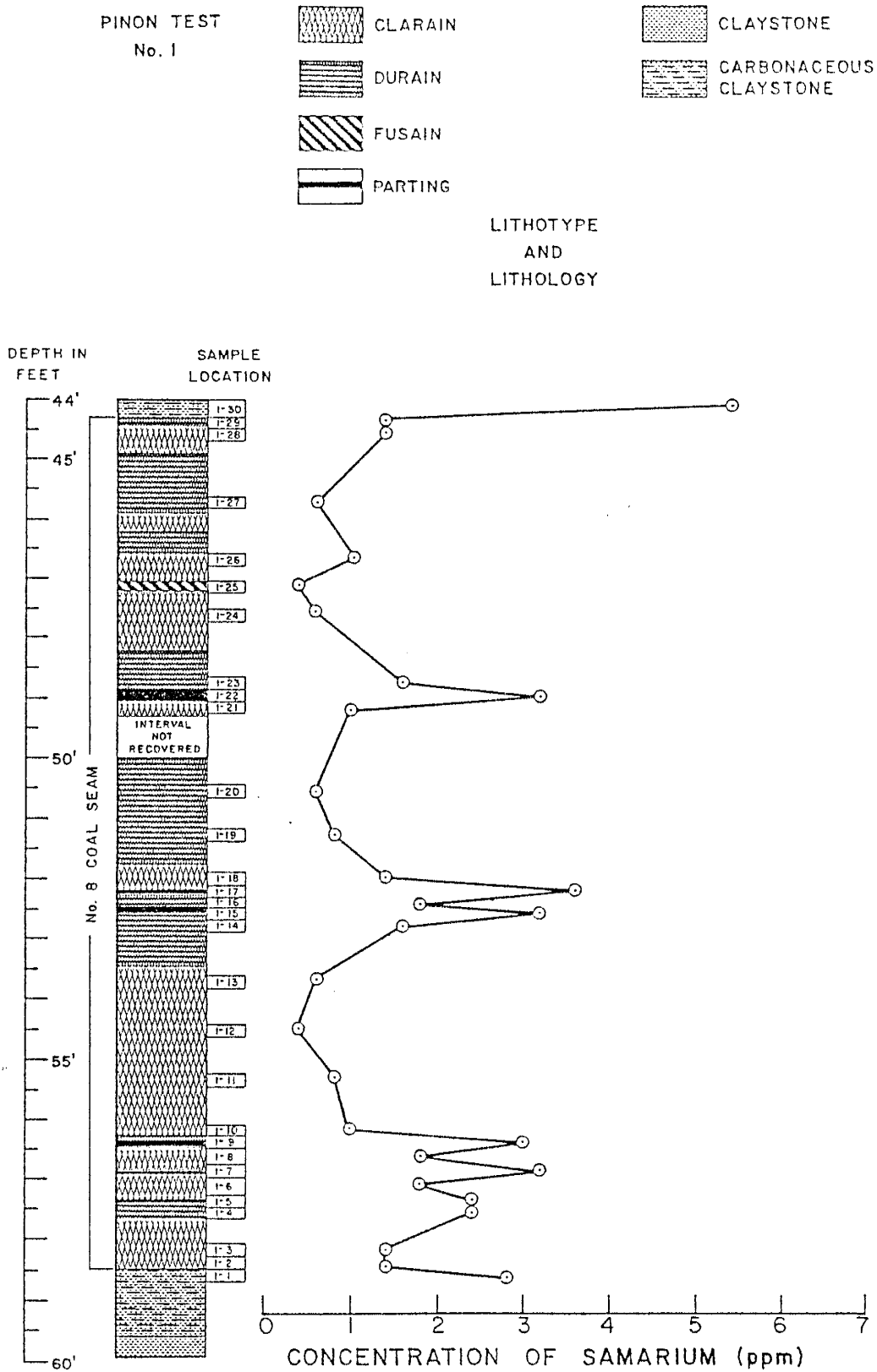
Figure A-7 - Distribution of Samarium
in Pinon Test No. 1.
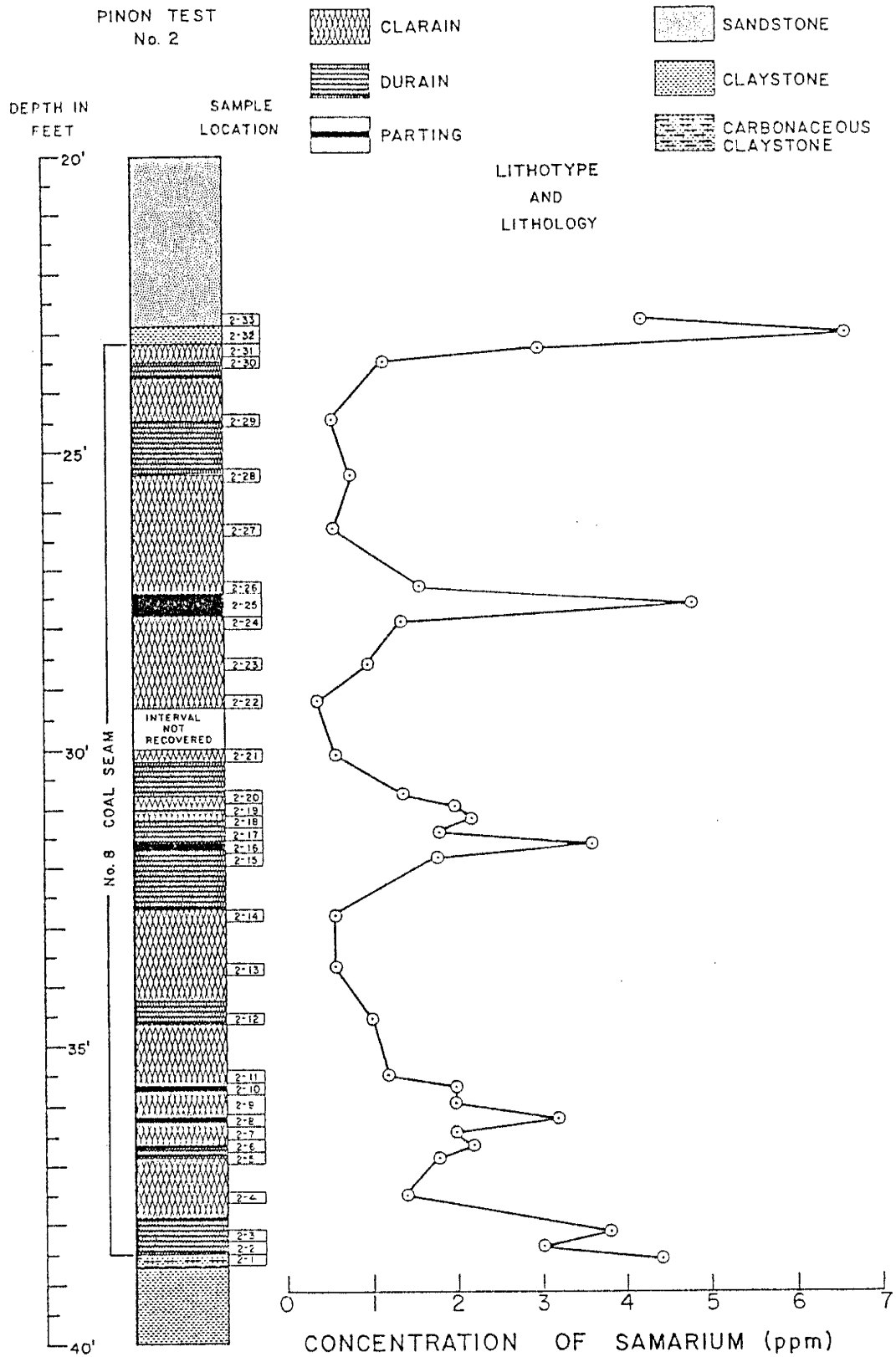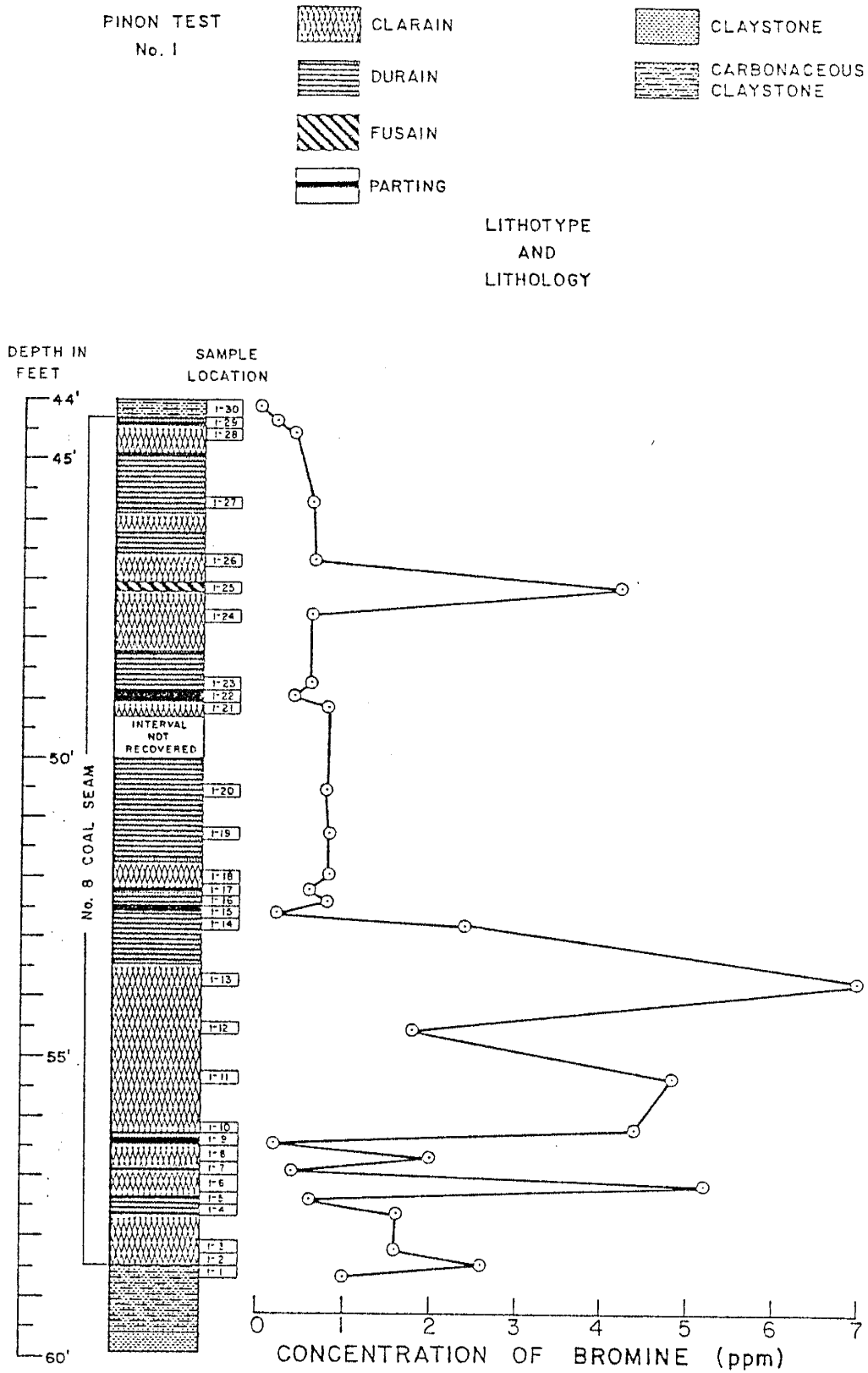
Figure A-8 – Distribution of Samarium
in Pinon Test No. 2.
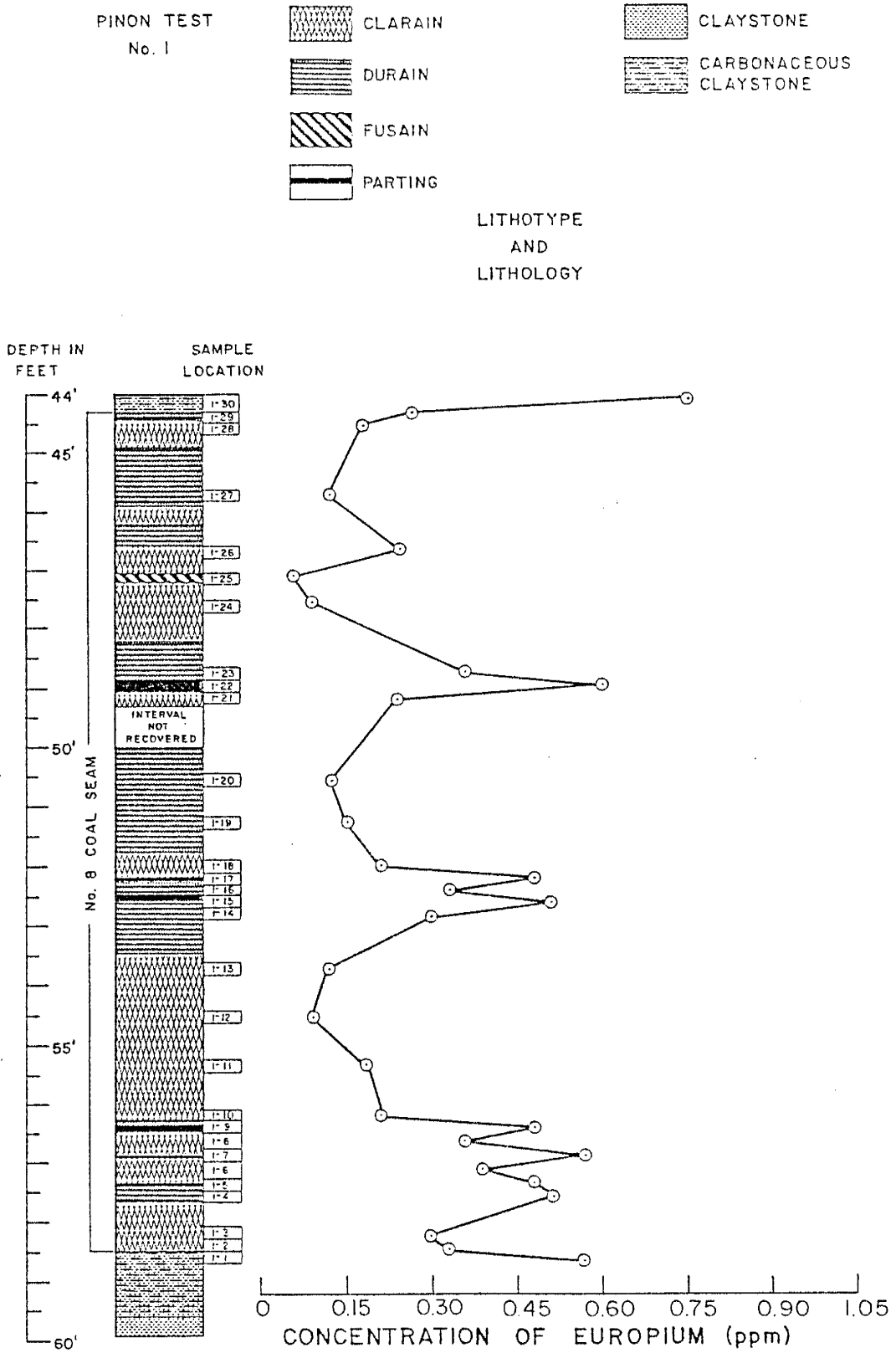
Figure A-9 — Distribution of Europium
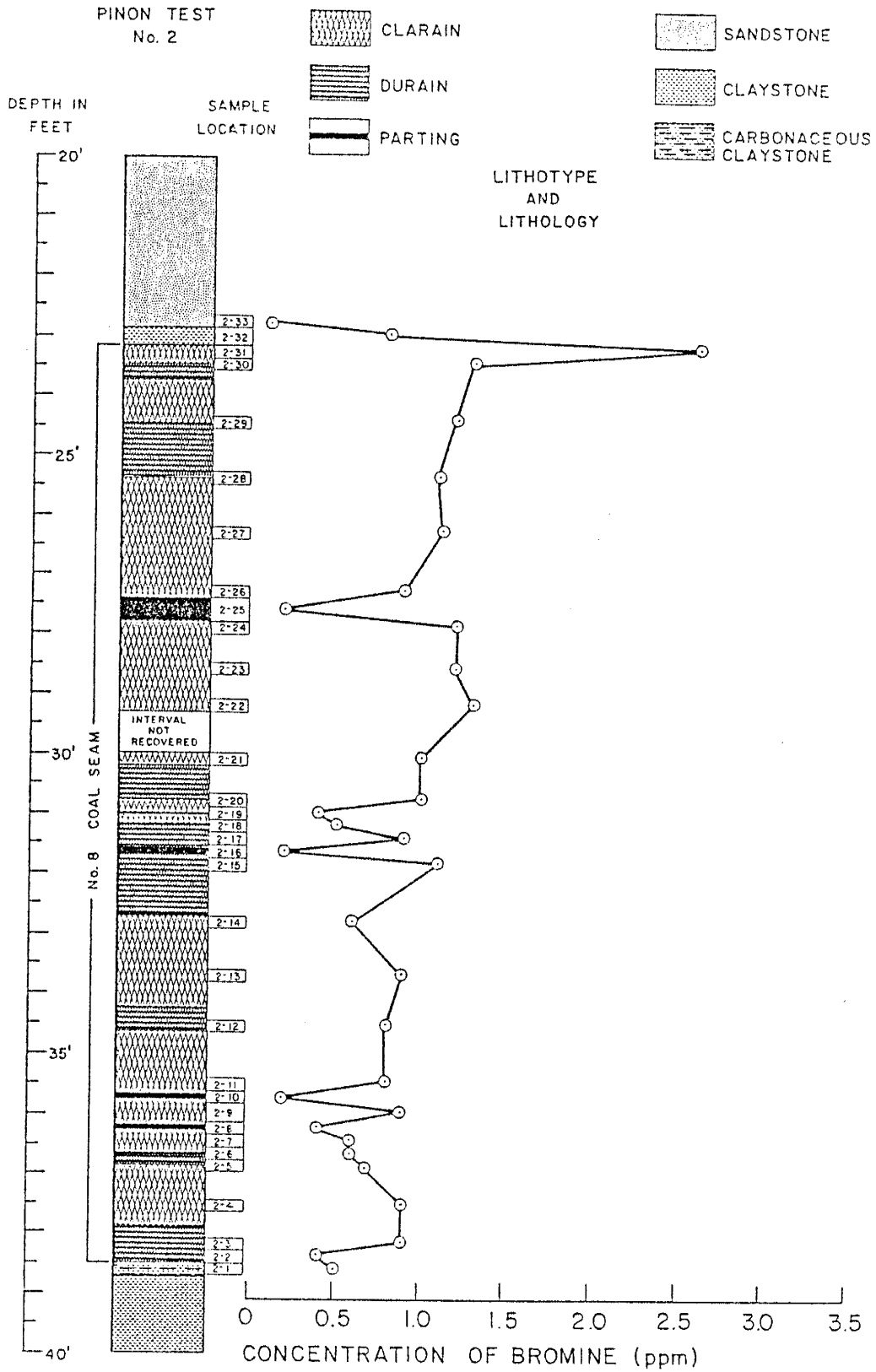in Pinon Test No. 1.
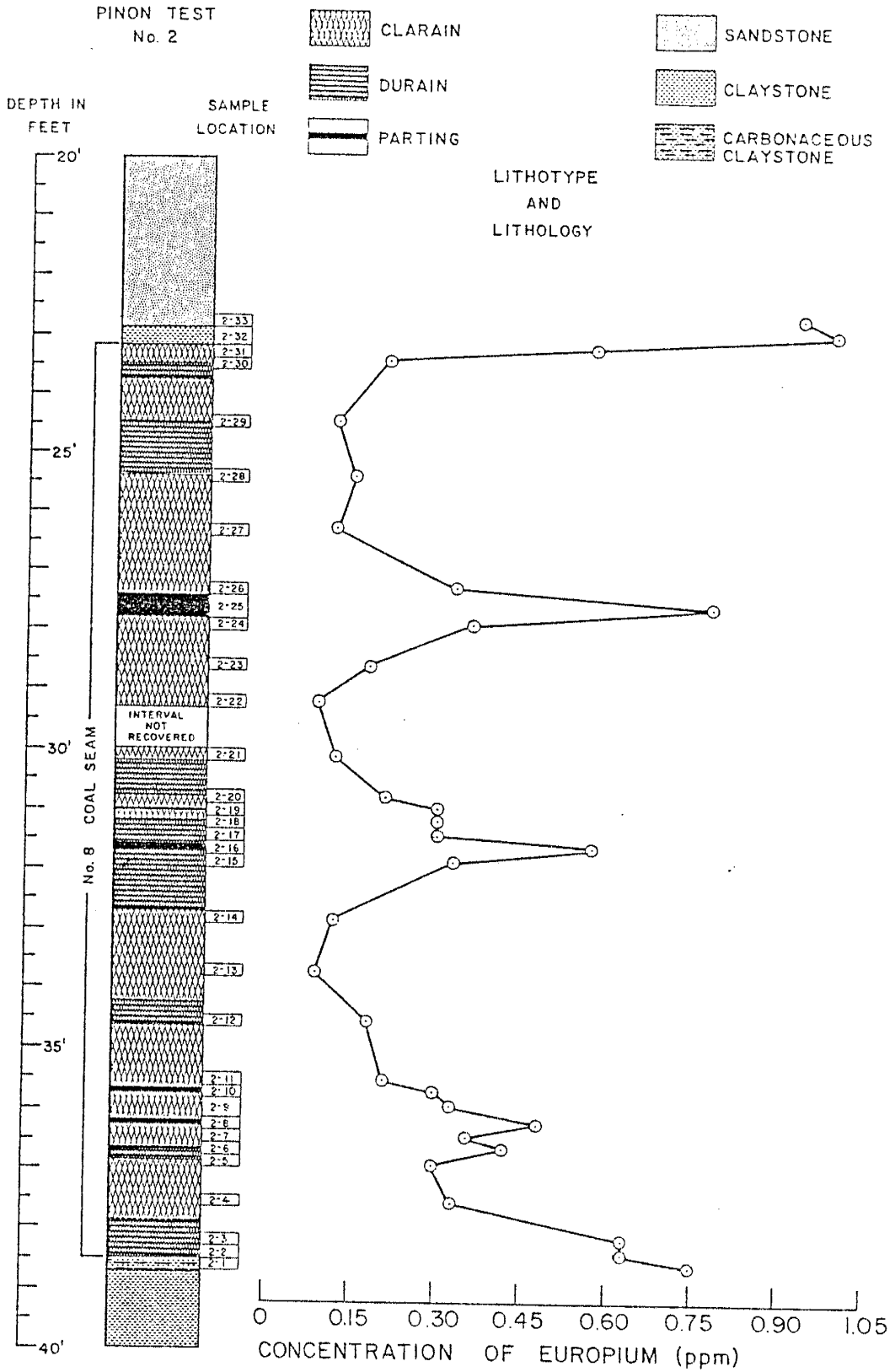
Figure A-10 – Distribution of Europium
in Pinon Test No. 2.

PINON TEST
No. I

CLARAIN

DURAIN

FUSAIN

PARTING

CLAYSTONE

CARBONACEOUS
CLAYSTONE

LITHOTYPE
AND
LITHOLOGY
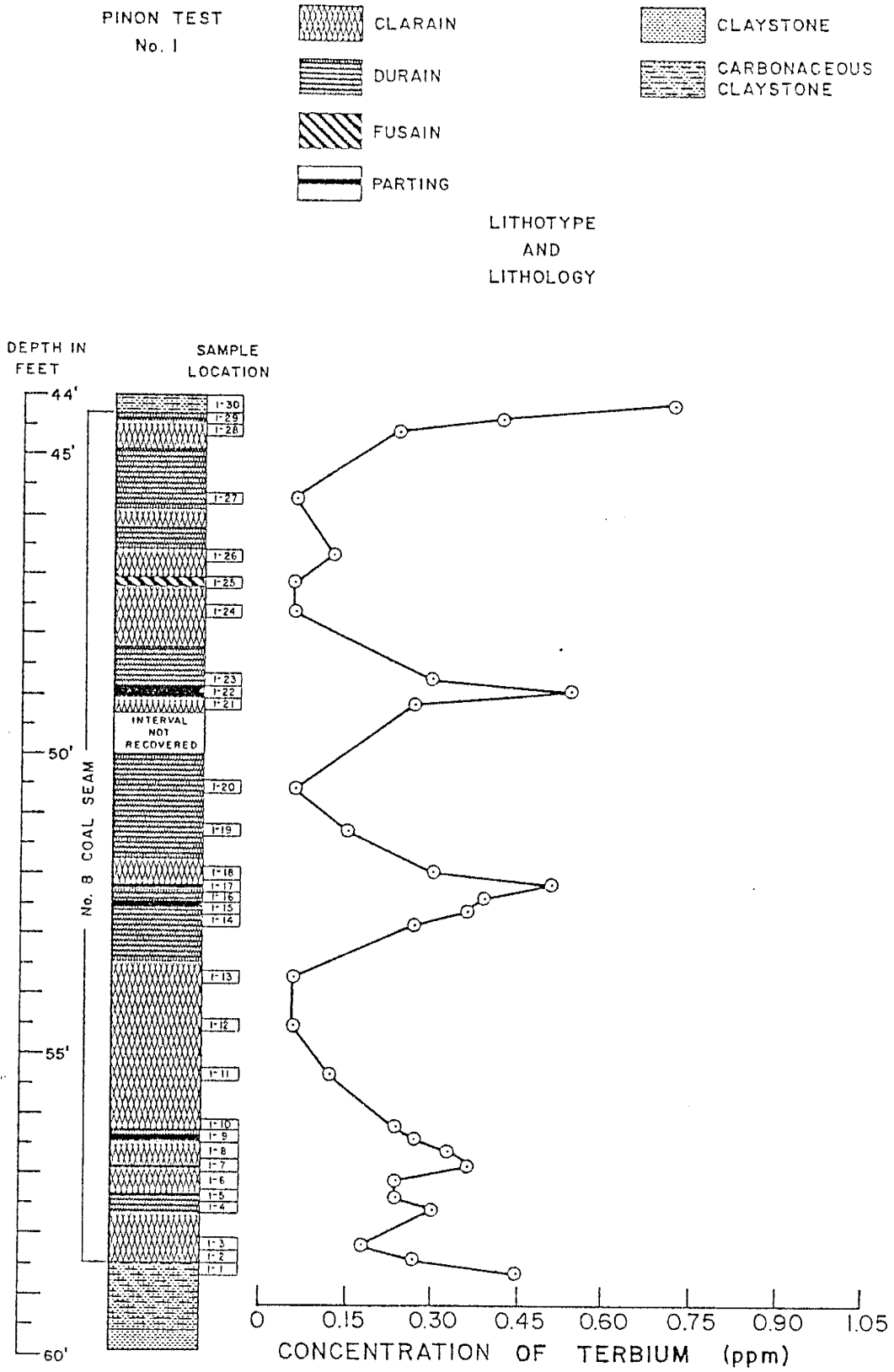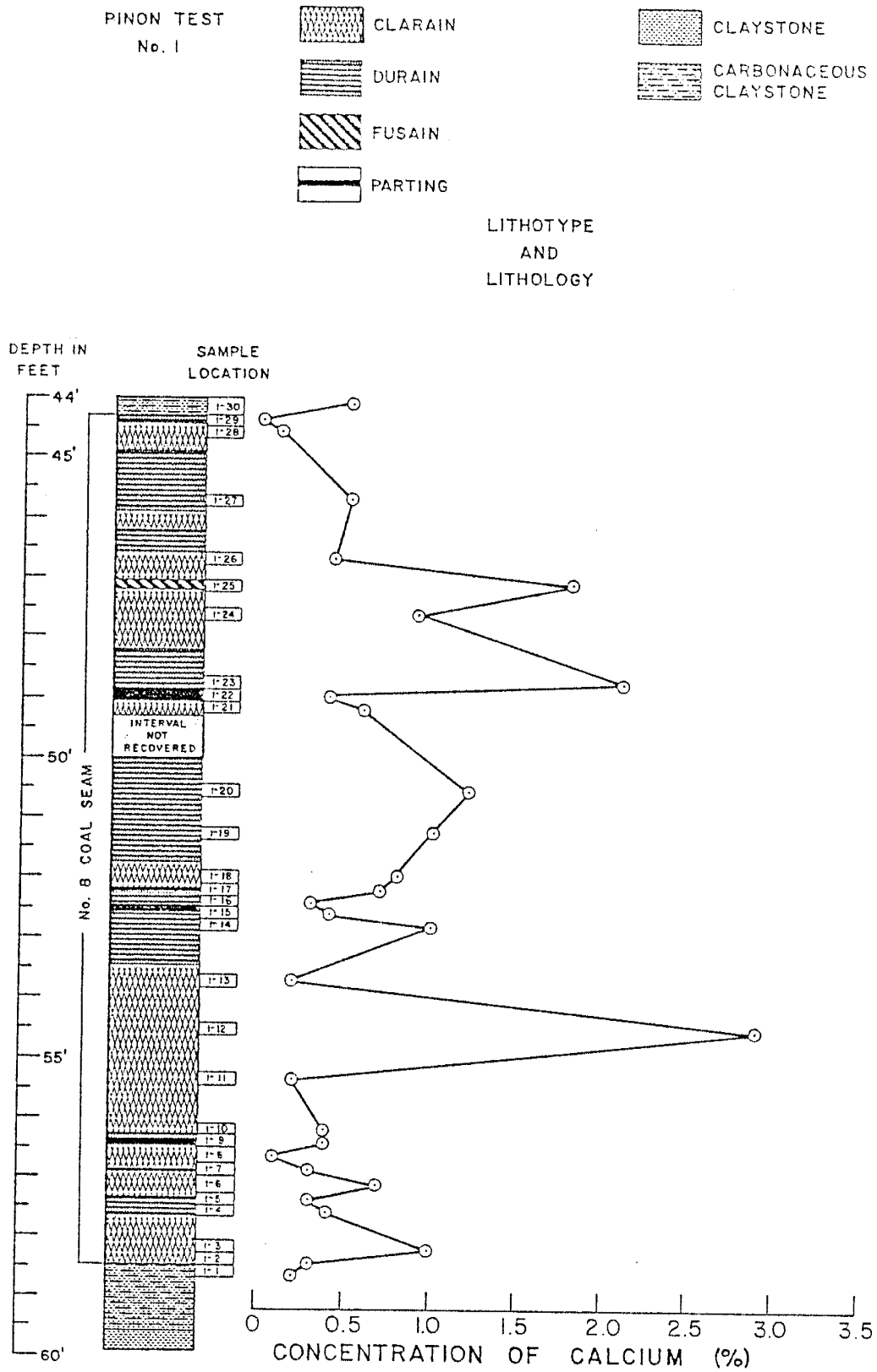


Figure A-11 - Distribution of Terbium
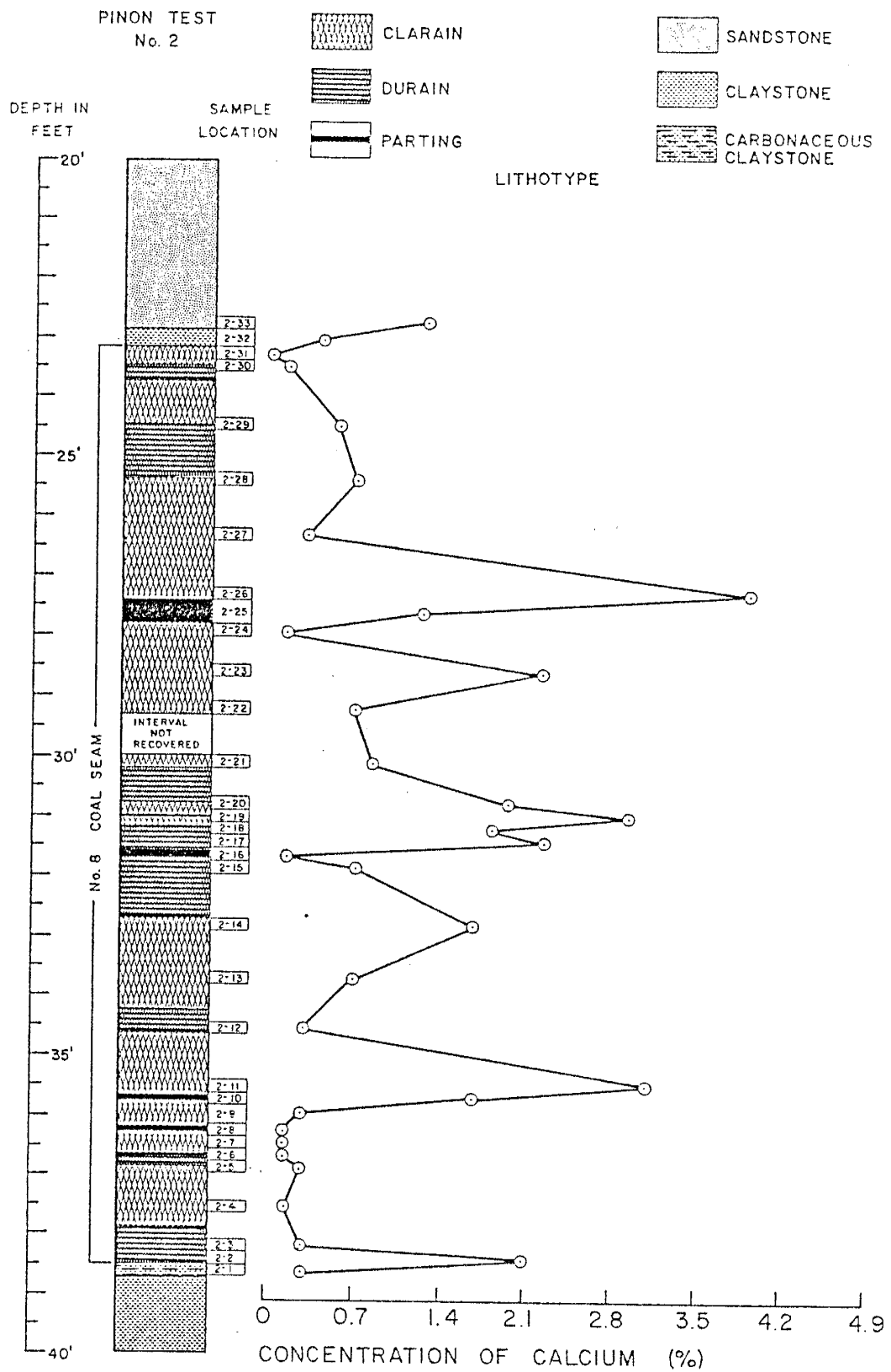in Pinon Test No. 1.
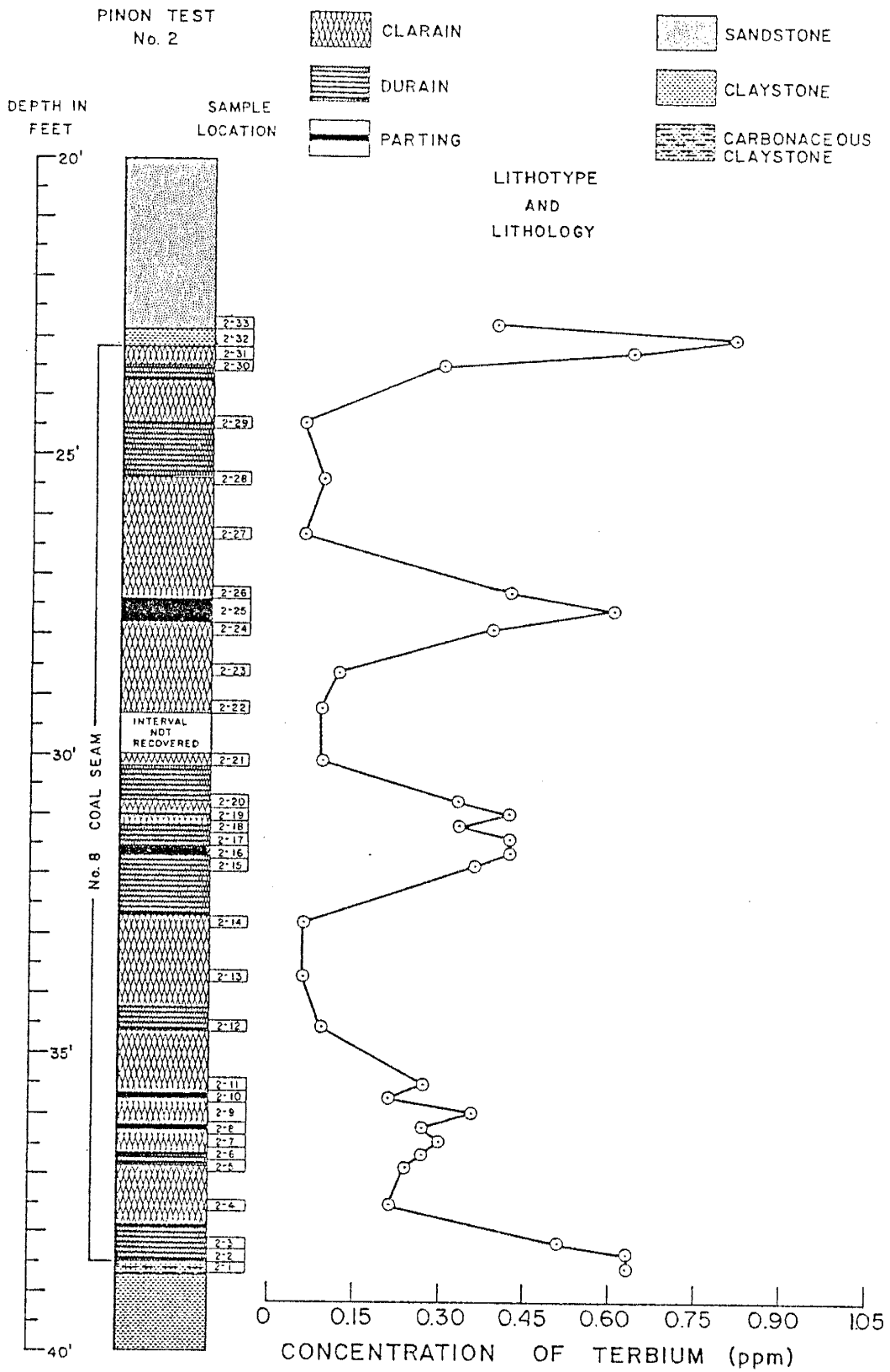
Figure A-12 – Distribution of Terbium
in Pinon Test No. 2.
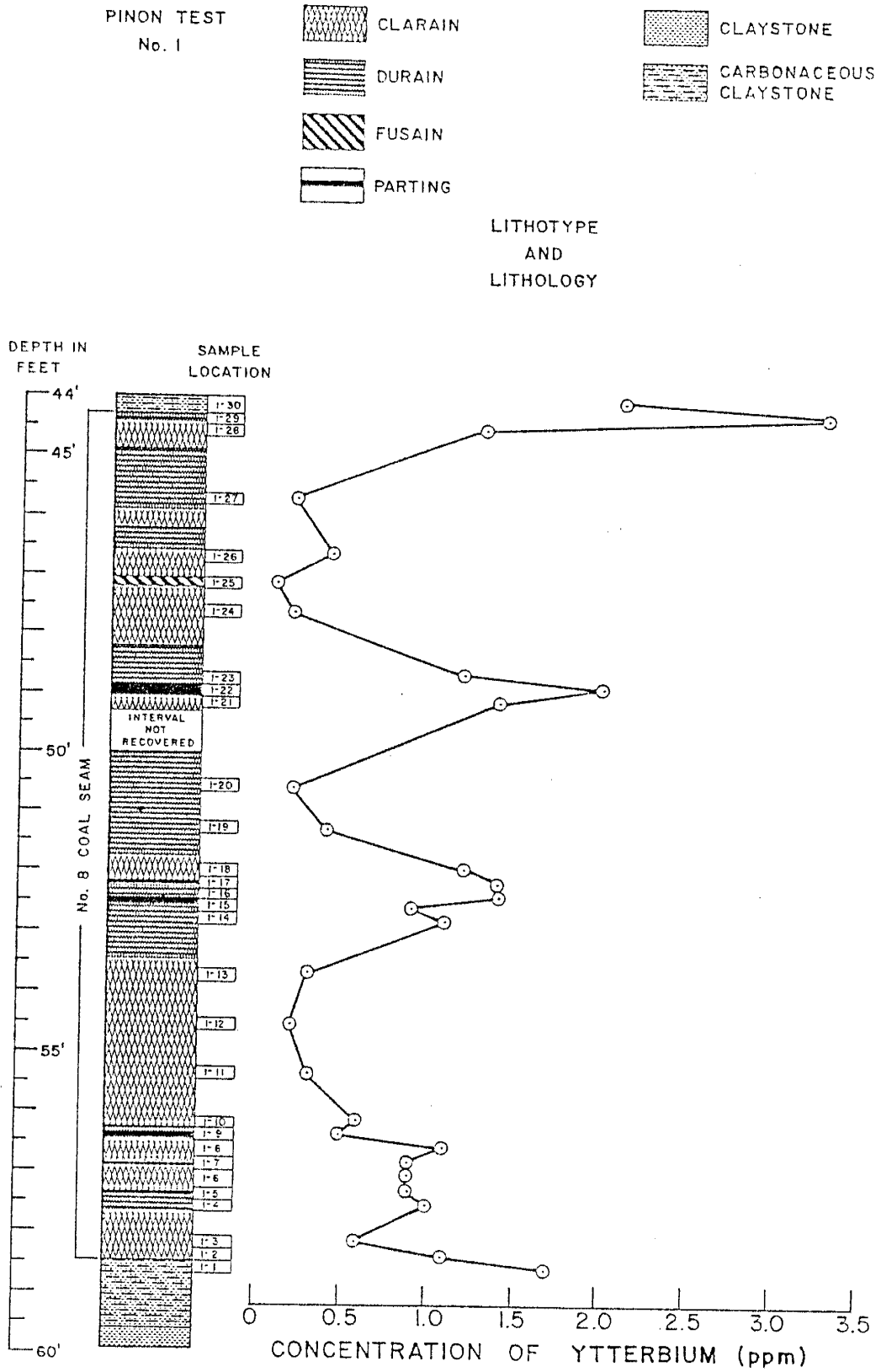
Figure A-13 - Distribution of Ytterbium
in Pinon Test No. 1.
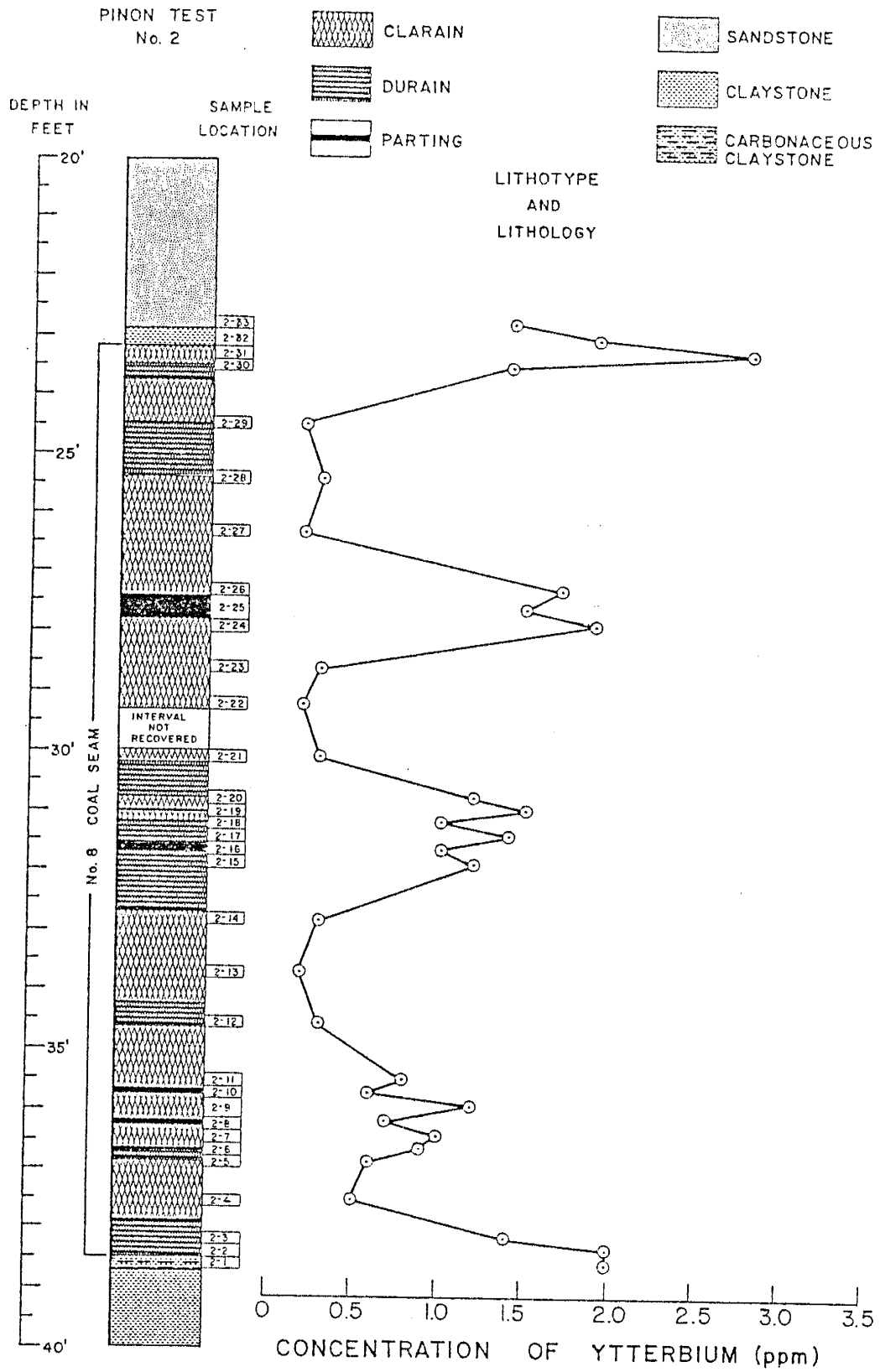
Figure A-14 - Distribution of Ytterbium
in Pinon Test No. 2.
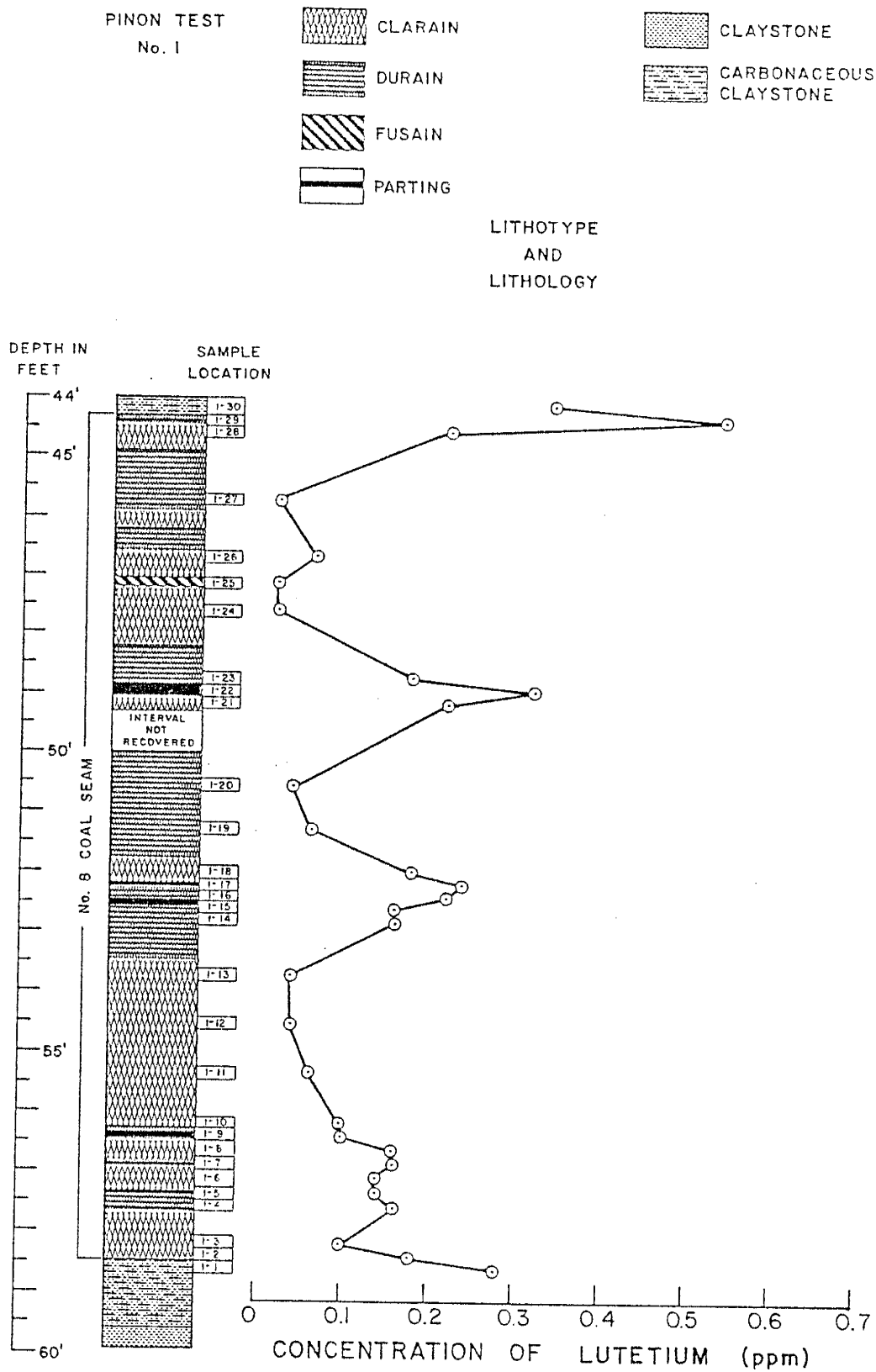
Figure A-15 - Distribution of Lutetium
in Pinon Test No. 1.

Figure A-16 - Distribution of Lutetium
in Pinon Test No. 2.

APPENDIX III

DISTRIBUTION PROFILES

FOR THE OTHER TRACE AND MINOR ELEMENTS

Figure A-17 - Distribution of Antimony
in Pinon Test No. 1.

Figure A-18 - Distribution of Antimony
in Pinon Test No. 2.

Figure A-19 – Distribution of Arsenic
in Pinon Test No. 1.

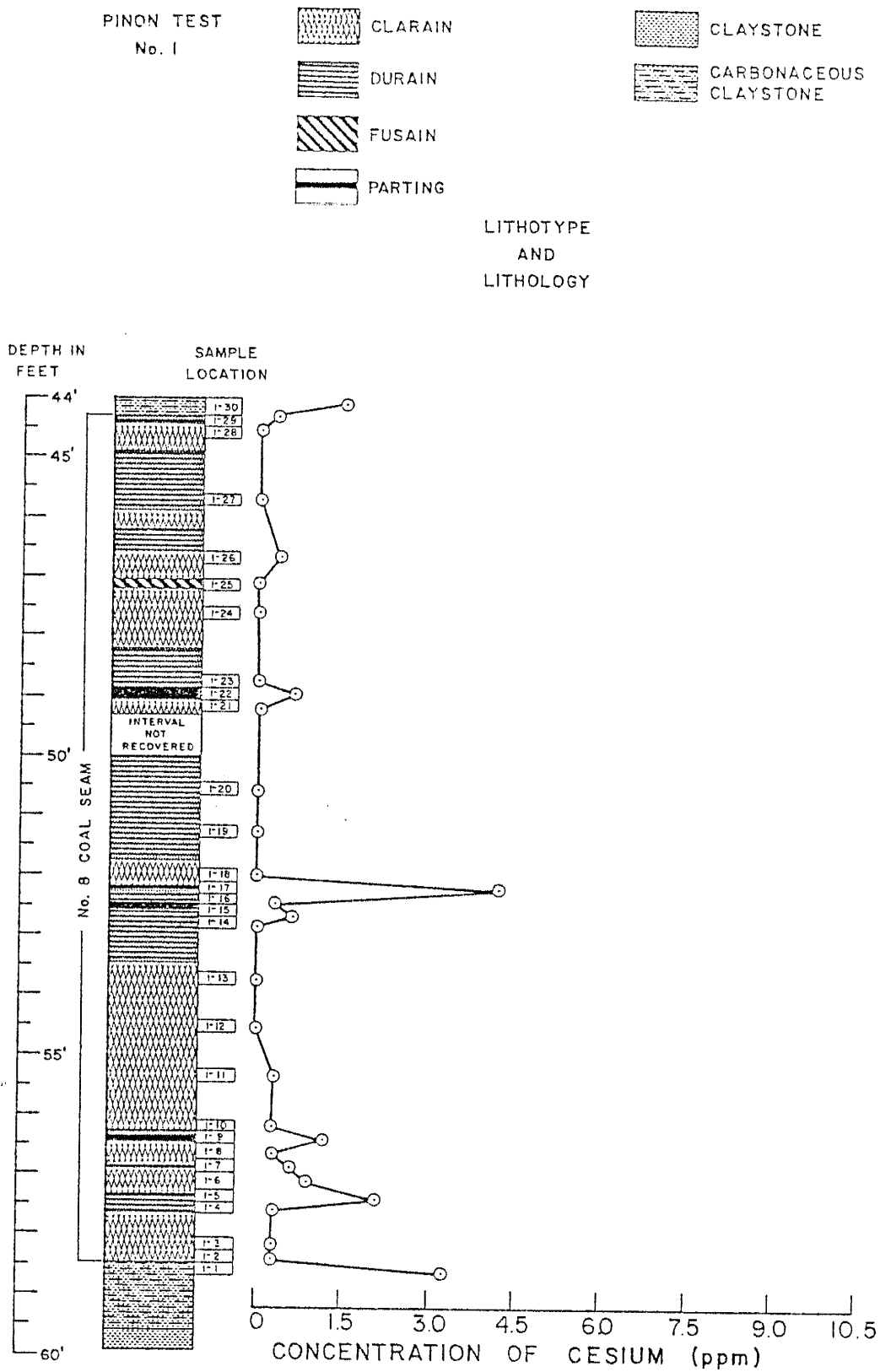Figure A-20 - Distribution of Arsenic
in Pinon Test No. 2.

Figure A-21 - Distribution of Barium
in Pinon Test No. 1.

Figure A-22 - Distribution of Barium
in Pinon Test No. 2.

Figure A-23 - Distribution of Bromine
in Pinon Test No. 1.

Figure A-24 – Distribution of Bromine
in Pinon Test No. 2.

Figure A-25 - Distribution of Calcium
in Pinon Test No. 1.

Figure A-26 — Distribution of Calcium
in Pinon Test No. 2.

Figure A-27 – Distribution of Cesium
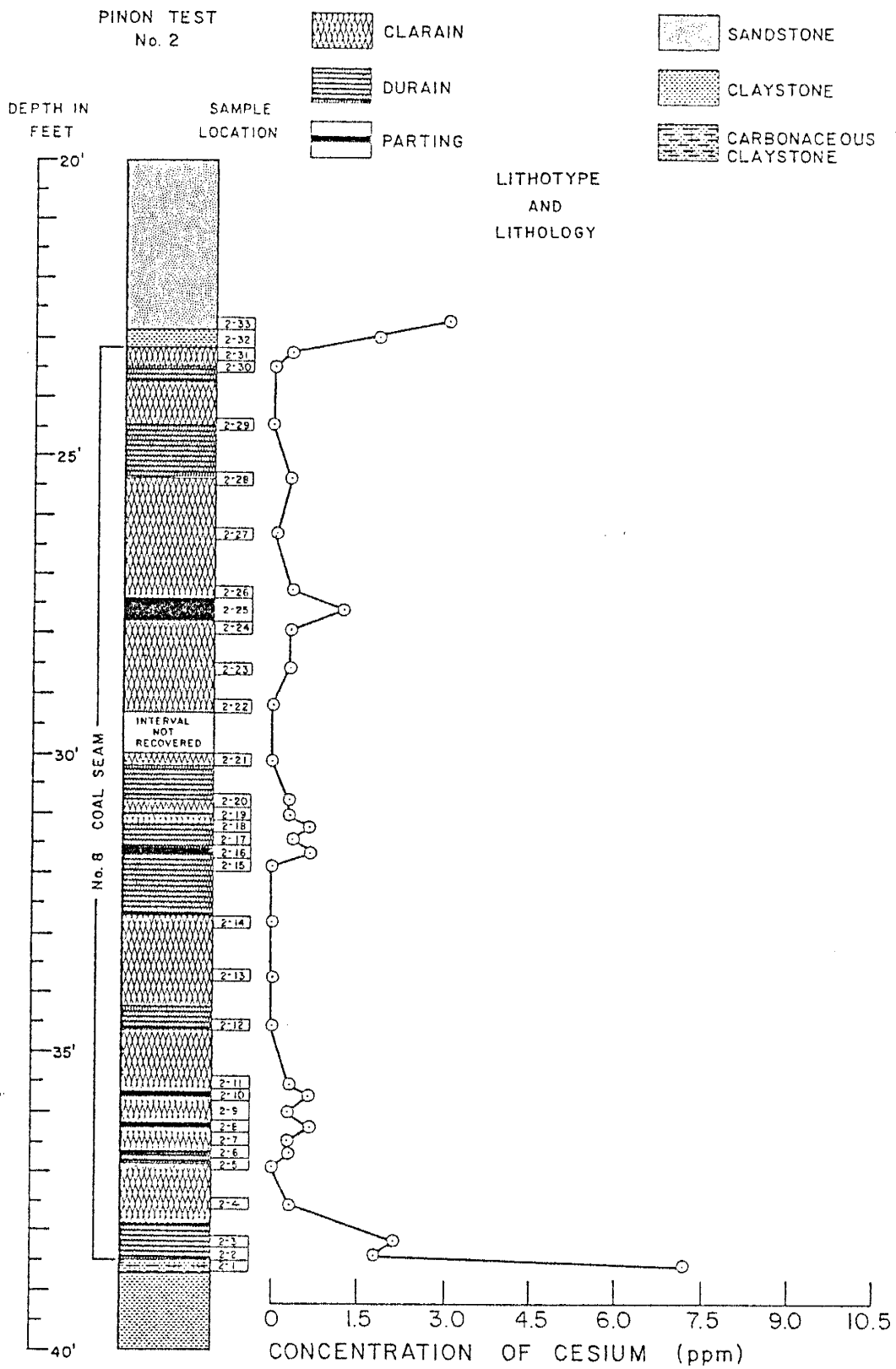in Pinon Test No. 1.

Figure A-28 - Distribution of Cesium
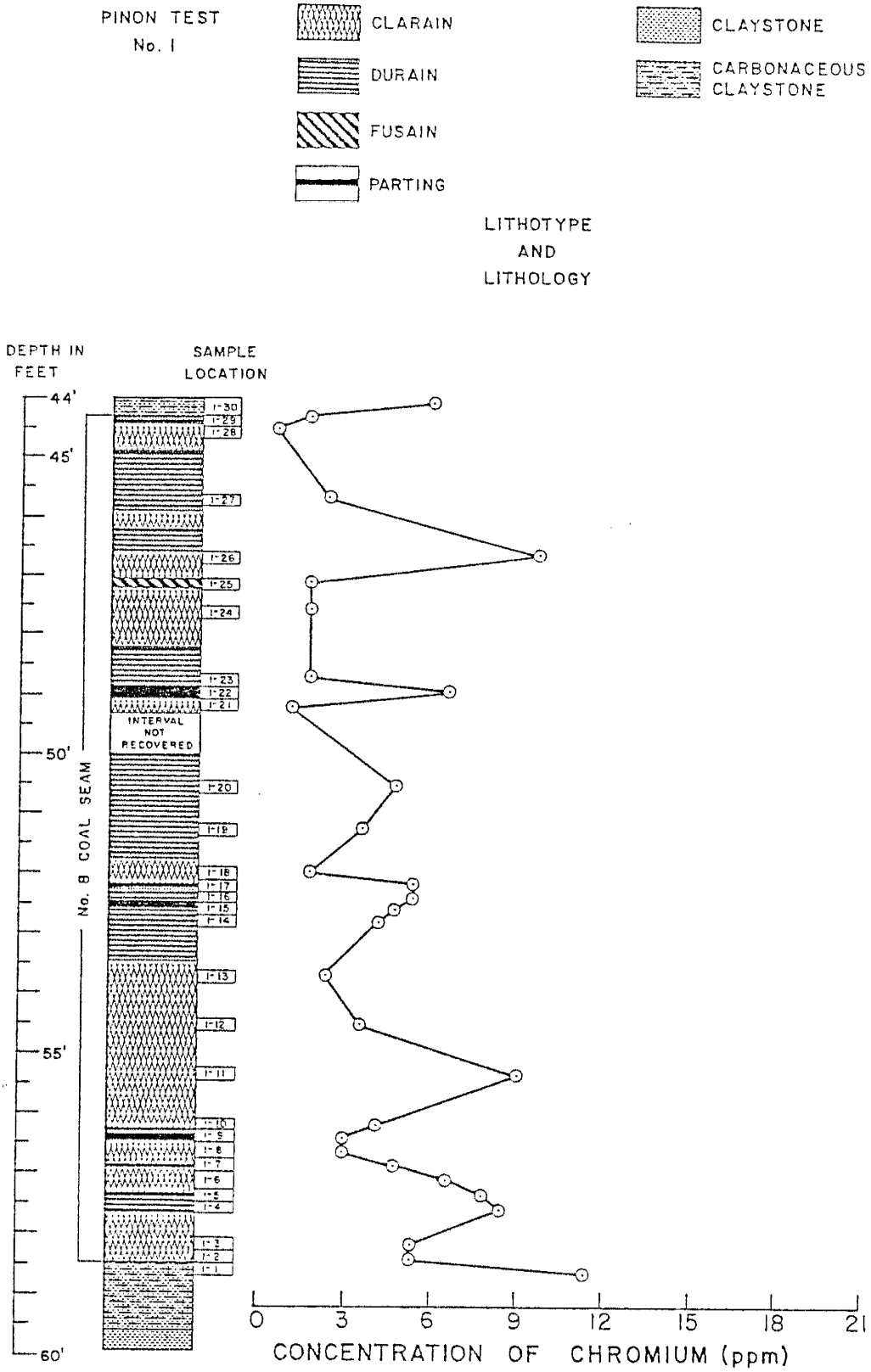in Pinon Test No. 2.

Figure A-29 – Distribution of Chromium
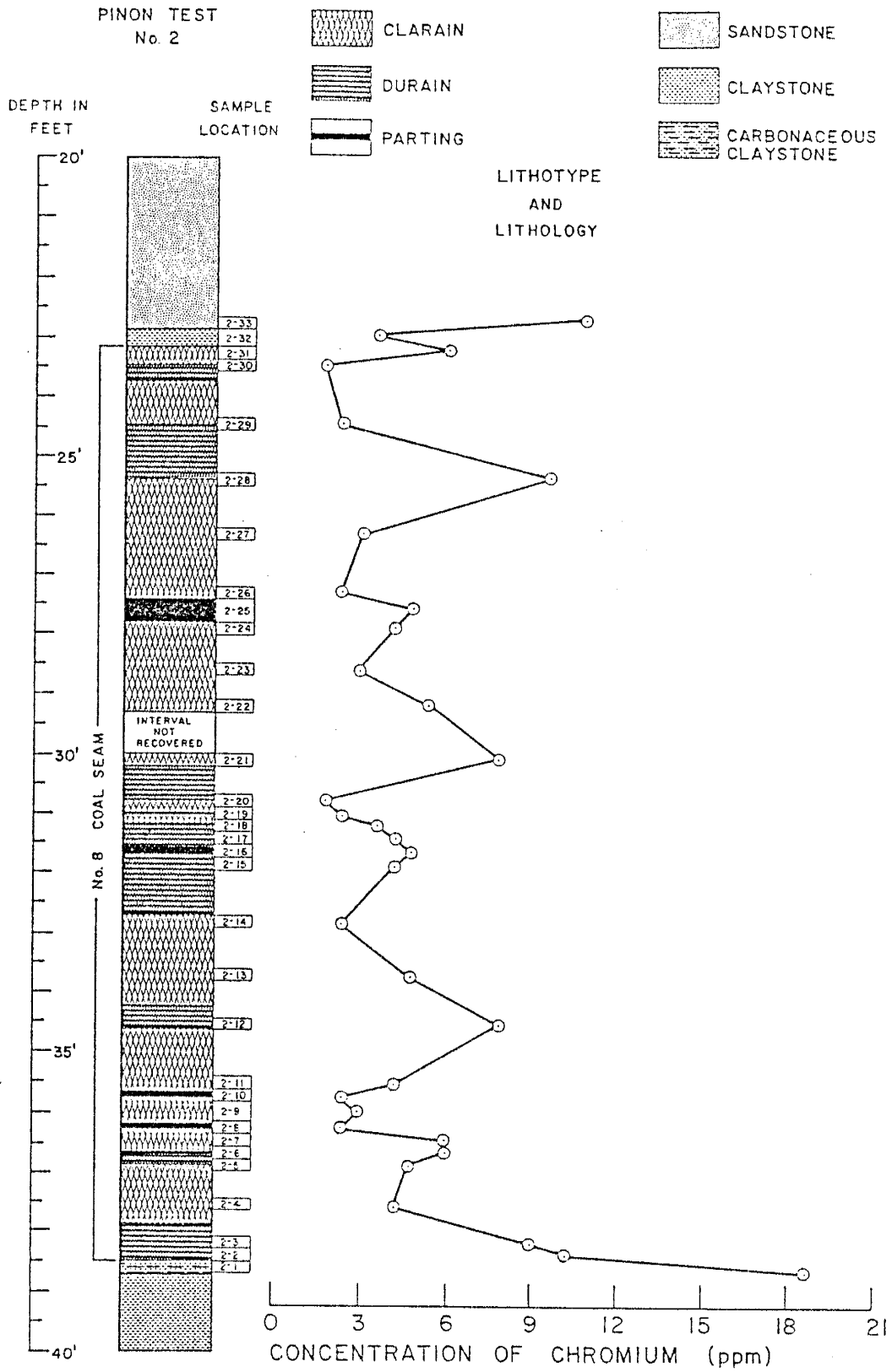in Pinon Test No. 1.

Figure A-30 - Distribution of Chromium
in Pinon Test No. 2.

PINON TEST
No. 1

CLARAIN

DURAIN

FUSAIN

PARTING

CLAYSTONE

CARBONACEOUS
CLAYSTONE
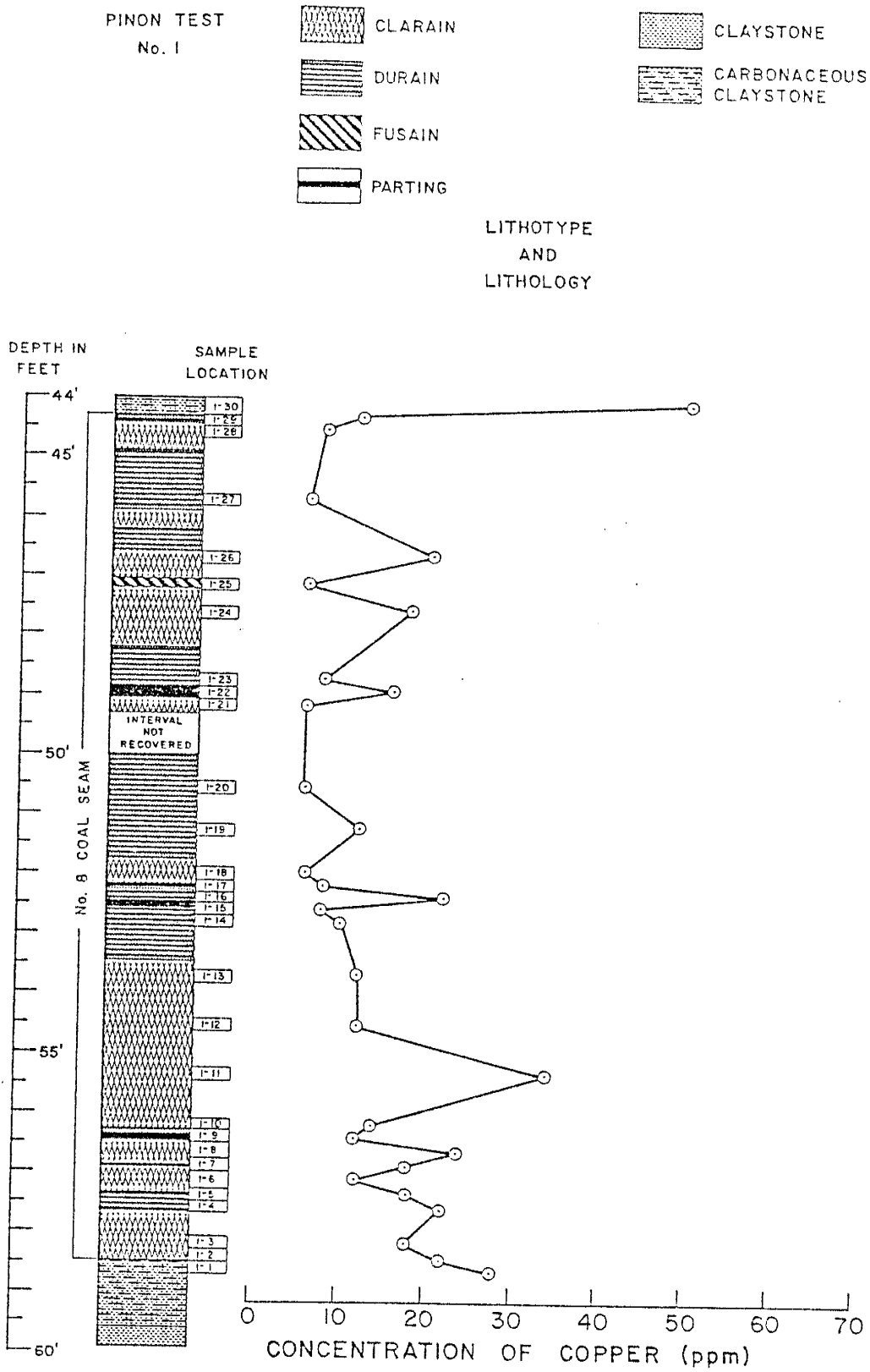
LITHOTYPE
AND
LITHOLOGY



Figure A-31 – Distribution of Copper
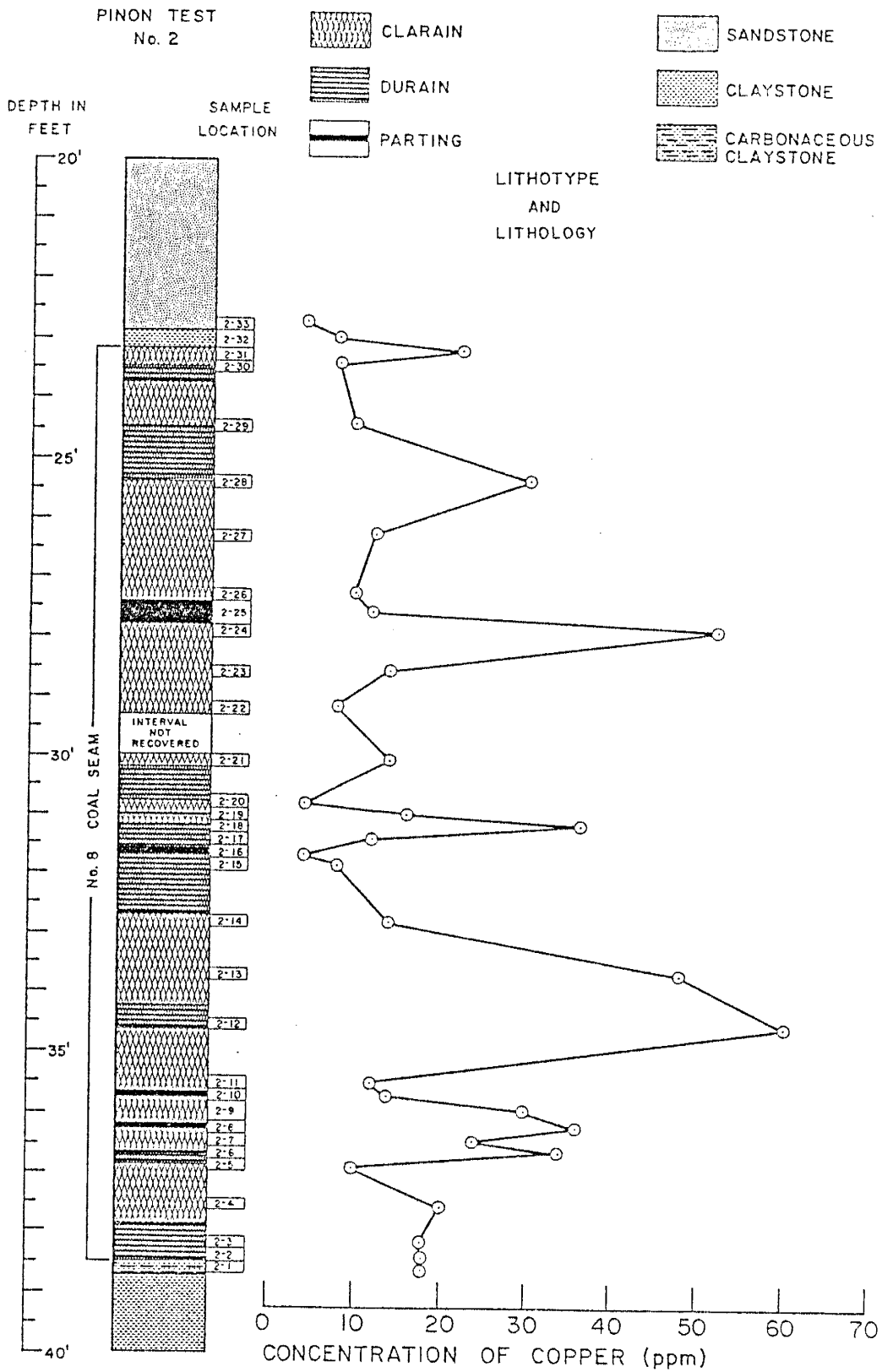in Pinon Test No. 1.

Figure A-32 - Distribution of Copper
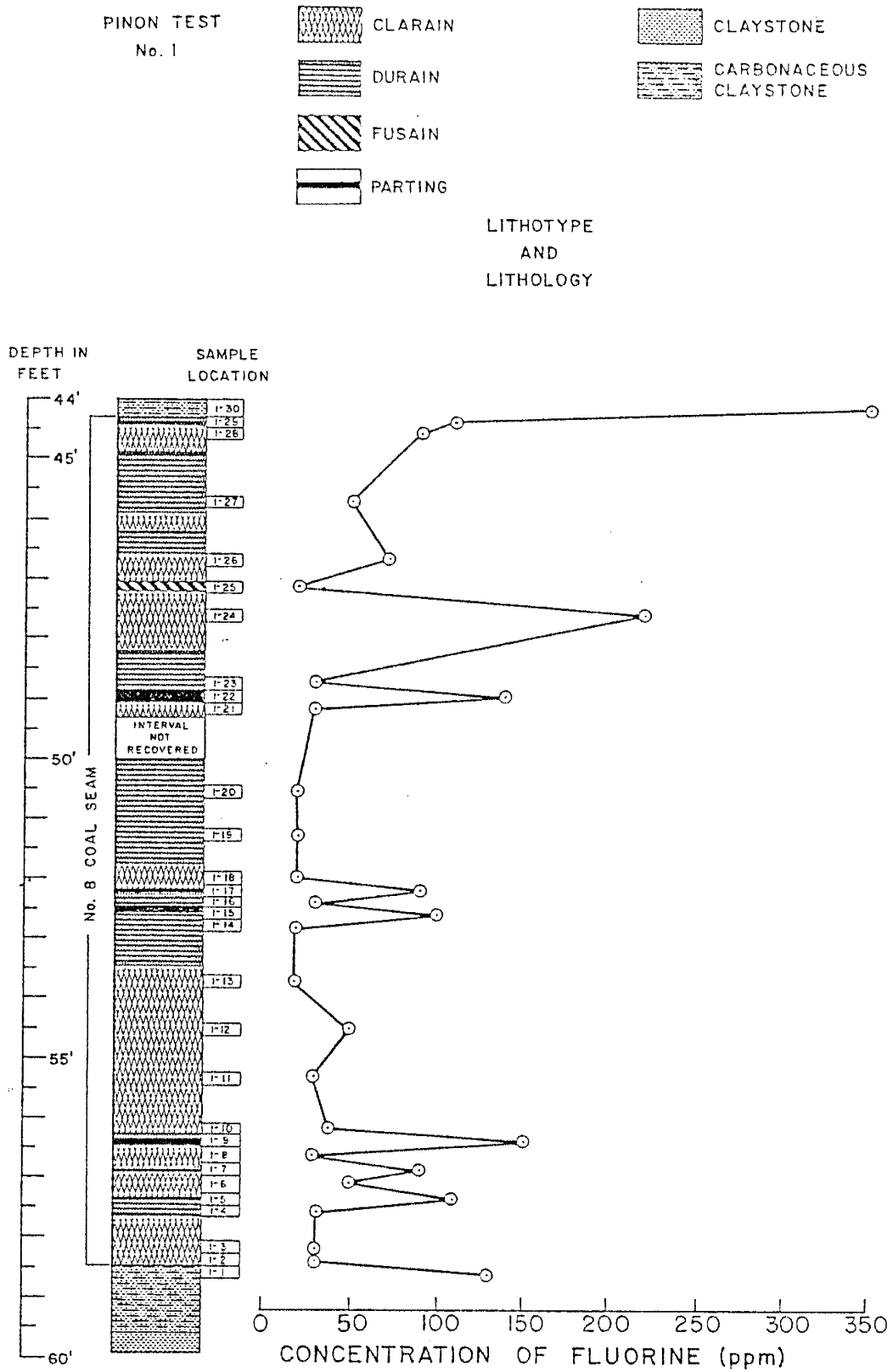in Pinon Test No. 2.

Figure A-33 - Distribution of Fluorine
in Pinon Test No. 1.
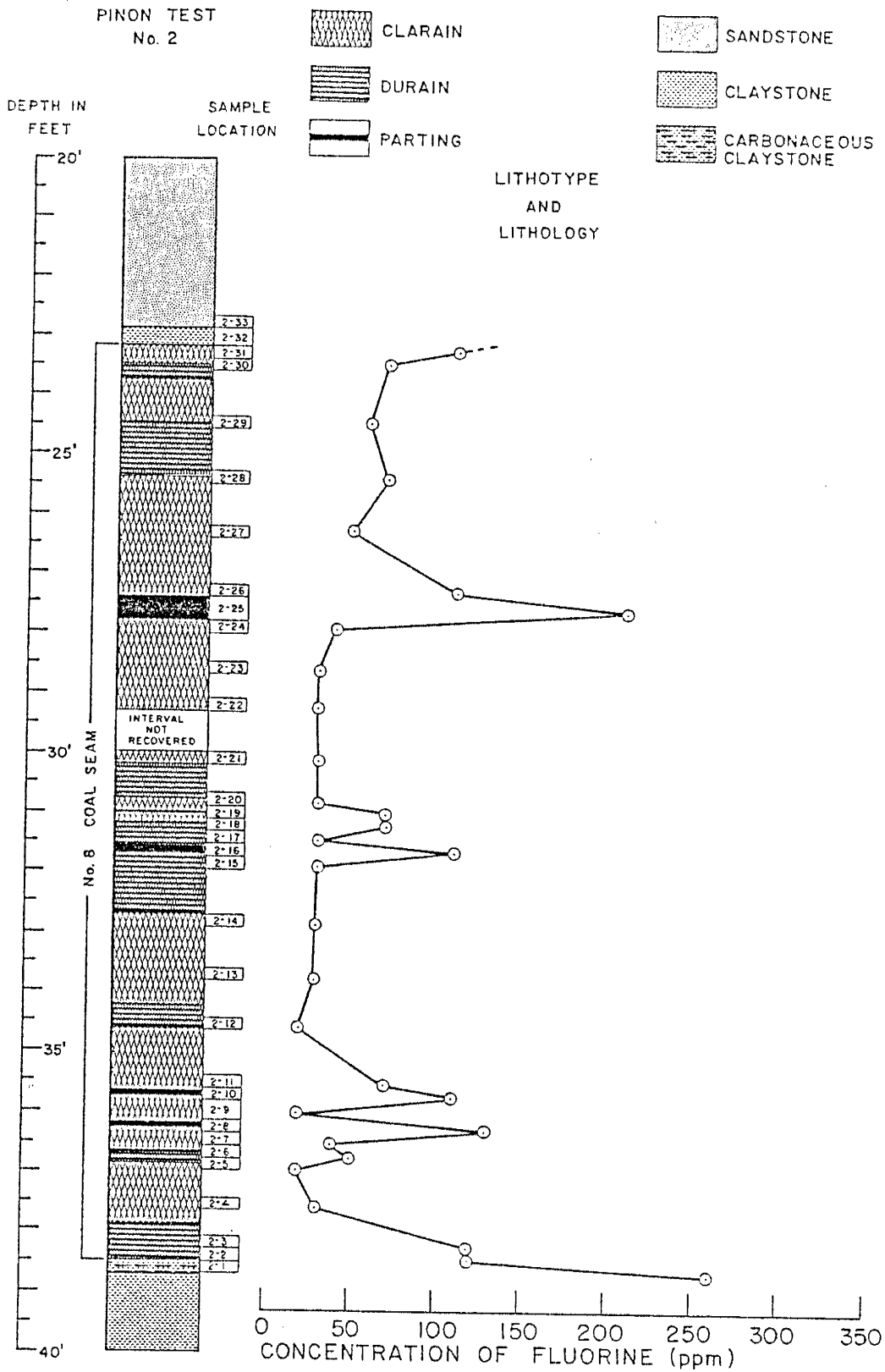
Figure A-34 - Distribution of Fluorine
in Pinon Test No. 2.

Figure A-35 – Distribution of Hafnium
in Pinon Test No. 1.

Figure A-36 - Distribution of Hafnium
in Pinon Test No. 2.

Figure A-37 - Ash normalized distribution of
Hafnium in Pinon Test No. 1.

Figure A-38 - Ash normalized distribution of
Hafnium in Pinon Test No. 2.

Figure A-39 – Distribution of Iron
in Pinon Test No. 1.

(122)



Figure A-40 - Distribution of Iron
in Pinon Test No. 2.
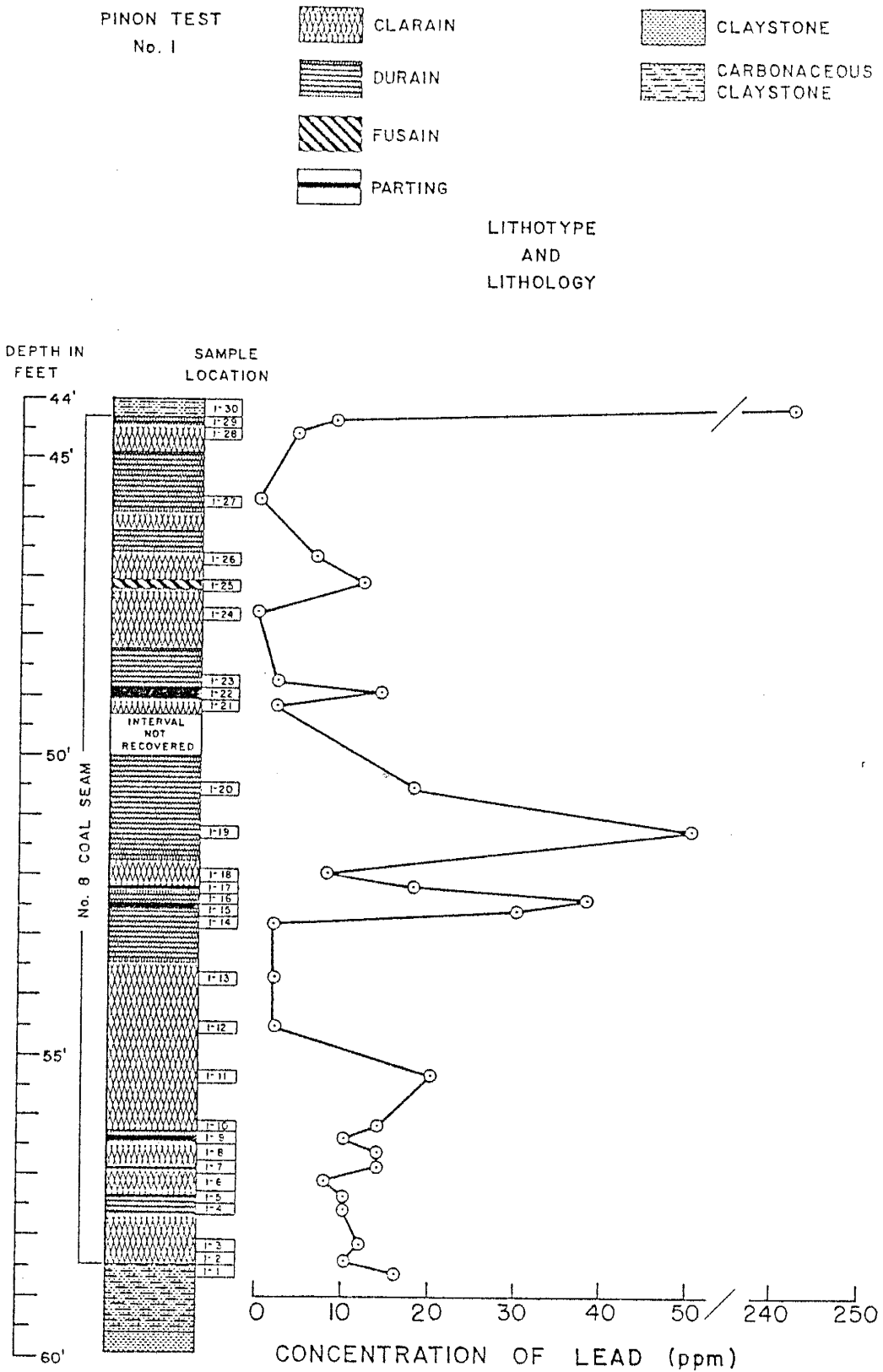
Figure A-41 - Distribution of Lead
in Pinon Test No. 1.
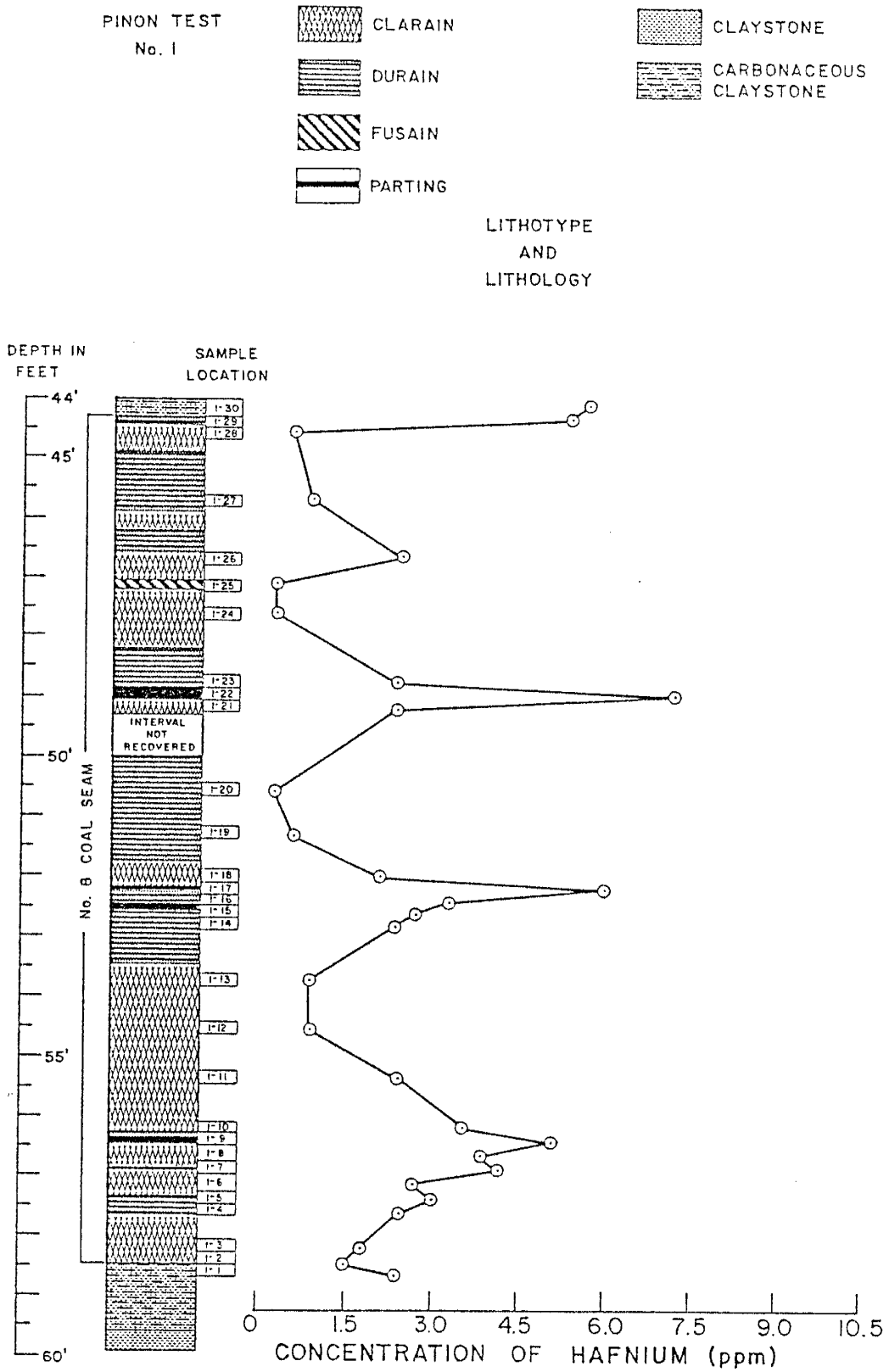
Figure A-42 - Distribution of Lead
in Pinon Test No. 2.

Figure A-43 - Distribution of Lithium
in Pinon Test No. 1.

Figure A-44 — Distribution of Lithium
in Pinon Test No. 2.

PINON TEST
No. 1

CLARAIN

DURAIN

FUSAIN

PARTING

CLAYSTONE

CARBONACEOUS
CLAYSTONE

LITHOTYPE
AND
LITHOLOGY

DEPTH IN
FEET

SAMPLE
LOCATION
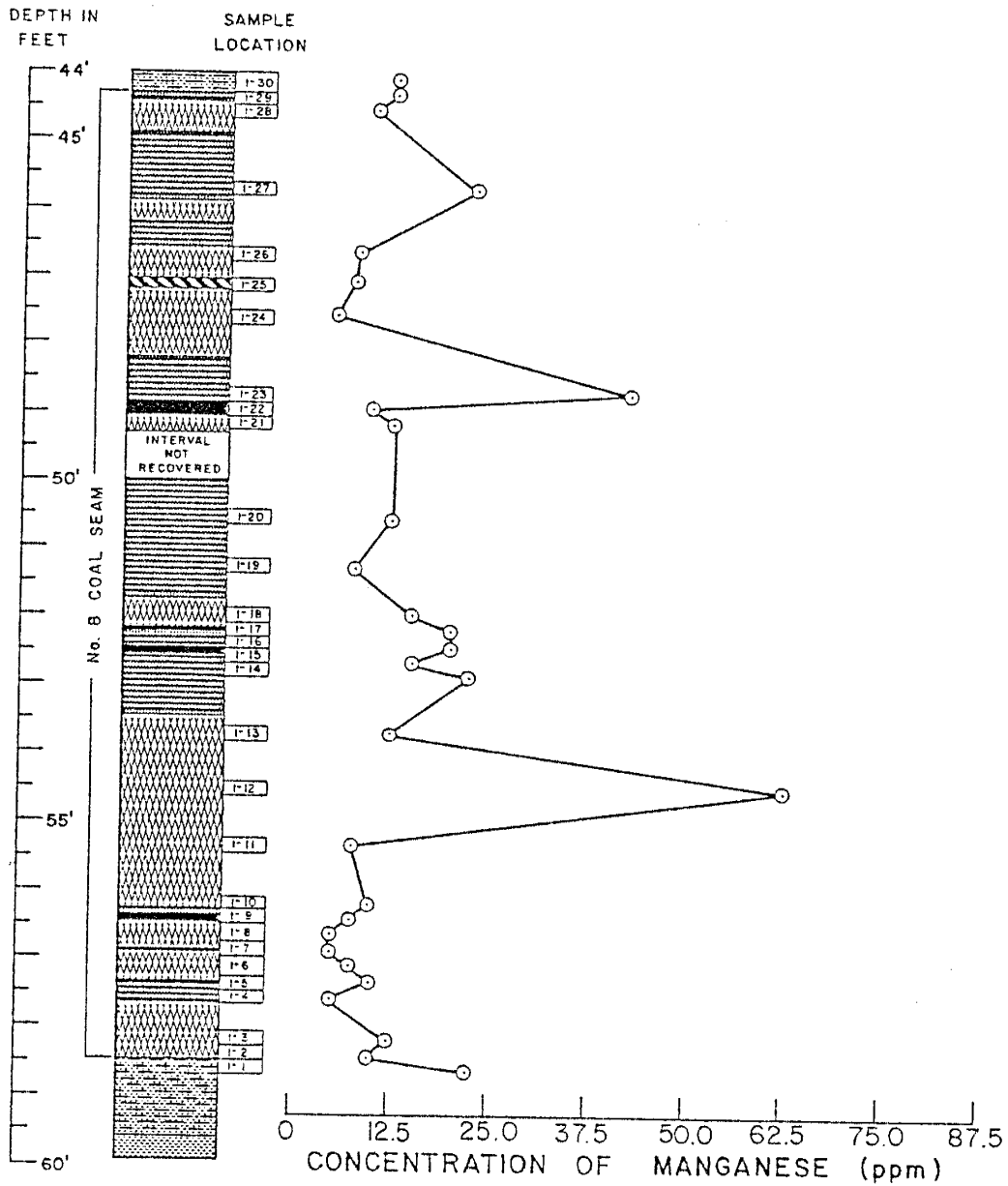
Figure A-45 - Distribution of Manganese
in Pinon Test No. 1.
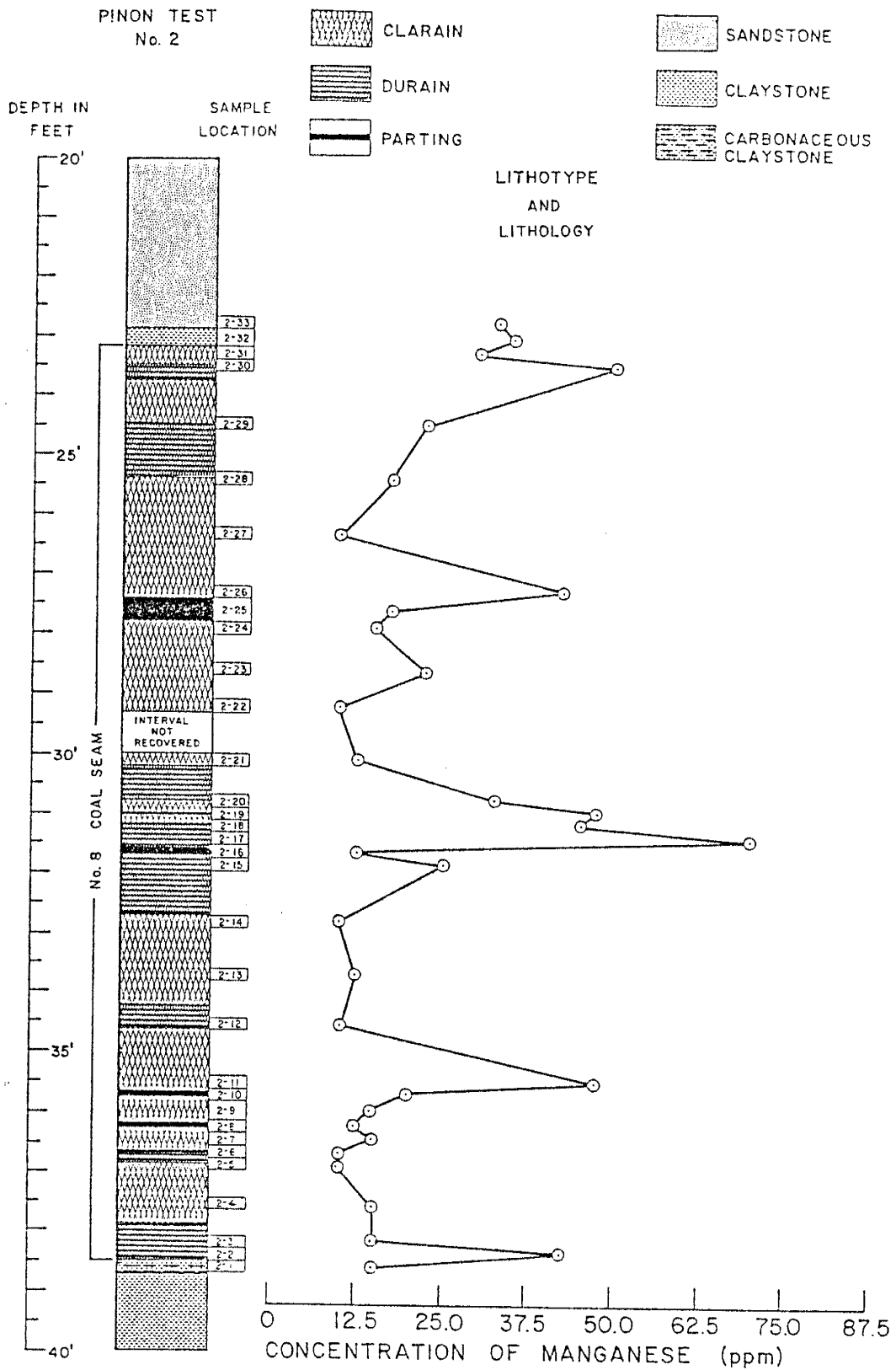
Figure A-46 - Distribution of Manganese
in Pinon Test No. 2.

PINON TEST
No. 1

CLARAIN

DURAIN

FUSAIN

PARTING

CLAYSTONE

CARBONACEOUS
CLAYSTONE

LITHOTYPE
AND
LITHOLOGY

DEPTH IN
FEET

SAMPLE
LOCATION
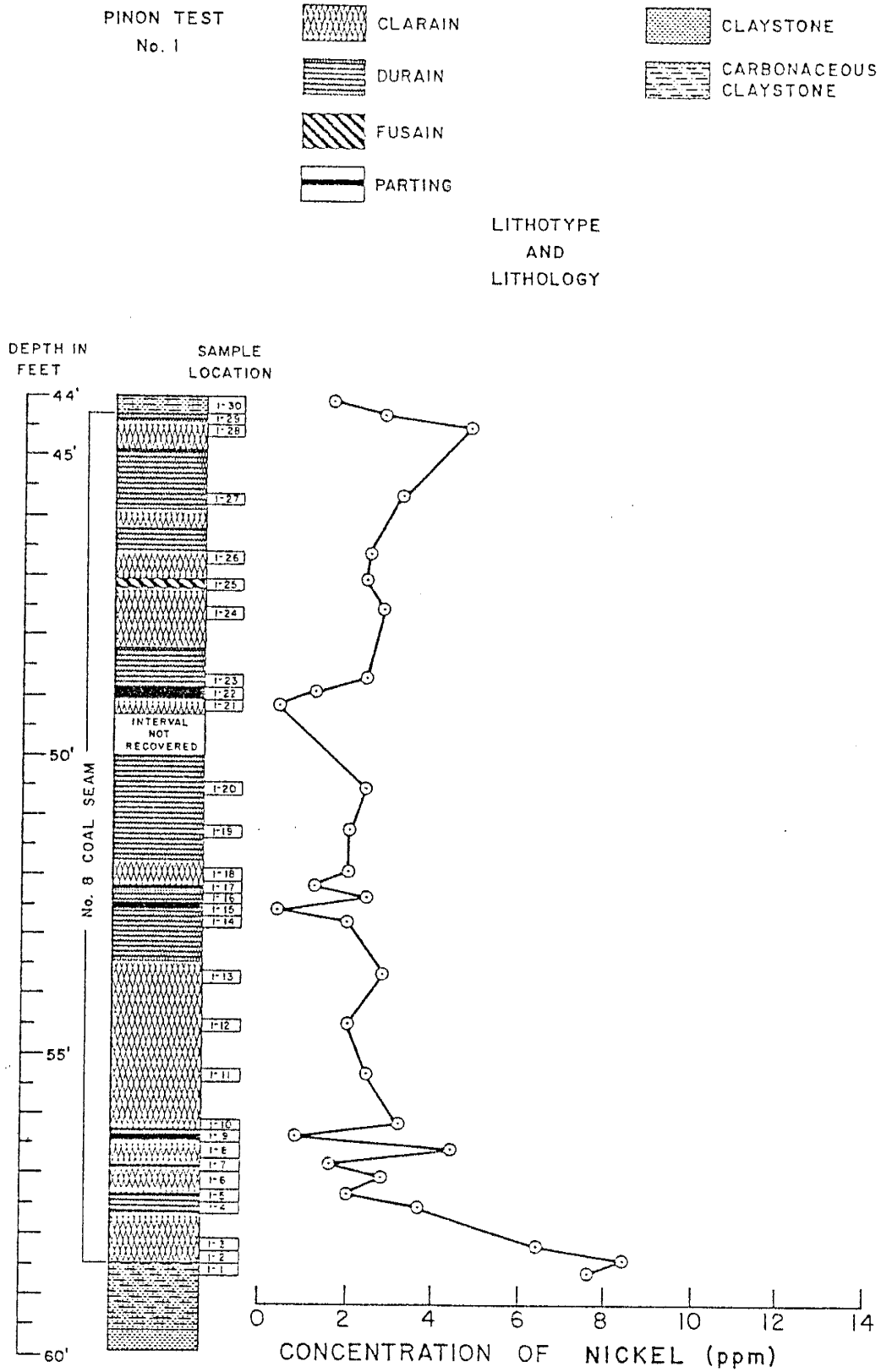
Figure A-47 - Distribution of Nickel
in Pinon Test No. 1.
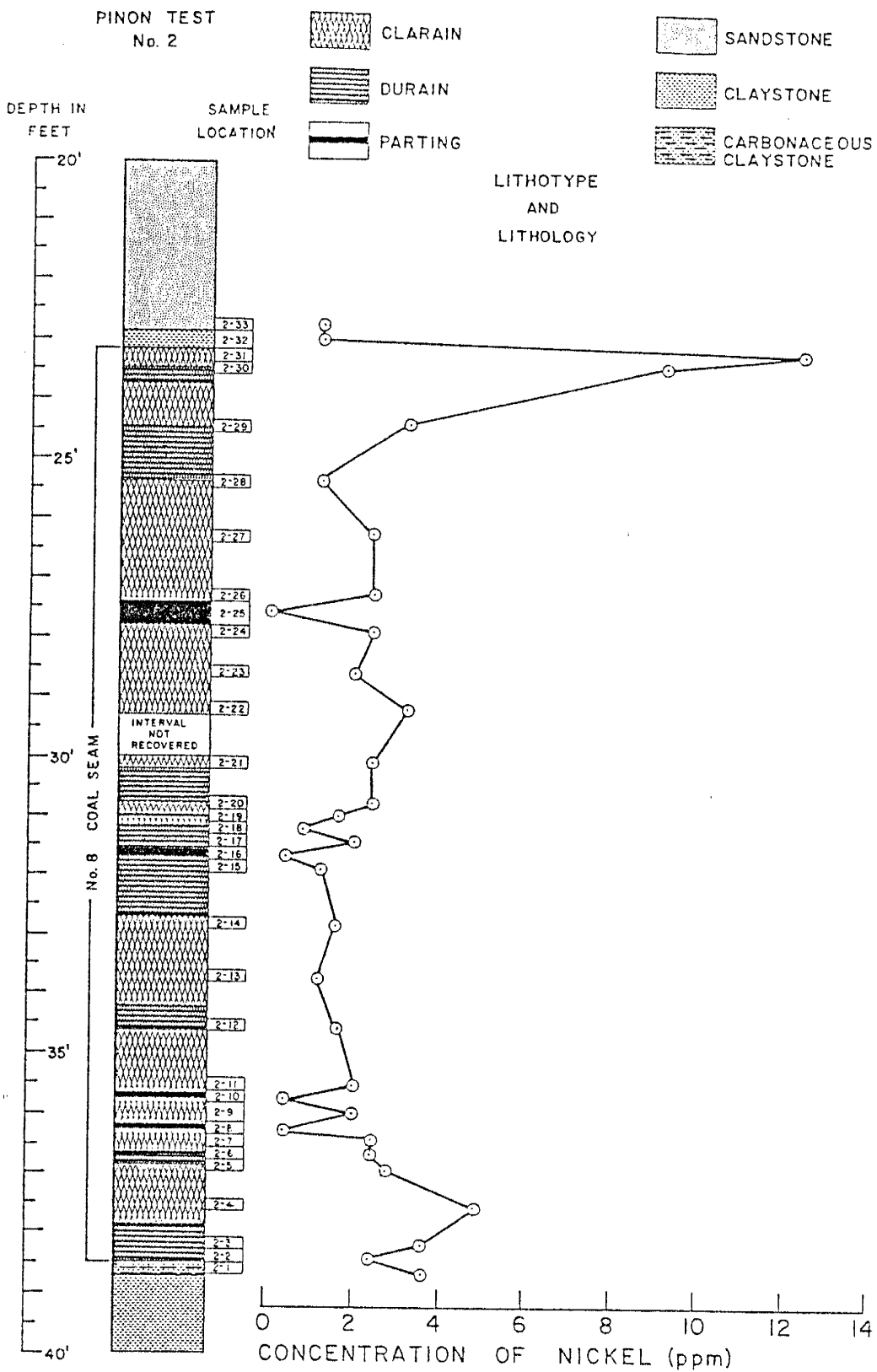
Figure A-48 – Distribution of Nickel
in Pinon Test No. 2.
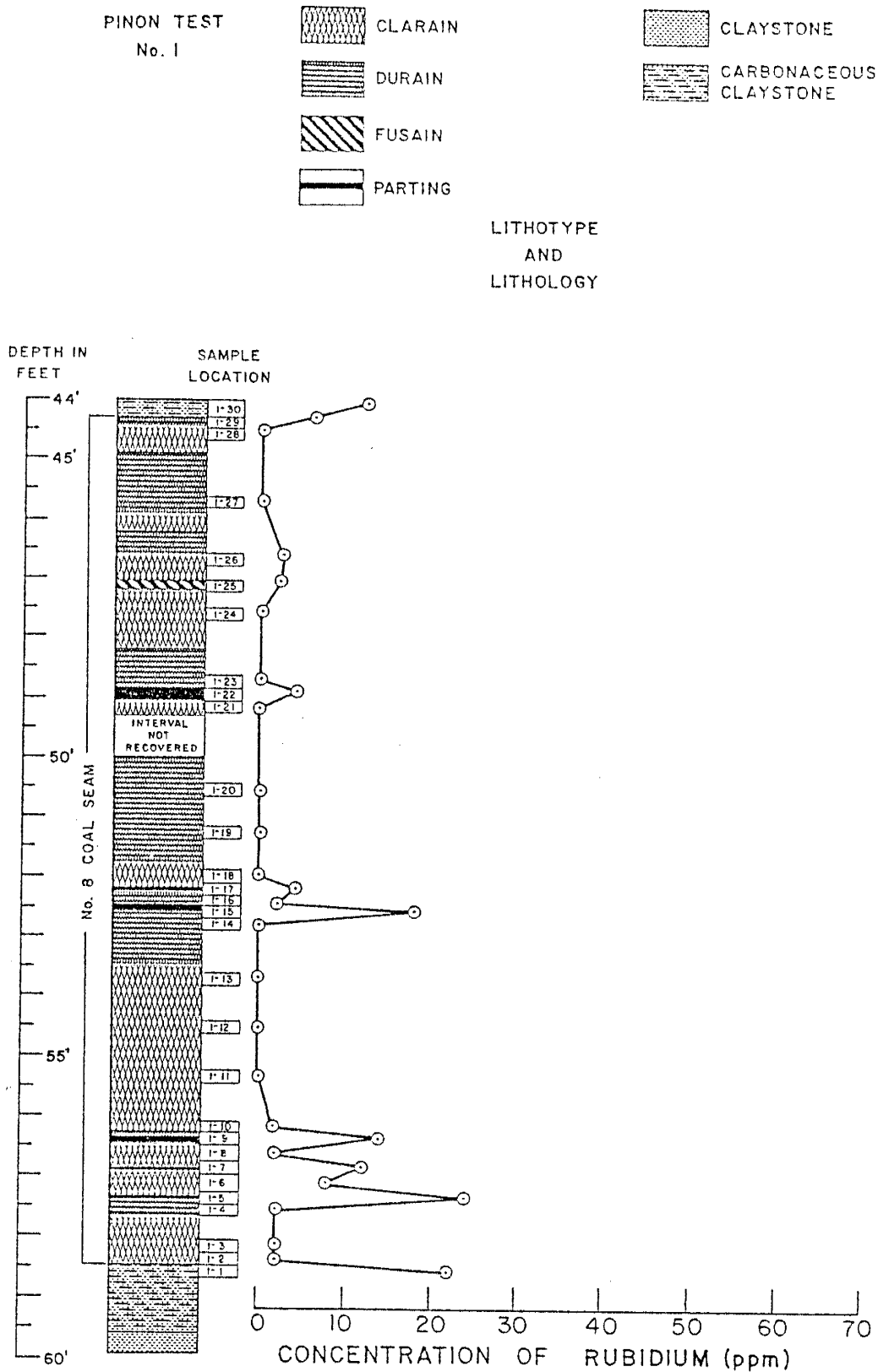
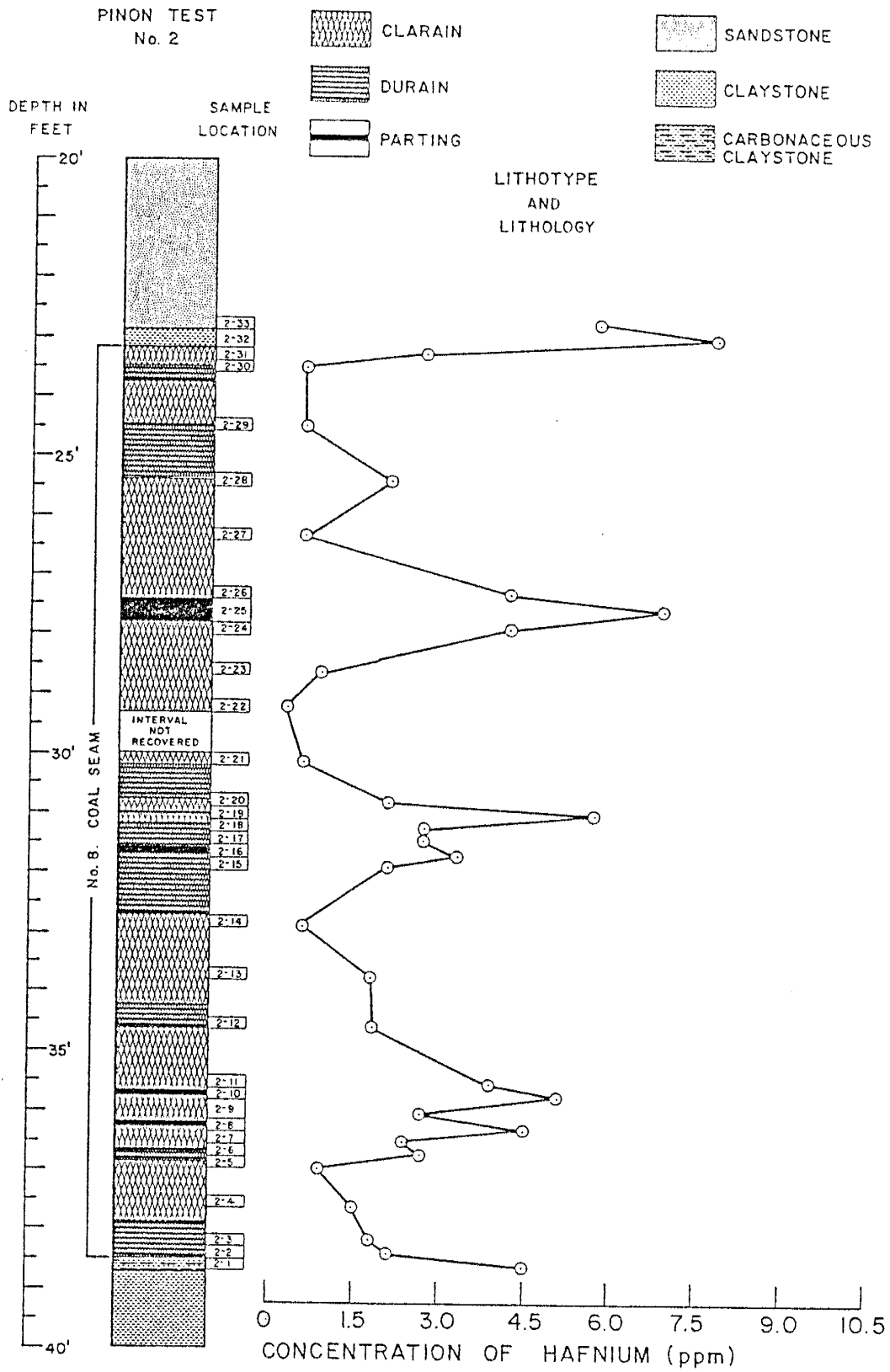Figure A-49 — Distribution of Rubidium
in Pinon Test No. 1.
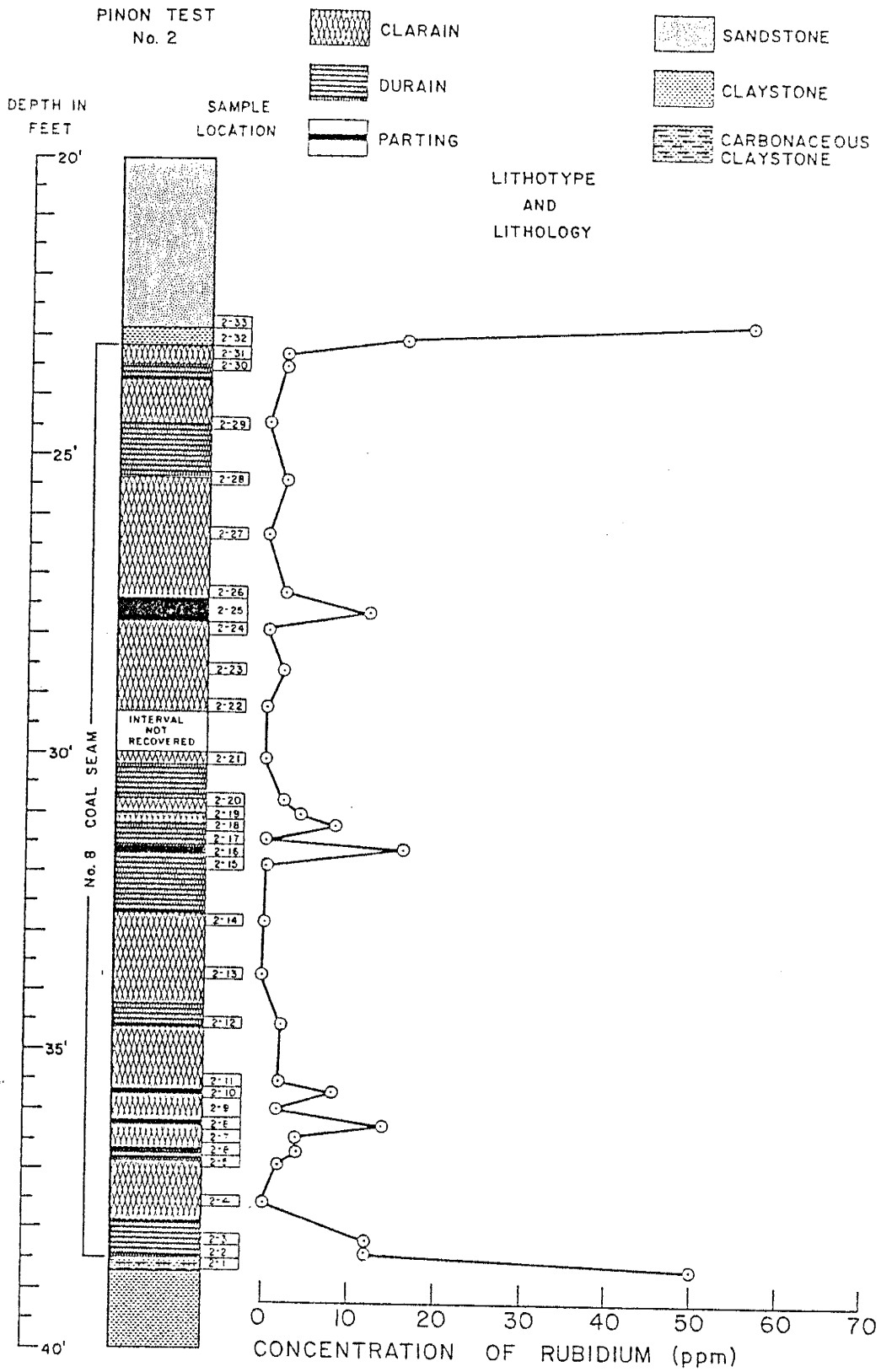
Figure A-50 — Distribution of Rubidium
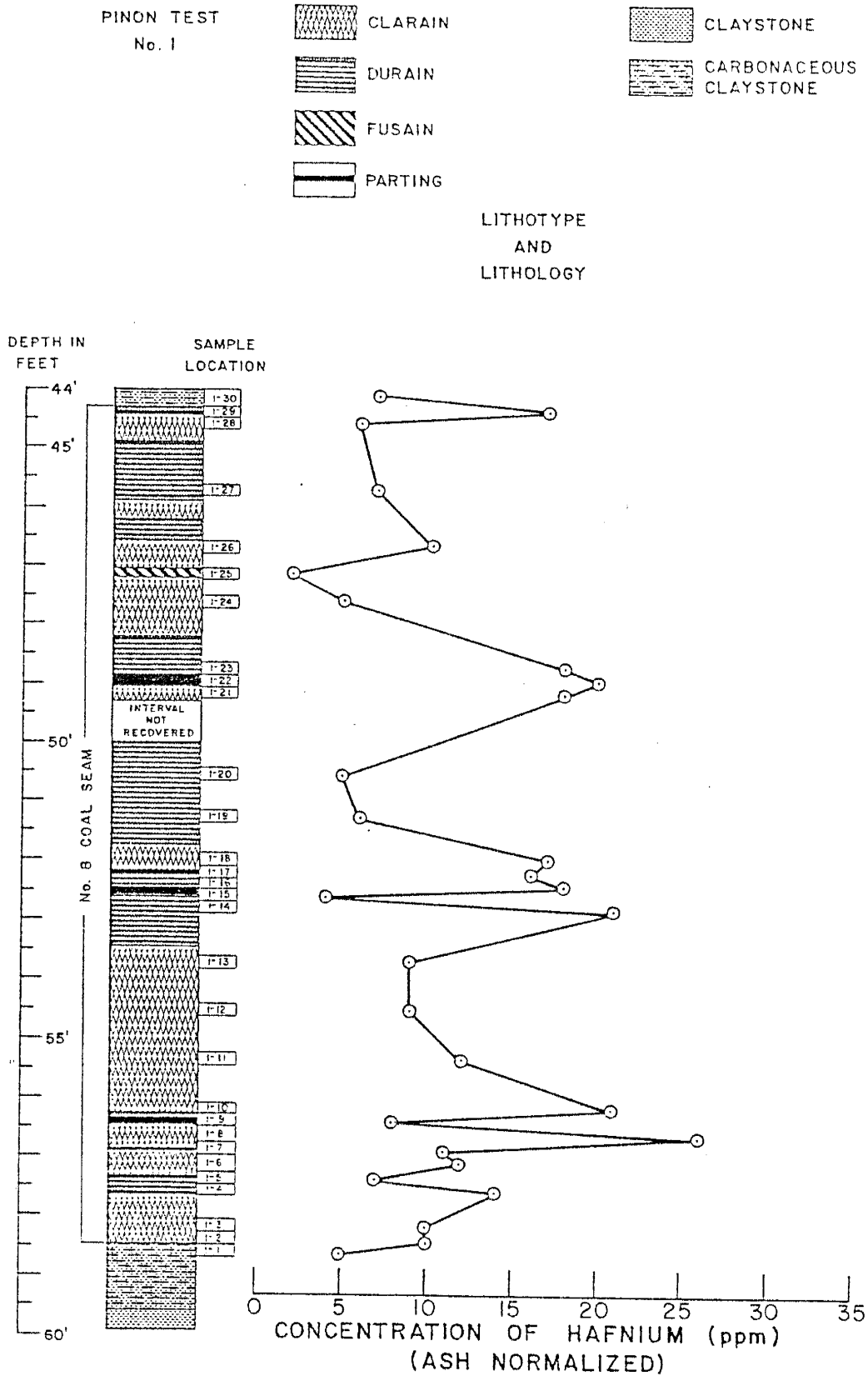in Pinon Test No. 2.

PINON TEST

PINON TEST
No. 1

CLARAIN

DURAIN

FUSAIN

PARTING

CLAYSTONE

CARBONACEOUS
CLAYSTONE

LITHOTYPE
AND
LITHOLOGY
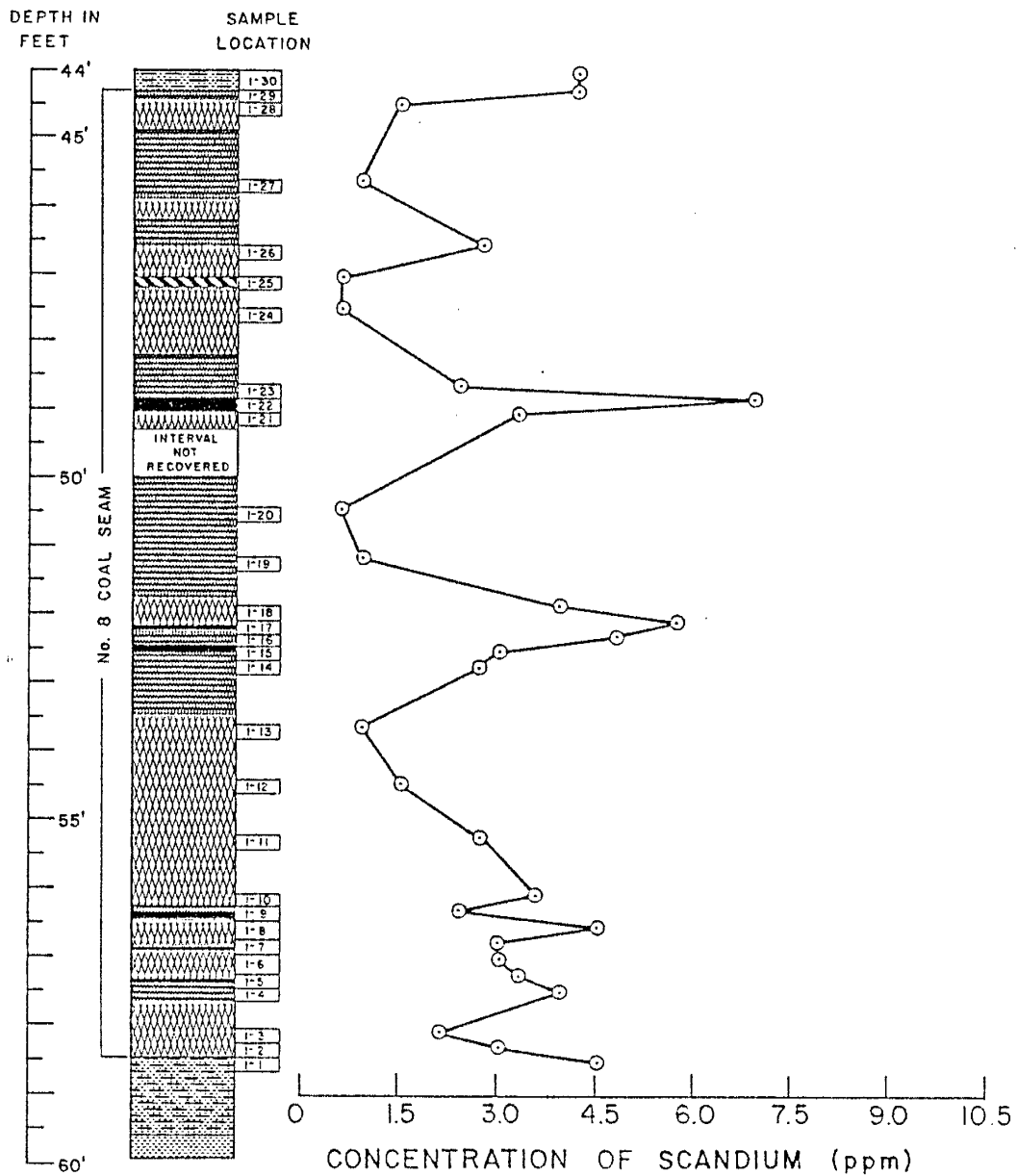


Figure A-51 - Distribution of Scandium
in Pinon Test No. 1.
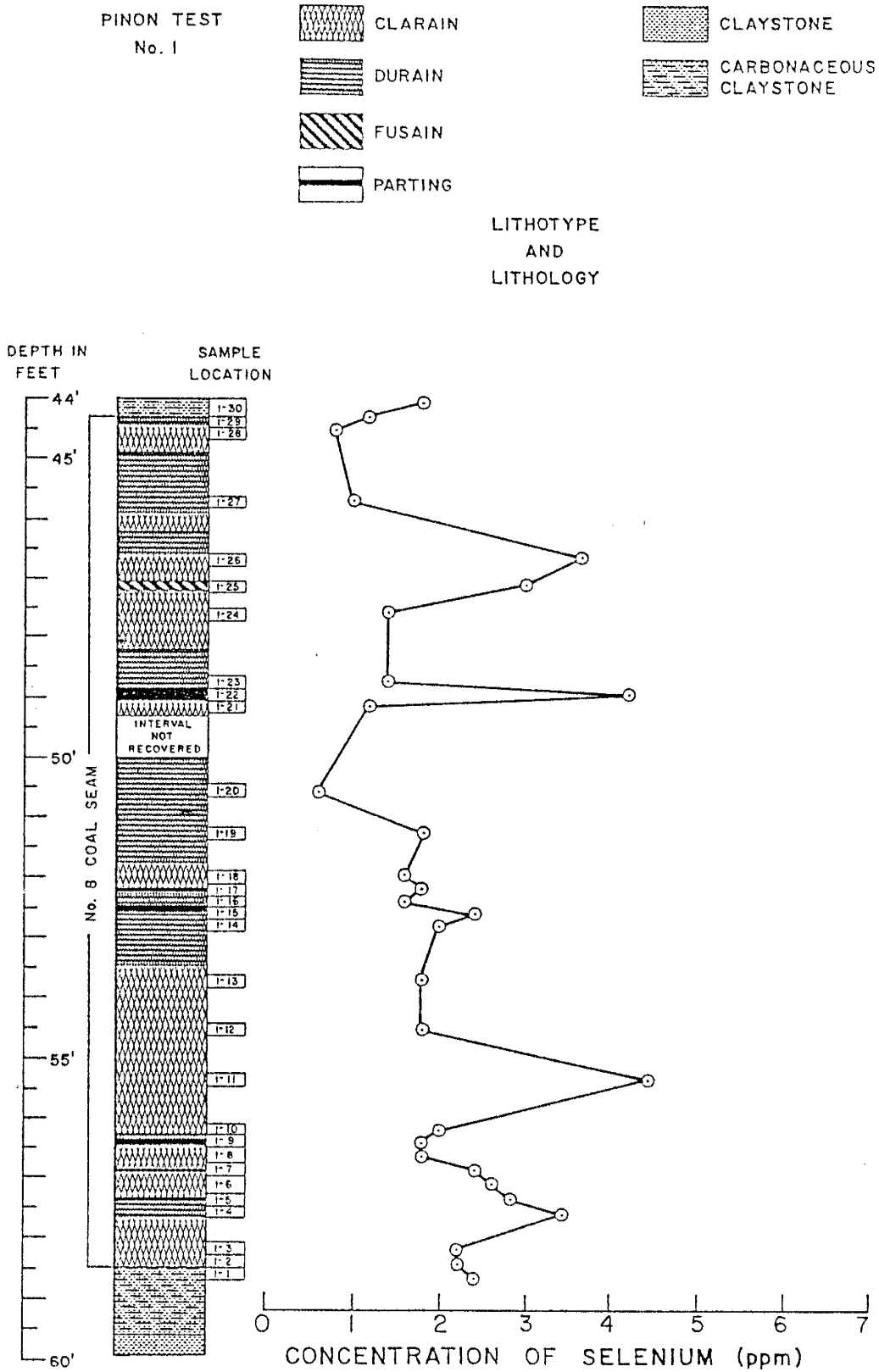
Figure A-53 – Distribution of Selenium
in Pinon Test No. 1.
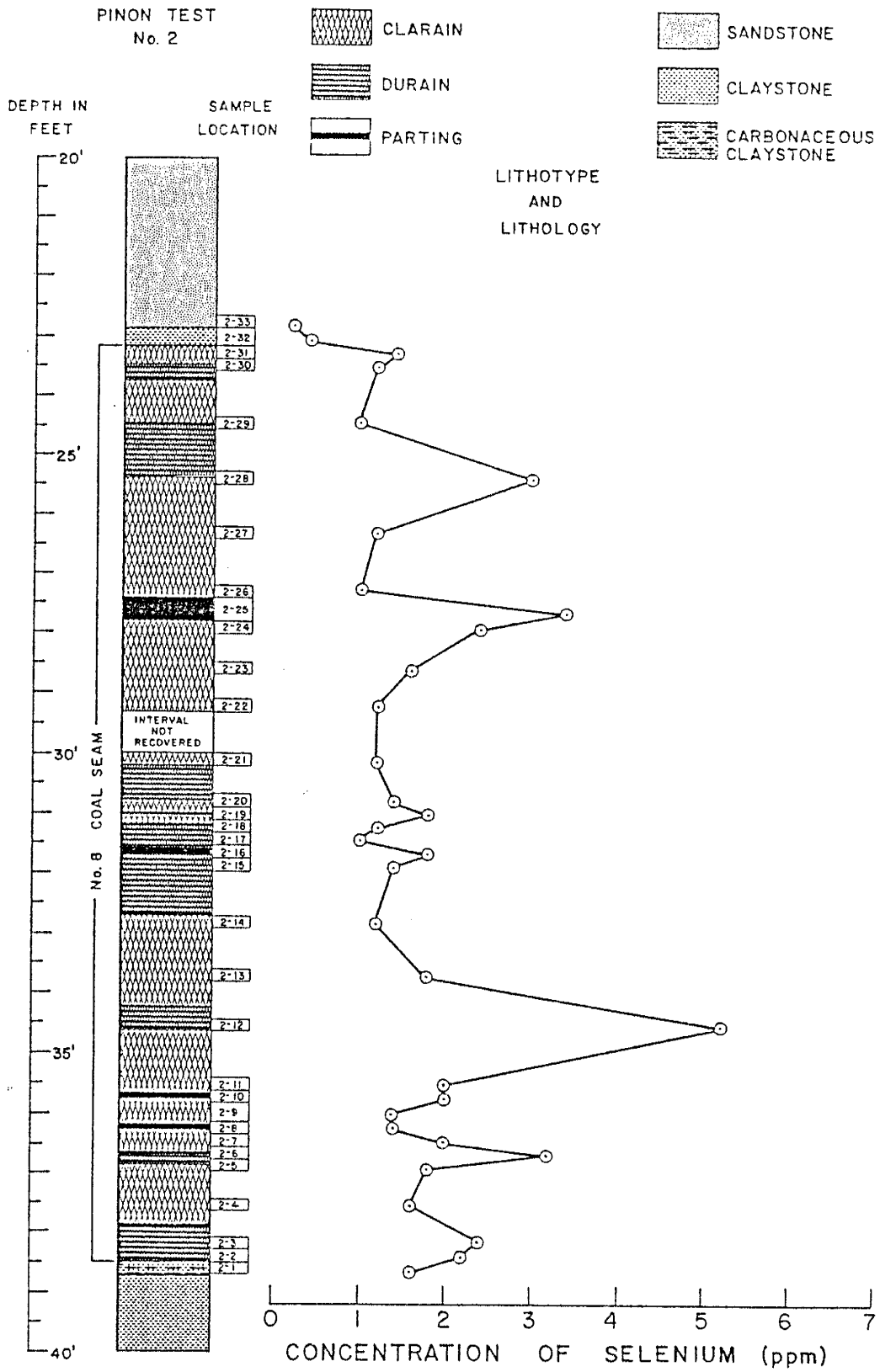
Figure A-54 - Distribution of Selenium
in Pinon Test No. 2.

PINON TEST
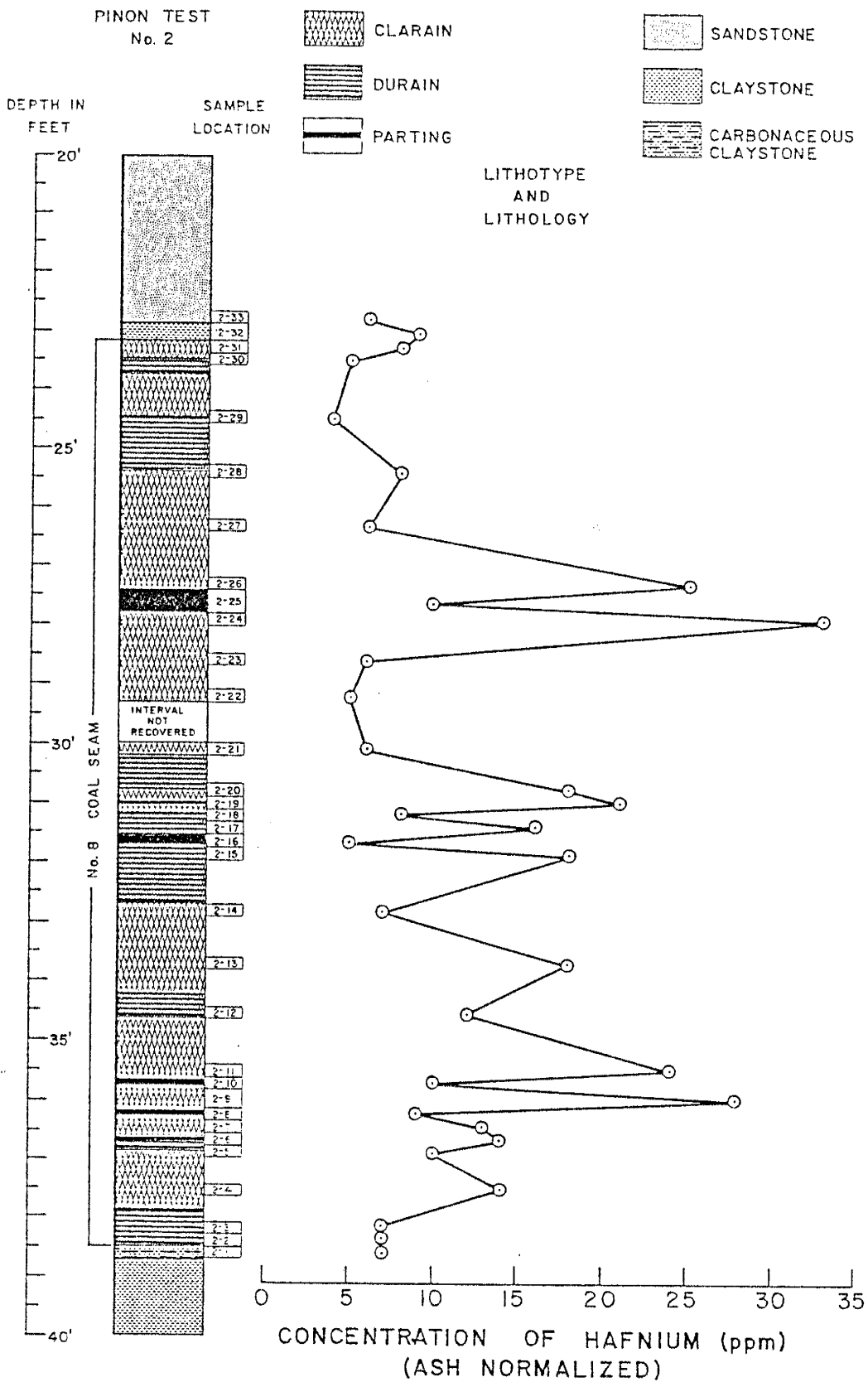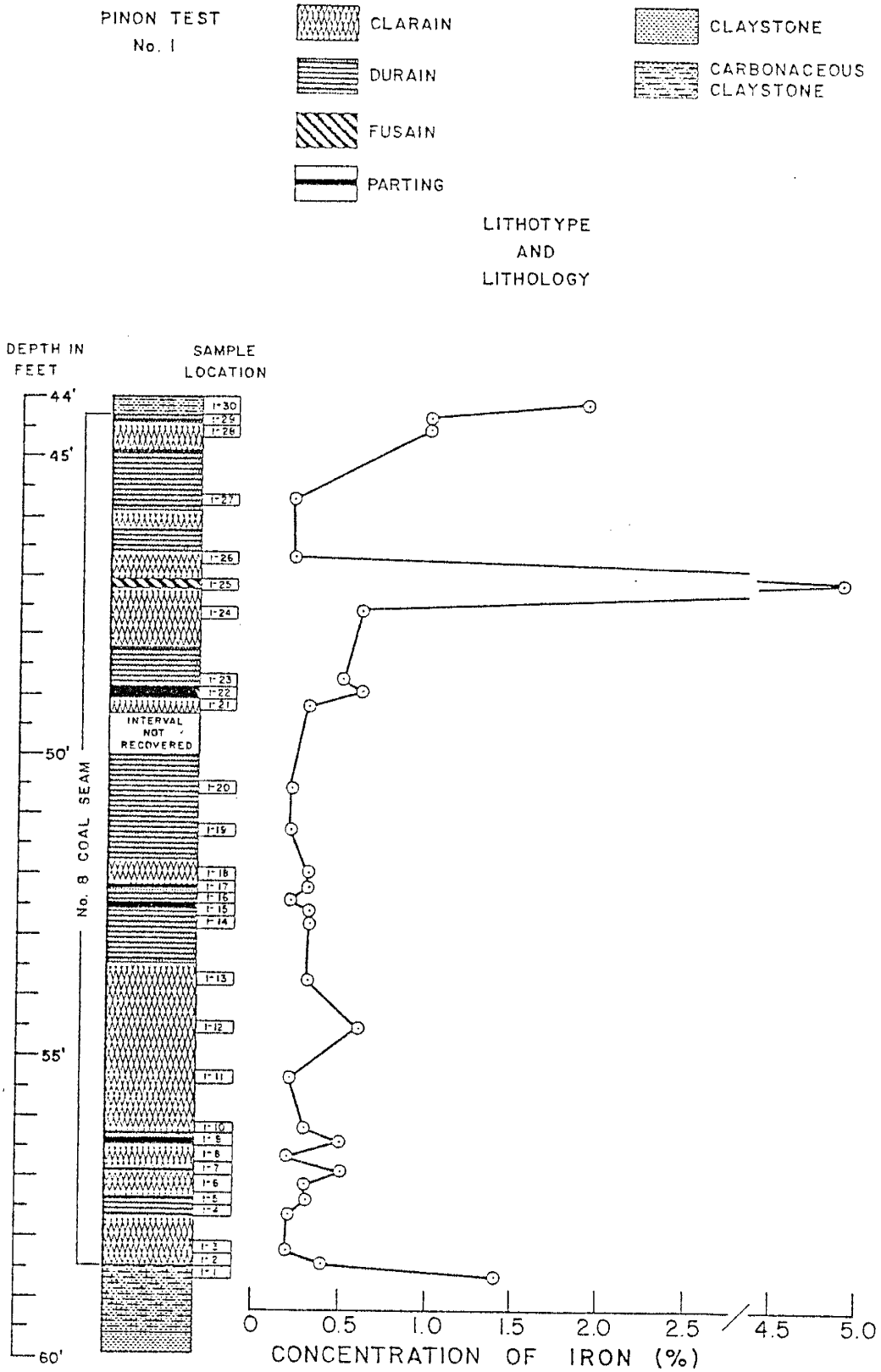No. I

CLARAIN

DURAIN

FUSAIN

PARTING

CLAYSTONE

CARBONACEOUS
CLAYSTONE

LITHOTYPE
AND
LITHOLOGY
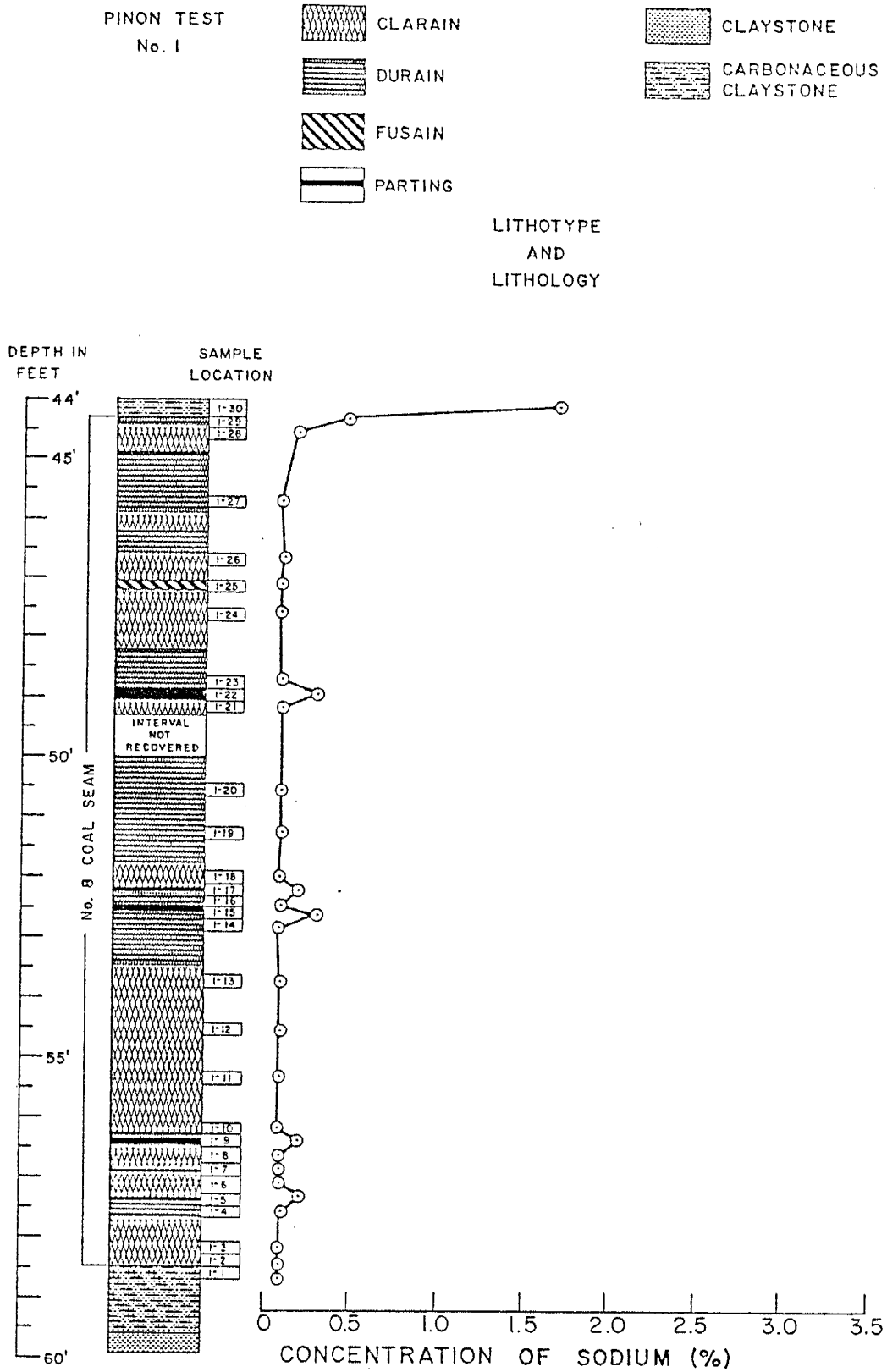


Figure A-55 - Distribution of Sodium
in Pinon Test No. 1.
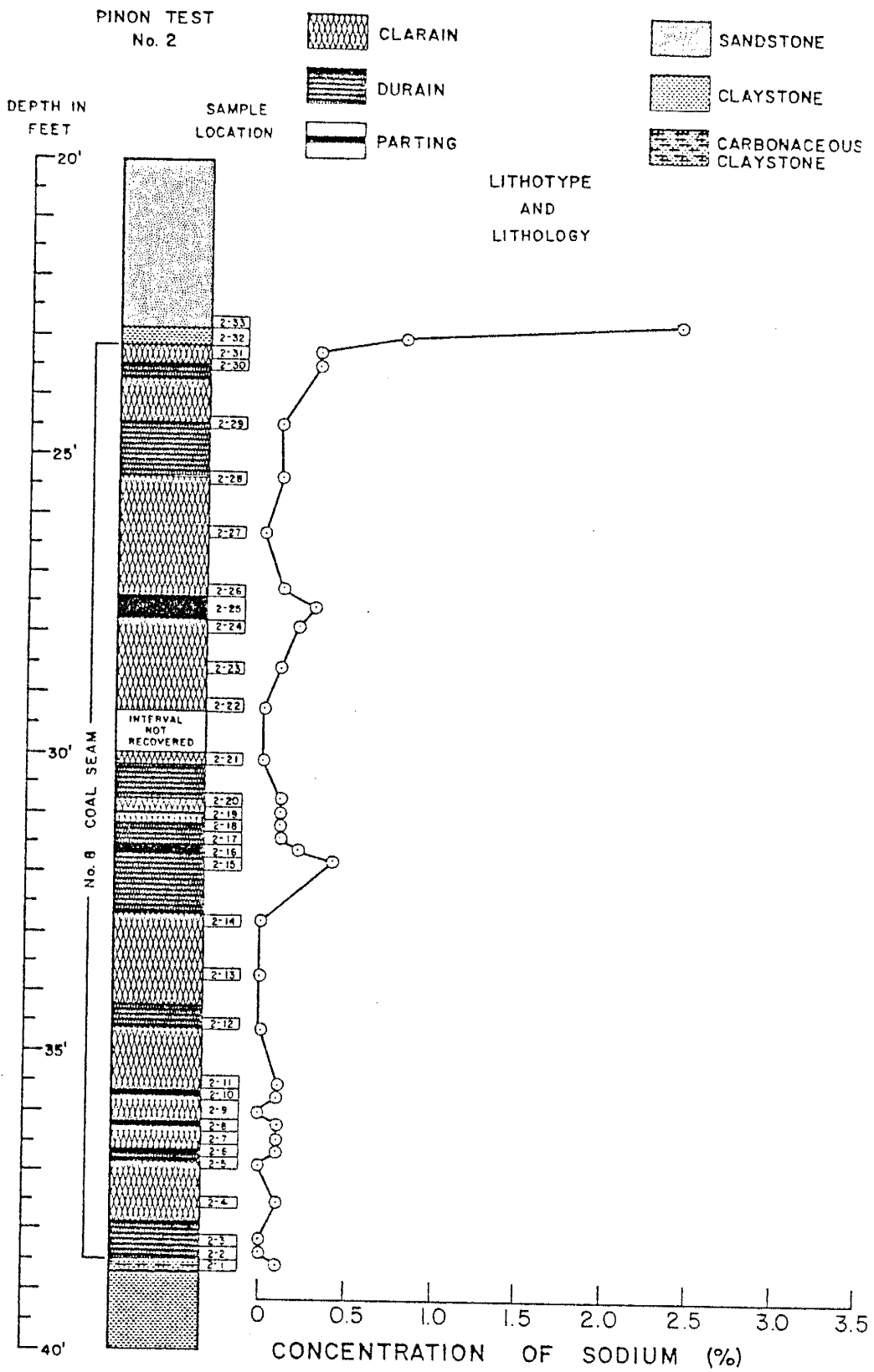
Figure A-56 – Distribution of Sodium
in Pinon Test No. 2.
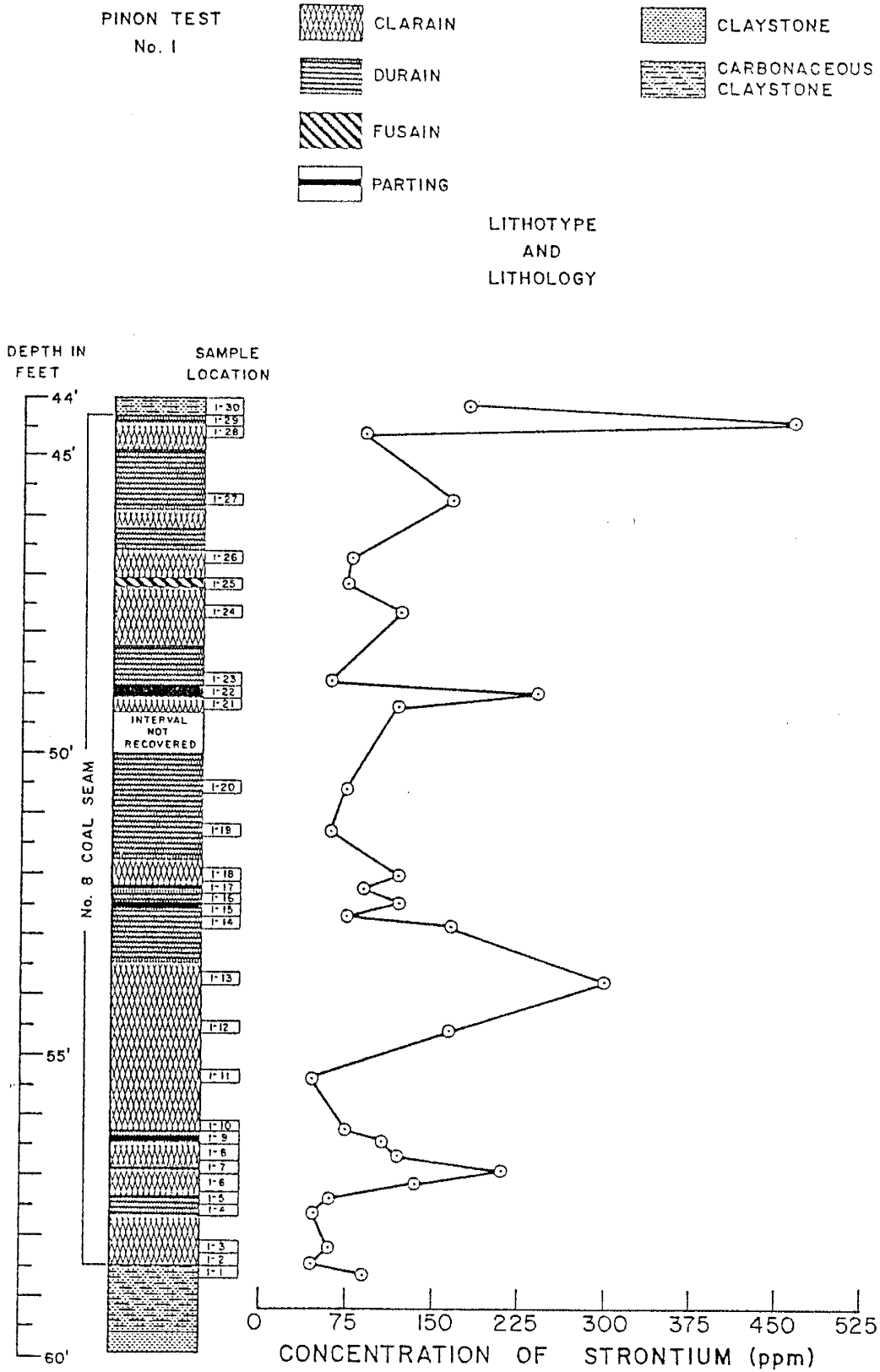
Figure A-57 - Distribution of Strontium
in Pinon Test No. 1.
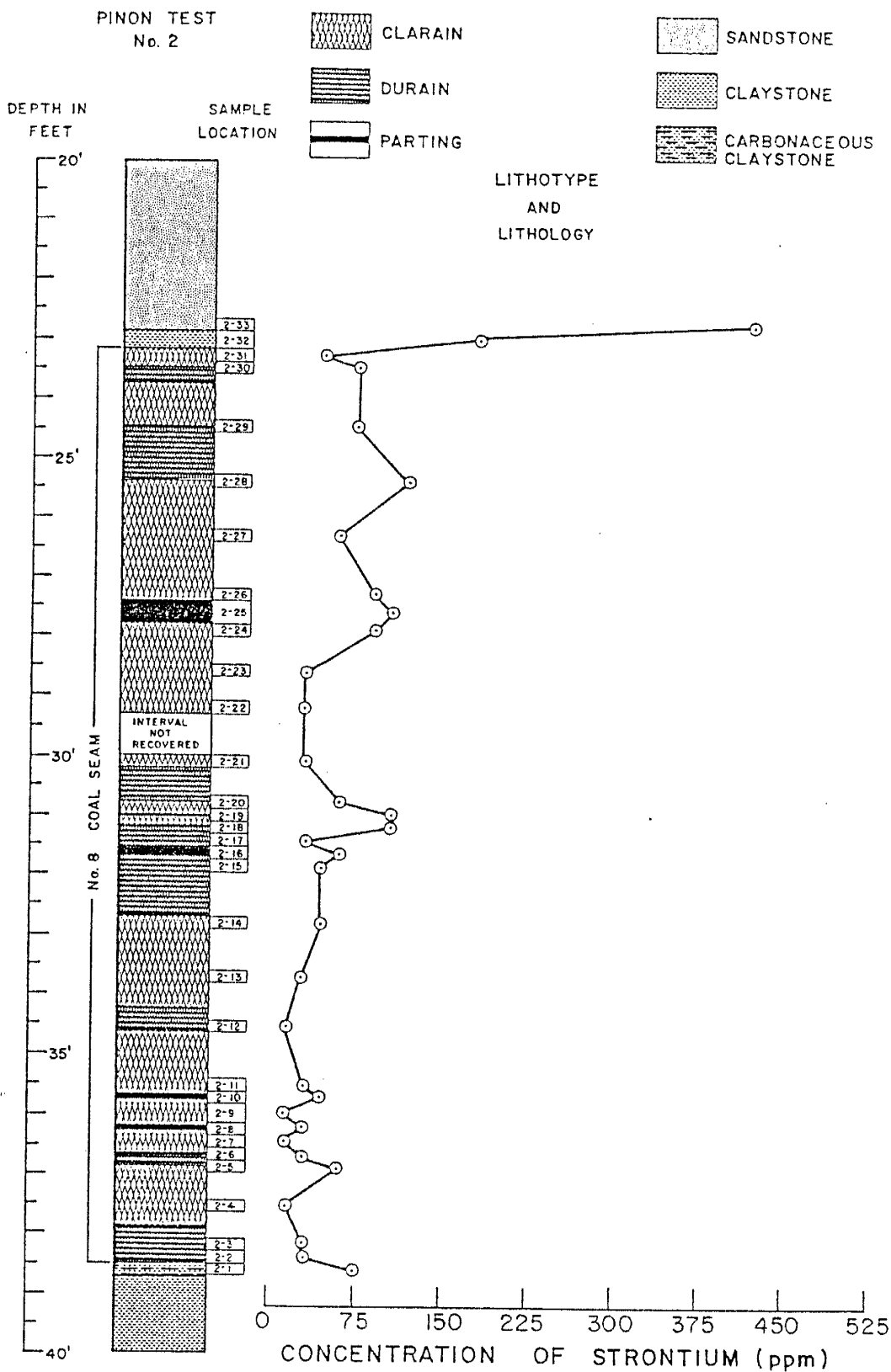
Figure A-58 – Distribution of Strontium
in Pinon Test No. 2.
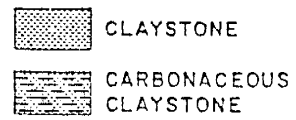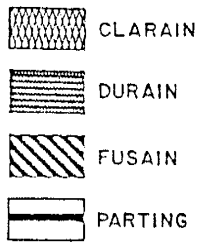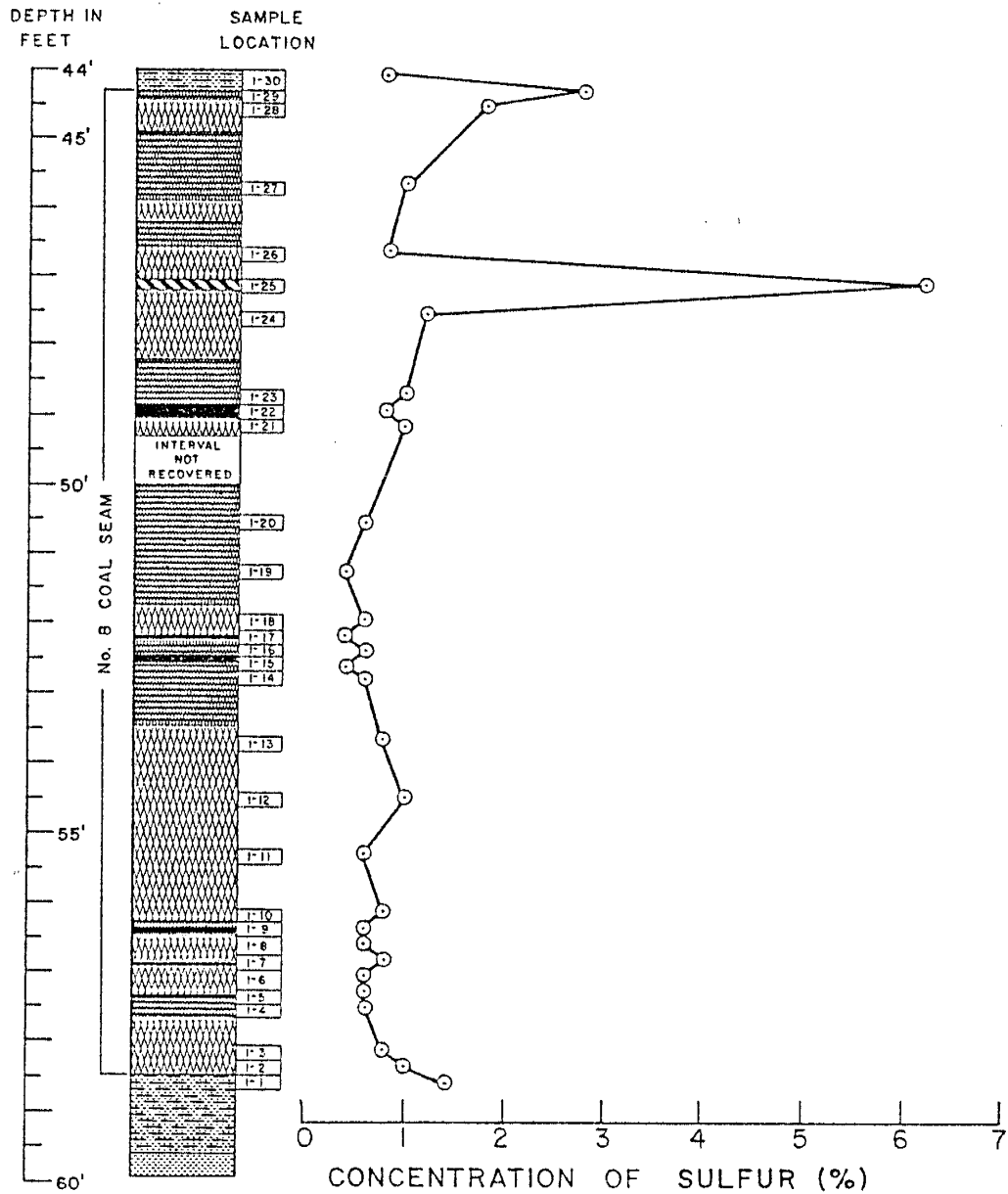
Figure A-59 - Distribution of Sulfur
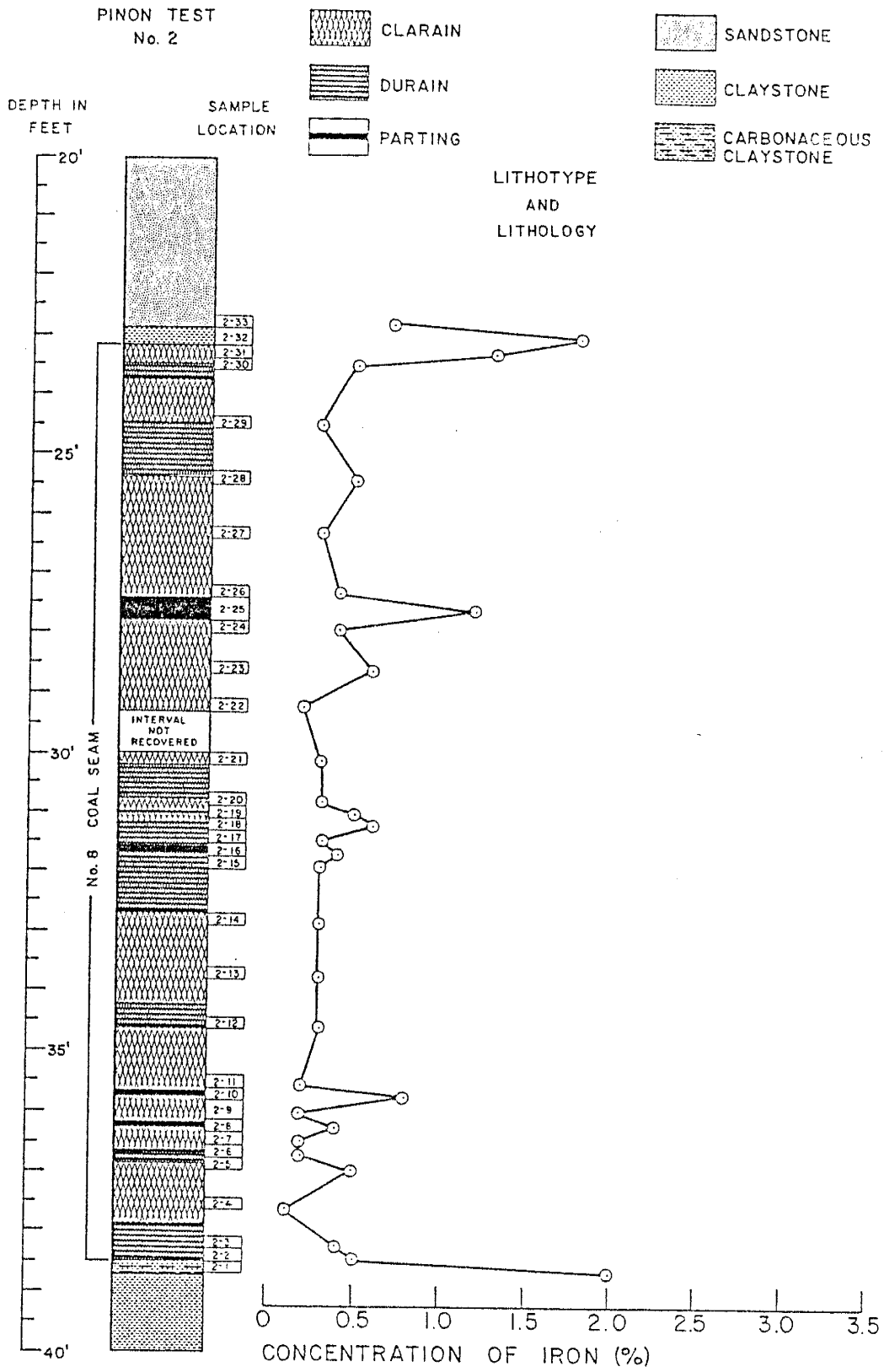in Pinon Test No. 1.
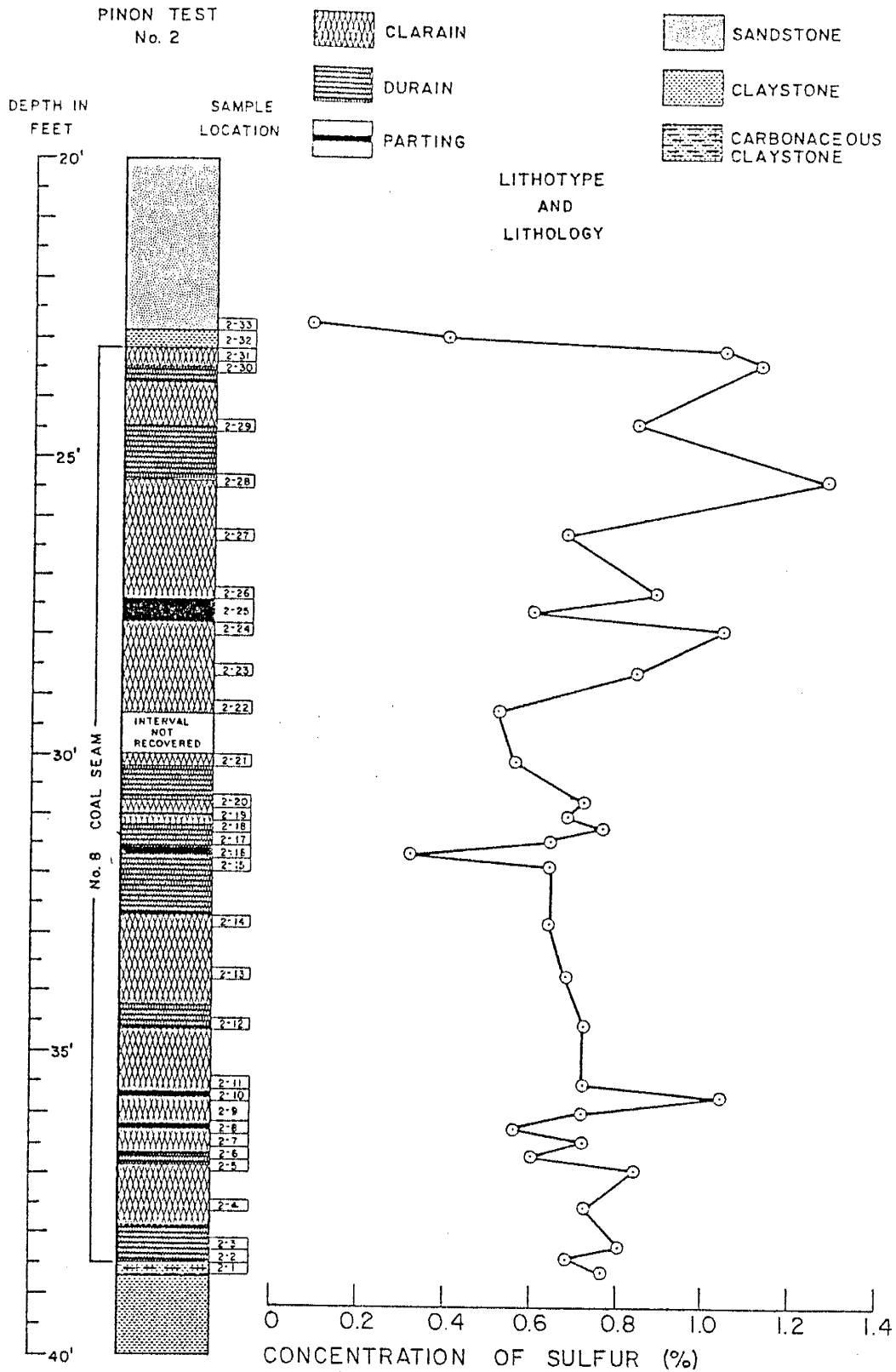
Figure A-60 - Distribution of Sulfur
in Pinon Test No. 2.
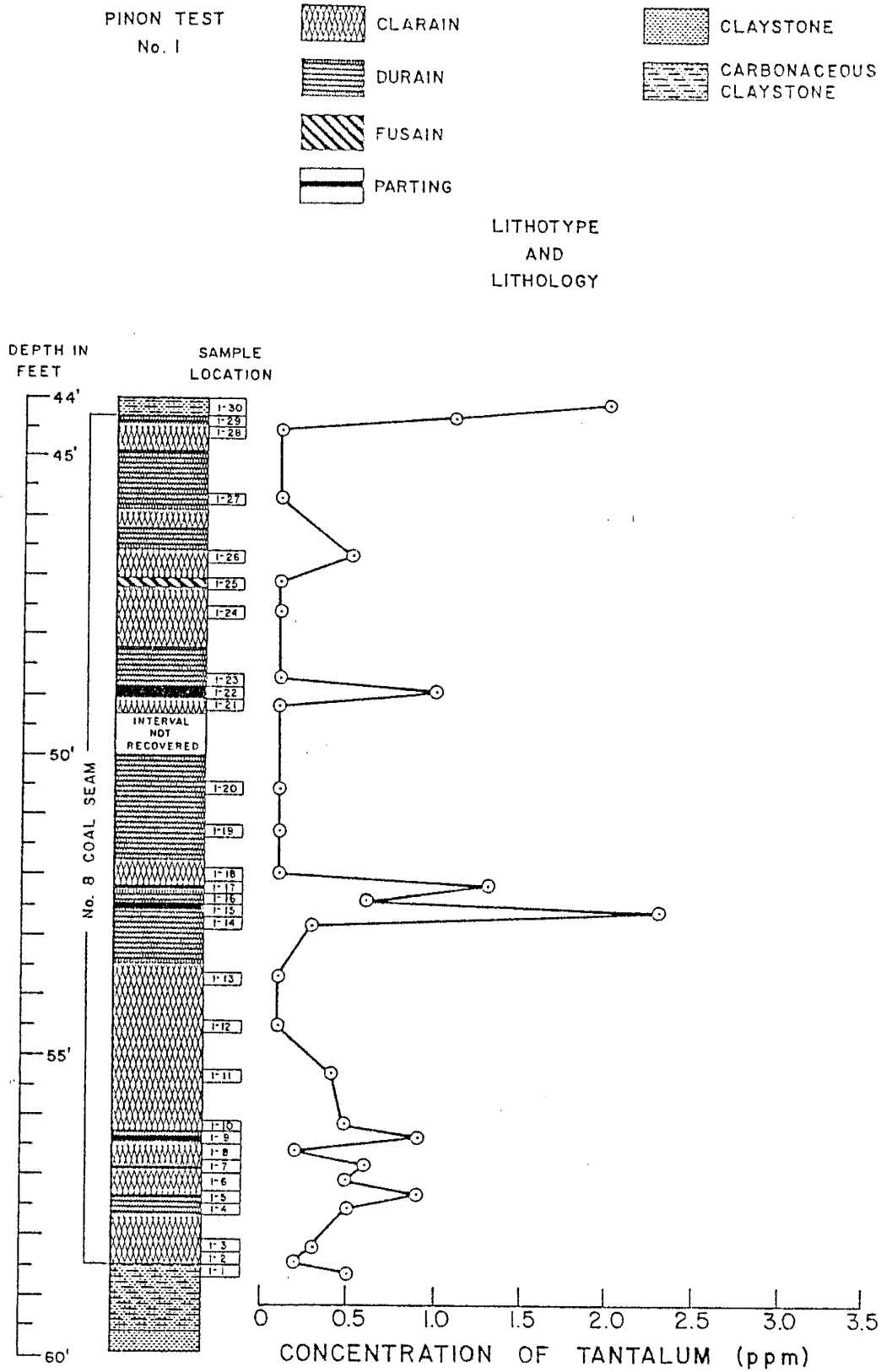
Figure A-61 - Distribution of Tantalum
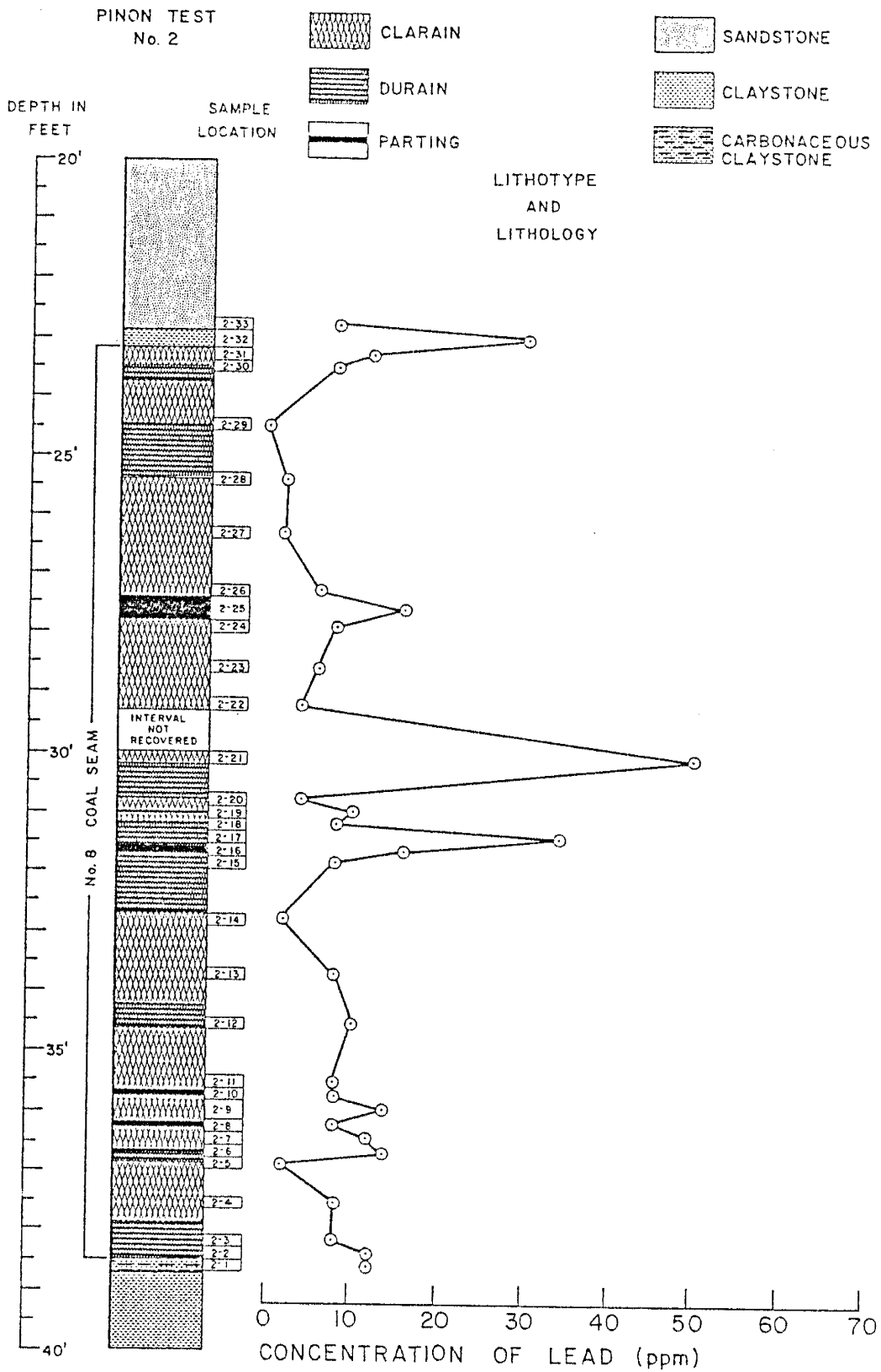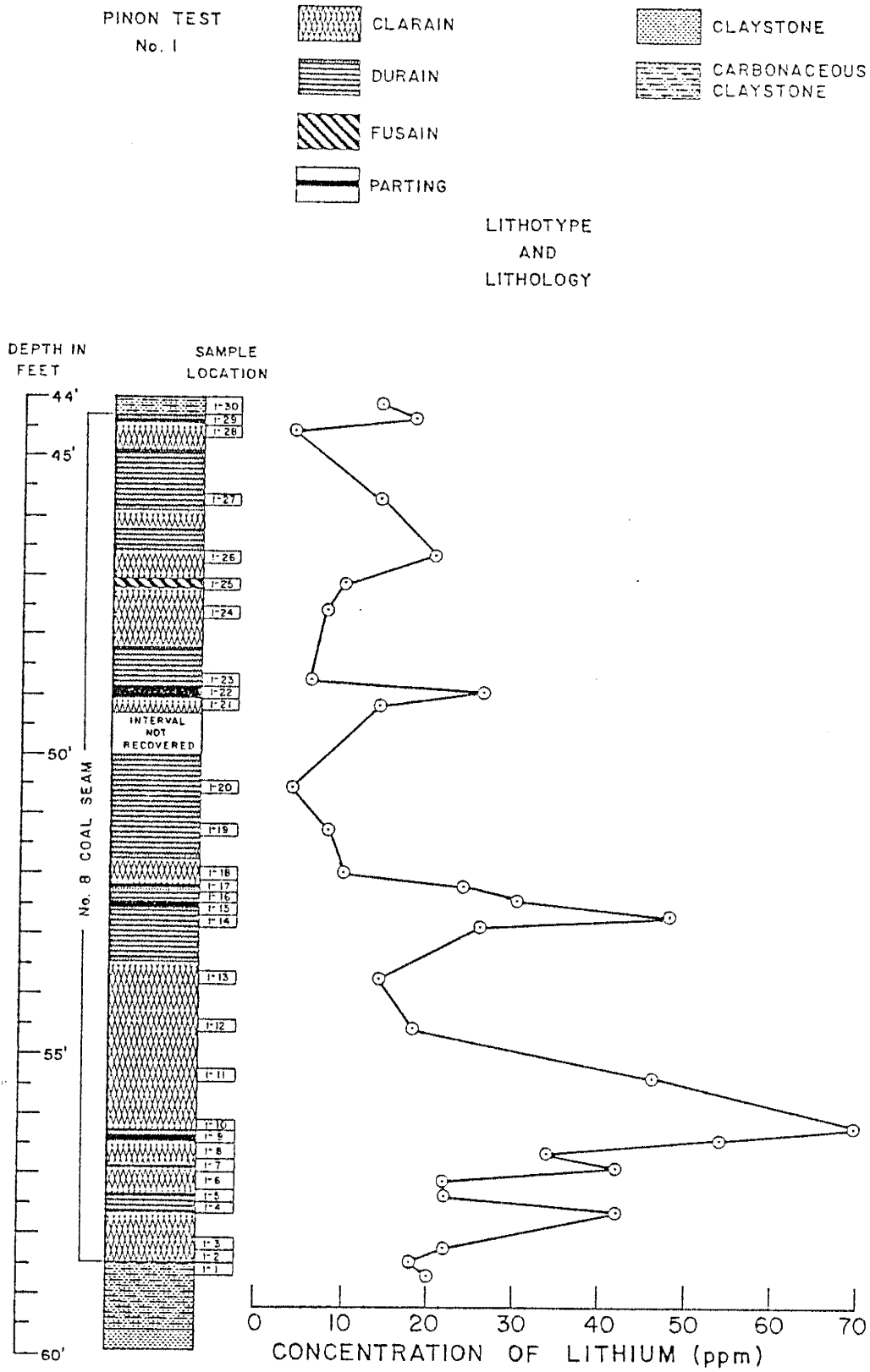in Pinon Test No. 1.
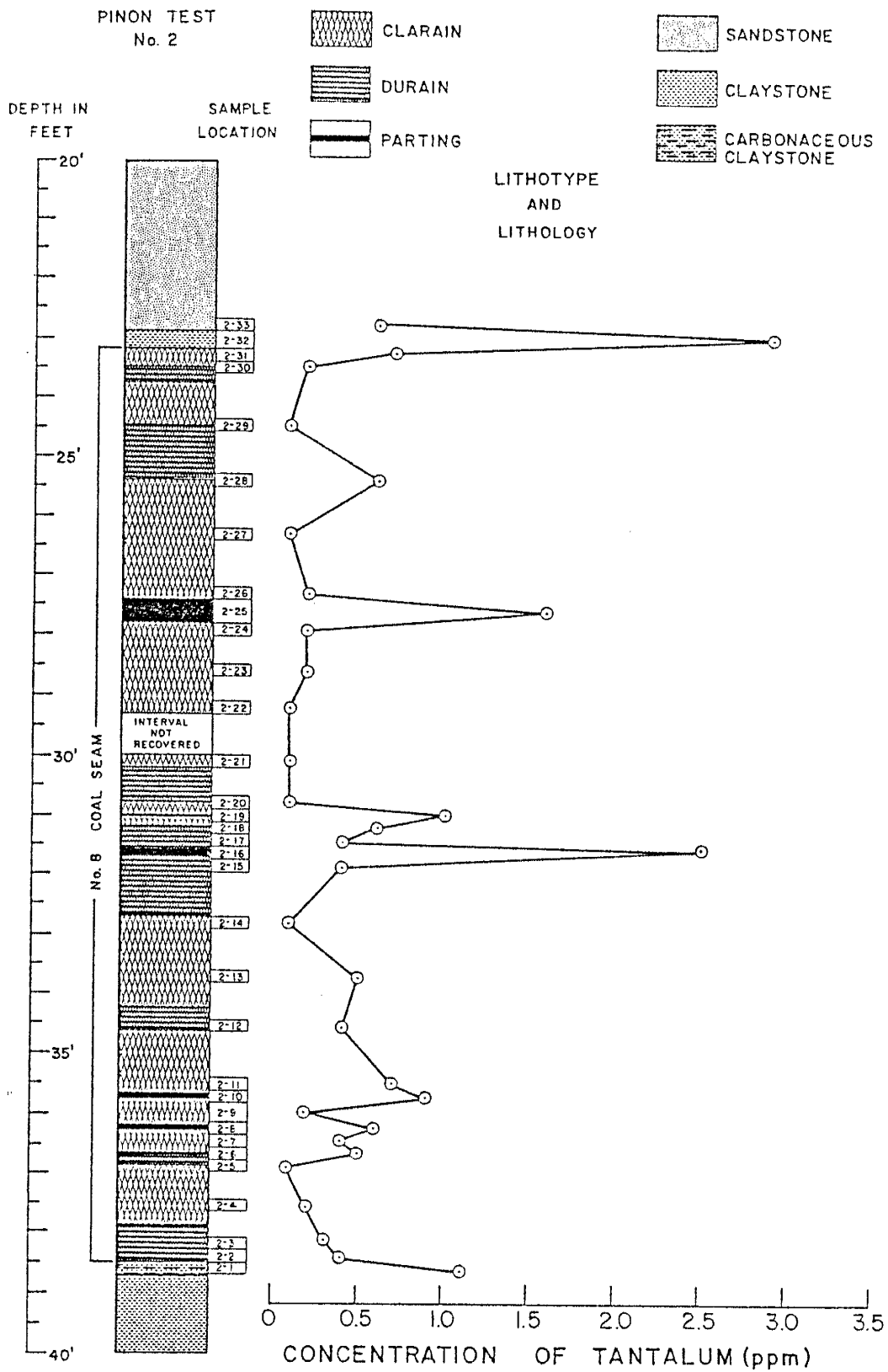
Figure A-62 - Distribution of Tantalum
in Pinon Test No. 2.
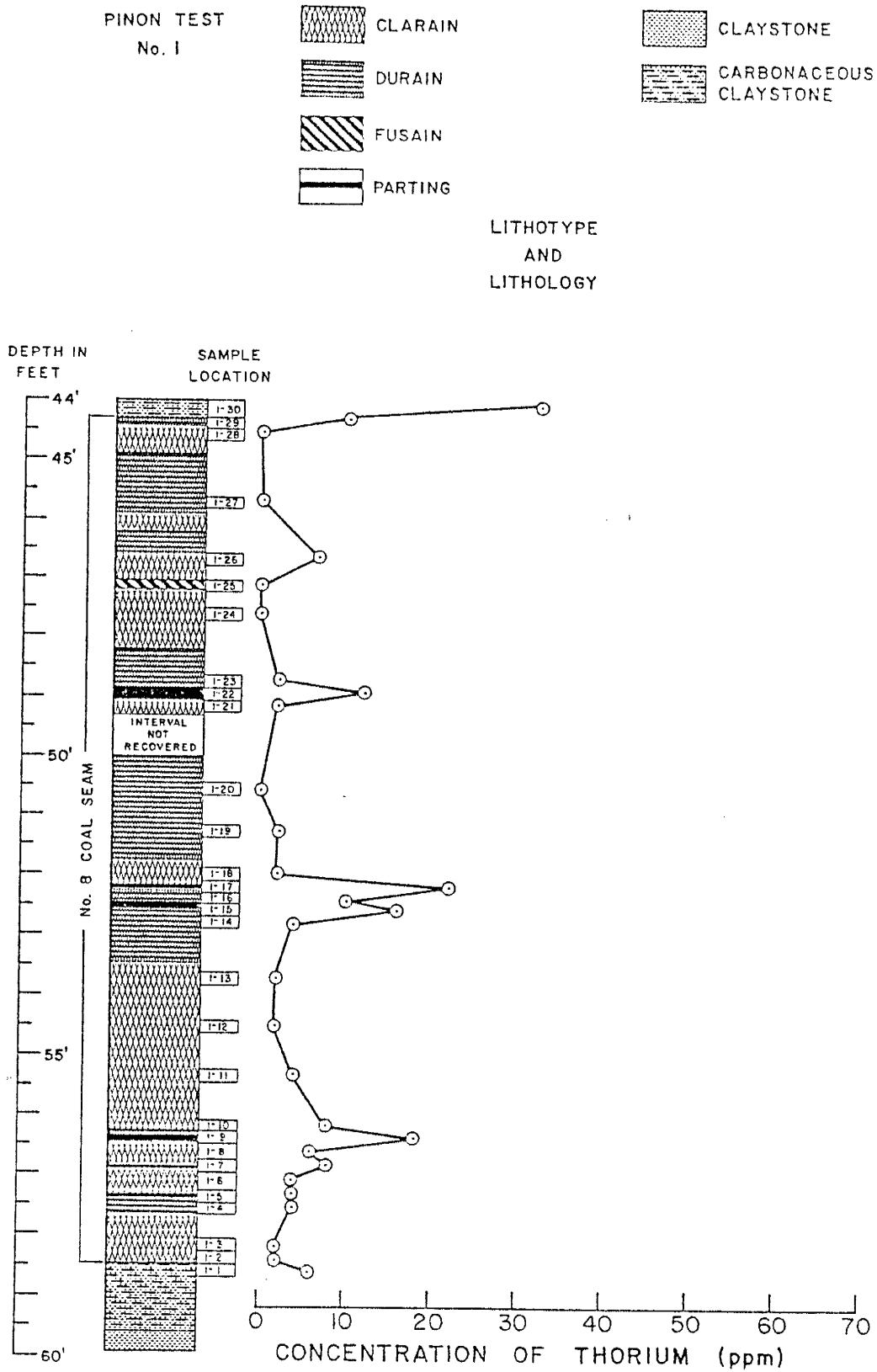
Figure A-63 – Distribution of Thorium
in Pinon Test No. 1.
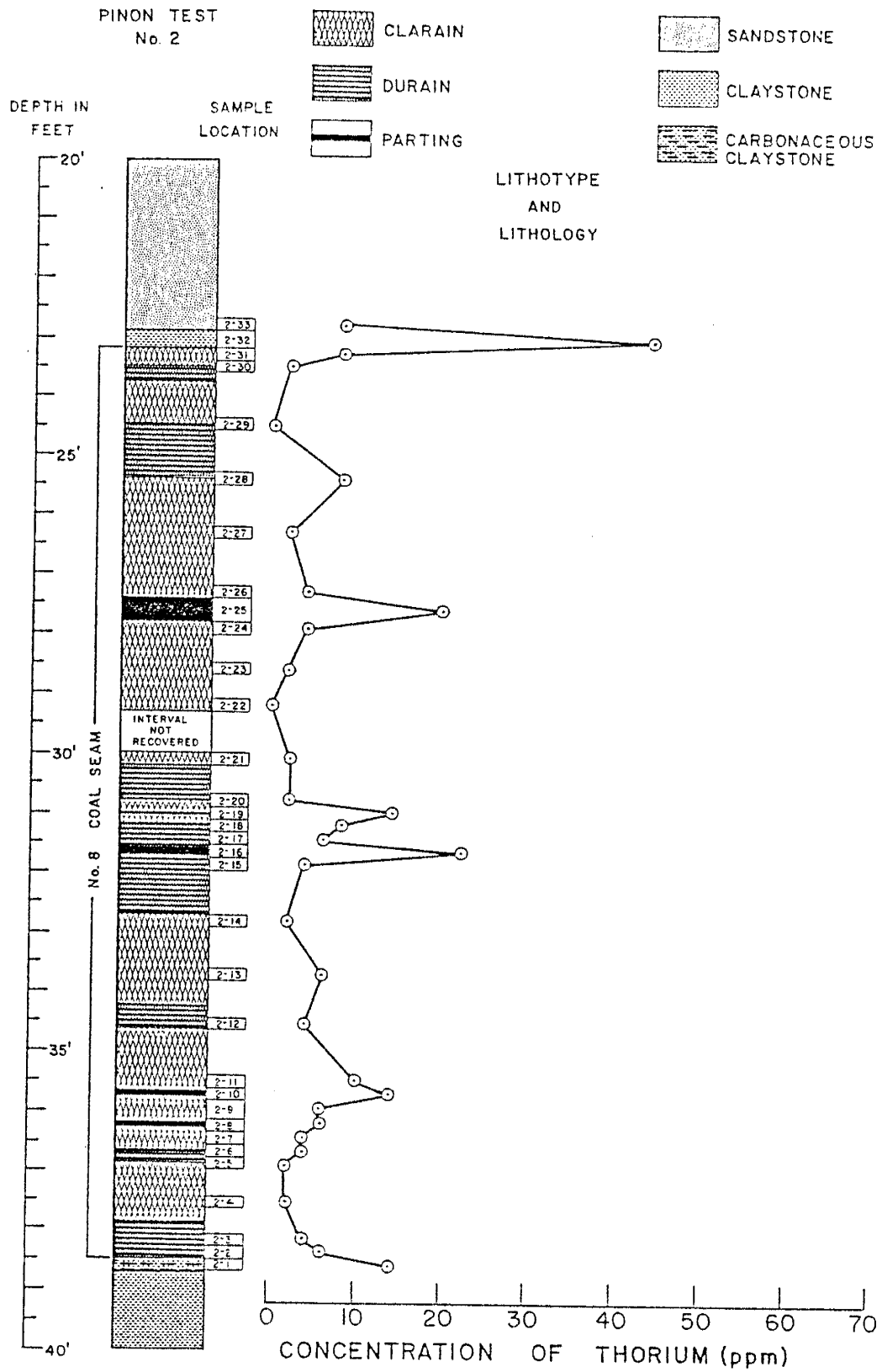
Figure A-66 – Distribution of Thorium
in Pinon Test No. 2.
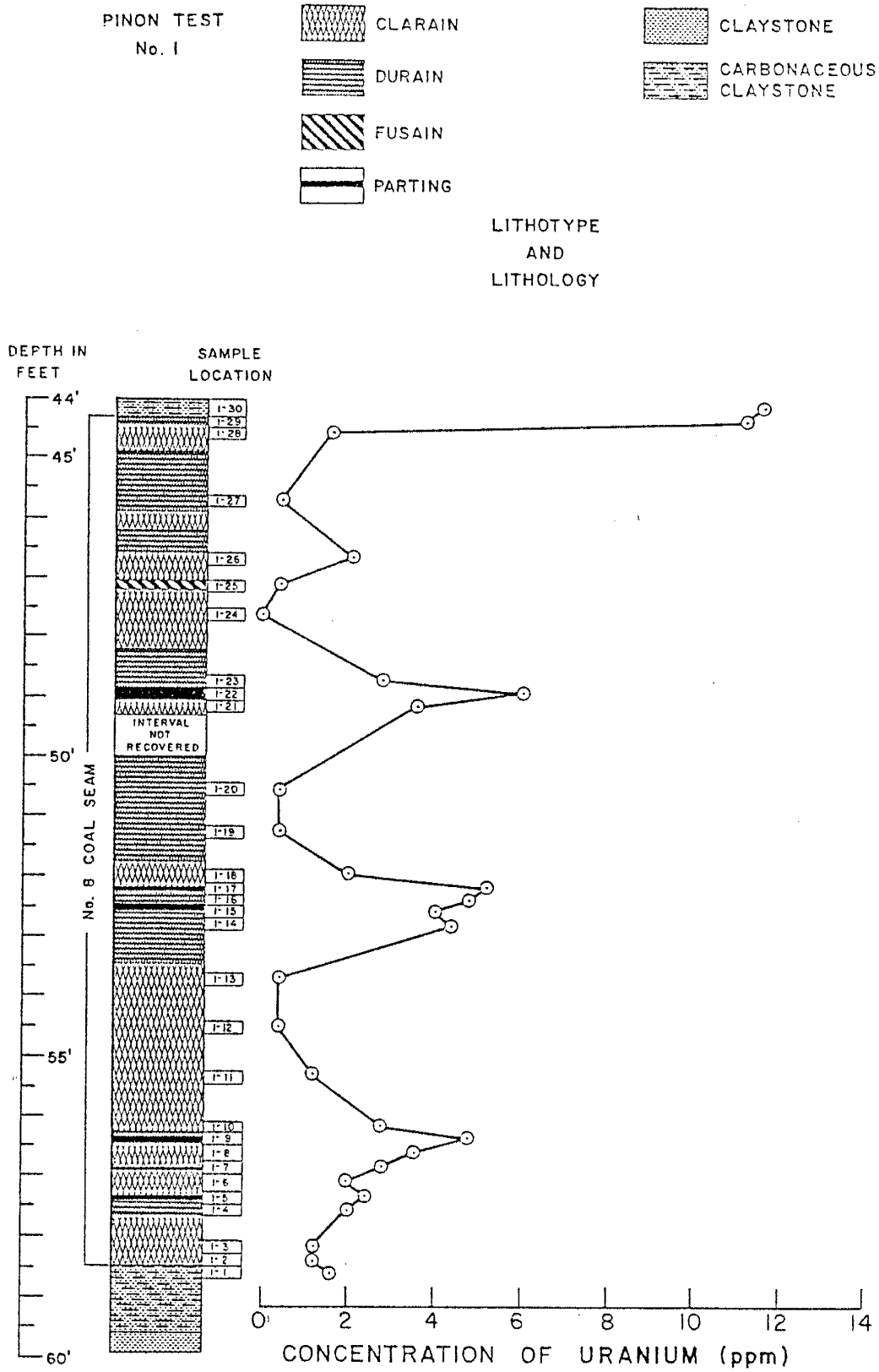
Figure A-65 - Distribution Of Uranium
in Pinon Test No. 1.
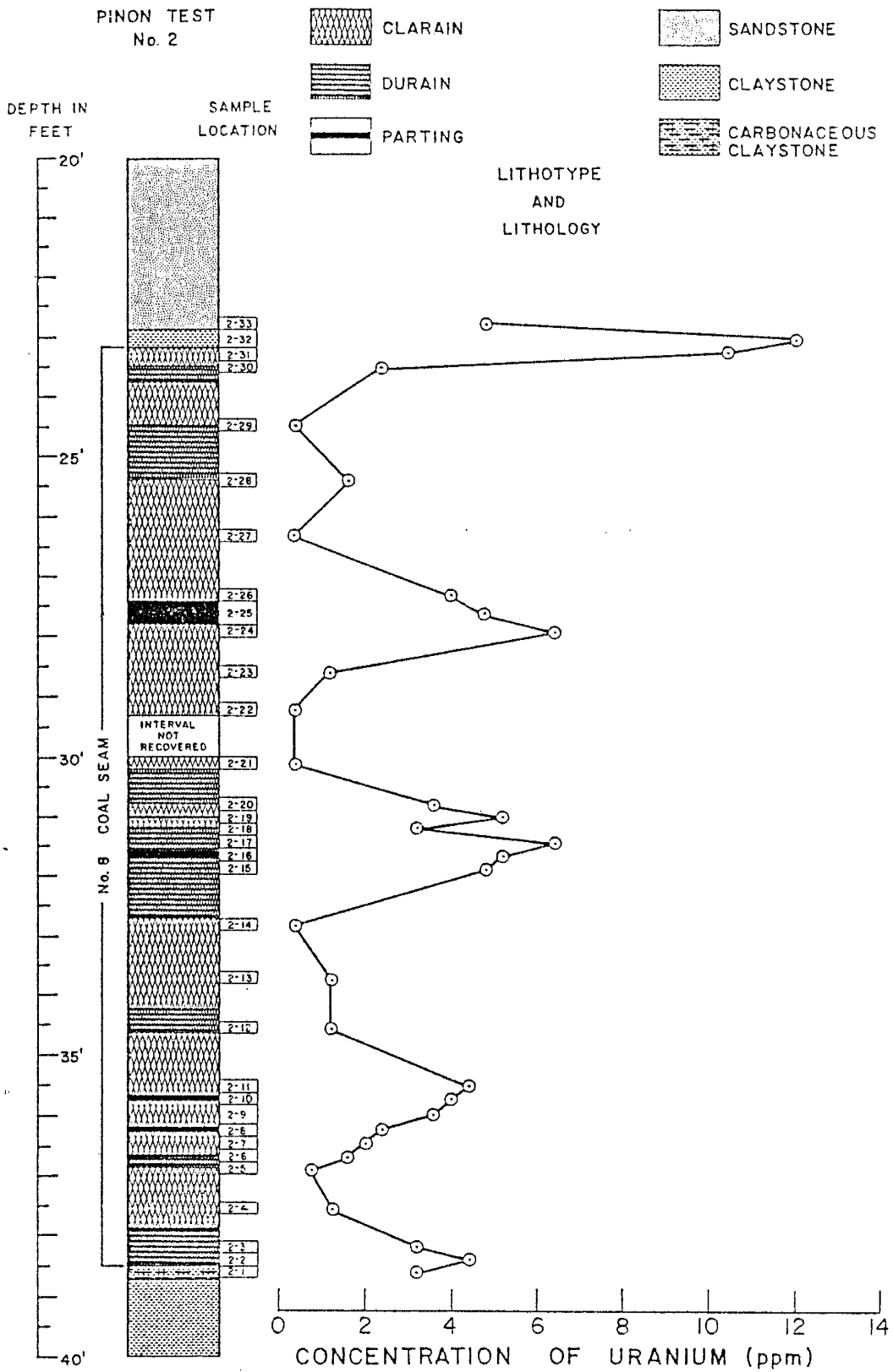
Figure A-66 - Distribution of Uranium
in Pinon Test No. 2.
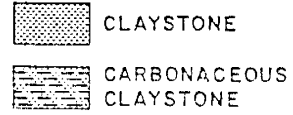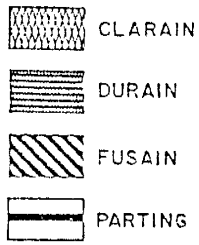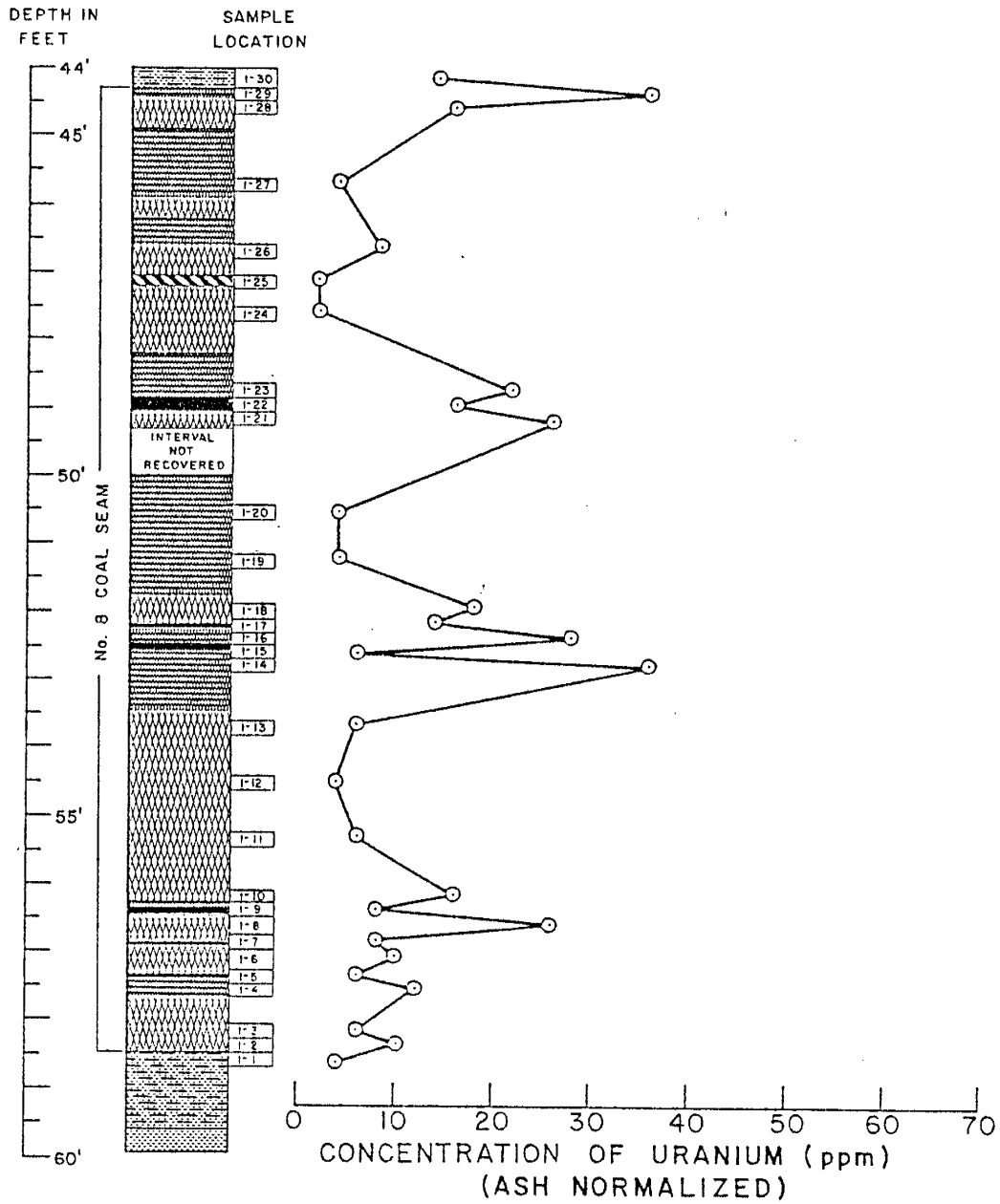
Figure A-67 - Ash normalized distribution of
Uranium in Pinon Test No. 1.
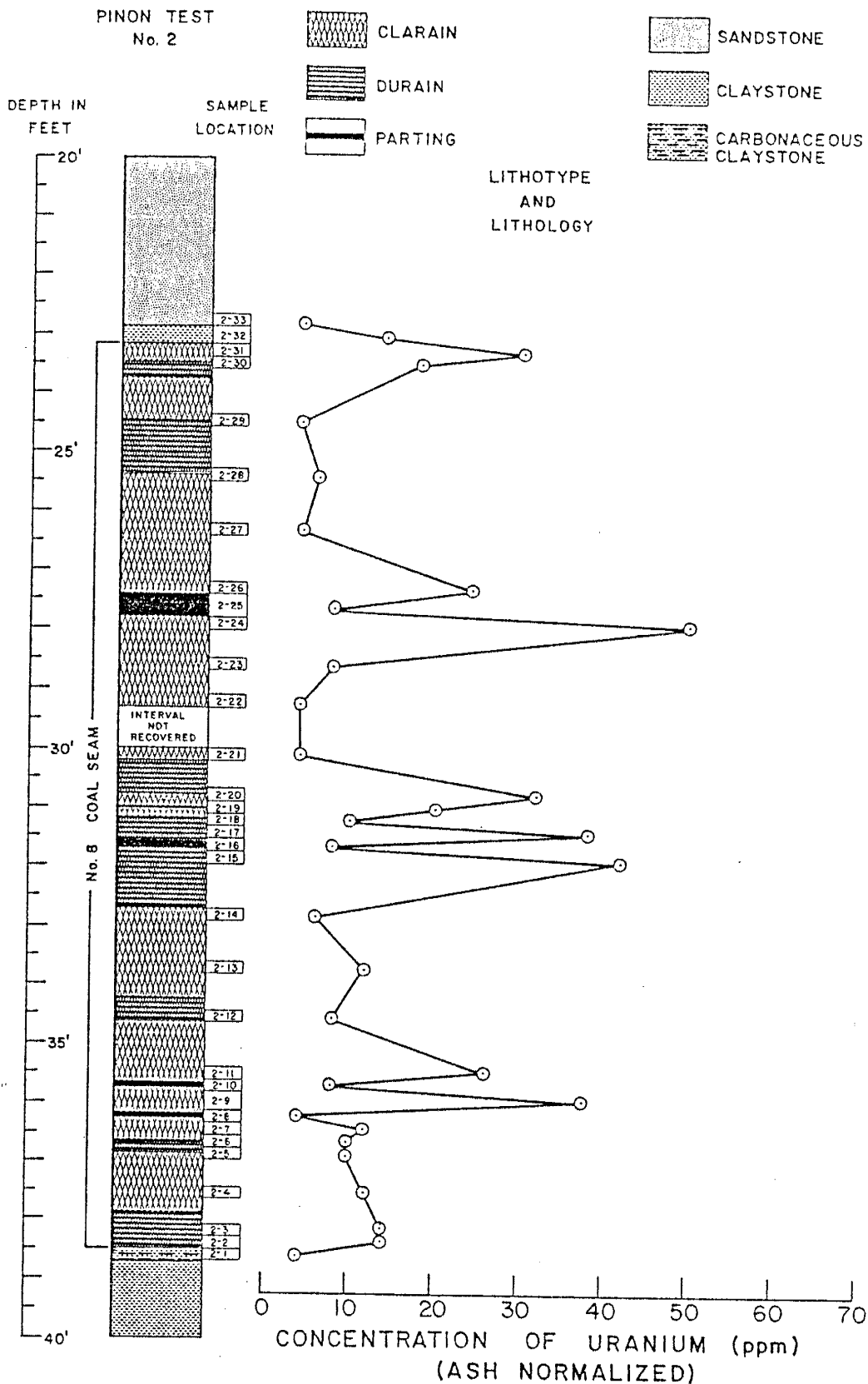
Figure A-68 - Ash normalized distribution of Uranium in Pinon Test No. 2.
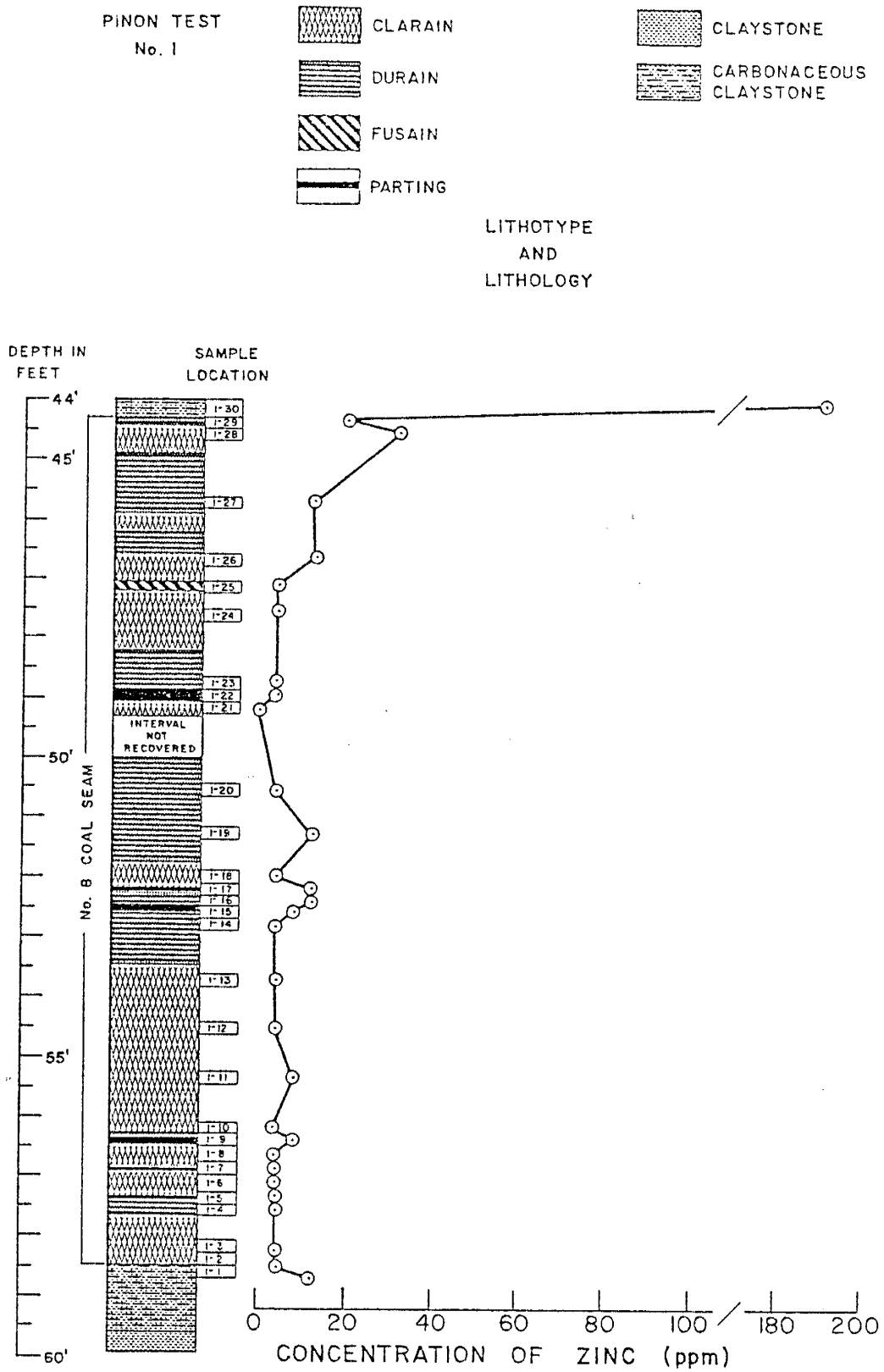
Figure A-69 - Distribution of Zinc
in Pinon Test No. 1.
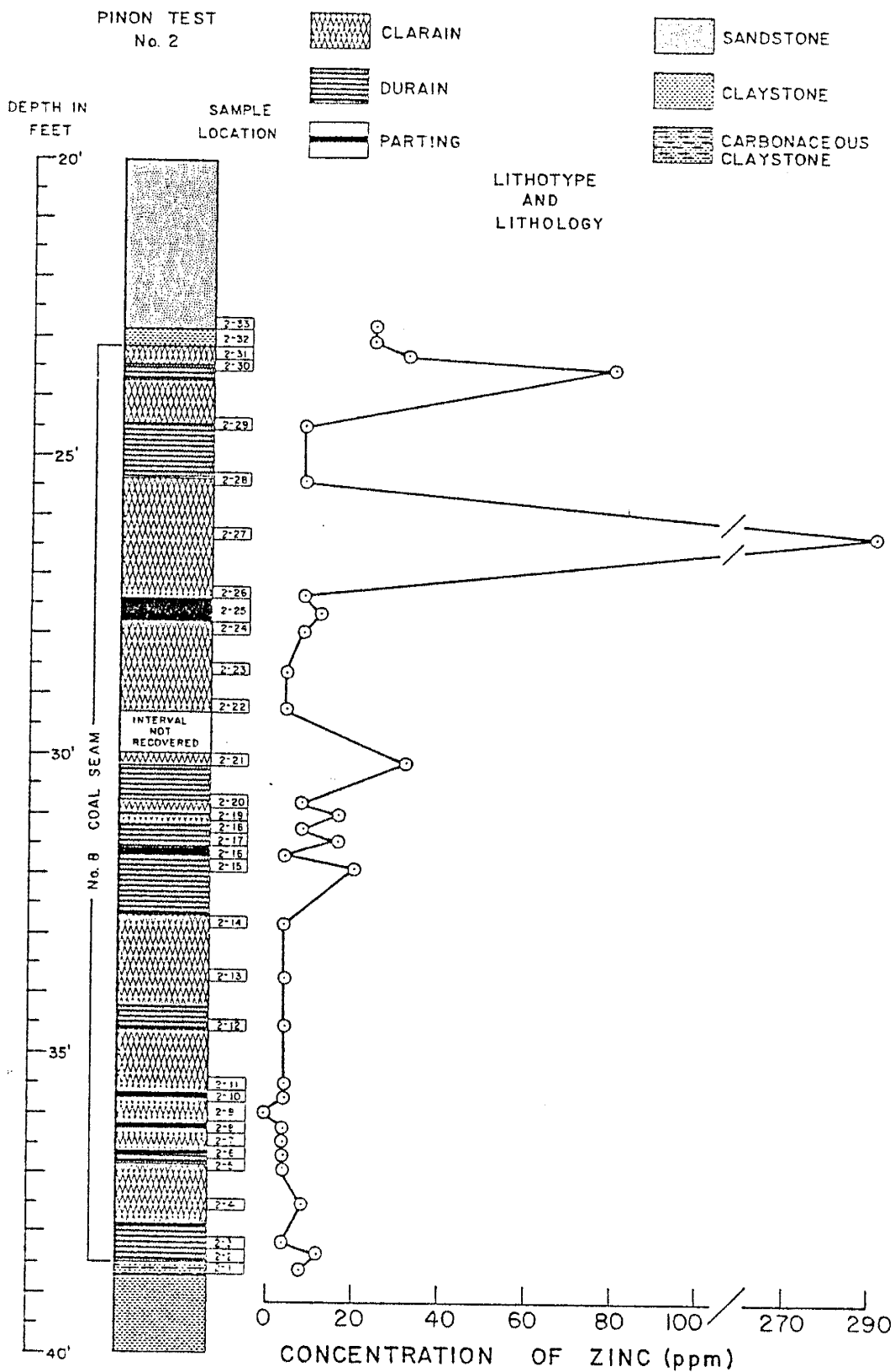
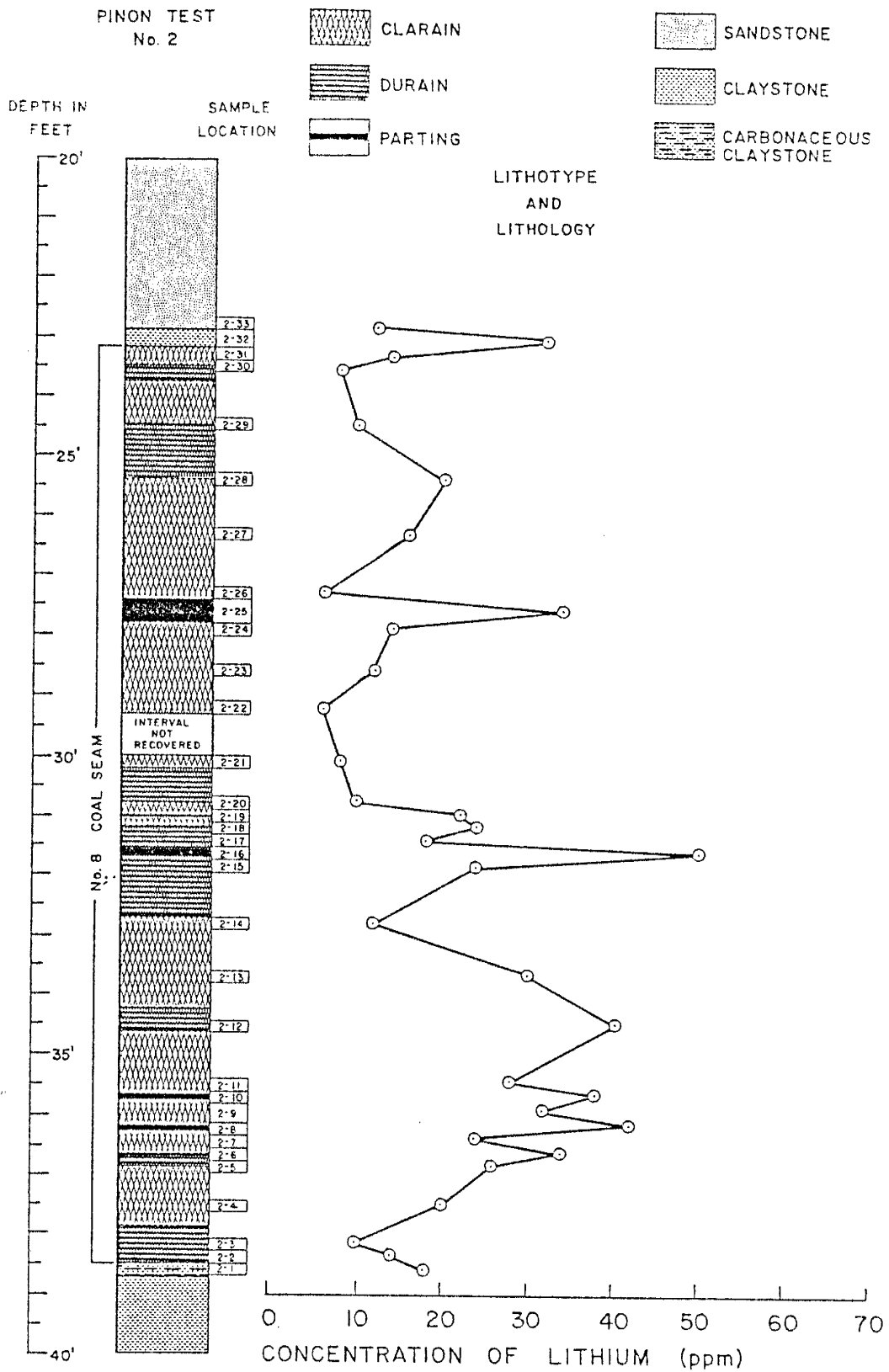Figure A-70 - Distribution of Zinc
in Pinon Test No. 2.

APPENDIX IV


INSTRUMENTAL NEUTRON ACTIVATION ANALYSIS


Instrumentation and Procedures


Analyses were made using a NUCLEAR DATA 6620 system, with two high purity germanium detectors. The signal from these detectors was preamplified, passed through a peak shaping circuit, an amplifier, and an analog to digital converter. Following processing by the ADC, the signal, (representing a spectra covering 70 Kev to 1700 Kev), was accumulated in the NUCLEAR DATA 6620 computer memory, and simultaneously displayed on a CRT. The resulting spectra was dumped from the computer memory to a magnetic disk, and subsequently processed to produce elemental abundances by a computer program known as "TEABAGS", Lundstrom and Korotev, (1982).

The procedure used generally followed that given by Jacobs et al., (1977), and is briefly described below. Approximately 100 mg of dried sample was weighed to the nearest 0.01 mg in a clean 3 mm I.D. ultra pure fused silica vial, and subsequently sealed. The vials were then washed, rinsed in distilled water, and reweighed for identification purposes.

The vials were wraped in aluminum foil forming a sleeve which was aligned around the inside of a 3.35 inch diameter irradiation capsule. The capsule was irradiated for approximately 48 hours in a flux of 2.0 x $10^{13}$ n $cm^{-2}$ $sec^{-1}$, at the 10 MW Research Reactor Facility, University of Missouri. Rotation of the capsule during irradiation assured that all samples were exposed to the same flux. Two irradiations, were necessary to handle all of the samples. The first and second irradiations were comprised of samples from Pinon Test No. 1, and Pinon Test No. 2, respectively.

Following a cooling-off period of approximately 60 hours, the irradiated samples were returned to New Mexico Institute of Mining and Technology for analysis. Because only one detector was available during the counting period following the first irradiation, the counting scheme differed from that used for samples from the second irradiation. The counting scheme for Pinon Test No. 1 samples was as follows:

| Count | Days Since Irradiation | Count Duration in Hours |
|---|---|---|
| Short # 1 | 5 | 1 |
| Short # 2 | 7 | 3 |
| Long | 40 | 3 |

The first, or short No. 1 count was necessary to maintain acceptable activities for some of the very short

half-lived isotopes such as arsenic. By extending the counting period for the second, or short No. 2 count, to three hours, a considerable improvement in counting statistics was realized. The third, or long count, was used to obtain better resolution on the longer half-lived isotopes.

The counting scheme used for Pinon Test No. 2 samples was an abbreviated form of that used for Pinon Test No. 1 samples, and is outlined below:

| Count | Days Since Irradiation | Count Duration In Hours |
|-------|------------------------|-------------------------|
| Short | 5 | 3 |
| Long | 40 | 3 |

Because two detectors were available to count samples from the second irradiation, the count duration for the first count was be extended to three hours, while still maintaining sufficient activity from the arsenic peaks to provide acceptable results. Therefore the need for the one hour, short count was eliminated.

Analysis of NBS coal standards showed no significant differences between results generated from the two different counting schemes.

## Precision and Accuracy

To estimate the precision of this technique two triplicate and one duplicate analyses were preformed on unknown samples. The results of these analyses are given in table C. The last column is a weighted average of the coefficient of variation, (based on the number of samples in the replicate set). Three analyses were run for P.T. 2-16 and P.T. 2-18, and two for P.T. 1-30. The coefficient of variation gives an estimate of the analytical precision.

To determine the analytical accuracy, two NBS standard coal reference materials (NBS 1632a and NBS 1635) were analyzed as unknowns. These results are summarized in table D and E along with the National Bureau of Standards values and a summary of quoted literature values compiled by Gladney et al., (1982).

TABLE C

Sample Replicate Analysis Summary (INAA)

| Element | P.T. 2-16 n = 3 | | P.T. 2-18 n = 3 | | P.T. 1-30 n = 2 | | |
|---|---|---|---|---|---|---|---|
| | X | Coef. of Var. | X | Coef. of Var. | X | Coef. of Var. | A ve. Coef. of Var. |
| As (ppm) | 0.20 | 32.2 | 0.60 | 10.6 | 1.54 | 2.3 | 16.6 |
| Ba (ppm) | 257. | 1.5 | 1526. | 0.8 | 627. | 5.2 | 2.1 |
| Br (ppm) | 0.18 | 30.6 | 0.52 | 4.4 | * 0.04 | 88.4 | 35.2 |
| Ca ( % ) | 0.87 | 1.6 | 1.87 | 3.9 | 0.51 | 11.1 | 4.9 |
| Ce (ppm) | 56.6 | 2.7 | 25.4 | 1.8 | 89.1 | 0.0 | 1.7 |
| Co (ppm) | 2.51 | 4.1 | 3.06 | 1.9 | 3.87 | 1.8 | 2.7 |
| Cr (ppm) | 4.7 | 3.7 | 3.5 | 12.5 | 5.8 | 7.3 | 7.9 |
| Cs (ppm) | 0.731 | 0.8 | 0.450 | 1.4 | 1.439 | 1.7 | 1.3 |
| Eu (ppm) | 0.563 | 1.5 | 0.297 | 1.3 | 0.757 | 0.3 | 1.1 |
| Fe ( % ) | 0.402 | 1.8 | 0.578 | 7.7 | 1.879 | 12.2 | 6.6 |
| Hf (ppm) | 3.15 | 3.8 | 2.63 | 4.2 | 5.78 | 6.0 | 4.5 |
| La (ppm) | 26.60 | 2.0 | 11.82 | 0.3 | 45.7 | 0.5 | 1.0 |
| Lu (ppm) | 0.166 | 2.3 | 0.174 | 3.5 | 0.341 | 3.7 | 3.1 |
| Na ( % ) | 0.2436 | 1.3 | 0.1124 | 2.1 | 1.6773 | 0.7 | 1.4 |
| Nd (ppm) | 20.4 | 2.7 | 10.1 | 1.0 | 34.6 | 0.6 | 1.5 |
| Rb (ppm) | 16.0 | 3.8 | 7.1 | 7.0 | 12.8 | 6.1 | 5.5 |
| Sb (ppm) | 0.221 | 5.2 | 0.678 | 2.0 | 0.81 | 3.5 | 3.6 |
| Sc (ppm) | 3.21 | 0.3 | 3.70 | 0.6 | 4.21 | 0.0 | 0.3 |
| Se (ppm) | 1.84 | 11.3 | 1.15 | 10.1 | 1.75 | 6.5 | 9.6 |
| Sm (ppm) | 3.61 | 1.7 | 2.13 | 0.8 | 4.93 | 0.6 | 1.1 |
| Sr (ppm) | 55. | 13.4 | 108. | 2.3 | 178. | 8.0 | 7.9 |
| Ta (ppm) | 2.51 | 1.2 | 0.604 | 0.7 | 1.99 | 1.4 | 1.1 |
| Tb (ppm) | 0.41 | 5.6 | 0.327 | 1.6 | 0.56 | 2.5 | 3.3 |
| Th (ppm) | 21.64 | 1.2 | 8.55 | 1.0 | 32.9 | 1.5 | 1.2 |
| U (ppm) | 5.08 | 2.0 | 3.15 | 1.0 | 12.45 | 0.6 | 1.2 |
| Yb (ppm) | 1.03 | 3.4 | 1.045 | 2.2 | 2.09 | 3.4 | 3.0 |

\* = value reported as upper limit only
n = number of analyses in replicate set
X = Mean value of replicate analyses

TABLE D

NBS 1632a REPLICATE ANALYSIS RESULTS (INAA)

| Element | | Mean | S.D. | NBS | Uncr. | Glad. | Uncr. | |
|---------|------|------|------|------|-------|-------|-------|---|
| As | (ppm) | 8.82 | 0.535 | 9.3 | 1.0 | 9.3 | 0.4 | |
| Ba | (ppm) | 105. | 5.13 | – | – | 124. | 16. | |
| Br | (ppm) | 44.0 | 1.48 | – | – | 42. | 2. | |
| Ca | (ppm) | 0.12 | 0.038 | – | – | 0.24 | 0.02 | @ |
| Ce | (ppm) | 29.3 | 0.781 | 30. | – | 29. | 2. | |
| Co | (ppm) | 6.48 | 0.231 | 6.8 | – | 6.4 | 0.3 | |
| Cr | (ppm) | 34.2 | 0.551 | 34.4 | 1.5 | 34. | 5. | |
| Cs | (ppm) | 2.17 | 0.030 | 2.4 | – | 2.3 | 0.2 | |
| Eu | (ppm) | 0.457 | 0.013 | 0.540 | – | 0.527 | 0.023 | @ |
| Fe | (%) | 1.11 | 0.049 | 1.11 | 0.02 | 1.12 | 0.02 | |
| Hf | (ppm) | 1.46 | 0.044 | 1.6 | – | 1.68 | 0.19 | |
| La | (ppm) | 13.5 | 0.534 | – | – | 15. | 3. | |
| Lu | (ppm) | 0.167 | 0.003 | – | – | 0.176 | 0.003 | |
| Na | (%) | 0.078 | 0.002 | – | – | 0.0830 | 0.0100 | |
| Nd | (ppm) | 14.7 | 1.617 | – | – | 11.4 | 1.3 | @ |
| Rb | (ppm) | 26.6 | 0.954 | 31. | – | 29.0 | 0.5 | @ |
| Sb | (ppm) | 0.563 | 0.023 | 0.58 | – | 0.60 | 0.12 | |
| Sc | (ppm) | 5.95 | 0.186 | 6.3 | – | 6.4 | 0.3 | |
| Se | (ppm) | 2.65 | 0.090 | 2.6 | 0.7 | 2.6 | 0.2 | |
| Sm | (ppm) | 2.48 | 0.087 | – | – | 2.4 | 0.3 | |
| Sr | (ppm) | 81. | 18.1 | – | – | 89. | 5. | |
| Ta | (ppm) | 0.370 | 0.004 | – | – | 0.410 | 0.030 | |
| Tb | (ppm) | 0.343 | 0.006 | – | – | 0.310 | 0.020 | |
| Th | (ppm) | 4.28 | 0.132 | 4.5 | 0.1 | 4.5 | 0.3 | |
| U | (ppm) | 1.27 | 0.046 | 1.28 | 0.02 | 1.22 | 0.07 | |
| Yb | (ppm) | 1.05 | 0.031 | – | – | 1.03 | 0.12 | |

S.D.  = Standard Deviation
Uncr. = Uncertainty
Glad. = Gladney et al., (1982)
 @    = determined value plus or minus one standard deviation
        lies outside the value range given by Gladney et al.
        or NBS.

## TABLE E

### NBS 1635 REPLICATE ANALYSIS SUMMARY (INAA)

| Element | Mean | S.D. | NBS | Uncr. | Glad. | Uncr. | |
|---|---|---|---|---|---|---|---|
| As (ppm) | 0.46 | 0.038 | 0.42 | 0.15 | 0.35 | 0.06 | |
| Ba (ppm) | 90.2 | 17.0 | – | – | 73. | 6. | |
| Br (ppm) | 1.46 | 0.095 | – | – | 1.9 | 0.8 | |
| Ca (%) | 0.54 | 0.084 | – | – | 0.5500 | 0.0200 | |
| Ce (ppm) | 3.12 | 0.150 | 3.6 | – | 3.4 | 0.1 | @ |
| Co (ppm) | 0.630 | 0.069 | 0.65 | – | 0.64 | 0.06 | |
| Cr (ppm) | 2.38 | 0.010 | 2.5 | 0.3 | 2.38 | 0.24 | |
| Cs (ppm) | 0.046 | 0.004 | – | – | 0.050 | – | |
| Eu (ppm) | 0.053 | 0.002 | 0.064 | – | 0.060 | – | @ |
| Fe (%) | 0.215 | 0.012 | 0.239 | 0.005 | 0.229 | 0.006 | |
| Hf (ppm) | 0.24 | 0.021 | 0.29 | – | 0.27 | 0.02 | |
| La (ppm) | 1.81 | 0.153 | – | – | 1.8 | 0.4 | |
| Lu (ppm) | 0.027 | 0.0006 | – | – | 0.032 | – | |
| Na (%) | 0.226 | 0.009 | – | – | 0.2400 | 0.0200 | |
| Nd (ppm) | 1.34 | 0.165 | – | – | 1.4 | – | |
| Rb (ppm) | 0.5 | 0.136 | – | – | 0.8 | – | @ |
| Sb (ppm) | 0.141 | 0.010 | 0.14 | – | 0.14 | 0.02 | |
| Sc (ppm) | 0.574 | 0.022 | 0.63 | – | 0.71 | 0.14 | |
| Se (ppm) | 0.85 | 0.085 | 0.9 | 0.3 | 0.89 | 0.08 | |
| Sm (ppm) | 0.260 | 0.012 | – | – | 0.29 | 0.04 | |
| Sr (ppm) | 109. | 5.00 | – | – | 128. | 9. | @ |
| Ta (ppm) | 0.040 | 0.001 | – | – | 0.045 | – | @ |
| Tb (ppm) | 0.044 | 0.005 | – | – | 0.035 | – | @ |
| Th (ppm) | 0.556 | 0.018 | 0.62 | 0.04 | 0.62 | 0.03 | @ |
| U (ppm) | 0.20 | 0.035 | 0.24 | 0.02 | 0.25 | 0.06 | |
| Yb (ppm) | 0.159 | 0.011 | – | – | 0.16 | 0.02 | |

S.D.  = Standard Deviation
Uncr. = Uncertainty
Glad. = Gladney et al., (1982)
 @    = determined value plus or minus one standard deviation lies outside the value range given by Gladney et al. or NBS.

In general the agreement is very good between the values determined in this study and the accepted values. Europium, rubidium, and tantalum consistently fall below the value range specified by either NBS, or Gladney (1982). Other

elements which lie outside the accepted value range on one, but not both analyses are: Ca, Ce, Fe, Nd, Sr, Tb, and Th. The determined mean, however, differs by less than 15 % from the accepted mean for most of these elements.

## ATOMIC ABSORPTION SPECTROPHOTOMETRY

### Instrumentation and Procedures

A Varian model 1250 atomic absorption spectrophotometer, equipped with a deuterium arc background correcting system, was used for all AA analyses. An air-acetylene flame, in conjunction with a 4 inch burner head was used for all elements determined. The burner head was occasionaly rotated during the analysis of Mn and Zn to reduce sensitivity.

The instrumental parameters used for the analyses were as prescribed in the operators' manual, and are given in table F.

TABLE F

INSTRUMENTAL PARAMETERS FOR ATOMIC ABSORPTION ANALYSIS

| Element | Wavelength in nm | Spectral Bandpass in nm | Lamp Current in mA | Optimum Working Range in (ppm) |
|---------|-----------------|------------------------|--------------------|-------------------------------|
| Co | 240.7 | 0.2 | 5.0 | 3.0 – 12.0 |
| Cr | 357.9 | 0.2 | 5.0 | 2.0 – 8.0 |
| Cu | 324.7 | 0.5 | 3.0 | 2.0 – 8.0 |
| Li | 670.8 | 0.2 | 5.0 | 1.0 – 4.0 |
| Mn | 279.5 | 0.2 | 5.0 | 1.0 – 4.0 |
| Ni | 232.0 | 0.2 | 5.0 | 3.0 – 12.0 |
| Pb | 217.0 | 0.2 | 5.0 | 5.0 – 20.0 |
| Zn | 213.9 | 0.5 | 5.0 | 0.4 – 1.6 |

Because of the complex sample matrix, it was necessary to use the methods of standard additions, as described in Beaty, (1978), to compensate for the various interferences observed. A standard additions set, consisting of three aliquot samples, was generated for each sample. This allowed determination of three points on the standard additions curve, from which a least squares regression analysis could be made. The regression analysis was then used to predict the x intercept, (the actual sample solution concentration) as well as a regression coefficient "r" which measures the linearity of the curve. This "r" value was used as an indication of the reliability of the determined value.

Preparation of the analysis sample involved ashing and digesting approximately 30 g of sample stock. Ashing of the coal was necessary to remove all organic material prior to

the acid digestion procedure, outlined below:

    25 ml hydrofluoric acid; fumed to dryness
    40 ml aqua regia; fumed to dryness
    10 ml nitric + 10 ml perchloric acid; fumed to dryness
    20 ml perchloric acid; fumed to dryness

Following acid decomposition the samples were brought up to about 30 ml volume in dilute nitric acid. Then 10 ml of 30 % hydrogen peroxide was added to ensure complete oxidation of all iron and manganese. The samples were filtered to remove excess silicate solids. The filter paper was washed with several small washings of warm dilute nitric acid to ensure quantitative transfer of all analyte ions. These samples were then brought up to 50 ml total volume, and subsequent aliquots taken to produce the standard additions set. A reagent blank was carried through the digestion procedure with each sample lot. All reagents used were ACS reagent grade chemicals.

## Precision and Accuracy

As previously mentioned the regression coefficient was used as a reliability indicator. A duplicate analysis of at least one sample in each lot was preformed to check reproducibility. A summary of these duplicate analyses is given in table G.

TABLE G

DUPLICATE ANALYSES SUMMARY FOR ATOMIC ABSORPTION

| Sample | | Cu | Li | Mn | Ni | Pb | Zn |
|---|---|---|---|---|---|---|---|
| 1 - 8 | Mean | 23.6 | 37.2 | 5.7 | 4.5 | 14.0 | 2.3 |
| | Range | 0.3 | 8.6 | 0.8 | 0.6 | 2.2 | 1.3 |
| 1 - 23 | Mean | 7.4 | 6.0 | 43.6 | 2.3 | 2.5 | 2.7 |
| | Range | 0.1 | 1.0 | 18.8 | 0.1 | 0.0 | 0.7 |
| 1 - 30 | Mean | 49.4 | 14.9 | 11.9 | 1.6 | 242.3 | 193.3 |
| | Range | 5.5 | 7.0 | 0.8 | 0.1 | 30.0 | 7.9 |
| 2 - 7 | Mean | 23.5 | 24.6 | 15.0 | 2.6 | 11.4 | 6.7 |
| | Range | 1.1 | 0.6 | 0.9 | 0.2 | 0.5 | 1.6 |
| 2 - 14 | Mean | 13.2 | 12.5 | 10.6 | 1.6 | 2.9 | 3.6 |
| | Range | 0.6 | 0.3 | 2.3 | 0.0 | 0.2 | 1.4 |
| 2 - 21 | Mean | 13.2 | 8.7 | 12.9 | 2.5 | 50.4 | 31.0 |
| | Range | 0.0 | 2.0 | 1.3 | 0.0 | 5.4 | 14.1 |
| 2 - 28 | Mean | 29.1 | 20.4 | 17.0 | 1.4 | 2.4 | 6.2 |
| | Range | 4.0 | 3.4 | 2.0 | 0.3 | 0.7 | 2.0 |

In general the precision is good for most elements. Zinc was the most difficult element to determine, and this shows up in the generaly poor level of precision compared to the other elements determined by AA.

An aliquot sample of NBS standard fly ash reference material 1633a was analyzed as a check of its overall accuracy. The results of this analysis are given in table H.

TABLE H

NBS 1633a ANALYSIS (AA)

| Element | Determined Value | NBS Value | | Difference |
|---|---|---|---|---|
| Cu (ppm) | 115 | 118 | + 3 | 3 |
| Li (ppm) | 204 | - - - | | - - - |
| Mn (ppm) | 192 | 190 | | 2 |
| Ni (ppm) | 144 | 127 | + 4 | 17 |
| Pb (ppm) | 77.9 | 72.4 | + 0.4 | 5.5 |
| Zn (ppm) | 272 | 220 | + 10 | 52 |

No value is given for lithium in either the NBS fly ash, or coal standards, therefore the relative accuracy is unknown. Both Cu and Mn show good agreement with the NBS values. While Ni and Pb lie outside the value range stated by NBS the agreement is still considered good. Zinc on the other hand shows poor agreement, but the difference is about the same magnitude as that seen in the duplicate analyses.

ION SELECTIVE ELECTRODE (FLUORINE)

Instrumentation and Procedures

A Corning model 94-09 A fluoride ion-selective electrode, a Orion model 90-02 double junction reference electrode, and an Orion model 407 A research meter were used to determine fluoride content in the sample solution. A

Parr model 1241 adiabatic oxygen bomb calorimeter was used

for combustion of the coal sample. The ASTM (D-3761)

procedure, Total Fluorine in Coal by the Oxygen Bomb

Combustion / Ion Selective Electrode Method was used with a

minor revision. This was the addition of benzoic acid to

high ash samples, as discussed in Thomas and Gluskoter

(1974).


## Precision and Accuracy


Five duplicate analyses, three without the addition of

benzoic acid and two with, were made to estimate the

precision of the technique. In addition a triplicate

analysis of NBS 1635 standard coal reference material was

analyzed as an accuracy check. These replicate analyses are

listed in table I.

TABLE I

FLUORIDE REPLICATE ANALYSES SUMMARY

| Sample | No. 1 | No. 2 | Mean | Range |
|--------|-------|-------|------|-------|
| 1 - 12 | 49.2 | 50.4 | 49.8 | 1.2 |
| 1 - 28 | 94.3 | 94.5 | 94.4 | 0.2 |
| 1 - 25 | 23.0 | 23.0 | 23.0 | 0.0 |
| * 1 - 22 | 133. | 138. | 136. | 5. |
| * 1 - 5 | 102. | 116. | 109. | 14. |

* = addition of benzoic acid

| Sample | Mean | S.D. | Coef. of Var. | Glad. |
|--------|------|------|---------------|-------|
| NBS 1635 | 20.1 | 0.757 | 3.7 | 20. |

Glad. = Gladney et al. (1982)

TOTAL SULFUR ANALYSIS

Instrumentation and Procedure

A Fisher model 475 Total Sulfur Analyzer was used to
determine the total sulfur content of all samples. A
detailed description and operation procedure for this
instrument may be found in the operators' manual. A brief
description of the procedure is given to familiarize the
reader with its operation.

The sample is combusted in a tube furnace at 1350
degrees centigrade. During combustion the tube is purged

with oxygen, and the resulting sulfur oxides are delivered from the furnace to a sealed reaction vessel through a length of heated tubing. Sulfur oxides entering the reaction vessel are bubbled into an organic solvent changing its potential. A titrant, pyridine, is delivered into the reaction vessel via a mechanical syringe. The potential of the solvent is monitored by a platinum electrode, which in turn controls titrant delivery.

The volume of titrant required is used in conjunction with an empirically determined titrant factor and the sample mass to calculate the percent sulfur. All operations are controlled by a microprocessor once the start sequence is initiated by the operator.

### Precision and Accuracy

Duplicate analyses were run for all samples, as is standard procedure for this analysis by the New Mexico Bureau of Mines and Mineral Resources Coal Lab. The range of duplicate samples expressed as a percentage of the mean averages six percent. Nine replicate analyses of an in-house standard were run as an estimate of both the relative precision and accuracy. The accepted value for this standard is 0.6897 % sulfur, as determined by calibration against a commercially available standard (Alpha Coal Standard). The mean value of the nine replicates was

0.6906 %, a difference of 0.0009 %. The coefficient of variance for the replicate set is 3.0 %. This value is also consistent with the variance observed in the duplicate analyses.


## PROXIMATE ANALYSIS AND HEATING VALUE


For the proximate analyses, moisture, ash, volatile matter, and fixed carbon, ASTM procedures D-3173, D-3174, and D-3175 were followed. The modified method, for use with sparking coals, was used for the volatile matter and fixed carbon analysis.

The heating value of the samples was determined as per ASTM procedure D-2015, Test for Gross Calorific Value of a Solid Fuel by the Adiabatic Bomb Calorimeter. A Parr model 1241 adiabatic oxygen bomb calorimeter was used. The calorimetry was determined concurrently with the generation of the fluoride analysis solutions, thus requiring a restandardization of the calorimeter to compensate for the addition of the 5 ml of NaOH to the bomb contents.

For both the proximate analysis and heating value determinations all values lie within the ranges stated by ASTM for repeatibility within the same laboratory.

## APPENDIX V
## TABLE J

Pearson Correlation Coefficients for Pinon Test No. 1 and No. 2

P E A R S O N   C O R R E L A T I O N   C O E F F I C I E N T S

|     | As | Ba | Br | Ca | Ce | Co | Cr | Cs | Cu | Eu |
|-----|----|----|----|----|----|----|----|----|----|----|
| As | 1.0000<br>(631)<br>P=**** | 0.0788<br>(631)<br>P=.539 | -0.2752<br>(631)<br>P=.029 | 0.1210<br>(631)<br>P=.345 | -0.1431<br>(631)<br>P=.263 | 0.0236<br>(631)<br>P=.854 | -0.0805<br>(631)<br>P=.530 | -0.0885<br>(631)<br>P=.490 | -0.0896<br>(631)<br>P=.485 | -0.1867<br>(631)<br>P=.143 |
| Ba | 0.0788<br>(631)<br>P=.539 | 1.0000<br>(631)<br>P=**** | -0.0970<br>(631)<br>P=.450 | -0.1298<br>(631)<br>P=.311 | -0.0029<br>(631)<br>P=.624 | -0.0049<br>(631)<br>P=.945 | -0.1320<br>(631)<br>P=.302 | -0.0827<br>(631)<br>P=.520 | -0.0573<br>(631)<br>P=.656 | -0.0970<br>(631)<br>P=.449 |
| Br | 0.2752<br>(631)<br>P=.029 | -0.0970<br>(631)<br>P=.450 | 1.0000<br>(631)<br>P=**** | 0.0946<br>(631)<br>P=.461 | -0.3390<br>(631)<br>P=.007 | 0.0041<br>(631)<br>P=.974 | 0.0234<br>(631)<br>P=.856 | -0.1767<br>(631)<br>P=.166 | -0.0162<br>(631)<br>P=.900 | -0.2959<br>(631)<br>P=.019 |
| Ca | -0.1210<br>(631)<br>P=.345 | -0.1298<br>(631)<br>P=.311 | -0.0946<br>(631)<br>P=.461 | 1.0000<br>(631)<br>P=**** | -0.2176<br>(631)<br>P=.087 | -0.1359<br>(631)<br>P=.288 | -0.2185<br>(631)<br>P=.085 | -0.1144<br>(631)<br>P=.372 | -0.2489<br>(631)<br>P=.049 | -0.1791<br>(631)<br>P=.160 |
| Ce | -0.1431<br>(631)<br>P=.263 | -0.0629<br>(631)<br>P=.624 | -0.3390<br>(631)<br>P=.007 | -0.2176<br>(631)<br>P=.087 | 1.0000<br>(631)<br>P=**** | -0.4223<br>(631)<br>P=.001 | 0.3283<br>(631)<br>P=.009 | 0.5917<br>(631)<br>P=0.000 | 0.0353<br>(631)<br>P=.783 | 0.9070<br>(631)<br>P=0.000 |
| Co | 0.0236<br>(631)<br>P=.854 | -0.0089<br>(631)<br>P=.945 | 0.0041<br>(631)<br>P=.974 | -0.1359<br>(631)<br>P=.288 | -0.4223<br>(631)<br>P=.001 | 1.0000<br>(631)<br>P=**** | -0.0511<br>(631)<br>P=.691 | 0.0958<br>(631)<br>P=.455 | -0.1377<br>(631)<br>P=.282 | 0.3653<br>(631)<br>P=.003 |
| Cr | -0.0805<br>(631)<br>P=.530 | -0.1320<br>(631)<br>P=.302 | 0.0234<br>(631)<br>P=.856 | -0.2185<br>(631)<br>P=.085 | 0.3283<br>(631)<br>P=.009 | -0.0511<br>(631)<br>P=.691 | 1.0000<br>(631)<br>P=**** | 0.6902<br>(631)<br>P=0.000 | 0.2718<br>(631)<br>P=.031 | 0.4516<br>(631)<br>P=0.000 |
| Cs | -0.0885<br>(631)<br>P=.490 | -0.0827<br>(631)<br>P=.520 | -0.1767<br>(631)<br>P=.166 | -0.1144<br>(631)<br>P=.372 | 0.5917<br>(631)<br>P=0.000 | 0.0958<br>(631)<br>P=.455 | 0.6902<br>(631)<br>P=0.000 | 1.0000<br>(631)<br>P=**** | -0.0171<br>(631)<br>P=.894 | 0.6236<br>(631)<br>P=0.000 |
| Cu | -0.0896<br>(631)<br>P=.485 | -0.0573<br>(631)<br>P=.656 | -0.0162<br>(631)<br>P=.900 | -0.2489<br>(631)<br>P=.049 | 0.0353<br>(631)<br>P=.783 | -0.1377<br>(631)<br>P=.282 | 0.2718<br>(631)<br>P=.031 | -0.0171<br>(631)<br>P=.894 | 1.0000<br>(631)<br>P=**** | -0.0383<br>(631)<br>P=.766 |
| Eu | -0.1867<br>(631)<br>P=.143 | -0.0970<br>(631)<br>P=.449 | -0.2959<br>(631)<br>P=.019 | -0.1791<br>(631)<br>P=.160 | 0.9070<br>(631)<br>P=0.000 | 0.3653<br>(631)<br>P=.003 | 0.4516<br>(631)<br>P=0.000 | 0.6236<br>(631)<br>P=0.000 | -0.0383<br>(631)<br>P=.766 | 1.0000<br>(631)<br>P=**** |
| F | -0.0701<br>(631)<br>P=.592 | 0.0849<br>(631)<br>P=.515 | -0.3426<br>(631)<br>P=.007 | -0.0752<br>(631)<br>P=.565 | 0.7764<br>(631)<br>P=0.000 | 0.0448<br>(631)<br>P=.732 | 0.3178<br>(631)<br>P=.013 | 0.5579<br>(631)<br>P=0.000 | -0.1570<br>(631)<br>P=.227 | 0.6624<br>(631)<br>P=0.000 |
| Fe | 0.7889<br>(631)<br>P=0.000 | 0.0713<br>(631)<br>P=.579 | -0.1242<br>(631)<br>P=.324 | 0.0653<br>(631)<br>P=.611 | 0.2942<br>(631)<br>P=.019 | 0.2548<br>(631)<br>P=.044 | 0.0727<br>(631)<br>P=.571 | 0.2774<br>(631)<br>P=.028 | -0.0493<br>(631)<br>P=.701 | 0.2238<br>(631)<br>P=.078 |

| | As | Ba | Br | Ca | Ce | Co | Cr | Cs | Cu | Eu |
|---|---|---|---|---|---|---|---|---|---|---|
| **Hf** | -0.1860 (63) P=.134 | 0.1372 (63) P=.284 | -0.2669 (63) P=.034 | 0.0209 (63) P=.871 | 0.7028 (63) P=0.000 | 0.2435 (63) P=.054 | 0.1509 (63) P=.238 | 0.4117 (63) P=.001 | 0.0970 (63) P=.450 | 0.7302 (63) P=0.000 |
| **Mn** | -0.0846 (63) P=.510 | -0.0586 (63) P=.648 | -0.1524 (63) P=.233 | 0.6777 (63) P=0.000 | -0.0414 (63) P=.747 | 0.2374 (63) P=.061 | -0.1315 (63) P=.304 | -0.0011 (63) P=.993 | -0.1845 (63) P=.148 | 0.0464 (63) P=.718 |
| **La** | -0.1377 (63) P=.296 | -0.0642 (63) P=.617 | -0.3436 (63) P=.006 | -0.2346 (63) P=.064 | 0.9890 (63) P=0.000 | 0.3916 (63) P=.002 | 0.3468 (63) P=.005 | 0.6118 (63) P=0.000 | 0.0270 (63) P=.834 | 0.8815 (63) P=0.000 |
| **Li** | -0.1532 (63) P=.231 | 0.0919 (63) P=.474 | -0.0783 (63) P=.542 | -0.2797 (63) P=.026 | 0.3083 (63) P=.014 | -0.0719 (63) P=.575 | 0.1123 (63) P=.381 | -0.0230 (63) P=.858 | 0.2503 (63) P=.048 | 0.2462 (63) P=.052 |
| **Lu** | -0.1515 (63) P=.236 | 0.3934 (63) P=.001 | -0.2254 (63) P=.076 | -0.0995 (63) P=.438 | 0.4578 (63) P=0.000 | 0.2719 (63) P=.031 | 0.1553 (63) P=.224 | 0.3533 (63) P=.005 | -0.0394 (63) P=.759 | 0.6225 (63) P=0.000 |
| **Na** | -0.0120 (63) P=.925 | -0.1119 (63) P=.383 | -0.1931 (63) P=.129 | -0.0691 (63) P=.590 | 0.5461 (63) P=0.000 | 0.2678 (63) P=.034 | 0.1796 (63) P=.159 | 0.2758 (63) P=.029 | -0.0091 (63) P=.944 | 0.5676 (63) P=0.000 |
| **Nd** | -0.1232 (63) P=.344 | -0.0849 (63) P=.516 | -0.3250 (63) P=.011 | -0.2033 (63) P=.116 | 0.9841 (63) P=0.000 | 0.3807 (63) P=.002 | 0.3267 (63) P=.010 | 0.5815 (63) P=0.000 | -0.0300 (63) P=.819 | 0.9456 (63) P=0.000 |
| **Ni** | 0.0225 (63) P=.861 | -0.0067 (63) P=.958 | -0.2566 (63) P=.042 | -0.2449 (63) P=.053 | -0.1974 (63) P=.121 | 0.2547 (63) P=.044 | 0.0982 (63) P=.444 | -0.0090 (63) P=.944 | 0.0096 (63) P=.941 | -0.0503 (63) P=.695 |
| **Pb** | -0.0439 (63) P=.738 | -0.0580 (63) P=.651 | -0.1325 (63) P=.300 | -0.0767 (63) P=.550 | 0.4042 (63) P=.001 | 0.0194 (63) P=.880 | 0.0925 (63) P=.471 | 0.1044 (63) P=.416 | 0.3130 (63) P=.013 | 0.2912 (63) P=.021 |
| **Rb** | -0.0599 (63) P=.641 | -0.0349 (63) P=.786 | -0.2465 (63) P=.051 | -0.1127 (63) P=.379 | 0.6688 (63) P=0.000 | 0.1308 (63) P=.307 | 0.6062 (63) P=0.000 | 0.7831 (63) P=0.000 | -0.0599 (63) P=.647 | 0.7173 (63) P=0.000 |
| **S** | 0.8954 (63) P=0.000 | 0.3197 (63) P=.011 | 0.2417 (63) P=.056 | 0.0738 (63) P=.566 | -0.2185 (63) P=.085 | -0.0204 (63) P=.874 | -0.2108 (63) P=.097 | -0.1231 (63) P=.337 | -0.0960 (63) P=.454 | -0.2628 (63) P=.037 |
| **Sb** | 0.0198 (63) P=.877 | 0.4725 (63) P=0.000 | -0.0478 (63) P=.710 | -0.1824 (63) P=.152 | -0.0125 (63) P=.923 | 0.2723 (63) P=.031 | -0.1791 (63) P=.160 | -0.0383 (63) P=.766 | -0.1177 (63) P=.358 | -0.0024 (63) P=.985 |
| **Sc** | -0.2012 (63) P=.114 | 0.0382 (63) P=.766 | -0.1703 (63) P=.182 | -0.0529 (63) P=.681 | 0.5346 (63) P=0.000 | 0.1799 (63) P=.158 | 0.4288 (63) P=0.000 | 0.5572 (63) P=0.000 | -0.1332 (63) P=.298 | 0.7327 (63) P=0.000 |
| **Se** | 0.1589 (63) P=.213 | -0.1213 (63) P=.341 | -0.1965 (63) P=.123 | -0.1951 (63) P=.125 | -0.0025 (63) P=.985 | -0.2566 (63) P=.042 | 0.3961 (63) P=.001 | 0.0027 (63) P=.983 | -0.4546 (63) P=0.000 | -0.0427 (63) P=.740 |

| | As | Ba | Br | Ca | Ce | Co | Cr | Cs | Cu | Eu |
|---|---|---|---|---|---|---|---|---|---|---|
| Sm | -0.1811 (636) P=.156 | -0.1120 (636) P=.342 | -0.3285 (636) P=.009 | -0.1704 (636) P=.182 | 0.9601 (636) P=0.000 | 0.4002 (636) P=.001 | 0.3610 (636) P=.004 | 0.6136 (636) P=0.000 | 0.0479 (636) P=.709 | 0.9642 (636) P=0.000 |
| Sr | 0.0408 (636) P=.751 | 0.5897 (636) P=0.000 | 0.0714 (636) P=.578 | -0.0815 (636) P=.525 | 0.2341 (636) P=.065 | 0.1440 (636) P=.260 | -0.0335 (636) P=.794 | 0.1126 (636) P=.380 | -0.2011 (636) P=.114 | 0.2524 (636) P=.046 |
| Ta | -0.1231 (636) P=.336 | 0.0875 (636) P=.495 | -0.2679 (636) P=.034 | -0.1406 (636) P=.272 | 0.7926 (636) P=0.000 | 0.3841 (636) P=.002 | 0.1598 (636) P=.211 | 0.3695 (636) P=.003 | 0.0010 (636) P=.994 | 0.6725 (636) P=0.000 |
| Tb | -0.1965 (636) P=.123 | 0.0222 (636) P=.863 | -0.2898 (636) P=.021 | -0.0570 (636) P=.657 | 0.7520 (636) P=0.000 | 0.3842 (636) P=.002 | 0.2753 (636) P=.029 | 0.5269 (636) P=0.000 | -0.0399 (636) P=.756 | 0.8612 (636) P=0.000 |
| Th | -0.1178 (636) P=.358 | 0.0110 (636) P=.932 | -0.2614 (636) P=.038 | -0.0869 (636) P=.498 | 0.8241 (636) P=0.000 | 0.4727 (636) P=0.000 | 0.1180 (636) P=.357 | 0.3966 (636) P=.001 | -0.0716 (636) P=.577 | 0.6907 (636) P=0.000 |
| U | -0.1322 (636) P=.302 | -0.3397 (636) P=.006 | -0.2210 (636) P=.082 | -0.0416 (636) P=.746 | 0.5835 (636) P=0.000 | 0.4261 (636) P=0.000 | -0.0072 (636) P=.955 | 0.1933 (636) P=.129 | 0.0765 (636) P=.551 | 0.6215 (636) P=0.000 |
| Yb | -0.1580 (636) P=.216 | 0.3781 (636) P=.002 | -0.2270 (636) P=.074 | -0.0822 (636) P=.522 | 0.4610 (636) P=0.000 | 0.2894 (636) P=.021 | 0.1540 (636) P=.228 | 0.3615 (636) P=.004 | 0.0368 (636) P=.775 | 0.6287 (636) P=0.000 |
| Zn | -0.0419 (636) P=.744 | 0.0167 (636) P=.897 | -0.1019 (636) P=.427 | -0.1185 (636) P=.355 | 0.1451 (636) P=.256 | 0.0936 (636) P=.466 | -0.0572 (636) P=.656 | -0.0009 (636) P=.995 | -0.0858 (636) P=.504 | -0.0493 (636) P=.701 |
| MOIST | 0.0170 (636) P=.895 | 0.1148 (636) P=.370 | -0.0132 (636) P=.918 | -0.0553 (636) P=.667 | -0.0089 (636) P=.945 | 0.6059 (636) P=0.000 | -0.1631 (636) P=.202 | -0.0789 (636) P=.539 | -0.0963 (636) P=.453 | -0.0276 (636) P=.830 |
| ASH | -0.0395 (636) P=.759 | -0.0000 (636) P=1.000 | -0.3065 (636) P=.015 | -0.1133 (636) P=.376 | 0.9051 (636) P=0.000 | 0.3354 (636) P=.007 | 0.3434 (636) P=.006 | 0.5760 (636) P=0.000 | 0.0052 (636) P=.968 | 0.8348 (636) P=0.000 |
| VM | -0.0197 (611) P=.880 | -0.0143 (611) P=.913 | -0.1700 (611) P=.190 | 0.1234 (611) P=.343 | -0.8463 (611) P=0.000 | 0.1295 (611) P=.320 | -0.3095 (611) P=.015 | -0.5311 (611) P=0.000 | -0.0617 (611) P=.637 | -0.7088 (611) P=0.000 |
| ATU | 0.0340 (636) P=.791 | -0.0052 (636) P=.968 | 0.3094 (636) P=.014 | 0.1108 (636) P=.387 | -0.8861 (636) P=0.000 | -0.4037 (636) P=.001 | -0.3630 (636) P=.012 | -0.5552 (636) P=0.000 | -0.0169 (636) P=.895 | -0.8153 (636) P=0.000 |
| FC | 0.0711 (611) P=.586 | -0.0173 (611) P=.895 | -0.3692 (611) P=.003 | 0.1323 (611) P=.309 | -0.8954 (611) P=0.000 | 0.0395 (611) P=.763 | -0.3337 (611) P=.009 | -0.5276 (611) P=0.000 | -0.1569 (611) P=.227 | -0.7633 (611) P=0.000 |

(Coefficient / (Cases) / Significance)    (A value of 99.0000 is printed if a coefficient cannot be computed)

|      | Ni | Nd | Na | Lu | Li | La | Mn | Hf | Fe | F |
|------|----|----|----|----|----|----|----|----|----|----|
| As   |    |    |    |    |    |    |    |    |    |   |
| Ba   |    |    |    |    |    |    |    |    |    |   |
| Br   |    |    |    |    |    |    |    |    |    |   |
| Ca   |    |    |    |    |    |    |    |    |    |   |
| Ce   |    |    |    |    |    |    |    |    |    |   |
| Co   |    |    |    |    |    |    |    |    |    |   |
| Cr   |    |    |    |    |    |    |    |    |    |   |
| Cs   |    |    |    |    |    |    |    |    |    |   |
| Cu   |    |    |    |    |    |    |    |    |    |   |
| Eu   |    |    |    |    |    |    |    |    |    |   |
| F    |    |    |    |    |    |    |    |    |    |   |
| Fe   |    |    |    |    |    |    |    |    |    |   |

| | F | Fc | Hf | Mn | La | Li | Lu | Na | Nd | Ni |
|---|---|---|---|---|---|---|---|---|---|---|
| **Hf** | 0.5285 (631) P=0.000 | 0.1464 (631) P=.252 | 1.0000 (631) P=.*** | 0.0924 (631) P=.471 | 0.6397 (631) P=0.000 | -0.4220 (631) P=.001 | 0.5909 (631) P=0.000 | -0.4378 (631) P=0.000 | 0.7280 (611) P=0.000 | -0.3093 (631) P=.014 |
| **Mn** | -0.0550 (611) P=.674 | -0.0106 (631) P=.934 | 0.0924 (631) P=.471 | 1.0000 (631) P=.*** | -0.0987 (631) P=.593 | -0.0687 (631) P=.593 | -0.2200 (631) P=.083 | 0.0748 (631) P=.560 | -0.0599 (611) P=.647 | -0.0567 (631) P=.659 |
| **La** | 0.7892 (611) P=0.000 | 0.3106 (631) P=.013 | 0.6397 (631) P=0.000 | -0.0987 (631) P=.593 | 1.0000 (631) P=.*** | 0.2512 (631) P=.047 | 0.4342 (631) P=0.000 | 0.5733 (631) P=0.000 | 0.9655 (611) P=0.000 | -0.1676 (631) P=.189 |
| **Li** | -0.0527 (611) P=.687 | -0.1364 (631) P=.286 | -0.4220 (631) P=.001 | -0.0687 (631) P=.593 | 0.2512 (631) P=.047 | 1.0000 (631) P=.*** | -0.0736 (631) P=.567 | 0.0767 (631) P=.550 | 0.2985 (611) P=.019 | -0.2719 (631) P=.029 |
| **Lu** | 0.4369 (611) P=0.000 | 0.2147 (631) P=.091 | 0.5909 (631) P=0.000 | -0.2498 (631) P=.048 | 0.4342 (631) P=0.000 | -0.0736 (631) P=.567 | 1.0000 (631) P=.*** | 0.3607 (631) P=.004 | 0.5128 (611) P=0.000 | 0.2568 (631) P=.042 |
| **Na** | 0.6511 (611) P=0.000 | -0.2394 (631) P=.059 | -0.4378 (631) P=0.000 | -0.2200 (631) P=.083 | 0.5733 (631) P=0.000 | 0.0767 (631) P=.550 | 0.3607 (631) P=.004 | 1.0000 (631) P=.*** | 0.5480 (611) P=0.000 | -0.1026 (631) P=.424 |
| **Nd** | 0.8325 (611) P=0.000 | -0.6527 (611) P=0.000 | 0.7280 (611) P=0.000 | 0.0748 (631) P=.560 | 0.9655 (611) P=0.000 | 0.2985 (631) P=.019 | 0.5128 (611) P=0.000 | 0.5480 (611) P=0.000 | 1.0000 (611) P=.*** | -0.1665 (611) P=.200 |
| **Ni** | -0.0447 (611) P=.733 | 0.0771 (611) P=.548 | -0.3093 (631) P=.014 | -0.0599 (631) P=.647 | -0.1676 (631) P=.189 | -0.2749 (631) P=.029 | 0.2568 (631) P=.042 | -0.1025 (631) P=.424 | -0.1665 (611) P=.200 | 1.0000 (631) P=.*** |
| **Pb** | 0.5186 (611) P=0.000 | 0.2321 (631) P=.067 | -0.2453 (631) P=.053 | 0.0567 (631) P=.659 | -0.4267 (631) P=0.000 | -0.0093 (631) P=.942 | 0.2206 (631) P=.082 | 0.4915 (631) P=0.000 | -0.4145 (611) P=.001 | -0.0934 (631) P=.467 |
| **Rb** | 0.6631 (611) P=0.000 | 0.2701 (631) P=.032 | -0.4527 (631) P=0.000 | 0.0675 (631) P=.599 | 0.6905 (631) P=0.000 | -0.1201 (631) P=.348 | 0.3200 (631) P=.011 | 0.6079 (631) P=0.000 | 0.6653 (611) P=0.000 | -0.1105 (631) P=.389 |
| **S** | -0.0271 (611) P=.836 | 0.7835 (631) P=0.000 | -0.1853 (631) P=.146 | 0.0169 (631) P=.895 | -0.1960 (631) P=.124 | -0.2178 (631) P=.086 | 0.0304 (631) P=.813 | -0.1001 (631) P=.435 | -0.2436 (611) P=.058 | -0.1367 (631) P=.286 |
| **Sb** | 0.1378 (611) P=.289 | -0.1520 (631) P=.231 | 0.0123 (631) P=.923 | -0.0053 (631) P=.506 | -0.0231 (631) P=.857 | -0.2181 (631) P=.086 | 0.5597 (631) P=0.000 | 0.1108 (631) P=.387 | -0.0197 (611) P=.880 | 0.5370 (631) P=0.000 |
| **Sc** | 0.4398 (611) P=0.000 | 0.1545 (631) P=.227 | -0.7344 (631) P=0.000 | 0.1673 (631) P=.190 | 0.4812 (631) P=0.000 | -0.2273 (631) P=.073 | 0.7922 (631) P=0.000 | 0.2165 (631) P=.088 | 0.6084 (611) P=0.000 | 0.0876 (631) P=.495 |
| **Se** | 0.0503 (611) P=.700 | 0.0379 (611) P=.768 | -0.1012 (631) P=.430 | -0.3450 (631) P=.006 | -0.0339 (631) P=.792 | 0.4160 (631) P=.001 | -0.1084 (631) P=.398 | -0.2458 (631) P=.052 | 0.0515 (611) P=.694 | -0.0779 (631) P=.544 |

| | F | Fe | Hf | Mn | La | Li | Lu | Na | Nd | Ni |
|---|---|---|---|---|---|---|---|---|---|---|
| Sm | 0.7231 (612) P=0.000 | 0.2654 (636) P=.036 | 0.7533 (630) P=0.000 | 0.0505 (634) P=.694 | 0.9313 (630) P=0.000 | 0.2837 (624) P=.024 | 0.5899 (630) P=0.000 | 0.5188 (630) P=0.000 | 0.9819 (612) P=0.000 | -0.1324 (630) P=.301 |
| Sr | 0.2178 (612) P=.092 | 0.1613 (636) P=.207 | 0.3895 (630) P=.002 | 0.0032 (636) P=.980 | 0.2450 (630) P=.053 | -0.0942 (633) P=.463 | 0.3806 (630) P=.002 | 0.5971 (630) P=0.000 | 0.2426 (612) P=.060 | -0.1287 (630) P=.315 |
| Ta | 0.6031 (612) P=0.000 | 0.2255 (636) P=.076 | 0.6940 (630) P=0.000 | 0.0032 (636) P=.980 | 0.7443 (630) P=0.000 | 0.4644 (630) P=0.000 | 0.3942 (630) P=.001 | 0.3933 (630) P=.001 | 0.7764 (612) P=0.000 | -0.2925 (630) P=.020 |
| Tb | 0.5977 (612) P=0.000 | 0.2501 (636) P=.048 | 0.7257 (630) P=0.000 | 0.2398 (636) P=.058 | 0.7137 (630) P=0.000 | 0.1108 (636) P=.387 | 0.8472 (630) P=0.000 | 0.3908 (632) P=.002 | 0.8060 (612) P=0.000 | 0.0676 (630) P=.599 |
| Th | 0.6867 (612) P=0.000 | 0.2787 (636) P=.027 | 0.7822 (630) P=0.000 | 0.0565 (636) P=.660 | 0.7765 (630) P=0.000 | 0.4033 (631) P=.001 | 0.4137 (630) P=.001 | 0.4381 (630) P=0.000 | 0.8097 (612) P=0.000 | -0.2810 (632) P=.026 |
| U | 0.4643 (612) P=.001 | 0.2297 (636) P=.070 | 0.7431 (630) P=0.000 | 0.2452 (633) P=.053 | 0.5292 (630) P=0.000 | 0.1496 (630) P=.242 | 0.8141 (630) P=0.000 | 0.4882 (630) P=0.000 | 0.6103 (612) P=0.000 | -0.0249 (632) P=.847 |
| Yb | 0.4290 (612) P=.001 | 0.2095 (636) P=.099 | 0.6022 (630) P=0.000 | 0.2382 (636) P=.060 | 0.4341 (630) P=0.000 | 0.0729 (630) P=.570 | 0.9972 (630) P=0.000 | 0.3494 (630) P=.005 | 0.5157 (630) P=0.000 | 0.2350 (630) P=.064 |
| Zn | 0.2857 (612) P=.026 | 0.1120 (636) P=.382 | -0.0120 (636) P=.926 | 0.0015 (631) P=.991 | 0.1910 (630) P=.134 | -0.1587 (633) P=.214 | 0.0825 (631) P=.521 | 0.2965 (630) P=.018 | 0.1197 (612) P=.358 | 0.0719 (630) P=.576 |
| MOIST | 0.1392 (612) P=.285 | 0.0975 (635) P=.447 | 0.0719 (630) P=.575 | 0.2944 (630) P=.019 | -0.0107 (630) P=.934 | -0.3903 (630) P=.002 | 0.2581 (630) P=.041 | 0.0609 (635) P=.635 | -0.0412 (612) P=.753 | 0.4483 (630) P=0.000 |
| ASH | 0.7881 (612) P=0.000 | 0.3637 (636) P=.003 | 0.7270 (630) P=0.000 | 0.0215 (637) P=.867 | 0.8877 (630) P=0.000 | 0.3328 (630) P=.008 | 0.4114 (630) P=.001 | 0.6717 (630) P=0.000 | 0.8939 (612) P=0.000 | -0.2243 (630) P=.065 |
| VM | -0.7531 (612) P=0.000 | -0.3971 (636) P=.002 | -0.6198 (630) P=0.000 | -0.1305 (636) P=.316 | -0.8189 (630) P=0.000 | -0.3465 (630) P=.006 | -0.3600 (630) P=.004 | -0.5636 (630) P=0.000 | -0.8569 (612) P=0.000 | 0.2447 (612) P=.057 |
| BTU | -0.7919 (612) P=0.000 | -0.3619 (636) P=.004 | -0.7093 (630) P=0.000 | -0.0817 (636) P=.524 | -0.8650 (630) P=0.000 | -0.2966 (630) P=.018 | -0.4362 (630) P=0.000 | -0.6520 (630) P=0.000 | -0.8703 (612) P=0.000 | 0.1605 (630) P=.209 |
| FC | -0.7707 (612) P=0.000 | -0.2751 (612) P=.032 | -0.6668 (612) P=0.000 | 0.0629 (612) P=.630 | -0.8445 (612) P=0.000 | -0.4397 (612) P=0.000 | -0.3853 (612) P=.002 | -0.4991 (612) P=0.000 | -0.8623 (612) P=0.000 | -0.1578 (612) P=.225 |

(Coefficient / (Cases) / Significance)    (A value of 99.0000 is printed if a coefficient cannot be computed)

|    | Tb | Ta | Sr | Sm | Se | Sc | Sb | S | Rb | Pb |
|----|----|----|----|----|----|----|----|---|----|----|
| As |    |    |    |    |    |    |    |   |    |    |
| Ba |    |    |    |    |    |    |    |   |    |    |
| Br |    |    |    |    |    |    |    |   |    |    |
| Ca |    |    |    |    |    |    |    |   |    |    |
| Ce |    |    |    |    |    |    |    |   |    |    |
| Co |    |    |    |    |    |    |    |   |    |    |
| Cr |    |    |    |    |    |    |    |   |    |    |
| Cs |    |    |    |    |    |    |    |   |    |    |
| Cu |    |    |    |    |    |    |    |   |    |    |
| Eu |    |    |    |    |    |    |    |   |    |    |
| F  |    |    |    |    |    |    |    |   |    |    |
| Fe |    |    |    |    |    |    |    |   |    |    |

|  | Tb | Ta | Sr | Sm | Se | Sc | Sb | S | Rb | Pb |
|---|---|---|---|---|---|---|---|---|---|---|
| **Hf** | 0.7257 (0.6366) P=0.000 | 0.6940 (0.6366) P=0.000 | 0.3895 (0.6302) P=.002 | 0.7533 (0.6366) P=0.000 | 0.1012 (0.6430) P=.430 | 0.7344 (0.6366) P=0.000 | 0.0123 (0.6366) P=.923 | -0.1853 (0.6366) P=.146 | 0.4527 (0.6366) P=0.000 | 0.2453 (0.6363) P=.053 |
| **Mn** | 0.2398 (0.6338) P=.058 | -0.0032 (0.6370) P=.980 | -0.0032 (0.6370) P=.980 | -0.0505 (0.6366) P=.694 | -0.3450 (0.6366) P=.006 | 0.1657 (0.6332) P=.194 | 0.1673 (0.6366) P=.190 | -0.0853 (0.6366) P=.506 | 0.0169 (0.6366) P=.895 | -0.0675 (0.6399) P=.599 |
| **La** | 0.7137 (0.6366) P=0.000 | 0.7443 (0.6366) P=0.000 | 0.2450 (0.6363) P=.053 | 0.9313 (0.6366) P=0.000 | -0.0339 (0.6392) P=.792 | 0.4812 (0.6366) P=0.000 | 0.0231 (0.6336) P=.857 | -0.1960 (0.6324) P=.124 | 0.6905 (0.6366) P=0.000 | 0.4267 (0.6366) P=0.000 |
| **Li** | 0.1108 (0.6387) P=.387 | 0.4644 (0.6366) P=0.000 | -0.0942 (0.6363) P=.463 | 0.2837 (0.6366) P=.024 | 0.4160 (0.6331) P=.001 | 0.2273 (0.6363) P=.073 | -0.2180 (0.6366) P=.086 | -0.2178 (0.6366) P=.086 | 0.1201 (0.6366) P=.348 | -0.0093 (0.6363) P=.942 |
| **Lu** | 0.8472 (0.6366) P=0.000 | 0.3942 (0.6301) P=.001 | 0.3806 (0.6302) P=.024 | 0.5899 (0.6366) P=0.000 | -0.1084 (0.6308) P=.399 | 0.7922 (0.6366) P=0.000 | 0.5997 (0.6366) P=0.000 | -0.0304 (0.6313) P=.813 | 0.3200 (0.6366) P=.011 | 0.2205 (0.6308) P=.082 |
| **Na** | 0.3908 (0.6302) P=.000 | 0.3933 (0.6301) P=.001 | 0.5971 (0.6302) P=0.000 | 0.5188 (0.6366) P=0.000 | 0.2458 (0.6332) P=.052 | 0.2165 (0.6388) P=.088 | 0.1108 (0.6366) P=.387 | -0.1001 (0.6366) P=.435 | 0.6079 (0.6366) P=0.000 | 0.4915 (0.6366) P=0.000 |
| **Nd** | 0.8060 (0.6110) P=0.000 | 0.7764 (0.6110) P=0.000 | 0.2426 (0.6110) P=.060 | 0.9819 (0.6110) P=0.000 | 0.0515 (0.6194) P=.694 | 0.6084 (0.6110) P=0.000 | -0.0197 (0.6110) P=.880 | -0.2436 (0.6110) P=.058 | 0.6653 (0.6110) P=0.000 | 0.4145 (0.6111) P=.001 |
| **Ni** | 0.0676 (0.6399) P=.599 | 0.2925 (0.6320) P=.020 | -0.1287 (0.6363) P=.315 | -0.1324 (0.6301) P=.301 | 0.0779 (0.6344) P=.544 | 0.0876 (0.6395) P=.495 | 0.5370 (0.6366) P=0.000 | -0.1367 (0.6286) P=.286 | -0.1105 (0.6366) P=.389 | -0.0934 (0.6301) P=.467 |
| **Pb** | 0.3613 (0.6304) P=.004 | 0.3833 (0.6302) P=.002 | 0.3435 (0.6306) P=.006 | 0.3874 (0.6302) P=.002 | 0.0140 (0.6331) P=.913 | 0.1402 (0.6301) P=.273 | -0.0476 (0.6311) P=.711 | -0.0760 (0.6366) P=.550 | 0.1011 (0.6366) P=.431 | 1.0000 (0.6363) P=*** |
| **Rb** | 0.4492 (0.6366) P=0.000 | 0.4431 (0.6366) P=0.000 | 0.1772 (0.6320) P=.320 | 0.6489 (0.6366) P=0.000 | -0.0958 (0.6366) P=.455 | 0.4189 (0.6301) P=.001 | -0.0212 (0.6369) P=.869 | -0.1559 (0.6366) P=.222 | 1.0000 (0.6363) P=*** | 0.1011 (0.6366) P=.431 |
| **S** | -0.1646 (0.6336) P=.197 | -0.1857 (0.6336) P=.145 | -0.2615 (0.6338) P=.038 | -0.2575 (0.6366) P=.042 | 0.0923 (0.6332) P=.472 | -0.1726 (0.6336) P=.176 | 0.2868 (0.6366) P=.023 | 1.0000 (0.6363) P=*** | -0.1559 (0.6366) P=.222 | -0.0760 (0.6366) P=.550 |
| **Sb** | 0.2270 (0.6374) P=.074 | -0.0034 (0.6379) P=.979 | -0.1548 (0.6336) P=.226 | -0.0013 (0.6332) P=.992 | -0.2187 (0.6335) P=.085 | 0.1436 (0.6361) P=.261 | 1.0000 (0.6363) P=*** | 0.2868 (0.6366) P=.023 | -0.0212 (0.6369) P=.869 | -0.0476 (0.6311) P=.711 |
| **Sc** | 0.8735 (0.6366) P=0.000 | 0.4865 (0.6366) P=0.000 | -0.1272 (0.6336) P= | 0.7106 (0.6366) P=0.000 | 0.1817 (0.6331) P=.154 | 1.0000 (0.6363) P=*** | 0.1436 (0.6361) P=.261 | -0.1726 (0.6336) P=.176 | 0.4189 (0.6301) P=.001 | 0.1402 (0.6301) P=.273 |
| **Se** | -0.0493 (0.6361) P=.701 | -0.0829 (0.6331) P=.518 | -0.1846 (0.6363) P=.147 | 0.0115 (0.6363) P=.929 | 1.0000 (0.6363) P=*** | 0.1817 (0.6331) P=.154 | -0.2187 (0.6335) P=.085 | 0.0923 (0.6366) P=.472 | -0.0958 (0.6366) P=.455 | -0.0140 (0.6331) P=.913 |

| | Ph | Rb | S | Sb | Sc | Se | Sm | Sr | Ta | Tb |
|---|---|---|---|---|---|---|---|---|---|---|
| Sm | 0.3874 (63) P=.002 | 0.6409 (63) P=0.000 | -0.2575 (63) P=.042 | -0.0013 (63) P=.992 | 0.7106 (63) P=0.000 | 0.0115 (63) P=.929 | 1.0000 (63) P=***** | 0.1933 (63) P=.129 | 0.7725 (63) P=0.000 | 0.8790 (63) P=0.000 |
| Sr | 0.0798 (63) P=.534 | 0.3435 (63) P=.006 | 0.1272 (63) P=.320 | 0.2615 (63) P=.030 | 0.1548 (63) P=.226 | -0.1846 (63) P=.147 | 0.1933 (63) P=.129 | 1.0000 (63) P=***** | 0.2059 (63) P=.105 | 0.1792 (63) P=.160 |
| Ta | 0.3830 (63) P=.002 | 0.4431 (63) P=0.000 | -0.1857 (63) P=.145 | -0.0034 (63) P=.979 | 0.4866 (63) P=0.000 | 0.0829 (63) P=.518 | 0.7725 (63) P=0.000 | 0.2059 (63) P=.105 | 1.0000 (63) P=***** | 0.6228 (63) P=0.000 |
| Tb | 0.3613 (63) P=.004 | 0.4492 (63) P=0.000 | -0.1616 (63) P=.197 | 0.2270 (63) P=.074 | 0.8735 (63) P=0.000 | -0.0493 (63) P=.701 | 0.8790 (63) P=0.000 | 0.1792 (63) P=.160 | 0.6228 (63) P=0.000 | 1.0000 (63) P=***** |
| Th | 0.4848 (63) P=0.000 | 0.3762 (63) P=.002 | -0.1843 (63) P=.148 | -0.0272 (63) P=.833 | 0.5369 (63) P=0.000 | 0.0052 (63) P=.968 | 0.8118 (63) P=0.000 | 0.2037 (63) P=.109 | 0.9195 (63) P=0.000 | 0.6940 (63) P=0.000 |
| U | 0.4284 (63) P=0.000 | 0.2333 (63) P=.066 | -0.0515 (63) P=.689 | 0.3214 (63) P=.010 | 0.6824 (63) P=0.000 | -0.1361 (63) P=.287 | 0.6635 (63) P=0.000 | 0.3822 (63) P=.002 | 0.6517 (63) P=0.000 | 0.8090 (63) P=0.000 |
| Yb | 0.2234 (63) P=.078 | 0.3142 (63) P=.012 | -0.0184 (63) P=.886 | 0.5346 (63) P=0.000 | 0.8035 (63) P=0.000 | -0.1140 (63) P=.374 | 0.5981 (63) P=0.000 | 0.3692 (63) P=.003 | 0.4007 (63) P=.001 | 0.8630 (63) P=0.000 |
| Zn | 0.4739 (63) P=0.000 | 0.0095 (63) P=.941 | -0.0343 (63) P=.789 | 0.1401 (63) P=.273 | -0.0500 (63) P=.697 | -0.1779 (63) P=.163 | 0.1091 (63) P=.395 | 0.0577 (63) P=.653 | -0.1049 (63) P=.413 | 0.1035 (63) P=.420 |
| MOIST | 0.0593 (63) P=.644 | -0.1611 (63) P=.206 | -0.0435 (63) P=.735 | 0.5227 (63) P=0.000 | 0.0246 (63) P=.848 | -0.2985 (63) P=.017 | 0.0115 (63) P=.929 | 0.0376 (63) P=.770 | -0.0195 (63) P=.880 | 0.1747 (63) P=.171 |
| ASH | 0.3737 (63) P=.003 | 0.7909 (63) P=0.000 | -0.1435 (63) P=.262 | -0.0219 (63) P=.865 | 0.4920 (63) P=0.000 | -0.0173 (63) P=.893 | -0.8591 (63) P=0.000 | 0.3541 (63) P=.004 | 0.8130 (63) P=0.000 | 0.6358 (63) P=0.000 |
| VM | -0.4668 (61) P=0.000 | -0.7233 (61) P=0.000 | -0.0002 (61) P=.998 | 0.0523 (61) P=.689 | -0.4401 (61) P=0.000 | -0.1784 (61) P=.169 | -0.7740 (61) P=0.000 | -0.2268 (61) P=.079 | -0.7939 (61) P=0.000 | -0.5636 (61) P=0.000 |
| BTU | -0.3526 (63) P=.005 | -0.7832 (63) P=0.000 | -0.1409 (63) P=.271 | -0.0628 (63) P=.625 | -0.4916 (63) P=0.000 | 0.0489 (63) P=.704 | -0.8456 (63) P=0.000 | -0.3746 (63) P=.007 | -0.8053 (63) P=0.000 | -0.6460 (63) P=0.000 |
| FC | -0.4055 (61) P=.001 | -0.7437 (61) P=0.000 | 0.1106 (61) P=.396 | -0.0112 (61) P=.932 | -0.5039 (61) P=0.000 | -0.2063 (61) P=.111 | -0.8286 (61) P=0.000 | -0.0658 (61) P=.614 | -0.8597 (61) P=0.000 | -0.6069 (61) P=0.000 |

(Coefficient / (Cases) / Significance)      (A value of 99.0000 is printed if a coefficient cannot be computed)

| | FC | BTU | VM | ASH | MOIST | Zn | Yb | U | Th |
|---|---|---|---|---|---|---|---|---|---|
| As | 0.0711 (611) P=.586 | 0.0340 (631) P=.791 | -0.0197 (611) P=.880 | -0.0395 (631) P=.759 | 0.0170 (631) P=.895 | -0.0419 (631) P=.744 | -0.1580 (631) P=.216 | -0.1322 (631) P=.302 | -0.1178 (631) P=.358 |
| Ba | -0.0173 (611) P=.895 | -0.0052 (631) P=.968 | -0.0143 (611) P=.913 | -0.0000 (631) P=1.000 | 0.1148 (631) P=.370 | 0.0167 (631) P=.897 | 0.3781 (631) P=.002 | 0.3997 (631) P=.006 | 0.0110 (631) P=.932 |
| Br | 0.3692 (611) P=.003 | 0.3094 (631) P=.014 | 0.1700 (611) P=.190 | -0.3065 (631) P=.015 | -0.0132 (631) P=.918 | -0.1019 (631) P=.427 | -0.2270 (631) P=.074 | -0.2210 (631) P=.082 | -0.2614 (631) P=.038 |
| Ca | 0.1323 (611) P=.309 | 0.1108 (631) P=.387 | 0.1234 (611) P=.343 | -0.1133 (631) P=.376 | 0.0553 (631) P=.667 | -0.1185 (631) P=.355 | -0.0822 (631) P=.522 | -0.0416 (631) P=.746 | -0.0869 (631) P=.498 |
| Ce | 0.8854 (611) P=0.000 | 0.8861 (631) P=0.000 | -0.8463 (611) P=0.000 | 0.9051 (631) P=0.000 | -0.0089 (631) P=.945 | 0.1451 (631) P=.256 | 0.4610 (631) P=0.000 | 0.5835 (631) P=0.000 | 0.8241 (631) P=0.000 |
| Co | 0.0395 (611) P=.763 | -0.4037 (631) P=.001 | 0.1295 (611) P=.320 | 0.3354 (631) P=.007 | 0.6059 (631) P=0.000 | 0.0936 (631) P=.466 | 0.2894 (631) P=.021 | 0.4261 (631) P=0.000 | 0.4727 (631) P=0.000 |
| Cr | -0.3377 (611) P=.009 | -0.3130 (631) P=.012 | -0.3095 (611) P=.015 | 0.3434 (631) P=.006 | -0.1631 (631) P=.202 | -0.0572 (631) P=.656 | -0.1540 (631) P=.228 | -0.0072 (631) P=.955 | 0.1180 (631) P=.357 |
| Cs | -0.5276 (611) P=0.000 | -0.5552 (631) P=0.000 | -0.5331 (611) P=0.000 | 0.5760 (631) P=0.000 | -0.0789 (631) P=.539 | -0.0009 (631) P=.995 | 0.3615 (631) P=.004 | 0.1933 (631) P=.129 | -0.3966 (631) P=.001 |
| Cu | -0.1569 (611) P=.227 | 0.0169 (631) P=.895 | -0.0617 (611) P=.637 | 0.0052 (631) P=.968 | -0.0963 (631) P=.453 | 0.0858 (631) P=.504 | 0.0368 (631) P=.775 | 0.0765 (631) P=.551 | 0.0716 (631) P=.577 |
| Eu | -0.7633 (611) P=0.000 | -0.8153 (631) P=0.000 | -0.7088 (611) P=0.000 | 0.8348 (631) P=0.000 | -0.0276 (631) P=.830 | 0.0493 (631) P=.701 | 0.6287 (631) P=0.000 | 0.6215 (631) P=0.000 | 0.6207 (631) P=0.000 |
| F | -0.7707 (611) P=0.000 | -0.7919 (611) P=0.000 | 0.7531 (611) P=0.000 | 0.7884 (611) P=0.000 | 0.1392 (611) P=.285 | 0.2857 (611) P=.026 | 0.4290 (631) P=.001 | 0.4643 (631) P=0.000 | 0.6867 (631) P=0.000 |
| Fe | -0.2751 (611) P=.032 | -0.3619 (631) P=.004 | -0.3971 (611) P=.002 | 0.3637 (631) P=.003 | 0.0975 (631) P=.447 | 0.1120 (631) P=.382 | 0.2095 (631) P=.099 | 0.2297 (631) P=.070 | 0.2787 (631) P=.027 |

| | FC | BTU | VM | ASH | MOIST | Zn | Yb | U | Th |
|---|---|---|---|---|---|---|---|---|---|
| Hf | -0.6668 .610 P=0.000 | -0.7093 .630 P=0.000 | -0.6198 .610 P=0.000 | 0.7270 .630 P=0.000 | -0.0719 .575 | -0.0120 .926 | 0.6022 .630 P=0.000 | 0.7431 .630 P=0.000 | 0.7822 .630 P=0.000 |
| Mn | 0.0629 .630 | -0.0817 .624 .524 | 0.1305 .316 | -0.0215 .867 | 0.2944 .019 | -0.0015 .991 | -0.2382 .060 | 0.2452 .053 | 0.0565 .660 |
| La | -0.8445 .610 P=0.000 | -0.8650 .630 P=0.000 | -0.8189 .610 P=0.000 | 0.8877 .630 P=0.000 | -0.0107 .934 | 0.1910 .134 | -0.4341 .630 P=0.000 | 0.5292 .630 P=0.000 | 0.7765 .630 P=0.000 |
| Li | -0.4397 .610 P=0.000 | -0.2966 .618 .018 | -0.3465 .006 | 0.3328 .008 | -0.3903 .002 | -0.1587 .214 | -0.0729 .570 | 0.1496 .242 | 0.4033 .001 |
| Lu | -0.3853 .612 .002 | -0.4362 .630 P=0.000 | -0.3601 .004 | 0.4114 .001 | 0.2581 .041 | 0.0825 .521 | 0.9972 .630 P=0.000 | 0.8141 .630 P=0.000 | 0.4137 .001 |
| Na | -0.4971 .610 P=0.000 | -0.6520 .630 P=0.000 | -0.5676 .610 P=0.000 | 0.6717 .630 P=0.000 | 0.0809 .035 | 0.2965 .018 | 0.3494 .005 | 0.4882 .630 P=0.000 | 0.4381 .630 P=0.000 |
| Nd | -0.8623 .590 P=0.000 | -0.8703 .610 P=0.000 | -0.8369 .590 P=0.000 | 0.8369 .000 | 0.0412 .753 | -0.1197 .358 | -0.5157 .610 P=0.000 | 0.6103 .610 P=0.000 | 0.8007 .610 P=0.000 |
| Ni | 0.1578 .225 | 0.1605 .209 | 0.2447 .057 | -0.2343 .065 | 0.0591 .644 | 0.0711 .577 | 0.2350 .064 | 0.0242 .847 | 0.2810 .026 |
| Pb | -0.4055 .601 .001 | -0.3526 .005 | -0.4668 .610 P=0.000 | 0.3737 .003 | -0.1614 .206 | 0.4730 .000 | 0.2234 .078 | 0.4284 .630 P=0.000 | 0.4849 .630 P=0.000 |
| Rb | -0.7437 .610 P=0.000 | -0.7632 .630 P=0.000 | -0.7233 .610 P=0.000 | 0.7909 .630 P=0.000 | 0.0435 .735 | 0.0095 .941 | 0.3142 .012 | 0.2333 .066 | 0.3762 .002 |
| S | 0.1106 .39 | 0.1409 .271 | 0.0002 .998 | -0.1435 .262 | 0.5227 .630 P=0.000 | -0.0343 .789 | 0.0184 .888 | 0.0515 .689 | -0.1843 .148 |
| Sb | -0.0112 .932 | -0.0628 .625 | 0.0523 .689 | -0.0219 .865 | 0.0246 .848 | 0.1401 .273 | 0.5346 .630 P=0.000 | 0.3214 .010 | 0.0272 .833 |
| Sc | -0.5039 .610 P=0.000 | -0.4916 .630 P=0.000 | -0.4401 .610 P=0.000 | 0.4920 .630 P=0.000 | -0.2985 .017 | -0.0500 .697 | 0.8035 .630 P=0.000 | 0.6824 .630 P=0.000 | 0.5369 .630 P=0.000 |
| Se | -0.2043 .111 | 0.0489 .704 | -0.1784 .169 | -0.0173 .893 | | -0.1779 .163 | 0.1140 .374 | -0.1361 .287 | 0.0052 .968 |

| | Th | U | Yb | Zn | MOIST | ASH | VM | BTU | FC |
|---|---|---|---|---|---|---|---|---|---|
| Sm | 0.8118 (631) P=0.000 | 0.6635 (631) P=0.000 | 0.5981 (631) P=0.000 | 0.1091 (631) P=.395 | 0.0115 (631) P=.929 | 0.8591 (631) P=0.000 | -0.7740 (611) P=0.000 | -0.8456 (631) P=0.000 | -0.8286 (611) P=0.000 |
| Sr | -0.2037 (631) P=.109 | 0.3822 (631) P=.002 | 0.3692 (631) P=.003 | 0.0577 (631) P=.653 | 0.0376 (631) P=.770 | 0.3541 (631) P=.004 | -0.2268 (611) P=.079 | -0.3346 (631) P=.007 | -0.0658 (611) P=.614 |
| Ta | 0.9195 (631) P=0.000 | 0.8517 (631) P=0.000 | 0.4007 (631) P=.001 | 0.1049 (631) P=.413 | -0.0195 (631) P=.880 | 0.8130 (631) P=0.000 | -0.7939 (611) P=0.000 | -0.8053 (631) P=0.000 | -0.8597 (611) P=0.000 |
| Tb | 0.6940 (631) P=0.000 | 0.8090 (631) P=0.000 | 0.8630 (631) P=0.000 | 0.1035 (631) P=.420 | 0.1747 (631) P=.171 | 0.6358 (631) P=0.000 | -0.5636 (611) P=0.000 | -0.6460 (631) P=0.000 | -0.6069 (611) P=0.000 |
| Th | 1.0000 (631) P=**** | 0.7308 (631) P=0.000 | 0.4279 (631) P=0.000 | 0.1710 (631) P=.180 | 0.0874 (631) P=.496 | 0.8001 (631) P=0.000 | -0.8034 (611) P=0.000 | -0.7978 (631) P=0.000 | -0.8452 (611) P=0.000 |
| U | 0.7308 (631) P=0.000 | 1.0000 (631) P=**** | 0.8225 (631) P=0.000 | 0.1676 (631) P=.189 | 0.2385 (631) P=.060 | 0.5678 (631) P=0.000 | -0.4938 (611) P=0.000 | -0.5841 (631) P=0.000 | -0.4814 (611) P=0.000 |
| Yb | 0.4279 (631) P=0.000 | 0.8225 (631) P=0.000 | 1.0000 (631) P=**** | 0.0815 (631) P=.525 | 0.2604 (631) P=.039 | 0.4060 (631) P=.001 | -0.3500 (611) P=.006 | -0.4295 (631) P=0.000 | -0.3720 (611) P=.003 |
| Zn | 0.1710 (631) P=.180 | 0.1676 (631) P=.189 | 0.0815 (631) P=.525 | 1.0000 (631) P=**** | 0.2483 (631) P=.050 | 0.1259 (631) P=.325 | -0.1225 (611) P=.347 | -0.1555 (631) P=.224 | -0.1325 (611) P=.309 |
| MOIST | 0.0874 (631) P=.496 | 0.2385 (631) P=.060 | 0.2604 (631) P=.039 | 0.2483 (631) P=.050 | 1.0000 (631) P=**** | -0.0605 (631) P=.638 | 0.1382 (611) P=.288 | 0.0888 (631) P=.489 | 0.1261 (611) P=.333 |
| ASH | 0.8001 (631) P=0.000 | 0.5678 (631) P=0.000 | 0.4060 (631) P=.001 | 0.1259 (631) P=.325 | -0.0605 (631) P=.638 | 1.0000 (631) P=**** | -0.9491 (611) P=0.000 | -0.9846 (631) P=0.000 | -0.9812 (611) P=0.000 |
| VM | -0.8034 (631) P=0.000 | -0.4938 (631) P=0.000 | -0.3500 (631) P=.006 | -0.1225 (631) P=.347 | 0.1382 (631) P=.288 | -0.9491 (631) P=0.000 | 1.0000 (611) P=**** | 0.9157 (631) P=0.000 | 0.8704 (611) P=0.000 |
| BTU | -0.7978 (631) P=0.000 | -0.5841 (631) P=0.000 | -0.4295 (631) P=0.000 | -0.1555 (631) P=.224 | 0.0888 (631) P=.489 | -0.9846 (631) P=0.000 | 0.9157 (611) P=0.000 | 1.0000 (631) P=**** | 0.9681 (611) P=0.000 |
| FC | -0.8452 (631) P=0.000 | -0.4844 (611) P=0.000 | -0.3720 (611) P=.003 | -0.1325 (611) P=.309 | 0.1261 (611) P=.333 | -0.9812 (611) P=0.000 | 0.8704 (611) P=0.000 | 0.9681 (611) P=0.000 | 1.0000 (611) P=**** |

(Coefficient / (Cases) / Significance)

(A value of 99.0000 is printed if a coefficient cannot be computed)

APPENDIX VI

TABLE K

Chondrite REE Values Used

| ELEMENT | VALUE IN (ppm) |
|---------|----------------|
| La | 0.315 |
| Ce | 0.813 |
| Nd | 0.597 |
| Sm | 0.192 |
| Eu | 0.0722 |
| Tb | 0.049 |
| Yb | 0.208 |
| Lu | 0.0323 |

Values from Taylor and Gorton, 1977.